Missouri S&T Library and Learning Resources

Scholars' Mine

Doctoral Dissertations | Student Theses and Dissertations

Fall 2017

Event-triggering architectures for adaptive control of uncertain dynamical systems

Ali Talib Oudah Albattat

Follow this and additional works at: https://scholarsmine.mst.edu/doctoral_dissertations

Part of the Mechanical Engineering Commons

Department: Mechanical and Aerospace Engineering

Recommended Citation

Albattat, Ali Talib Oudah, "Event-triggering architectures for adaptive control of uncertain dynamical systems" (2017). *Doctoral Dissertations*. 2616.
https://scholarsmine.mst.edu/doctoral_dissertations/2616

This thesis is brought to you by Scholars' Mine, a service of the Missouri S&T Library and Learning Resources. This work is protected by U. S. Copyright Law. Unauthorized use including reproduction for redistribution requires the permission of the copyright holder. For more information, please contact scholarsmine@mst.edu.

EVENT-TRIGGERING ARCHITECTURES FOR ADAPTIVE CONTROL OF UNCERTAIN DYNAMICAL SYSTEMS

by

ALI TALIB OUDAH ALBATTAT

A DISSERTATION

Presented to the Graduate Faculty of the

MISSOURI UNIVERSITY OF SCIENCE AND TECHNOLOGY

In Partial Fulfillment of the Requirements for the Degree

DOCTOR OF PHILOSOPHY

in

MECHANICAL ENGINEERING

2017

Approved by

Dr. Tansel Yucelen, Advisor
Dr. Jagannathan Sarangapani
Dr. S.N. Balakrishnan
Dr. Robert Landers
Dr. Douglas A. Bristow

Copyright 2017

ALI TALIB OUDAH ALBATTAT

All Rights Reserved

PUBLICATION DISSERTATION OPTION

This dissertation consists of the six articles which have been submitted, or will be submitted for publication as follows

Paper I: Pages 13-36 have been published in Journal of Dynamic Systems, Measurement, and Control.

Paper II: Pages 37-75 have been published as a chapter in Adaptive Control for Robotic Manipulators, CRC Press/Taylor & Francis Group.

Paper III: Pages 76-126 have been published in Sensors Journal.

Paper IV: Pages 127-148 have been accepted by ASME Dynamic Systems and Control Conference.

Paper V: Pages 149-177 have been submitted to American Control Conference.

Paper VI: Pages 178-220 have been accepted by AIAA Guidance, Navigation, and Control Conference.

ABSTRACT

In this dissertation, new approaches are presented for the design and implementation of networked adaptive control systems to reduce the wireless network utilization while guaranteeing system stability in the presence of system uncertainties. Specifically, the design and analysis of state feedback adaptive control systems over wireless networks using event-triggering control theory is first presented. The state feedback adaptive control results are then generalized to the output feedback case for dynamical systems with unmeasurable state vectors. This event-triggering approach is then adopted for large-scale uncertain dynamical systems. In particular, decentralized and distributed adaptive control methodologies are proposed with reduced wireless network utilization with stability guarantees.

In addition, for systems in the absence of uncertainties, a new observer-free output feedback cooperative control architecture is developed. Specifically, the proposed architecture is predicated on a nonminimal state-space realization that generates an expanded set of states only using the filtered input and filtered output and their derivatives for each vehicle, without the need for designing an observer for each vehicle. Building on the results of this new observer-free output feedback cooperative control architecture, an event-triggering methodology is next proposed for the output feedback cooperative control to schedule the exchanged output measurements information between the agents in order to reduce wireless network utilization. Finally, the output feedback cooperative control architecture is generalized to adaptive control for handling exogenous disturbances in the follower vehicles.

For each methodology, the closed-loop system stability properties are rigorously analyzed, the effect of the user-defined event-triggering thresholds and the controller design parameters on the overall system performance are characterized, and Zeno behavior is shown not to occur with the proposed algorithms.

ACKNOWLEDGMENTS

I would like to thank HCED for giving me the scholarship and all financial support to accomplish my study in the United States of America. I also would like to introduce special thanks to my advisor, Tansel Yucelen, for his tireless effort, guidance, patience, and kindness. He is the person who is responsible for my success and the source of my scientific inspiration. I would like also to deeply thank Dr. Jag for his support and for his valuable suggestions during my work with him. In addition, I thank my other committee members, Dr. Balakrishnan, Dr. Landers, and Dr. Bristow, for their guidance and constructive critiques to enhance my research work.

I would like to thank my labmates who gave me all the help and support during my research time and I enjoyed so much working with them, especially Benjamin Gruenwald and Daniel Peterson. I am deeply indebted for Benjamin for his help during my work with him.

I would like to thank all my friends for their support, especially Ethar Alkamil for supporting me and giving me the positive energy. I also would like to thank my parents, brothers, and sisters for their support and for praying for me. Finally, special thanks and appreciation to my warm nest, my wife, without her my achieved work would be not possible.

TABLE OF CONTENTS

Page

PUBLICATION DISSERTATION OPTION iii

ABSTRACT iv

ACKNOWLEDGMENTS v

LIST OF ILLUSTRATIONS xii

LIST OF TABLES xv

SECTION

1. INTRODUCTION 1
   - 1.1. NETWORKED SYSTEMS AND ADAPTIVE CONTROL 1
   - 1.2. EVENT-TRIGGERED ADAPTIVE STATE FEEDBACK CONTROL 2
   - 1.3. EVENT-TRIGGERED OUTPUT FEEDBACK ADAPTIVE CONTROL 3
   - 1.4. EVENT-TRIGGERED ADAPTIVE ARCHITECTURES FOR DECENTRALIZED AND DISTRIBUTED CONTROL OF LARGE-SCALE MODULAR SYSTEMS 4
   - 1.5. AN OBSERVER-FREE OUTPUT FEEDBACK COOPERATIVE CONTROL ARCHITECTURE FOR MULTIVEHICLE SYSTEMS 7
   - 1.6. AN OBSERVER-FREE OUTPUT FEEDBACK COOPERATIVE CONTROL ARCHITECTURE FOR LINEAR MULTIAGENT SYSTEMS WITH EVENT-TRIGGERING 8
   - 1.7. OBSERVER-FREE OUTPUT FEEDBACK ADAPTIVE CONTROL FOR MULTIVEHICLE SYSTEMS WITH EXOGENOUS DISTURBANCES 9
   - 1.8. ORGANIZATION 11

PAPER

I. DESIGN AND ANALYSIS OF ADAPTIVE CONTROL SYSTEMS OVER WIRELESS NETWORKS 13

ABSTRACT 13

1. INTRODUCTION 14

2. MATHEMATICAL PRELIMINARIES 16

3. EVENT-TRIGGERED STATE FEEDBACK ADAPTIVE CONTROL 20

4. STABILITY AND PERFORMANCE ANALYSIS 22

4.1. Scheduling Data Exchange and Uniform Ultimate Boundedness 23

4.2. Computation of the Ultimate Bound 26

4.3. Computation of the Event-triggered Intersample Time Lower Bound 28

5. ILLUSTRATIVE NUMERICAL EXAMPLE 29

6. CONCLUSION 31

REFERENCES 32

II. OUTPUT FEEDBACK ADAPTIVE CONTROL OF UNCERTAIN DYNAMICAL SYSTEMS WITH EVENT-TRIGGERING 37

ABSTRACT 37

1. INTRODUCTION 38

1.1. Motivation and Literature Review 38

1.2. Contribution 39

1.3. Notation 40

2. OUTPUT FEEDBACK ADAPTIVE CONTROL OVERVIEW 41

3. EVENT-TRIGGERED OUTPUT FEEDBACK ADAPTIVE CONTROL 47

3.1. Proposed Event-triggered Adaptive Control Algorithm 48

3.2. Scheduling Two-way Data Exchange 49

4. STABILITY AND PERFORMANCE ANALYSIS 50

4.1. Uniform Ultimate Boundedness Analysis 51
4.2. Ultimate Bound Computation 57
4.3. Zeno Behavior Analysis 58
5. ILLUSTRATIVE NUMERICAL EXAMPLE 64
6. CONCLUSION 66
REFERENCES 70

III. ON EVENT-TRIGGERED ADAPTIVE ARCHITECTURES FOR DECENTRALIZED AND DISTRIBUTED CONTROL OF LARGE-SCALE MODULAR SYSTEMS 76
ABSTRACT 76
1. INTRODUCTION 77
1.1. Motivation and Literature Review 77
1.2. Contribution 79
1.3. Organization 80
1.4. Notation 80
2. EVENT-TRIGGERED DECENTRALIZED ADAPTIVE CONTROL 81
2.1. Overview of a Standard Decentralized Adaptive Control Architecture Without Event-triggering 81
2.2. Proposed Event-triggered Decentralized Adaptive Control Architecture 84
2.2.1. Stability analysis and uniform ultimate boundedness 86
2.2.2. Computation of the ultimate bound for system performance assessment 91
2.2.3. Computation of the event-triggered inter-sample time lower bound 92
2.2.4. Generalizations to the event-triggered decentralized adaptive control with state emulator 94
3. EVENT-TRIGGERED DISTRIBUTED ADAPTIVE CONTROL 101

3.1. Overview of a Standard Distributed Adaptive Control Architecture Without Event-triggering 101

3.2. Proposed Event-triggered Distributed Adaptive Control Architecture 103

3.2.1. Stability analysis and uniform ultimate boundedness 104

3.2.2. Computation of the ultimate bound for system performance assessment 107

3.2.3. Computation of the event-triggered inter-sample time lower bound 108

3.2.4. Generalizations to the event-triggered distributed adaptive control with state emulator 109

4. ILLUSTRATIVE NUMERICAL EXAMPLE 114

5. CONCLUSIONS 117

REFERENCES 121

IV. AN OBSERVER-FREE OUTPUT FEEDBACK COOPERATIVE CONTROL ARCHITECTURE FOR MULTIVEHICLE SYSTEMS 127

ABSTRACT 127

1. INTRODUCTION 127

2. MATHEMATICAL PRELIMINARIES 129

3. NONMINIMAL STATE SPACE REALIZATION FOR FOLLOWER VEHICLES 132

4. COOPERATIVE CONTROL DESIGN BASED ON NONMINIMAL STATE SPACE REALIZATION 134

4.1. Vehicle-level Control Law 135

4.2. Local Cooperative Control Law 136

5. ANALYSIS 138

6. ILLUSTRATIVE NUMERICAL EXAMPLES 142

7. CONCLUSIONS 145

ACKNOWLEDGMENT 146

REFERENCES 146

V. AN OBSERVER-FREE OUTPUT FEEDBACK COOPERATIVE CONTROL ARCHITECTURE FOR LINEAR MULTIAGENT SYSTEMS WITH EVENT-TRIGGERING 149

ABSTRACT 149

1. INTRODUCTION 149

2. NECESSARY PRELIMINARIES 151

3. AN OVERVIEW OF THE NONMINIMAL STATE SPACE REALIZATION 155

4. COOPERATIVE CONTROL DESIGN BASED ON NONMINIMAL STATE SPACE REALIZATION 157

4.1. Vehicle-level Control Law 158

4.2. Local Cooperative Control Law with Event-triggering 158

5. USER-DEFINED EVENT-TRIGGERING RULES 161

6. SYSTEM-THEORETIC ANALYSIS 162

7. ZENO ANALYSIS 168

8. ILLUSTRATIVE NUMERICAL EXAMPLES 169

9. CONCLUSIONS 171

ACKNOWLEDGMENT 174

REFERENCES 174

VI. OBSERVER-FREE OUTPUT FEEDBACK ADAPTIVE CONTROL FOR MULTIVEHICLE SYSTEMS WITH EXOGENOUS DISTURBANCES 178

ABSTRACT 178

1. INTRODUCTION 179

1.1. Literature Review 179

1.2. Contribution 180

2. NOTATION AND MATHEMATICAL PRELIMINARIES 181

3. NONMINIMAL STATE SPACE REALIZATION: AN OVERVIEW 185

4. $(OF)^2AC$ CONSTRUCTION FOR THE FOLLOWER VEHICLES 188

4.1. Vehicle-level Controller Design 191

4.2. Local Cooperative Control Design 192
4.3. Actual Control Construction 196
5. STABILITY ANALYSIS OF THE (OF)^{2}AC 196
5.1. Constant Disturbance Case 196
5.2. Time-varying Disturbance Case 199
5.3. Low-frequency Learning in Adaptive Control: A Practical Extension 202
6. CONVERGENCE ANALYSIS OF THE (OF)^{2}AC 206
7. ILLUSTRATIVE NUMERICAL EXAMPLES 212
8. CONCLUSION 215
ACKNOWLEDGMENT 216
REFERENCES 216

SECTION

2. CONCLUDING REMARKS AND FUTURE WORK 221
2.1. CONCLUDING REMARKS 221
2.2. FUTURE RESEARCH SUGGESTIONS 223

APPENDICES

A. SYSTEM CONTROLLABILITY AND THE STRUCTURAL MATCHING CONDITION IN PAPER I 225

B. NONMINIMAL STATE SPACE REALIZATION FOR THE FOLLOWER VEHICLE SYSTEMS IN PAPER IV 231

C. INTERSAMPLING TIME ANALYSIS FOR THE EVENT-TRIGGERED OUTPUT OF THE LEADER SYSTEMS IN PAPER V 237

D. COPYRIGHT PERMISSION FOR PAPER II 239

REFERENCES 245

VITA 261

LIST OF ILLUSTRATIONS

Figure Page

PAPER I

1 Event-Triggered Adaptive Control System. 21

2 Effect of a) $\gamma \in [1,100]$ and $L \in [0,10]$ to the ultimate bound (28) for $\epsilon_x = 1$ and $\epsilon_u = 1$, where the arrow indicates the direction γ is increased (dashed line denotes the case with $\gamma = 100$); b) $\epsilon_x \in [0,1.5]$ to the ultimate bound (28) for $\epsilon_u = 1$, $L \in [0,10]$, and $\gamma = 100$, where the arrow indicates the direction ϵ_x is increased (dashed line denotes that case with $\epsilon_x = 1$); c) $\epsilon_u \in [0,3]$ to the ultimate bound (28) for $\epsilon_x = 1$, $L \in [0,10]$, and $\gamma = 100$, where the arrow indicates the direction ϵ_u is increased (dashed line denotes that case with $\epsilon_u = 1$). 27

3 Command following performance for the proposed event-triggered adaptive control approach. 31

4 Event triggers in Figures 3a-3d and comparison with a conventional periodic strategy in terms of state and control transmission. 32

PAPER II

1 Event-triggered adaptive control system. 47

2 Effect of $\Gamma \in [5,100]$ and $v \in [0.01,1]$ to the ultimate bound (58) for $\eta = 5$, $\epsilon_y = 0.1$ and $\epsilon_u = 0.1$, where the arrow indicates the increase in Γ (dashed line denotes the case with $\Gamma = 100$). 59

3 Effect of $\eta \in [5,20]$ to the ultimate bound (58) for $\epsilon_y = 0.1$, $\epsilon_u = 0.1$, $v \in [0.01,1]$, and $\Gamma = 100$, where the arrow indicates the increase in η (dashed line denotes the case with $\eta = 5$). 59

4 Effect of $\epsilon_y \in [0,1]$ to the ultimate bound (58) for $\eta = 5$, $\epsilon_u = 0.1$, $v \in [0.01,1]$, and $\Gamma = 100$, where the arrow indicates the increase in ϵ_y (dashed line denotes the case with $\epsilon_y = 0.1$ and blue bottom line denotes the case with $\epsilon_y = 0$). 60

5 Effect of $\epsilon_u \in [0,1]$ to the ultimate bound (58) for $\eta = 5$, $\epsilon_y = 0.1$, $v \in [0.01,1]$, and $\Gamma = 100$, where the arrow indicates the increase in ϵ_u (dashed line denotes the case with $\epsilon_u = 0.1$). 60

6 Command following performance for the proposed event-triggered output feedback adaptive control approach with $\Gamma = 50I$, $\epsilon_y = 0.3$, and $\epsilon_u = 0.3$. 67

7 Command following performance for the proposed event-triggered output feedback adaptive control approach with $\Gamma = 50I$, $\epsilon_y = 0.3$, and $\epsilon_u = 0.1$. 67

8 Command following performance for the proposed event-triggered output feedback adaptive control approach with $\Gamma = 50I$, $\epsilon_y = 0.3$, and $\epsilon_u = 0.5$. 68

9 Command following performance for the proposed event-triggered output feedback adaptive control approach with $\Gamma = 50I$, $\epsilon_y = 0.1$, and $\epsilon_u = 0.3$. 68

10 Command following performance for the proposed event-triggered output feedback adaptive control approach with $\Gamma = 50I$, $\epsilon_y = 0.5$, and $\epsilon_u = 0.3$. 69

11 Output and control event triggers for the cases in Figures 7–10. 69

PAPER III

1 Event-triggered adaptive control for large-scale modular systems. 87

2 Connected mass-damper-spring system. 115

3 Command following performance for the proposed event-triggered decentralized adaptive control approach with $\gamma_i = 50$ and $L_i = 0$. 117

4 Command following performance for the proposed event-triggered decentralized adaptive control approach with $\gamma_i = 50$ and $L_i = 9$. 118

5 Command following performance for the proposed event-triggered decentralized adaptive control approach with $\gamma_i = 200$ and $L_i = 9$. 118

6 Command following performance for the proposed event-triggered distributed adaptive control approach with $\gamma_i = 50$ and $L_i = 0$. 119

7 Command following performance for the proposed event-triggered distributed adaptive control approach with $\gamma_i = 50$ and $L_i = 9$. 119

8 Command following performance for the proposed event-triggered distributed adaptive control approach with $\gamma_i = 200$ and $L_i = 9$. 120

9 Number of triggers with respect to the controller design parameters. 120

PAPER IV

1 Proposed output feedback control performance for multivehicle system with one leader following a constant command. 144

2 Proposed output feedback control performance for multivehicle system with one leader following a time varying command. 144

3 Proposed output feedback control performance for multivehicle system with two leaders creating a constant convex hull. 145

4 Proposed output feedback control performance for multivehicle system with two leaders creating a time varying convex hull. 145

PAPER V

1 System connection graph. 170

2 Responses of $y_f(t)$, $y_L(t)$, $y_{fs}(t)$, $y_{Ls}(t)$, $u_v(t)$, and $u_c(t)$ for the multiagent system with one leader following a constant command. 171

3 Responses of $y_f(t)$, $y_L(t)$, $y_{fs}(t)$, $y_{Ls}(t)$, $u_v(t)$, and $u_c(t)$ for the multiagent system with one leader following a time varying command. 171

4 Single leader case; a) Output triggers for constant command; b) Triggers comparison for constant command; c) Output triggers for time varying command; d) Triggers comparison for time varying command. 172

5 Responses of $y_f(t)$, $y_L(t)$, $y_{fs}(t)$, $y_{Ls}(t)$, $u_v(t)$, and $u_c(t)$ for the multiagent system with two leaders creating a constant convex hull. 172

6 Responses of $y_f(t)$, $y_L(t)$, $y_{fs}(t)$, $y_{Ls}(t)$, $u_v(t)$, and $u_c(t)$ for the multiagent system with two leaders creating a time varying convex hull. 173

7 Two leaders case; a) Output triggers for constant commands; b) Triggers comparison for constant commands; c) Output triggers for time varying commands; d) Triggers comparison for time varying commands. 173

PAPER VI

1 Responses of $y(t)$, $y_L(t)$, and $u(t)$ for the multivehicle system for Example 1.... 214

2 Responses of $y(t)$, $y_L(t)$, and $u(t)$ for the multivehicle system with input disturbance for Example 1..... 214

3 Responses of $y(t)$, $y_L(t)$, and $u(t)$ for multivehicle system with proposed adaptive output feedback control architecture in presence of input disturbance for Example 1..... 215

4 Responses of $y(t)$, $y_L(t)$, and $u(t)$ for the multivehicle system with low-frequency version of the proposed adaptive output feedback control architecture in presence of input disturbance for Example 1. 215

5 Responses of $y(t)$, $y_L(t)$, and $u(t)$ for the multivehicle system with low-frequency version of the proposed adaptive output feedback control architecture in presence of input disturbance for Example 2. 216

LIST OF TABLES

Table Page

1 Event-triggered output feedback adaptive control algorithm. 49

SECTION

1. INTRODUCTION

1.1. NETWORKED SYSTEMS AND ADAPTIVE CONTROL

The last decade has witnessed an increased interest in physical systems controlled over wireless networks (networked control systems) for their advantages in reducing cost for the design and implementation of control systems [1, 2, 3, 4, 5]. These systems allow the computation of control signals via processors that are not attached to the physical systems and the feedback loops are closed over wireless networks. A critical task in the design and implementation of networked control systems is to guarantee system stability while reducing wireless network utilization and achieving a given system performance in the presence of system uncertainties.

One of the fundamental problems in feedback control design is the capability of the control system to guarantee system stability and performance in the presence of system uncertainties resulting from mathematical modeling and degraded modes of operations. To this end, adaptive control theory along with robust control theory have been developed to address the problem of system uncertainties in control system design [6, 7, 8, 9, 10]. Specifically, robust control methods require the knowledge of characterized bounds resulting from system uncertainty parameterizations. From a practical standpoint, determination of these bounds is not necessarily easy since they can require excessive modeling and ground testing efforts [11, 12]. In addition, adaptive control methods require less modeling information than do robust control methods and are able to deal with high levels of system uncertainties [8, 9, 10]. These facts make adaptive control theory an appealing candidate for many applications.

1.2. EVENT-TRIGGERED ADAPTIVE STATE FEEDBACK CONTROL

In the networked control systems literature, notable contributions that utilize adaptive control approaches to suppress the effect of system uncertainties include [13, 14, 15, 16]. In particular, the authors of [13, 14] develop adaptive control approaches to deal with system uncertainties, where their results only consider data transmission from a physical system to the controller, but not vice versa. The authors of [15, 16] consider the case where data transmits from a physical system to the controller and from the controller to this physical system (i.e., two-way data exchange is allowed over a wireless network). Although this approach is promising, their methodology requires the knowledge of a conservative upper bound on the unknown constant gain resulting from their uncertainty parameterization. While this conservative upper bound may be available for some applications, the actual upper bound may change and exceed its conservative estimate; for example, when an aircraft undergoes a sudden change in dynamics as a result of reconfiguration, deployment of a payload, docking, or structural damage [17].

In this dissertation, we first study the design and analysis of adaptive control systems over wireless networks using event-triggering control theory (see, for example, [18, 19, 20, 21, 22, 23, 24, 25] and references therein), where two-way data exchange between the physical system and the proposed adaptive controller is considered. The proposed event-triggered adaptive control methodology schedules the data exchange dependent upon errors exceeding user-defined thresholds to reduce wireless network utilization and guarantees system stability and command following performance in the presence of system uncertainties. Specifically, we consider a state emulator-based adaptive control methodology [26, 27, 28, 29, 30, 31, 32, 33] since this framework has the capability to achieve stringent performance specifications without causing high-frequency oscillations in the controller response [32, 33] unlike standard adaptive controllers.

First contribution of the dissertation, in particular, we analyze stability and boundedness of the overall closed-loop dynamical system, characterize the effect of user-defined thresholds and adaptive controller design parameters to the system performance, and discuss conditions to make the resulting command following performance error sufficiently small. As a byproduct, we also show that the resulting closed-loop dynamical system performance is more sensitive to the changes in the data transmission threshold from the physical system to the adaptive controller (sensing threshold) than the data transmission threshold from the adaptive controller to the physical system (actuation threshold). This means that the actuation threshold can be chosen large enough to reduce wireless network utilization between the physical system and the adaptive controller without sacrificing closed-loop dynamical system performance.

1.3. EVENT-TRIGGERED OUTPUT FEEDBACK ADAPTIVE CONTROL

As discussed in the previous section, the first contribution of this dissertation is a new event-triggered state-feedback adaptive control architecture. Although the assumption of full state feedback leads to computationally simpler control algorithms, in certain applications of control systems the entire state vector is not available. Therefore, output feedback is required for these applications the ones that involve high-dimensional models such as active noise suppression, active control of flexible structures, fluid flow control systems, and combustion control processes [34, 35, 36, 37, 38, 39, 40, 41].

Since a critical task in the design and implementation of networked control systems is to reduce wireless network utilization while guaranteeing system stability in the presence of system uncertainties, an event-triggered adaptive control architecture is presented in an output feedback setting to schedule two-way data exchange dependent upon errors exceeding user-defined thresholds. Specifically, we consider the output feedback adaptive control architecture predicated on the asymptotic properties of LQG/LTR controllers [39, 33, 40, 41], since this framework has the capability to achieve stringent per-

formance specifications without causing high-frequency oscillations in the controller response, asymptotically satisfies a strictly positive real condition for the closed-loop dynamical system, and is less complex than other approaches to output feedback adaptive control (see, for example, [35, 36, 37]). While this part of dissertation considers a particular yet effective output feedback adaptive control formulation to present its main contributions, the proposed approach can be used in a complimentary way with many other approaches to output feedback adaptive control (see, for example, [42, 43, 44, 45]).

1.4. EVENT-TRIGGERED ADAPTIVE ARCHITECTURES FOR DECENTRALIZED AND DISTRIBUTED CONTROL OF LARGE-SCALE MODULAR SYSTEMS

The design and implementation of decentralized and distributed architectures for controlling complex, large-scale systems is a nontrivial control engineering task involving the consideration of components interacting with the physical processes to be controlled. In particular, large-scale systems are characterized by a large number of highly coupled components exchanging matter, energy or information and have become ubiquitous given the recent advances in embedded sensor and computation technologies. Examples of such systems include, but are not limited to, multivehicle systems, communication systems, power systems, process control systems and water systems (see, for example, [46, 47, 48, 49, 50, 51] and the references therein). This part of dissertation concentrates on an important class of large-scale systems; namely, large-scale modular systems that consist of physically-interconnected and generally heterogeneous modules.

Two sweeping generalizations can be made about large-scale modular systems. The first is that their complex structure and large-scale nature yield to inaccurate mathematical module models, since it is a challenge to precisely model each module of a large-scale system and the interconnections between these modules. As a consequence, the discrepancies between the modules and their mathematical models, that is system uncertainties, result in

the degradation of overall system stability and the performance of the large-scale modular systems. To this end, adaptive control methodologies [8, 11, 10, 52, 9, 53, 31] offer an important capability for this class of dynamical systems to learn and suppress the effect of system uncertainties resulting from modeling and degraded modes of operation, and hence, they offer system stability and desirable closed-loop system performance in the presence of system uncertainties without excessively relying on mathematical models.

The second generalization about large-scale modular systems is that these systems are often controlled over wireless networks, and hence, the communication costs between the modules and their remote processors increase proportionally with the increase in the number of modules and often the interconnection between these modules. To this end, event-triggered control methodologies [54, 18, 55] offer new control execution paradigms that relax the fixed periodic demand of computational resources and allow for the aperiodic exchange of sensor and actuator information with the remote processor to reduce overall communication cost over a wireless network. Note that adaptive control methodologies and event-triggered control methodologies are often studied separately in the literature, where it is of practical importance to theoretically integrate these two approaches to guarantee system stability and the desirable closed-loop system performance of uncertain large-scale modular systems with reduced communication costs over wireless networks, which is the main focus of this part of dissertation.

More specifically, the authors of [56, 57, 58, 59, 60, 61, 17, 51] proposed decentralized and distributed adaptive control architectures for large-scale systems; however, these approaches do not make any attempts to reduce the overall communication cost over wireless networks using, for example, event-triggered control methodologies. In addition, the authors of [62, 63, 64, 65, 66, 67, 68] present decentralized and distributed control architectures with event triggering; however, these approaches do not consider adaptive control architectures and assume perfect models of the processes to be controlled; hence, they are not practical for large-scale modular systems with significant system uncertain-

ties. Only the authors of [13, 14, 15, 69, 70, 71] present event-triggered adaptive control approaches for uncertain dynamical systems. In particular, the authors of [13, 14] consider data transmission from a physical system to the controller, but not vice versa, while developing their adaptive control approaches to deal with system uncertainties. On the other hand, the adaptive control architectures of the authors in [15, 69, 70, 71] consider two-way data transmission over wireless networks; that is, from a physical system to the controller and from the controller to this physical system. However, none of these approaches can be directly applied to large-scale modular systems. This is due to the fact that large-scale modular systems require decentralized and distributed architectures, and direct application of the results in [13, 14, 15, 69, 70, 71] to this class of systems can result in centralized architectures, which is not practically desired due to the large-scale nature of modular systems. To summarize, there do not exist resilient adaptive control architectures for large-scale systems in the literature to deal with system uncertainties while reducing the communication costs between the models and their remote processors.

Building of our other contributions highlighted above, the third contribution of this dissertation is to design and analyze event-triggered decentralized and distributed adaptive control architectures for uncertain large-scale systems controlled over wireless networks. Specifically, the proposed decentralized and distributed adaptive architectures of this dissertation guarantee overall system stability while reducing wireless network utilization and achieving a given system performance in the presence of system uncertainties that can result from modeling and degraded modes of operation of the modules and their interconnections between each other. From a theoretical viewpoint, the proposed event-triggered adaptive architectures here can be viewed as a significant generalization of our prior work documented in [70, 71] to large-scale modular systems, which consider a state emulator-based adaptive control methodology with robustness against high-frequency oscillations in the controller response [52, 26, 27, 28, 29, 30, 31, 32]. In this generalization, we also adopt necessary tools and methods from [17, 51] on decentralized and distributed adaptive con-

troller construction for large-scale modular systems. In addition to the theoretical findings including rigorous system stability and boundedness analysis of the closed-loop dynamical system and the characterization of the effect of user-defined event-triggering thresholds, as well as the design parameters of the proposed adaptive architectures on the overall system performance, an illustrative numerical example is further provided to demonstrate the efficacy of the proposed decentralized and distributed control approaches.

1.5. AN OBSERVER-FREE OUTPUT FEEDBACK COOPERATIVE CONTROL ARCHITECTURE FOR MULTIVEHICLE SYSTEMS

Owing to the ever-increasing advances in embedded systems technologies, we are rapidly moving toward a future in which squadrons of vehicles (henceforth, referred as multivehicle systems) will autonomously perform a broad spectrum of tasks in both military and civilian domains. Examples of such tasks include but are not limited to collaborative exploration; search and rescue; nuclear, biological, and chemical attack detection; and target tracking. Motivated from this standpoint, cooperative control enabling multivehicle systems to work in coherence through local information exchange between vehicles has been the focus of high research activity during the last two decades (e.g., see books [46, 47, 72, 73] for a thorough coverage of the recent progress).

In this part of dissertation, we focus on the output feedback cooperative control problem in the context of a containment problem (i.e., outputs of the follower vehicles convergence to the convex hull spanned by those of the leader vehicles). While full state feedback designs lead to computationally simpler cooperative control laws, output feedback designs are required for most applications that involve high-dimensional vehicle models with inaccessible states. To this end, several output feedback cooperative control approaches are proposed in the literature for multivehicle systems (e.g., see [74, 75, 76, 77, 78, 79, 80, 81] and references therein), where the common denominator of these approaches is that they utilize an observer in their cooperative control laws.

Unlike the existing literature, the fourth contribution is a new, observer-free output feedback cooperative control architecture for continuous-time, minimum phase, and high-order multivehicle systems. The proposed architecture is predicated on a nonminimal state-space realization originally proposed in [82, 38] that generates an expanded set of states only using the filtered input and filtered output and their derivatives for each follower vehicle, without the need for designing an observer for each vehicle. Specifically, the proposed observer-free output feedback control law consists of a vehicle-level controller and a local cooperative controller for each vehicle as in [49], where the former addresses internal stability of vehicles and the latter addresses the containment problem.

1.6. AN OBSERVER-FREE OUTPUT FEEDBACK COOPERATIVE CONTROL ARCHITECTURE FOR LINEAR MULTIAGENT SYSTEMS WITH EVENT-TRIGGERING

Building on the theoretical study of the previous section, in this part of dissertation, we propose an event-triggering methodology for the output feedback cooperative control to schedule the exchanged output measurements information between the agents in order to reduce wireless network utilization. The utilized output feedback cooperative control architecture is in the context of a containment problem (i.e., outputs of the follower agents convergence to the convex hull spanned by those of the leader agents). While full state feedback designs lead to computationally simpler cooperative control laws [83, 84], output feedback designs are required for most applications that involve high-dimensional agent models with inaccessible states, as also outlined before. To this end, several output feedback cooperative control with event triggering approaches are proposed in the literature for multiagent systems (e.g., see [85, 86] and references therein), where the common denominator of these approaches is that they utilize an observer in their cooperative control laws.

Unlike the aforementioned existing literature, our fifth contribution is an event-triggering mechanism on the exchanged output measurements between agents that are controlled by an observer-free output feedback cooperative control architecture for continuous-time, minimum phase, and high-order linear multiagent systems, where the results reported here can be viewed as a generalization of our recent papers in [87, 88] that do not consider event-triggering. The key feature of our adopted controller scheme is that it is predicated on a nonminimal state-space realization originally proposed in [82, 38] that generates an expanded set of states only using the filtered input and filtered output and their derivatives for each follower agent, without the need for designing an observer for each agent. In addition, the proposed event-triggering methodology is applied on the relative output measurements of the agents, where each agent has its own event-triggering threshold to transmit its own output measurements to the neighbor agents asynchronously. Note that our cooperative controller scheme operates in a periodic sampling instances and it uses event-triggered output measurements transmitted from the neighboring agents.

1.7. OBSERVER-FREE OUTPUT FEEDBACK ADAPTIVE CONTROL FOR MULTIVEHICLE SYSTEMS WITH EXOGENOUS DISTURBANCES

In general, vehicle system models are represented by the first principles of physics and derived using fundamental physical laws. Due to the system complexity, nonlinearity, and uncertainty, the simplistic approximations create inaccuracies between the model and the the actual system as discussed. As a result of this modeling error, it is very important for the cooperative control design to not only achieve system level objectives, but also possess the ability to maintain the stability of each vehicle in the presence of system uncertainties. The most notable results that address cooperative control of uncertain vehicle systems include [89, 90, 91, 92, 93, 94, 95, 96, 97, 98, 49]. Specifically, the authors in [89, 90, 91, 92, 93], consider the uncertain multivehicle systems problem as first and/or

second order models which are suitable for a limited number of applications. For more applicable system dynamics, [94, 95, 96, 97, 98, 49] use high-order vehicle models with system uncertainties.

In particular, the authors in [94] consider linear single input and single output vehicle systems with parametric uncertainties that range over an known compact set. The work in [95] uses an internal model based distributed control scheme that makes the vehicle controllers robust to small variation in their models. A finite-time disturbance observer is proposed in [96] to estimate the system uncertainties. A distributed adaptive control for both the uncertain follower and uncertain leaders is considered in [97], where the distributed adaptive control law is designed based on local consensus error feedback. The authors of [98] design a decentralized adaptive tracking controller under the assumption that the uncertain follower vehicles with Lipschitz-type disturbances are guided by a leader with unknown input. The authors in [49] introduce cooperative control for higher-order multivehicle systems having nonidentical nonlinear uncertain dynamics and large parametric uncertainties with no a prior information on their bound. While the above results are promising, full state feedback is necessary for each proposed controller which requires knowledge of the vehicle system state variables and this is not applicable when the multivehicle system state variables are unknown. Therefore, output feedback is necessary for most applications that involve high-dimensional models with unknown system state variables, such as multiple unmanned aerial vehicles, multiple mobile robots, and multiple manipulators.

To address this problem, [99, 100, 101, 102] propose adaptive output feedback controllers for uncertain dynamical multivehicle systems. In particular, in [99, 100] the adaptive output feedback controller is design for consensus protocols, where the gains rely on the global information of the network which is represented by the Laplacian matrix. The authors of [101] adopt two observer designs, a local observer and an adaptive estimator, for the distributed adaptive output-feedback consensus tracking control for unknown agent

dynamics without depending on the Laplacian matrix information. Among the above mentioned works, the common feature is that the adaptive output feedback controller requires an observer for estimating the unknown state variables. In a recent result [87], we employ an output feedback control architecture for dynamical multivehicle systems without observers (outside the context of adaptive control). Specifically, the observer-free nature of our work is an expansion of the original observer-free output feedback adaptive control idea proposed in [103, 104, 38, 17]. In this part of dissertation, a new observer-free output feedback adaptive control, $(OF)^2AC$, method is proposed for continuous-time, minimum phase, and high-order linear multivehicle systems subject to exogenous disturbances (hereinafter referred to as "uncertain multivehicle systems"), where the results reported here can be viewed as an expansion of our recent paper in [87]. In particular, similar to the observer-free methods studied in [103, 104, 38, 17, 87], the $(OF)^2AC$ is based on a nonminimal state-space realization for each follower vehicle of the multivehicle system, where this realization generates an expanded set of states using the filtered input, filtered output, and their derivatives of the follower vehicles. The $(OF)^2AC$ consists of *i)* a local cooperative controller in [49] and *ii)* a vehicle-level controller for each follower vehicle Specifically, part *i)* of the proposed control method addresses the leader-follower containment control problem by receiving the relative output measurements of the neighboring vehicles and its part *ii)* consists of an augmenting adaptive controller for stabilization and command following in the presence of exogenous disturbances.

1.8. ORGANIZATION

The organization of this dissertation report is as follows. Paper I presents the proposed event-triggered state feedback adaptive control architecture. The results of this paper are generalized in Paper II to the output feedback case. Paper III presents the event-triggered decentralized and distributed adaptive control architectures for uncertain network large scale modular systems. An observer-free output feedback cooperative control archi-

tecture for multivehicle systems is presented in Paper IV. On the results of this paper, an event-triggering architecture is applied in Paper V. Then, Paper VI presents the generalization of Paper IV to adaptive control to handle the system uncertainties. Finally, conclusions and future research suggestions are presented in Section 2.

PAPER

I. DESIGN AND ANALYSIS OF ADAPTIVE CONTROL SYSTEMS OVER WIRELESS NETWORKS

Ali Albattat[1], Benjamin Gruenwald[2], and Tansel Yucelen[2]

[1] Department of Mechanical & Aerospace Engineering

Missouri University of Science and Technology

[2] Department of Mechanical Engineering

University of South Florida

ABSTRACT

In this paper, we study the design and analysis of adaptive control systems over wireless networks using event-triggering control theory. The proposed event-triggered adaptive control methodology schedules the data exchange dependent upon errors exceeding user-defined thresholds to reduce wireless network utilization and guarantees system stability and command following performance in the presence of system uncertainties. Specifically, we analyze stability and boundedness of the overall closed-loop dynamical system, characterize the effect of user-defined thresholds and adaptive controller design parameters to the system performance, and discuss conditions to make the resulting command following performance error sufficiently small. An illustrative numerical example is provided to demonstrate the efficacy of the proposed approach.

Keywords: Networked control systems; adaptive control; event-triggering control; system uncertainties; system stability; system performance

1. INTRODUCTION

The last decade has witnessed an increased interest in physical systems controlled over wireless networks (networked control systems) for their advantages in reducing cost for the design and implementation of control systems [1, 2, 3, 4, 5]. These systems allow the computation of control signals via processors that are not attached to the physical systems and the feedback loops are closed over wireless networks. A critical task in the design and implementation of networked control systems is to guarantee system stability while reducing wireless network utilization and achieving a given system performance in the presence of system uncertainties.

One of the fundamental problems in feedback control design is the capability of the control system to guarantee system stability and performance in the presence of system uncertainties resulting from mathematical modeling and degraded modes of operations. To this end, adaptive control theory along with robust control theory have been developed to address the problem of system uncertainties in control system design [6, 7, 8, 9, 10]. Specifically, robust control methods require the knowledge of characterized bounds resulting from system uncertainty parameterizations. From a practical standpoint, determination of these bounds is not necessarily easy since they can require excessive modeling and ground testing efforts [11, 12]. In addition, adaptive control methods require less modeling information than do robust control methods and are able to deal with high levels of system uncertainties [8, 9, 10]. These facts make adaptive control theory an appealing candidate for many applications.

In the networked control systems literature, notable contributions that utilize adaptive control approaches to suppress the effect of system uncertainties include [13, 14, 15, 16]. In particular, the authors of [13, 14] develop adaptive control approaches to deal with system uncertainties, where their results only consider data transmission from a physical system to the controller, but not vice versa. The authors of [15, 16] consider the case where data transmits from a physical system to the controller and from the controller to this phys-

ical system (i.e., two-way data exchange is allowed over a wireless network). Although this approach is promising, their methodology requires the knowledge of a conservative upper bound on the unknown constant gain resulting from their uncertainty parameterization. While this conservative upper bound may be available for some applications, the actual upper bound may change and exceed its conservative estimate; for example, when an aircraft undergoes a sudden change in dynamics as a result of reconfiguration, deployment of a payload, docking, or structural damage [17].

In this paper, we study the design and analysis of adaptive control systems over wireless networks using event-triggering control theory (see, for example, [18, 19, 20, 21, 22, 23, 24, 25] and references therein), where two-way data exchange between the physical system and the proposed adaptive controller is considered. The proposed event-triggered adaptive control methodology schedules the data exchange dependent upon errors exceeding user-defined thresholds to reduce wireless network utilization and guarantees system stability and command following performance in the presence of system uncertainties. Specifically, we consider a state emulator-based adaptive control methodology[26, 27, 28, 29, 30, 31, 32, 33] since this framework has the capability to achieve stringent performance specifications without causing high-frequency oscillations in the controller response [32, 33] unlike standard adaptive controllers. We analyze stability and boundedness of the overall closed-loop dynamical system, characterize the effect of user-defined thresholds and adaptive controller design parameters to the system performance, and discuss conditions to make the resulting command following performance error sufficiently small. As a byproduct, we show that the resulting closed-loop dynamical system performance is more sensitive to the changes in the data transmission threshold from the physical system to the adaptive controller (sensing threshold) than the data transmission threshold from the adaptive controller to the physical system (actuation threshold). This means that the actua-

tion threshold can be chosen large enough to reduce wireless network utilization between the physical system and the adaptive controller without sacrificing closed-loop dynamical system performance.

2. MATHEMATICAL PRELIMINARIES

Throughout this paper, we use $\mathbb{R}$ for the set of real numbers, $\mathbb{R}^n$ for the set of $n \times 1$ real column vectors, $\mathbb{R}^{n\times m}$ for the set of $n \times m$ real matrices, $\mathbb{R}_+$ for the set of positive real numbers, $\mathbb{R}_+^{n\times n}$ for the set of $n \times n$ positive-definite real matrices, $\mathbb{S}^{n\times n}$ for the set of $n \times n$ symmetric real matrices, $\mathbb{D}^{n\times n}$ for the set of $n\times n$ real matrices with diagonal scalar entries, $\lambda_{\min}(A)$ (resp., $\lambda_{\max}(A)$) for the minimum (resp., maximum) eigenvalue of the Hermitian matrix A, $\|\cdot\|$ for the Euclidean norm, $\|\cdot\|_{\mathrm{F}}$ for the Frobenius matrix norm, "$\vee$" for the "or" logic operator, and "$\overline{(\cdot)}$" for the "not" logic operator. We also define the projection operator needed for the results of this paper.

Definition 1. Let $\phi : \mathbb{R}^n \to \mathbb{R}$ be a continuously differentiable convex function given by $\phi(\theta) \triangleq ((\epsilon_\theta + 1)\,\theta^T\theta - \theta_{\max}^2)/(\epsilon_\theta\theta_{\max}^2)$, where $\theta_{\max} \in \mathbb{R}$ is a projection norm bound imposed on $\theta \in \mathbb{R}^n$ and $\epsilon > 0$ is a projection tolerance bound. Then, for $y \in \mathbb{R}^n$, the projection operator $\mathrm{Proj} : \mathbb{R}^n \times \mathbb{R}^n \to \mathbb{R}^n$ is defined by

$$\mathrm{Proj}(\theta, y) \triangleq \begin{cases} y, & \text{if } \phi(\theta) < 0, \\ y, & \text{if } \phi(\theta) \geq 0 \text{ and } \phi'(\theta)y \leq 0, \\ y - \dfrac{\phi'^{\mathrm{T}}(\theta)\phi'(\theta)y}{\phi'(\theta)\phi'^{\mathrm{T}}(\theta)}\phi(\theta), & \text{if } \phi(\theta) \geq 0 \text{ and } \phi'(\theta)y > 0. \end{cases} \tag{1}$$

It follows from Definition 1 that $(\theta - \theta^*)^{\mathrm{T}}(\mathrm{Proj}(\theta, y) - y) \leq 0$, $\theta^* \in \mathbb{R}^n$ holds [34]. The definition of the projection operator can be generalized to matrices as $\mathrm{Proj}_{\mathrm{m}}(\Theta, Y) = (\mathrm{Proj}(\mathrm{col}_1(\Theta), \mathrm{col}_1(Y)), \ldots, \mathrm{Proj}(\mathrm{col}_m(\Theta), \mathrm{col}_m(Y)))$, where $\Theta \in \mathbb{R}^{n\times m}$, $Y \in \mathbb{R}^{n\times m}$, and $\mathrm{col}_i(\cdot)$ denotes the ith column operator. In this case, $\mathrm{tr}\left[(\Theta - \Theta^*)^{\mathrm{T}}(\mathrm{Proj}_{\mathrm{m}}(\Theta, Y) - Y)\right] = \sum_{i=1}^m \left[\mathrm{col}_i(\Theta - \Theta^*)^{\mathrm{T}}(\mathrm{Proj}(\mathrm{col}_i(\Theta), \mathrm{col}_i(Y)) - \mathrm{col}_i(Y))\right] \leq 0$ holds, where $\Theta^* \in \mathbb{R}^{n\times m}$.

We now overview necessary preliminaries on standard model reference adaptive control problem needed for the results of this paper. Consider the uncertain dynamical system given by

$$\dot{x}(t) = Ax(t) + Bu(t), \quad x(0) = x_0, \tag{2}$$

where $x(t) \in \mathbb{R}^n$ is the state vector available for feedback, $u(t) \in \mathbb{R}^m$ is the control input, and $A \in \mathbb{R}^{n\times n}$ and $B \in \mathbb{R}^{n\times m}$ are unknown system and control input matrices, respectively, such that the pair (A, B) is controllable.

Assumption 1. Unknown control input matrix is parameterized as $B = D\Lambda$, where $D \in \mathbb{R}^{n\times m}$ is a known input matrix and $\Lambda \in \mathbb{R}_+^{m\times m} \cap \mathbb{D}^{m\times m}$ is an unknown control effectiveness matrix.

Next, consider the reference system capturing a desired, ideal closed-loop dynamical system performance given by

$$\dot{x}_{\mathrm{ri}}(t) = A_{\mathrm{r}}x_{\mathrm{ri}}(t) + B_{\mathrm{r}}c(t), \quad x_{\mathrm{ri}}(0) = x_{\mathrm{ri}0}, \tag{3}$$

where $x_{\mathrm{ri}}(t) \in \mathbb{R}^n$ is the ideal reference state vector, $c(t) \in \mathbb{R}^m$ is a given uniformly continuous bounded command with a bounded derivative, $A_{\mathrm{r}} \in \mathbb{R}^{n\times n}$ is the Hurwitz reference system matrix, and $B_{\mathrm{r}} \in \mathbb{R}^{n\times m}$ is the command input matrix.

Assumption 2. There exist gain matrices $K_1 \in \mathbb{R}^{m\times n}$ and $K_2 \in \mathbb{R}^{m\times m}$ such that $A_{\mathrm{r}} = A + DK_1$ and $B_{\mathrm{r}} = DK_2$ hold.

Note that Assumptions 1 and 2 are standard in the model reference adaptive control literature (see, for example, [9, 8, 33]). Using Assumptions 1 and 2, (2) can be equivalently written by

$$\dot{x}(t) = A_{\mathrm{r}}x(t) + B_{\mathrm{r}}c(t) + D\Lambda[u(t) + W_1^{\mathrm{T}}x(t) + W_2^{\mathrm{T}}c(t)], \tag{4}$$

where $W_1 \triangleq -K_1^{\mathrm{T}}\Lambda^{-1} \in \mathbb{R}^{n\times m}$ and $W_2 \triangleq -K_2^{\mathrm{T}}\Lambda^{-1} \in \mathbb{R}^{m\times m}$ are unknown matrices. Based on the structure of the uncertain terms in (4), let the adaptive feedback control law be given by

$$u(t) = -\hat{W}^{\mathrm{T}}(t)\sigma\left(x(t), c(t)\right), \tag{5}$$

where $\sigma(x(t), c(t)) = \left[x^{\mathrm{T}}(t), c^{\mathrm{T}}(t)\right]^{\mathrm{T}} \in \mathbb{R}^{n+m}$ and $\hat{W}(t) \in \mathbb{R}^{(n+m)\times m}$ is the estimate of $W \triangleq [W_1^{\mathrm{T}}, W_2^{\mathrm{T}}]^{\mathrm{T}} \in \mathbb{R}^{(n+m)\times m}$ satisfying the weight update law

$$\dot{\hat{W}}(t) = \gamma\sigma\left(x(t), c(t)\right) e_{\mathrm{o}}^{\mathrm{T}}(t)PD, \quad \hat{W}(0) = \hat{W}_0. \tag{6}$$

In (6), $\gamma \in \mathbb{R}_+$ is the learning rate, $e_o(t) \triangleq x(t) - x_{\mathrm{ri}}(t) \in \mathbb{R}^n$ is the ideal system error, and $P \in \mathbb{R}_+^{n\times n} \cap \mathbb{S}^{n\times n}$ is a unique solution [35] of the Lyapunov equation

$$0 = A_{\mathrm{r}}^{\mathrm{T}}P + PA_{\mathrm{r}} + R, \quad R \in \mathbb{R}_+^{n\times n} \cap \mathbb{S}^{n\times n}. \tag{7}$$

Next, using (5), (4) can be rewritten as

$$\dot{x}(t) = A_{\mathrm{r}}x(t) + B_{\mathrm{r}}c(t) - D\Lambda\tilde{W}^{\mathrm{T}}(t)\sigma\left(x(t), c(t)\right), \tag{8}$$

where the ideal system error dynamics can be given using (3) and (8) as

$$\dot{e}_{\mathrm{o}}(t) = A_{\mathrm{r}}e_{\mathrm{o}}(t) - D\Lambda\tilde{W}^{\mathrm{T}}(t)\sigma\left(x(t), c(t)\right), \quad e_{\mathrm{o}}(0) = e_{\mathrm{o}0}, \tag{9}$$

where $\tilde{W}(t) \triangleq \hat{W}(t) - W \in \mathbb{R}^{(n+m)\times m}$. Note from [9, 8, 33] that $e_o(t)$ satisfying (9) asymptotically goes to zero with the standard model reference adaptive controller given by (5) and (6).

Finally, we overview the state emulator-based adaptive control framework [26, 27, 28, 29, 30, 31, 32, 33] considered for the results of this paper. Consider the (modified) reference system so-called the state emulator given by

$$\dot{x}_{\mathrm{r}}(t) = A_{\mathrm{r}}x_{\mathrm{r}}(t) + B_{\mathrm{r}}c(t) + L\left(x(t) - x_{\mathrm{r}}(t)\right), \quad x_{\mathrm{r}}(0) = x_{\mathrm{r}0}, \tag{10}$$

where $L \in \mathbb{R}^{n\times n} \cap \mathbb{S}^{n\times n}$ is the state emulator gain. Letting $\tilde{x}(t) \triangleq x_{\mathrm{r}}(t) - x_{\mathrm{ri}}(t) \in \mathbb{R}^n$, the reference system error dynamics capturing the difference between the ideal reference model (3) and the state emulator-based (modified) reference model (10) is given by

$$\dot{\tilde{x}}(t) = A_{\mathrm{r}}\tilde{x}(t) + L(x(t) - x_{\mathrm{r}}(t)), \quad \tilde{x}(0) = \tilde{x}_0. \tag{11}$$

In addition, letting $e(t) \triangleq x(t) - x_{\mathrm{r}}(t) \in \mathbb{R}^n$ to denote the system state error vector, the (state emulator-based) system error dynamics is given by

$$\dot{e}(t) = \tilde{A}e(t) - D\Lambda\tilde{W}^{\mathrm{T}}(t)\sigma\left(x(t), c(t)\right), \quad e(0) = e_0, \tag{12}$$

using (8) and (10), where $\tilde{A} \triangleq A_{\mathrm{r}} - L \in \mathbb{R}^{n\times n}$ is Hurwitz by a suitable selection of the state emulator gain L (e.g., $\tilde{A}$ is Hurwitz with $L = \kappa I$, $\kappa \in \mathbb{R}^+$, since A_{r} is Hurwitz). It can be shown that $\tilde{x}(t)$ satisfying (11) and $e(t)$ satisfying (12) asymptotically go to zero with the adaptive controller given by (5), (6), and (7) with $e_o(t)$ replaced with $e(t)$ in (6) and A_{r} replaced with $\tilde{A}$ in (7) [33].

Note from [32, 33] that the state emulator-based adaptive control framework achieves stringent transient and steady-state system performance specifications by judiciously choosing the learning rate γ and the state emulator gain L without causing high-frequency oscillations in the controller response unlike standard model reference adaptive controllers overviewed earlier in this section. We also note that if one selects $L = 0$, then the results of

this paper holds for standard model reference adaptive controllers, and hence, there is no loss in generality in using a state emulator-based adaptive control framework for the results of this paper.

3. EVENT-TRIGGERED STATE FEEDBACK ADAPTIVE CONTROL

In this section, we present a state emulator-based adaptive control approach, which reduces wireless network utilization and allows a desirable command tracking performance during the two-way data exchange between the physical system (uncertain dynamical system) and this controller over a wireless network. For this purpose, we utilize event-triggering control theory to schedule the data exchange dependent upon errors exceeding user-defined thresholds. In particular, when a predefined event occurs, the uncertain dynamical system sends its state signal to the adaptive controller. The kth time instants of the state transmission is represented by the monotonic sequence $\{s_k\}_{k=1}^{\infty}$, where $s_k \in \mathbb{R}_+$. The controller uses this triggered system state signal to compute the control signal using state emulator-based adaptive control architecture. When another predefined event occurs, the updated feedback control input is transmitted to the uncertain dynamical system. The jth time instants of the feedback control transmission is then represented by the monotonic sequence $\left\{r_j\right\}_{j=1}^{\infty}$, where $r_j \in \mathbb{R}_+$. As shown in Figure 1, each system state signal and control input is held by a zero-order-hold operator (ZOH) until the next triggering event for that signal takes place.

Considering the two-way data exchange depicted in Figure 1, the controller generates a control signal $u(t)$ and the uncertain dynamical system is driven by the sampled version of this control signal $u_{\mathrm{s}}(t)$ depending on the event-triggering mechanism to be discussed later. Likewise, the controller utilizes $x_{\mathrm{s}}(t)$ that represents the sampled version of the uncertain dynamical system state $x(t)$. Mathematically speaking, consider the uncertain dynamical system given by

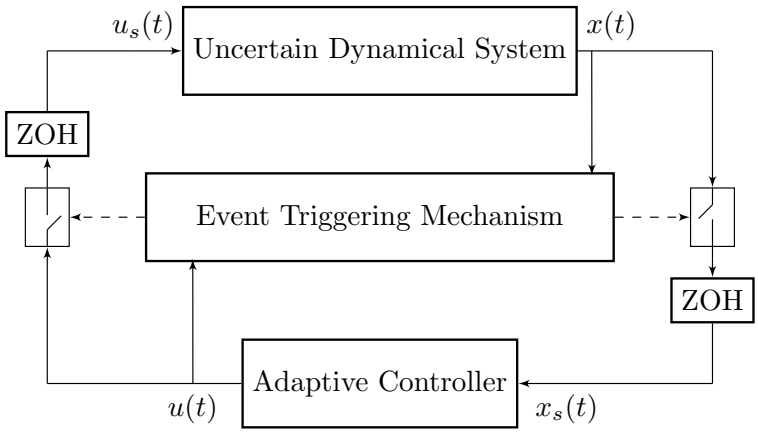

Figure 1. Event-Triggered Adaptive Control System.

$$\dot{x}(t) = Ax(t) + Bu_{\mathrm{s}}(t), \quad x(0) = x_0, \tag{13}$$

where $u_{\mathrm{s}}(t) \in \mathbb{R}^m$ is the sampled control input vector. Using Assumptions 1 and 2, (13) can be equivalently written by

$$\dot{x}(t) = A_{\mathrm{r}}x(t) + B_{\mathrm{r}}c(t) + D\Lambda[u_{\mathrm{s}}(t) + W_1^{\mathrm{T}}x(t) + W_2^{\mathrm{T}}c(t)]. \tag{14}$$

Now, let the adaptive feedback control law be given by

$$u(t) = -\hat{W}^{\mathrm{T}}(t)\sigma_{\mathrm{s}}\left(x_{\mathrm{s}}(t), c(t)\right), \tag{15}$$

where $x_{\mathrm{s}}(t) \in \mathbb{R}^n$ is the sampled state vector, $\sigma_{\mathrm{s}}\left(x_{\mathrm{s}}(t), c(t)\right) = \left[x_{\mathrm{s}}^{\mathrm{T}}(t), c^{\mathrm{T}}(t)\right]^{\mathrm{T}} \in \mathbb{R}^{n+m}$, and $\hat{W}(t)$ satisfies the weight update law

$$\dot{\hat{W}}(t) = \gamma\, \mathrm{Proj}_{\mathrm{m}}[\hat{W}(t), \sigma_{\mathrm{s}}(x_{\mathrm{s}}(t), c(t))e_{\mathrm{s}}^{\mathrm{T}}(t)PD], \quad \hat{W}(0) = \hat{W}_0, \tag{16}$$

with $e_{\mathrm{s}}(t) \triangleq x_{\mathrm{s}}(t) - x_{\mathrm{r}}(t) \in \mathbb{R}^n$ being the error of the triggered system state vector and $P \in \mathbb{R}_+^{n\times n} \cap \mathbb{S}^{n\times n}$ being a unique solution of the Lyapunov equation

$$0 = \tilde{A}^{\mathrm{T}}P + P\tilde{A} + R. \tag{17}$$

Note that using (15), (14) can be rewritten as

$$\begin{aligned}\dot{x}(t) &= A_{\mathrm{r}}x(t) + B_{\mathrm{r}}c(t) + D\Lambda\left(u_{\mathrm{s}}(t) - u(t)\right) - D\Lambda\tilde{W}^{\mathrm{T}}(t)\sigma\left(x(t), c(t)\right) \\ &\quad -D\Lambda\hat{W}^{\mathrm{T}}(t)\left[\sigma_{\mathrm{s}}\left(x_{\mathrm{s}}(t), c(t)\right) - \sigma\left(x(t), c(t)\right)\right],\end{aligned} \tag{18}$$

Next, consider the state emulator-based reference system given by

$$\dot{x}_{\mathrm{r}}(t) = A_{\mathrm{r}}x_{\mathrm{r}}(t) + B_{\mathrm{r}}c(t) + Le_{\mathrm{s}}(t), \quad x_{\mathrm{r}}(0) = x_{\mathrm{r}0}, \tag{19}$$

The (state emulator-based) system error dynamics and the reference system error dynamics are now respectively given by

$$\begin{aligned}\dot{e}(t) &= \tilde{A}e(t) + D\Lambda\left(u_{\mathrm{s}}(t) - u(t)\right) - D\Lambda\tilde{W}^{\mathrm{T}}(t)\sigma\left(x(t), c(t)\right)) \\ &\quad - D\Lambda\hat{W}^{\mathrm{T}}(t)\left[\sigma_{\mathrm{s}}\left(x_{\mathrm{s}}(t), c(t)\right) - \sigma\left(x(t), c(t)\right)\right] - L\left(x_{\mathrm{s}}(t) - x(t)\right), \quad e(0) = e_0,\end{aligned} \tag{20}$$

$$\dot{\tilde{x}}(t) = A_{\mathrm{r}}\tilde{x}(t) + Le_{\mathrm{s}}(t), \quad \tilde{x}(0) = \tilde{x}_0. \tag{21}$$

In the next section, we present user-defined event thresholds for scheduling the data exchange and analyze the stability and performance of the state emulator-based adaptive control approach introduced in this section using the error dynamics given by (21) and (20) along with the adaptive feedback control law given by (15) and (16).

4. STABILITY AND PERFORMANCE ANALYSIS

In this section, we first present the user-defined event thresholds for scheduling the two-way data exchange and analyze the uniform ultimate boundedness of the resulting closed-loop dynamical system (Section 4.1). Then, we compute the ultimate bound and discuss the effect of user-defined thresholds and the adaptive controller design parameters

to this ultimate bound (Section 4.2). Since a Zeno behavior implies a continuous two-way data exchange between the proposed controller and the physical system, and hence, is not desired in the context of reducing wireless network utilization, we finally show that the proposed state emulator-based adaptive controller does not yield to a Zeno behavior (Section 4.3).

4.1. Scheduling Data Exchange and Uniform Ultimate Boundedness. Let $\epsilon_x \in \mathbb{R}_+$ be a given, user-defined sensing threshold to allow for data transmission from the uncertain dynamical system to the controller. In addition, let $\epsilon_u \in \mathbb{R}_+$ be a given, user-defined actuation threshold to allow for data transmission from the controller to the uncertain dynamical system. We now define three logic rules for scheduling the two-way data exchange

$$E_1 : \quad \|x_s(t) - x(t)\| \leq \epsilon_x, \tag{22}$$

$$E_2 : \quad \|u_s(t) - u(t)\| \leq \epsilon_u, \tag{23}$$

$$E_3 : \quad \text{The controller receives } x_s(t). \tag{24}$$

Specifically, when the inequality (22) is violated at the s_k moment of the kth time instant, the uncertain dynamical system triggers the system state signal information such that $x_s(t)$ is sent to the controller. Likewise, when (23) is violated or the controller receives a new transmitted system state from the uncertain dynamical system (i.e., when $\bar{E}_2 \vee E_3$ is true), then the adaptive controller sends a new control input $u_s(t)$ to the uncertain dynamical system at the r_j moment of the jth time instant. Note that the three logic rules given above and the ones in [15] are not the same; that is, the proposed approach of this paper does not require the second and third logic rules of [15] and our second logic rule is different than the logic rules of [15].

Next, we show the uniform ultimate boundedness of the closed-loop dynamical system subject to the proposed state emulator-based event-triggered adaptive control methodology utilizing the data exchange rules E_1, E_2, and E_3 given by (22), (23), and (24), respectively.

Theorem 1. Consider the uncertain dynamical system given by (13) subject to Assumptions 1 and 2, the ideal reference system given by (3), the state emulator given by (19), and the adaptive feedback control law given by (15) with the weight update law given by (16). In addition, let the data transmission from the uncertain dynamical system to the controller occur when $\bar{E}_1$ is true and let the data transmission from the controller to the uncertain dynamical system occur when $\bar{E}_2 \vee E_3$ is true. Then, the closed-loop solution $(e(t), \tilde{W}(t), \tilde{x}(t))$ is uniformly ultimately bounded for all initial conditions.

Proof. Since the data transmission from the uncertain dynamical system to the controller and from the controller to the uncertain dynamical system occur when $\bar{E}_1$ and $\bar{E}_2 \vee E_3$ are true, respectively, note that $\|x_{\mathrm{s}}(t) - x(t)\| \leq \epsilon_x$ and $\|u_{\mathrm{s}}(t) - u(t)\| \leq \epsilon_u$ hold.

Consider the Lyapunov-like function $\mathcal{V}(e, \tilde{W}, \tilde{x}) = e^{\mathrm{T}} P e + \gamma^{-1} \mathrm{tr}(\tilde{W}\Lambda^{\frac{1}{2}})^{\mathrm{T}}(\tilde{W}\Lambda^{\frac{1}{2}}) + \beta \tilde{x}^{\mathrm{T}} \tilde{P} \tilde{x}$, where $\beta \in \mathbb{R}_+$, $P \in \mathbb{R}_+^{n\times n} \cap \mathbb{S}^{n\times n}$ is a solution of the Lyapunov equation given by (17) with $R \in \mathbb{R}_+^{n\times n} \cap \mathbb{S}^{n\times n}$, and $\tilde{P} \in \mathbb{R}_+^{n\times n} \cap \mathbb{S}^{n\times n}$ is a unique solution of the Lyapunov equation given by $0 = A_{\mathrm{r}}^{\mathrm{T}} \tilde{P} + \tilde{P} A_{\mathrm{r}} + \tilde{R}$, $\tilde{R} \in \mathbb{R}_+^{n\times n} \cap \mathbb{S}^{n\times n}$. Note that $\mathcal{V}(0,0,0) = 0$ and $\mathcal{V}(e, \tilde{W}, \tilde{x}) > 0$ for all $(e, \tilde{W}, \tilde{x}) \neq (0,0,0)$. The time-derivative of $\mathcal{V}(e, \tilde{W}, \tilde{x})$ is given by

$$
\begin{aligned}
&\dot{\mathcal{V}}(e(t), \tilde{W}(t), \tilde{x}(t)) \\
&\quad \leq \; -\lambda_{\min}(R) \left\| e(t) \right\|^2 + 2 \left\| x_{\mathrm{s}}(t) - x(t) \right\| \left\| PD \right\|_{\mathrm{F}} \left\| \Lambda \right\|_{\mathrm{F}} \left\| \tilde{W}(t) \right\|_{\mathrm{F}} \left\| \sigma_{\mathrm{s}} \left(x_{\mathrm{s}}(t), c(t) \right) \right\| \\
&\qquad + 2 \left\| e(t) \right\| \left\| PD \right\|_{\mathrm{F}} \left\| \Lambda \right\|_{\mathrm{F}} \left\| W \right\|_{\mathrm{F}} \left\| \sigma_{\mathrm{s}} \left(x_{\mathrm{s}}(t), c(t) \right) - \sigma \left(x(t), c(t) \right) \right\| \\
&\qquad + 2 \left\| e(t) \right\| \left\| PD \right\|_{\mathrm{F}} \left\| \Lambda \right\|_{\mathrm{F}} \left\| u_{\mathrm{s}}(t) - u(t) \right\| + 2 \left\| e(t) \right\| \left\| P \right\|_{\mathrm{F}} \left\| L \right\|_{\mathrm{F}} \left\| x_{\mathrm{s}}(t) - x(t) \right\| \\
&\qquad - \beta \lambda_{\min}(\tilde{R}) \left\| \tilde{x}(t) \right\|^2 + 2\beta \left\| \tilde{x}(t) \right\| \left\| \tilde{P} \right\|_{\mathrm{F}} \left\| L \right\|_{\mathrm{F}} \left\| e_{\mathrm{s}}(t) \right\| . \qquad (25)
\end{aligned}
$$

We now determine an upper bound for $\|\sigma_{\rm s}\left(x_{\rm s}(t),c(t)\right)\|$ in (25). To this end, one can write $\|\sigma_{\rm s}(x_{\rm s}(t),c(t))\|^2 = \left\|x_{\rm s}^{\rm T}(t)x_{\rm s}(t) + c^{\rm T}(t)c(t)\right\| \leq \|x_{\rm s}(t)\|^2 + \|c(t)\|^2 \leq (\|x_{\rm s}(t)\| + \|c(t)\|)^2$, and hence, $\|\sigma_{\rm s}(x_{\rm s}(t),c(t))\| \leq \|x_{\rm s}(t)\| + \|c(t)\|$. Furthermore, letting $\tilde{\epsilon}_x$ to be an upper bound of $\|x_{\rm ri}(t)\| + \epsilon_x + \|c(t)\|$, i.e., $\|x_{\rm ri}(t)\| + \epsilon_x + \|c(t)\| \leq \tilde{\epsilon}_x$, and using $\|x_{\rm s}(t) - x(t)\| \leq \epsilon_x$, we have $\|\sigma_{\rm s}(x_{\rm s}(t),c(t))\| \leq \|x_{\rm s}(t)\| + \|c(t)\| = \|e(t) + x_{\rm r}(t) + x_{\rm s}(t) - x(t)\| + \|c(t)\| \leq \|e(t)\| + \|x_{\rm r}(t)\| + \epsilon_x + \|c(t)\| \leq \|e(t)\| + \|\tilde{x}(t)\| + \|x_{\rm ri}(t)\| + \epsilon_x + \|c(t)\| \leq \|e(t)\| + \|\tilde{x}(t)\| + \tilde{\epsilon}_x$. In addition, we determine an upper bound for $\|e_{\rm s}(t)\|$ in (25) as $\|e_{\rm s}(t)\| = \|e(t) + x_{\rm s}(t) - x(t)\| \leq \|e(t)\| + \epsilon_x$. Using these upper bounds, $\|x_{\rm s}(t) - x(t)\| \leq \epsilon_x$, and $\|u_{\rm s}(t) - u(t)\| \leq \epsilon_u$, (25) can be rewritten as

$$
\begin{aligned}
&\dot{\mathcal{V}}(e(t),\tilde{W}(t),\tilde{x}(t))\\
&\quad\leq -\lambda_{\min}(R)\,\|e(t)\|^2 + 2\,\|PD\|_{\rm F}\,\|\Lambda\|_{\rm F}\left\|\tilde{W}(t)\right\|_{\rm F}\|e(t)\|\,\epsilon_x + 2\,\|PD\|_{\rm F}\,\|\Lambda\|_{\rm F}\left\|\tilde{W}(t)\right\|_{\rm F}\\
&\qquad\cdot\,\|\tilde{x}(t)\|\,\epsilon_x + 2\,\|PD\|_{\rm F}\,\|\Lambda\|_{\rm F}\left\|\tilde{W}(t)\right\|_{\rm F}\tilde{\epsilon}_x\epsilon_x + 2\,\|e(t)\|\,\|PD\|_{\rm F}\,\|\Lambda\|_{\rm F}\,\|W\|_{\rm F}\,\epsilon_x\\
&\qquad+ 2\,\|e(t)\|\|\,PD\|_{\rm F}\,\|\Lambda\|_{\rm F}\,\epsilon_u + 2\,\|e(t)\|\,\|P\|_{\rm F}\,\|L\|_{\rm F}\,\epsilon_x - \beta\lambda_{\min}(\tilde{R})\,\|\tilde{x}(t)\|^2\\
&\qquad+ 2\beta\,\|\tilde{x}(t)\|\left\|\tilde{P}\right\|_{\rm F}\|L\|_{\rm F}\,\epsilon_x + 2\beta\,\|\tilde{x}(t)\|\left\|\tilde{P}\right\|_{\rm F}\|L\|_{\rm F}\,\|e(t)\|\,. \qquad (26)
\end{aligned}
$$

Next, consider $2xy \leq \alpha x^2 + \frac{1}{\alpha}y^2$, $x \in \mathbb{R}$, $y \in \mathbb{R}$, $\alpha \in \mathbb{R}_+$ [36], where using this inequality for the last term in (26) yields

$$
\dot{\mathcal{V}}(e(t),\tilde{W}(t),\tilde{x}(t)) \leq -d_1\,\|e(t)\|^2 - d_2\,\|\tilde{x}(t)\|^2 + d_3\,\|e(t)\| + d_4\,\|\tilde{x}(t)\| + d_5, \qquad (27)
$$

where $d_1 \triangleq \lambda_{\min}(R) - \alpha\left\|\tilde{P}\right\|_{\rm F}^2\|L\|_{\rm F}^2 > 0$, $d_2 \triangleq \beta\lambda_{\min}(\tilde{R}) - \frac{\beta^2}{\alpha} > 0$, $d_3 \triangleq 2\,\|PD\|_{\rm F}\,\|\Lambda\|_{\rm F}\,\tilde{w}^*\epsilon_x$ $+2\,\|PD\|_{\rm F}\,\|\Lambda\|_{\rm F}\,\|W\|_{\rm F}\,\epsilon_x + 2\,\|PD\|_{\rm F}\,\|\Lambda\|_{\rm F}\,\epsilon_u + 2\,\|P\|_{\rm F}\,\|L\|_{\rm F}\,\epsilon_x$, $d_4 \triangleq 2\,\|PD\|_{\rm F}\,\|\Lambda\|_{\rm F}\,\tilde{w}^*\epsilon_x + 2\beta\left\|\tilde{P}\right\|_{\rm F}\|L\|_{\rm F}\,\epsilon_x$, and $d_5 \triangleq 2\,\|PD\|_{\rm F}\,\|\Lambda\|_{\rm F}\,\tilde{w}^*\tilde{\epsilon}_x\epsilon_x$ with $||\tilde{W}(t)||_{\rm F} \leq \tilde{w}^*$ due to utilizing the projection operator in the weight update law given by (16). Note that the positiveness of d_1 and d_2 can be readily assured by letting (arbitrary) positive constants α and β to be sufficiently small. We now rearrange (27) as $\dot{\mathcal{V}}(e(t),\tilde{W}(t),\tilde{x}(t)) \leq -\left(\sqrt{d_1}\,\|e(t)\| - \frac{d_3}{2\sqrt{d_1}}\right)^2 - \left(\sqrt{d_2}\,\|\tilde{x}(t)\| - \frac{d_4}{2\sqrt{d_2}}\right)^2 + \left(d_5 + \frac{d_3^2}{4d_1} + \frac{d_4^2}{4d_2}\right)$, which shows that $\dot{\mathcal{V}}(e(t),\tilde{W}(t),\tilde{x}(t)) \leq 0$

when $\|e(t)\| \geq \psi_1$ and $\|\tilde{x}(t)\| \geq \psi_2$, where $\psi_1 \triangleq \left[\frac{d_3}{2\sqrt{d_1}} + \sqrt{d_5 + \frac{d_3^2}{4d_1} + \frac{d_4^2}{4d_2}}\right]/\sqrt{d_1}$ and $\psi_2 \triangleq \left[\frac{d_4}{2\sqrt{d_2}} + \sqrt{d_5 + \frac{d_3^2}{4d_1} + \frac{d_4^2}{4d_2}}\right]/\sqrt{d_2}$. This argument proves uniform ultimate boundedness of the solution $(e(t), \tilde{W}(t), \tilde{x}(t))$ for all initial conditions [37, 33]. ■

4.2. Computation of the Ultimate Bound. The next corollary computes the ultimate bound for the system error between the uncertain dynamical system and the ideal reference model, where this bound explicitly shows the effect of user-defined thresholds and the adaptive control design parameters to the system performance and how the resulting command following performance error can be made sufficiently small.

Corollary 1. Consider the uncertain dynamical system given by (13) subject to Assumptions 1 and 2, the ideal reference system given by (3), the state emulator given by (19), and the adaptive feedback control law given by (15) with the weight update law given by (16). In addition, let the data transmission from the uncertain dynamical system to the controller occur when $\bar{E}_1$ is true and let the data transmission from the controller to the uncertain dynamical system occur when $\bar{E}_2 \vee E_3$ is true. Then, the ultimate bound of the system error between the uncertain dynamical system and the ideal reference model is given by

$$||e_o(t)|| \quad = \quad ||x(t) - x_{\mathrm{ri}}(t)|| \;\leq\; \bar{e}_o \;\triangleq\; \tilde{\Phi}\left[\lambda_{\min}^{-1}(P) + \left(\beta\lambda_{\min}(\tilde{P})\right)^{-1}\right]^{\frac{1}{2}}, \quad t \geq T \quad (28)$$

where $\tilde{\Phi} \triangleq \left[\lambda_{\max}(P)\psi_1^2 + \beta\lambda_{\max}(\tilde{P})\psi_2^2 + \gamma^{-1}\tilde{w}^{*2}\,\|\Lambda\|_{\mathrm{F}}\right]^{\frac{1}{2}}$.

Proof. It follows from the proof of Theorem 1 that $\dot{\mathcal{V}}(e(t), \tilde{W}(t), \tilde{x}(t)) \leq 0$ outside the compact set given by $\mathcal{S} \triangleq \{(e(t), \tilde{x}(t)) : \|e(t)\| \leq \psi_1\} \bigcap \{(e(t), \tilde{x}(t)) : \|\tilde{x}(t)\| \leq \psi_2\}$. That is, since $\mathcal{V}(e(t), \tilde{W}(t), \tilde{x}(t))$ cannot grow outside $\mathcal{S}$, evolution of $\mathcal{V}(e(t), \tilde{W}(t), \tilde{x}(t))$ is upper bounded by $\mathcal{V}(e(t), \tilde{W}(t), \tilde{x}(t)) \leq \max_{(e(t), \tilde{x}(t)) \in \mathcal{S}} \mathcal{V}(e(t), \tilde{W}(t), \tilde{x}(t)) = \lambda_{\max}(P)\psi_1^2 + \beta\lambda_{\max}(\tilde{P})\psi_2^2 + \gamma^{-1}\tilde{w}^{*2}\,\|\Lambda\|_{\mathrm{F}} = \tilde{\Phi}^2$. Now, it follows from $e^{\mathrm{T}}Pe \leq \mathcal{V}(e, \tilde{W}, \tilde{x})$ and $\beta\tilde{x}^{\mathrm{T}}\tilde{P}\tilde{x} \leq$

$\mathcal{V}(e,\tilde{W},\tilde{x})$ that $\|e(t)\|^2 \leq \frac{\tilde{\Phi}^2}{\lambda_{\min}(P)}$ and $\|\tilde{x}(t)\|^2 \leq \frac{\tilde{\Phi}^2}{\beta\lambda_{\min}(P)}$. Finally, since $e_o(t) = x(t) - x_{\mathrm{r}}(t) + x_{\mathrm{r}}(t) - x_{\mathrm{ri}}(t) = e(t) + \tilde{x}(t)$, and hence, $\|e_o(t)\| \leq \|e(t)\| + \|\tilde{x}(t)\|$, the ultimate bound given by (28) is now immediate. ■

Remark 1. The ultimate bound given by (28) depends on Φ_1 and Φ_2, where Φ_1 and Φ_2 depend on the magnitude of d_1, d_2, d_3, d_4, and d_5. Note that, among these $d_i, (i = 1,\cdots,5)$ terms only d_3, d_4, and d_5 depend on ϵ_x and ϵ_u. In general, since the magnitude of the terms multiplied by ϵ_x in d_3, d_4, and d_5 is larger than the magnitude of the only term multiplied by ϵ_u (i.e. in the presence of large system uncertainties), then it is expected that ϵ_x has a more dominating effect on the ultimate bound (28) than ϵ_u on the ultimate bound.

Remark 2. To elucidate the effect of the user-defined thresholds and the adaptive controller design parameters to the ultimate bound given by (28) and discussed in Remark 1, let $A_{\mathrm{r}} = -5$, $D = 1$, $\Lambda = 1$, $W = 1$, $R = 1$, $\tilde{R} = 1$, $\alpha = 0.5$, and $\beta = 0.25$. In this case, Figure 2a shows the effect of the variation in L and γ to (28) for $\epsilon_x = 1$ and $\epsilon_u = 1$. Specifically, one can conclude from this figure that increasing γ reduces the ultimate bound and the minimum value of this bound is obtained for $L = 2$. Figures 2b and 2c show the effect of the variations in ϵ_x and ϵ_u, respectively. From these figures and in general from

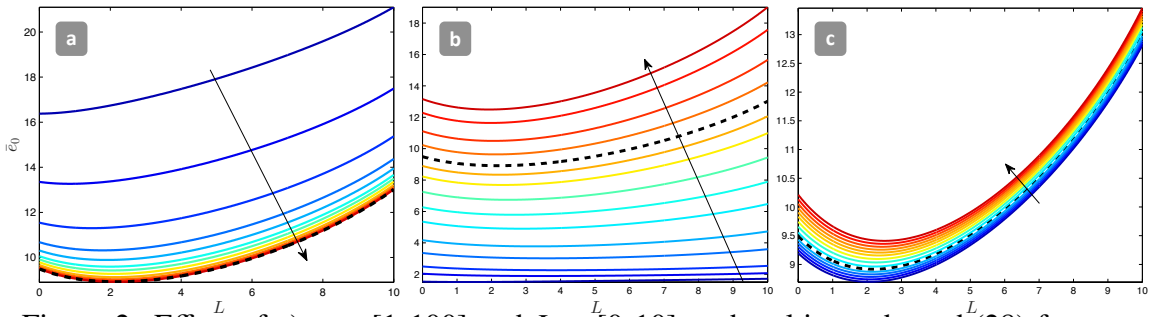

Figure 2. Effect of a) $\gamma \in [1,100]$ and $L \in [0,10]$ to the ultimate bound (28) for $\epsilon_x = 1$ and $\epsilon_u = 1$, where the arrow indicates the direction γ is increased (dashed line denotes the case with $\gamma = 100$); b) $\epsilon_x \in [0,1.5]$ to the ultimate bound (28) for $\epsilon_u = 1$, $L \in [0,10]$, and $\gamma = 100$, where the arrow indicates the direction ϵ_x is increased (dashed line denotes that case with $\epsilon_x = 1$); c) $\epsilon_u \in [0,3]$ to the ultimate bound (28) for $\epsilon_x = 1$, $L \in [0,10]$, and $\gamma = 100$, where the arrow indicates the direction ϵ_u is increased (dashed line denotes that case with $\epsilon_u = 1$).

the structure of the ultimate bound given by (28), it is of practical importance to note that the resulting closed-loop dynamical system performance, which is characterized by the upper bound on $e_o(t)$, is more sensitive to the changes in the sensing threshold ϵ_x (the data transmission threshold from the physical system to the adaptive controller) than the actuation threshold ϵ_u (the data transmission threshold from the adaptive controller to the physical system). This means that the actuation threshold can be chosen large enough to reduce wireless network utilization between the physical system and the adaptive controller without necessarily sacrificing closed-loop dynamical system performance.

4.3. Computation of the Event-triggered Intersample Time Lower Bound. For the following result, similar to [15], we consider $r_i^k \in (s_k, s_{k+1})$ to be the ith time instant when E_2 is violated over (s_k, s_{k+1}), and since $\{s_k\}_{k=1}^{\infty}$ is a subsequence of $\left\{r_j\right\}_{j=1}^{\infty}$, it follows that $\left\{r_j\right\}_{j=1}^{\infty} = \{s_k\}_{k=1}^{\infty} \bigcup \left\{r_i^k\right\}_{k=1,i=1}^{\infty,m_k}$, where $m_k \in \mathbb{N}$ is the number of violation times of E_2 over (s_k, s_{k+1}). We also let Φ_1 and Φ_2 to denote $\|A\|_{\mathrm{F}} \|x(t)\| + \|D\|_{\mathrm{F}} \|\Lambda\|_{\mathrm{F}} \|u_{\mathrm{s}}(t)\| \leq \Phi_1$, and $\gamma\big(\|e(t)\| + \|\tilde{x}(t)\| + \bar{\epsilon}_x\big)^2 \left(\|e(t)\| + \epsilon_x\right) \|PD\|_{\mathrm{F}} + \left\|\hat{W}(t)\right\|_{\mathrm{F}}$
$\cdot \|\dot{c}(t)\| \leq \Phi_2$, respectively, where the existence of positive constants Φ_1 and Φ_2 are guaranteed by Theorem 1.

Corollary 2. Consider the uncertain dynamical system given by (13) subject to Assumptions 1 and 2, the ideal reference system given by (3), the state emulator given by (19), and the adaptive feedback control law given by (15) with the weight update law given by (16). In addition, let the data transmission from the uncertain dynamical system to the controller occur when $\bar{E}_1$ is true and let the data transmission from the controller to the uncertain dynamical system occur when $\bar{E}_2 \vee E_3$ is true. Then, there exist positive scalars $\alpha_x \triangleq \frac{\epsilon_x}{\Phi_1}$ and $\alpha_u \triangleq \frac{\epsilon_u}{\Phi_2}$, such that

$$s_{k+1} - s_k \geq \alpha_x, \quad \forall k \in \mathbb{N}, \tag{29}$$

$$r_{i+1}^k - r_i^k \geq \alpha_u, \quad \forall i \in \{0, \ldots, m_k\}, \quad \forall k \in \mathbb{N}. \tag{30}$$

Proof. The time derivative of $\|x_{\mathrm{s}}(t) - x(t)\|$ over $t \in (s_k, s_{k+1})$, $\forall k \in \mathbb{N}$, is given by

$$\frac{\mathrm{d}}{\mathrm{d}t}\left\|x_{\mathrm{s}}(t)-x(t)\right\| \leq \left\|\dot{x}_{\mathrm{s}}(t)-\dot{x}(t)\right\| = \left\|\dot{x}(t)\right\| \leq \left\|A\right\|_{\mathrm{F}}\left\|x(t)\right\| + \left\|D\right\|_{\mathrm{F}}\left\|\Lambda\right\|_{\mathrm{F}}\left\|u_{\mathrm{s}}(t)\right\|. \quad (31)$$

Using Φ_1 for the upper bound of (31) and with initial condition satisfying $\lim_{t\to s_k^+}||x_s(t) - x(t)|| = 0$, it follows from (31) that $\|x_{\mathrm{s}}(t) - x(t)\| \leq \Phi_1(t - s_k)$, $t \in (s_k, s_{k+1})$. Therefore, when $\bar{E}_1$ is true, then $\lim_{t\to s_{k+1}^-}\|x_{\mathrm{s}}(t) - x(t)\| = \epsilon_x$ and it then follows that $s_{k+1} - s_k \geq \alpha_x$.

Next, the time derivative of $\|u_{\mathrm{s}}(t) - u(t)\|$ over $t \in \left(r_i^k, r_{i+1}^k\right), \forall i \in \mathbb{N}$, is given by

$$\begin{aligned}\frac{\mathrm{d}}{\mathrm{d}t}\left\|u_{\mathrm{s}}(t)-u(t)\right\| &\leq \left\|\dot{u}_{\mathrm{s}}(t)-\dot{u}(t)\right\| = \left\|\dot{u}(t)\right\| \\ &\leq \gamma\left(\left\|e(t)\right\| + \left\|\tilde{x}(t)\right\| + \tilde{\epsilon}_x\right)^2\left(\left\|e(t)\right\| + \epsilon_x\right)\left\|PD\right\|_{\mathrm{F}} \\ &\quad + \left\|\hat{W}(t)\right\|_{\mathrm{F}}\left\|\dot{c}(t)\right\|. \end{aligned} \quad (32)$$

Once again, using Φ_2 for the upper bound of (32) and with initial condition satisfying $\lim_{t\to r_i^{k+}}\|u_{\mathrm{s}}(t) - u(t)\| = 0$, it follows from (32) that $\|u_{\mathrm{s}}(t) - u(t)\| \leq \Phi_2(t - r_i^k)$, $t \in \left(r_i^k, r_{i+1}^k\right)$. Therefore, when $\bar{E}_2 \vee E_3$ is true, then $\lim_{t\to r_{i+1}^{k-}}\|u_{\mathrm{s}}(t) - u(t)\| = \epsilon_u$ and it then follows that $r_{i+1}^k - r_i^k \geq \alpha_u$. ■

Remark 3. Zeno behavior implies a continuous two-way data exchange between the proposed controller and the physical system (for example, when $\epsilon_x = \epsilon_u = 0$ that yields to an asymptotic command following performance), which is not desired in the context of reducing wireless network utilization. Corollary 2 shows that the intersample times for the system state vector and feedback control vector are positive scalars, and hence, the proposed event-triggered adaptive control approach does not yield to a Zeno behavior and reduces wireless network utilization.

5. ILLUSTRATIVE NUMERICAL EXAMPLE

To illustrate the proposed event-triggered adaptive control approach, consider an uncertain dynamical system given by

$$\begin{bmatrix} \dot{x}_1(t) \\ \dot{x}_2(t) \end{bmatrix} = \begin{bmatrix} 0 & 1 \\ 0.2 & -0.2 \end{bmatrix} \begin{bmatrix} x_1(t) \\ x_2(t) \end{bmatrix} + \begin{bmatrix} 0 \\ 1 \end{bmatrix} u_{\mathrm{s}}(t), \quad \begin{bmatrix} x_1(0) \\ x_2(0) \end{bmatrix} = \begin{bmatrix} 0 \\ 0 \end{bmatrix}. \tag{33}$$

For this example, let $x_1(t)$ represent an angle in radians and $x_2(t)$ represent an angular rate in radians per second. We choose a second-order ideal reference system that has a natural frequency of 0.40 rad/s and a damping ratio of 0.707. Furthermore, we set $R = I_2$ and $\tilde{R} = I_2$.

Figures 3a-3d show the proposed event-triggered adaptive control approach for various γ and L settings. In particular, we set $\gamma = 2.5$ and $L = 0$ in Figure 3a that results in a control response with high-frequency oscillations. In order to get rid of these oscillations, we set $L = 5I$ in Figure 3b. In this figure, even though such oscillations are reduced, the command tracking performance becomes worse as we increase L. Following the discussion in Remark 2, in addition to increasing L, we also increase γ in Figures 3c and 3d, where the command tracking performance is improved without causing high-frequency oscillations. Finally, the state and control event triggers for the cases in Figures 3a-3d are given in Figure 4a. If we compare $L = 0$ case (standard adaptive control) with $L \neq 0$ cases (state emulator-based adaptive control), we can observe that the state emulator approach has a recognizable effect in reducing state and control event triggers. Figure 4b also shows a comparison of the proposed event-triggered adaptive control approach in Figures 3a-3d with a conventional periodic (i.e., non-event-triggered) strategy in terms of state and control transmission (a fixed period of 0.005 seconds[1] is used in the execution of the conventional periodic strategy).

[1] Since a continuous-time formulation is adopted in this paper, we chose a sufficiently small sampling time of 0.005 seconds in all simulations for discretization purposes. Specifically, to make a fair comparison with the proposed event-triggered control law subject to this sampling time, we also used the same sampling time in the execution of the conventional periodic strategy that corresponds to a fixed period of 0.005 seconds for the two-way communication between this controller and the considered uncertain dynamical system.

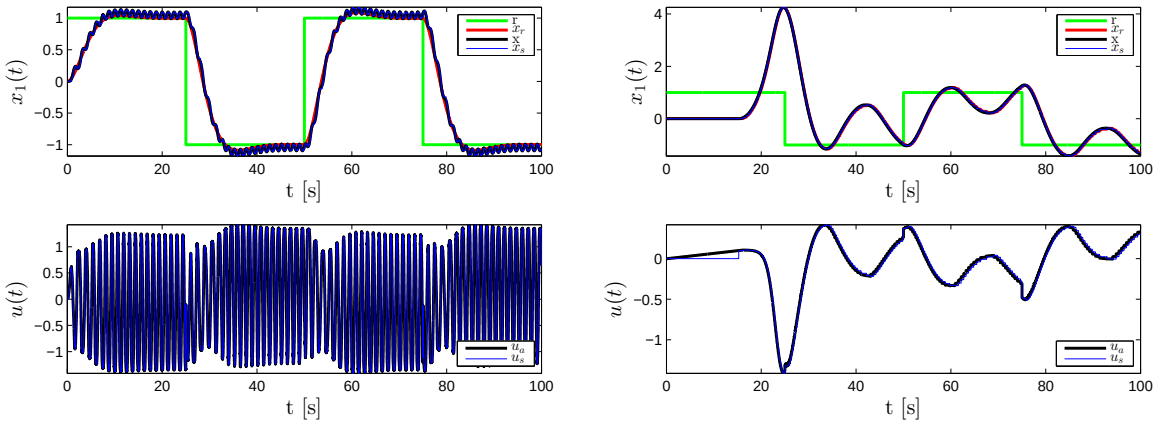

(a) $\epsilon_x = 0.1$, $\epsilon_u = 0.1$, $\gamma = 2.5$, and $L = 0$.

(b) $\epsilon_x = 0.1$, $\epsilon_u = 0.1$, $\gamma = 2.5$, and $L = 5I$.

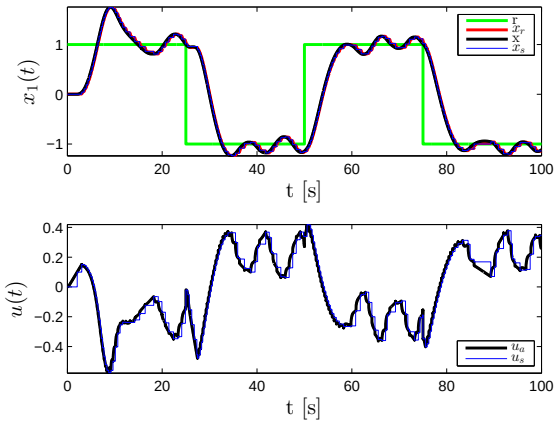

(c) $\epsilon_x = 0.1$, $\epsilon_u = 0.1$, $\gamma = 20$, and $L = 5I$.

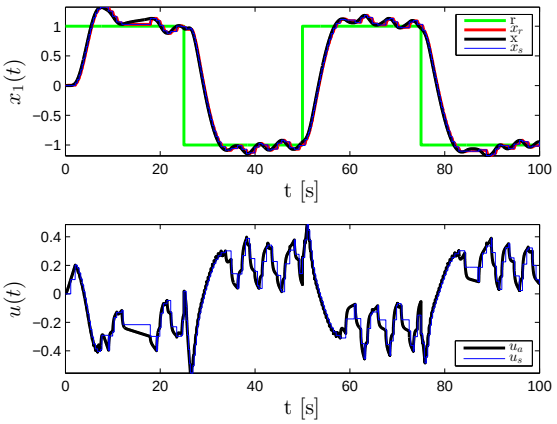

(d) $\epsilon_x = 0.1$, $\epsilon_u = 0.1$, $\gamma = 40$, and $L = 5I$.

Figure 3. Command following performance for the proposed event-triggered adaptive control approach.

6. CONCLUSION

Design and analysis of an event-triggered adaptive control methodology is presented in this paper for a class of uncertain dynamical systems in the presence of two-way data exchange between the physical system and the proposed controller over a wireless network. In particular, using tools and methods from nonlinear systems and Lyapunov stability, we showed that the proposed approach reduces wireless network utilization, guarantees system stability and command following performance in the presence of system

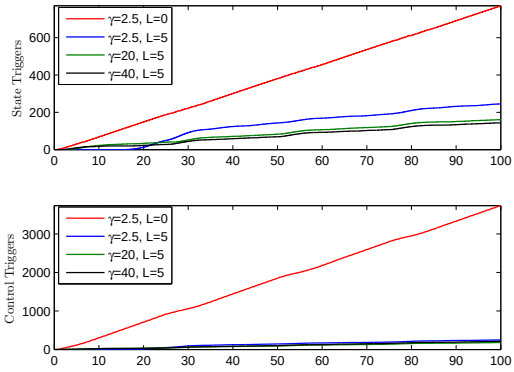

(a) State and control event triggers for the cases presented in Figures 3a-3d.

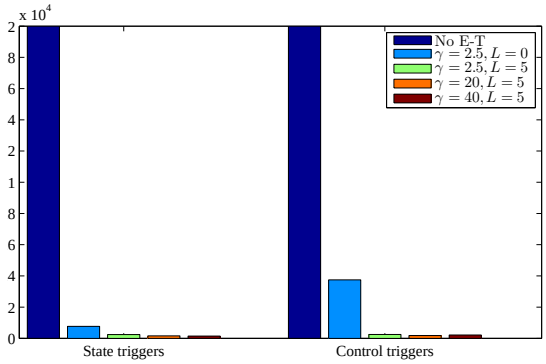

(b) Comparison of the proposed event-triggered adaptive control approach in Figures 3a-3d with a conventional periodic strategy.

Figure 4. Event triggers in Figures 3a-3d and comparison with a conventional periodic strategy in terms of state and control transmission.

uncertainties, and does not yield to a Zeno behavior. In addition, the effect of user-defined thresholds and adaptive controller design parameters to the system performance is characterized and discussed. As a byproduct, we found that the actuation threshold (the data transmission threshold from the adaptive controller to the physical system) can be chosen larger than the sensing threshold (the data transmission threshold from the physical system to the adaptive controller) to reduce wireless network utilization between the physical system and the adaptive controller without necessarily sacrificing closed-loop dynamical system performance. Finally, we illustrated the efficacy of the proposed adaptive control approach in a numerical example.

REFERENCES

[1] W. Zhang, M. S. Branicky, and S. M. Phillips, "Stability of networked control systems," *IEEE Control Systems Magazine*, vol. 21, no. 1, pp. 84–99, 2001.

[2] Y. Tipsuwan and M.-Y. Chow, "Control methodologies in networked control systems," *Control engineering practice*, vol. 11, no. 10, pp. 1099–1111, 2003.

[3] J. P. Hespanha, P. Naghshtabrizi, and Y. Xu, "A survey of recent results in networked control systems," *Proceedings of the IEEE*, vol. 95, no. 1, pp. 138–162, 2007.

[4] F.-Y. Wang and D. Liu, *Networked Control Systems*. Springer, 2008.

[5] A. Bemporad, M. Heemels, and M. Johansson, *Networked Control Systems*. Springer, 2010.

[6] K. Zhou and J. C. Doyle, *Essentials of Robust Control*. Upper Saddle River, NJ: Prentice Hall, 1998.

[7] G. Dullerud and F. Paganini, *Course in Robust Control Theory*. Springer-Verlag New York, 2000.

[8] P. A. Ioannou and J. Sun, *Robust Adaptive Control*. Courier Corporation, 2012.

[9] K. S. Narendra and A. M. Annaswamy, *Stable Adaptive Systems*. Courier Corporation, 2012.

[10] K. J. Åström and B. Wittenmark, *Adaptive Control*. Courier Corporation, 2013.

[11] T. Yucelen and W. M. Haddad, "A robust adaptive control architecture for disturbance rejection and uncertainty suppression with $\mathcal{L}_\infty$ transient and steady-state performance guarantees," *International Journal of Adaptive Control and Signal Processing*, vol. 26, no. 11, pp. 1024–1055, 2012.

[12] T. Yucelen and E. Johnson, "A new command governor architecture for transient response shaping," *International Journal of Adaptive Control and Signal Processing*, vol. 27, no. 12, pp. 1065–1085, 2013.

[13] A. Sahoo, H. Xu, and S. Jagannathan, "Neural network-based adaptive event-triggered control of nonlinear continuous-time systems," *IEEE International Symposium on Intelligent Control*, pp. 35–40, 2013.

[14] A. Sahoo, H. Xu, and S. Jagannathan, "Neural network approximation-based event-triggered control of uncertain mimo nonlinear discrete time systems," *IEEE American Control Conference*, pp. 2017–2022, 2014.

[15] X. Wang and N. Hovakimyan, "$\mathcal{L}_1$ adaptive control of event-triggered networked systems," *IEEE American Control Conference*, pp. 2458–2463, 2010.

[16] X. Wang, E. Kharisov, and N. Hovakimyan, "Real-time adaptive control for uncertain networked control systems," *IEEE Transactions on Automatic Control*, vol. 60, no. 9, pp. 2500–2505, 2015.

[17] T. Yucelen and A. J. Calise, "Derivative-free model reference adaptive control," *Journal of Guidance, Control, and Dynamics*, vol. 34, no. 4, pp. 933–950, 2011.

[18] P. Tabuada, "Event-triggered real-time scheduling of stabilizing control tasks," *IEEE Transactions on Automatic Control*, vol. 52, no. 9, pp. 1680–1685, 2007.

[19] M. Mazo Jr and P. Tabuada, "On event-triggered and self-triggered control over sensor/actuator networks," in *IEEE Conference on Decision and Control*, pp. 435–440, 2008.

[20] M. Mazo Jr, A. Anta, and P. Tabuada, "On self-triggered control for linear systems: Guarantees and complexity," in *IEEE European Control Conference*, pp. 3767–3772, 2009.

[21] J. Lunze and D. Lehmann, "A state-feedback approach to event-based control," *Automatica*, vol. 46, no. 1, pp. 211–215, 2010.

[22] R. Postoyan, A. Anta, D. Nesic, and P. Tabuada, "A unifying Lyapunov-based framework for the event-triggered control of nonlinear systems," in *IEEE Conference on Decision and Control and European Control Conference*, pp. 2559–2564, 2011.

[23] W. Heemels, K. H. Johansson, and P. Tabuada, "An introduction to event-triggered and self-triggered control," in *IEEE Annual Conference on Decision and Control*, pp. 3270–3285, 2012.

[24] H. Li and Y. Shi, "Event-triggered robust model predictive control of continuous-time nonlinear systems," *Automatica*, vol. 50, no. 5, pp. 1507–1513, 2014.

[25] D. Shi, T. Chen, and L. Shi, "An event-triggered approach to state estimation with multiple point-and set-valued measurements," *Automatica*, vol. 50, no. 6, pp. 1641–1648, 2014.

[26] E. Lavretsky, R. Gadient, and I. M. Gregory, "Predictor-based model reference adaptive control," *Journal of Guidance, Control, and Dynamics*, vol. 33, no. 4, pp. 1195–1201, 2010.

[27] J. A. Muse and A. J. Calise, "H_∞ adaptive flight control of the generic transport model," *AIAA Infotech@Aerospace*, 2010.

[28] V. Stepanyan and K. Krishnakumar, "MRAC revisited: guaranteed performance with reference model modification," *IEEE American Control Conference*, pp. 93–98, 2010.

[29] V. Stepanyan and K. Krishnakumar, "M-MRAC for nonlinear systems with bounded disturbances," *IEEE Decision and Control and European Control Conference*, pp. 5419–5424, 2011.

[30] T. E. Gibson, A. M. Annaswamy, and E. Lavretsky, "Improved transient response in adaptive control using projection algorithms and closed loop reference models," *AIAA Guidance Navigation and Control Conference*, 2012.

[31] T. Yucelen, G. De La Torre, and E. N. Johnson, "Improving transient performance of adaptive control architectures using frequency-limited system error dynamics," *International Journal of Control*, vol. 87, no. 11, pp. 2383–2397, 2014.

[32] T. E. Gibson, A. M. Annaswamy, and E. Lavretsky, "Adaptive systems with closed-loop reference models: Stability, robustness and transient performance," *arXiv preprint arXiv:1201.4897*, 2012.

[33] E. Lavretsky and K. Wise, *Robust and Adaptive Control: With Aerospace Applications*. Springer, 2012.

[34] J.-B. Pomet and L. Praly, "Adaptive nonlinear regulation: estimation from the Lyapunov equation," *IEEE Transactions on Automatic Control*, vol. 37, no. 6, pp. 729–740, 1992.

[35] W. M. Haddad and V. Chellaboina, *Nonlinear Dynamical Systems and Control:* A L*yapunov-Based Approach*. Princeton University Press, 2008.

[36] D. S. Bernstein, *Matrix mathematics: Theory, Facts, and Formulas*. Princeton University Press, 2009.

[37] H. K. Khalil, *Nonlinear Systems*. Upper Saddle River, NJ: PrenticeHall, 1996.

II. OUTPUT FEEDBACK ADAPTIVE CONTROL OF UNCERTAIN DYNAMICAL SYSTEMS WITH EVENT-TRIGGERING

Ali Albattat, Benjamin Gruenwald , and Tansel Yucelen
Department of Mechanical & Aerospace Engineering
Missouri University of Science and Technology

ABSTRACT

Networked control for a class of uncertain dynamical systems is studied, where the control signals are computed via processors that are not attached to the dynamical systems and the feedback loops are closed over wireless networks. Since a critical task in the design and implementation of networked control systems is to reduce wireless network utilization while guaranteeing system stability in the presence of system uncertainties, an event-triggered adaptive control architecture is presented in an output feedback setting to schedule the data exchange dependent upon errors exceeding user-defined thresholds. Specifically, using tools and methods from nonlinear systems theory and Lyapunov stability in particular, it is shown that the proposed approach guarantees system stability in the presence of system uncertainties and does not yield to a Zeno behavior. In addition, the effect of user-defined thresholds and output feedback adaptive controller design parameters to the system performance is rigorously characterized and discussed. The efficacy of the proposed event-triggered output feedback adaptive control approach is demonstrated in an illustrative numerical example.

Keywords: Networked control systems; output feedback adaptive control; event-triggering control; system uncertainties; system stability; system performance.

1. INTRODUCTION

Networked control of dynamical systems is an appealing methodology in reducing cost for the development and implementation of control systems [1, 2, 3, 4, 5, 6, 7, 8]. These systems allow the computation of control signals via processors that are not attached to the dynamical systems and the feedback loops are closed over wireless networks. In a networked control setting, since the processors computing control signals are separated from the dynamical systems, not only the feedback control algorithms can be easily modified as necessary but also this setting allows to develop small-size physical systems for low-cost control theory applications.

1.1. Motivation and Literature Review. A challenge in the design and implementation of networked control systems is to reduce wireless network utilization. To this end, the last decade has witnessed an increased interest in event-triggering control theory [9, 10, 11, 12, 13, 14], where it relaxes periodic data exchange demand of the feedback loops closed over wireless networks. Specifically, this theory allows aperiodic data exchange between the processors computing control signals and the dynamical systems, and hence, asynchronous data can be exchanged only when needed.

In networked control systems, another challenge is to guarantee system stability in the presence of system uncertainties. Often when designing feedback controllers for dynamical systems, idealized assumptions, linearization, model-order reduction, exogenous disturbances, and unexpected system changes lead to modeling inaccuracies. If not mitigated, the uncertainties present in the system model can result in poor system performance and system instability [15, 16, 17, 18, 19, 20, 21, 22]. Therefore, it is essential in the feedback control design process to achieve robust stability and a desired level of system performance when dealing with dynamical systems subject to system uncertainties.

Motivated by these two challenges of networked control systems, this chapter studies control of uncertain dynamical systems over wireless networks with event-triggering. To this end, we consider an adaptive control approach rather than a robust control ap-

proach, since the former approach requires less system modeling information than the latter and can address system uncertainties and failures effectively in response to system variations. Notable contributions that utilize event-triggered adaptive control approaches include [23, 24, 25, 26, 27].

In particular, [23, 24] develop neural networks-based adaptive control approaches to guarantee system stability in the presence of system uncertainties, where these results only consider one-way data transmission from a dynamical system to the controller. Two-way data transmission over a wireless network; that is, from a dynamical system to the controller and from the controller to this dynamical system, is considered in [25, 26, 27] to guarantee system stability under system uncertainties. The major difference between the results in [25, 26] and [27] is that the latter does not require the knowledge of a conservative upper bound on the unknown constant gain resulting from the system uncertainty parameterization. Finally, it should be noted that all these approaches documented in [23, 24, 25, 26, 27] consider an event-triggered state feedback adaptive control approach. Yet, output feedback is required for most applications that involve high-dimensional models such as active noise suppression, active control of flexible structures, fluid flow control systems, and combustion control processes [28, 29, 30, 31, 32, 33, 34, 35].

1.2. Contribution. In this chapter, networked control for a class of uncertain dynamical systems is studied. Since a critical task in the design and implementation of networked control systems is to reduce wireless network utilization while guaranteeing system stability in the presence of system uncertainties, an event-triggered adaptive control architecture is presented in an output feedback setting to schedule two-way data exchange dependent upon errors exceeding user-defined thresholds. Specifically, we consider the output feedback adaptive control architecture predicated on the asymptotic properties of LQG/LTR controllers [33, 21, 34, 35], since this framework has the capability to achieve stringent performance specifications without causing high-frequency oscillations

in the controller response, asymptotically satisfies a strictly positive real condition for the closed-loop dynamical system, and is less complex than other approaches to output feedback adaptive control (see, for example, [29, 30, 31]).

Building on this output feedback adaptive control architecture as well as our previous event-triggered state feedback adaptive control methodology [27], it is shown using tools and methods from nonlinear systems theory and Lyapunov stability in particular that the proposed feedback control approach guarantees system stability in the presence of system uncertainties. In addition, the effect of user-defined thresholds and output feedback adaptive controller design parameters to the system performance is rigorously characterized and discussed. Moreover, we show that the proposed event-triggered output feedback adaptive control methodology does not yield to a Zeno behavior, which implies that it does not require a continuous two-way data exchange and reduces wireless network utilization. Similar to the state feedback case [27], we also show that the resulting closed-loop dynamical system performance is more sensitive to the changes in the data transmission threshold from the physical system to the adaptive controller (sensing threshold) than the data transmission threshold from the adaptive controller to the physical system (actuation threshold), which implies that the actuation threshold can be chosen large enough to reduce wireless network utilization between the physical system and the adaptive controller without sacrificing closed-loop dynamical system performance. The efficacy of the proposed event-triggered output feedback adaptive control approach is demonstrated in an illustrative numerical example. Although this chapter considers a particular output feedback adaptive control formulation to present its main contributions, the proposed approach can be used in a complimentary way with many other approaches to output feedback adaptive control concerning robotic manipulators (see, for example, [36, 37, 38, 39]).

1.3. Notation. The notation used in this chapter is fairly standard. Specifically, $\mathbb{R}$ denotes the set of real numbers, $\mathbb{R}^n$ denotes the set of $n \times 1$ real column vectors, $\mathbb{R}^{n\times m}$ denotes the set of $n \times m$ real matrices, $\mathbb{R}_+$ denotes the set of positive real numbers, $\mathbb{R}_+^{n\times n}$ denotes the set of $n \times n$ positive-definite real matrices, $\mathbb{S}^{n\times n}$ denotes the set of $n \times n$

symmetric real matrices, $\mathbb{D}^{n\times n}$ denotes the set of $n \times n$ real matrices with diagonal scalar entries, $(\cdot)^{\mathrm{T}}$ denotes transpose, $(\cdot)^{-1}$ denotes inverse, $\mathrm{tr}(\cdot)$ denotes the trace operator, and "$\triangleq$" denotes equality by definition. In addition, we write $\lambda_{\min}(A)$ (respectively, $\lambda_{\max}(A)$) for the minimum and respectively maximum eigenvalue of the Hermitian matrix A, $\|\cdot\|$ for the Euclidean norm, and $\|\cdot\|_{\mathrm{F}}$ for the Frobenius matrix norm. Furthermore, we use "$\vee$" for the "or" logic operator and "$\overline{(\cdot)}$" for the "not" logic operator.

2. OUTPUT FEEDBACK ADAPTIVE CONTROL OVERVIEW

In this section, we overview the output feedback adaptive control architecture predicated on the asymptotic properties of LQG/LTR controllers [33, 21, 34, 35], which are needed for the main results of this chapter. For this purpose, consider the uncertain dynamical system given by

$$\dot{x}_{\mathrm{p}}(t) = A_{\mathrm{p}}x_{\mathrm{p}}(t) + B_{\mathrm{p}}\Lambda\left[u(t) + \Delta\left(x_{\mathrm{p}}(t)\right)\right], \quad x_{\mathrm{p}}(0) = x_{\mathrm{p}0}, \tag{1}$$

$$y_{\mathrm{reg}}(t) = C_{\mathrm{reg}}x_{\mathrm{p}}(t), \tag{2}$$

where $A_{\mathrm{p}} \in \mathbb{R}^{n_{\mathrm{p}}\times n_{\mathrm{p}}}$, $B_{\mathrm{p}} \in \mathbb{R}^{n_{\mathrm{p}}\times m}$, and $C_{\mathrm{reg}} \in \mathbb{R}^{m\times n_{\mathrm{p}}}$ are known system matrices, $x_{\mathrm{p}}(t) \in \mathbb{R}^{n_{\mathrm{p}}}$ is the state vector, which is not available for state feedback design, $u(t) \in \mathbb{R}^m$ is the control input, $\Lambda \in \mathbb{R}_+^{m\times m} \cap \mathbb{D}^{m\times m}$ is an unknown control effectiveness matrix, $\Delta : \mathbb{R}^n \to \mathbb{R}^m$ is a system uncertainty, and $y_{\mathrm{reg}}(t) \in \mathbb{R}^m$ is the regulated output vector. In addition, we assume that the uncertain dynamical system given by (1) and (2) has a measured output vector

$$y_{\mathrm{p}}(t) = C_{\mathrm{p}}x_{\mathrm{p}}(t), \tag{3}$$

where $y_{\mathrm{p}}(t) \in \mathbb{R}^{l_{\mathrm{p}}}, C_{\mathrm{p}} \in \mathbb{R}^{l_{\mathrm{p}}\times n_{\mathrm{p}}}$, and $l_{\mathrm{p}} \geq m$ such that the elements of $y_{\mathrm{reg}}(t)$ are a subset of the elements of $y_{\mathrm{p}}(t)$. Throughout this chapter, we assume that the triple $(A_{\mathrm{p}}, B_{\mathrm{p}}, C_{\mathrm{p}})$ is minimal, the system uncertainty in (1) can be linearly parameterized as

$$\Delta(x_{\mathrm{p}}(t)) = W_o^{\mathrm{T}}\sigma_o(x_{\mathrm{p}}(t)), \tag{4}$$

where $W_o \in \mathbb{R}^{s\times m}$ is an unknown weight matrix satisfying $\|W_o\|_{\mathrm{F}} \leq \omega^*$, $\omega^* \in \mathbb{R}_+$, and $\sigma_o(x_{\mathrm{p}}(t))$ is a known Lipschitz continuous basis vector satisfying

$$\|\sigma_o(x_{\mathrm{p}}) - \sigma_o(\hat{x}_{\mathrm{p}})\| \leq L_\sigma\|x_{\mathrm{p}} - \hat{x}_{\mathrm{p}}\|, \tag{5}$$

with $L_\sigma \in \mathbb{R}_+$. These assumptions are standard in the output feedback adaptive control literature (see, for example, [33, 21, 34, 35, 40, 41]). For the case when the system uncertainty given by (4) cannot be perfectly parameterized and/or the basis vector does not satisfy (5), note that universal approximation tools such as neural networks can be used in the basis vector on a compact subset of the state space (see, for example, [42, 43]).

Similar to the approaches documented in [40, 41, 33], we consider a state observer-based nominal control architecture to achieve command following, where control of the regulated outputs that are commanded include integral action and the regulated outputs that are not commanded are subject to proportional control. For this purpose, let

$$y_{\mathrm{reg}}(t) = \begin{bmatrix} y_{\mathrm{reg1}}(t) \\ y_{\mathrm{reg2}}(t) \end{bmatrix} = \begin{bmatrix} C_{\mathrm{reg1}} \\ C_{\mathrm{reg2}} \end{bmatrix} x_{\mathrm{p}}(t), \tag{6}$$

where $y_{\mathrm{reg1}}(t) \in \mathbb{R}^r, r \leq m$, is regulated with proportional and integral control to track a given command vector $r(t) \in \mathbb{R}^r$, $y_{\mathrm{reg2}}(t) \in \mathbb{R}^{m-r}$ is regulated with proportional control, $C_{\mathrm{reg1}} \in \mathbb{R}^{r\times n_{\mathrm{p}}}$, and $C_{\mathrm{reg2}} \in \mathbb{R}^{(m-r)\times n_{\mathrm{p}}}$. Now, we define the integrator dynamics as

$$\dot{x}_{\mathrm{int}}(t) = -y_{\mathrm{reg1}}(t) + r(t) = -C_{\mathrm{reg1}}x_{\mathrm{p}}(t) + I_r r(t), \tag{7}$$

where $x_{\mathrm{int}}(t) \in \mathbb{R}^r$ is the integral state vector. Utilizing (1), (2), and (7), the augmented

system dynamics are now given by

$$\dot{x}(t) = \underbrace{\begin{bmatrix} A_{\mathrm{p}} & 0 \\ -C_{\mathrm{p1}} & 0 \end{bmatrix}}_{A} x(t) + \underbrace{\begin{bmatrix} B_{\mathrm{p}} \\ 0 \end{bmatrix}}_{B} \Lambda \left[u(t) + \Delta(x_{\mathrm{p}}(t)) \right] + \underbrace{\begin{bmatrix} 0 \\ I_r \end{bmatrix}}_{B_{\mathrm{r}}} r(t), \tag{8}$$

$$y_{\mathrm{reg}}(t) = \underbrace{\begin{bmatrix} C_{\mathrm{reg}} & 0 \end{bmatrix}}_{C_{\mathrm{Reg}}} x(t), \tag{9}$$

where $x(t) = [x_{\mathrm{p}}^{\mathrm{T}}(t), x_{\mathrm{int}}^{\mathrm{T}}(t)]^{\mathrm{T}} \in \mathbb{R}^n$, $A \in \mathbb{R}^{n \times n}$, $B \in \mathbb{R}^{n \times m}$, $B_{\mathrm{r}} \in \mathbb{R}^{n \times r}$,$C_{\mathrm{Reg}} \in \mathbb{R}^{m \times n}$, and $n = n_{\mathrm{p}} + r$. In addition, the augmented measured output vector becomes

$$y(t) = \begin{bmatrix} y_{\mathrm{p}}(t) \\ x_{\mathrm{int}}(t) \end{bmatrix} = \underbrace{\begin{bmatrix} C_{\mathrm{p}} & 0 \\ 0 & I_r \end{bmatrix}}_{C} x(t) \tag{10}$$

where $y(t) \in \mathbb{R}^l$, $C \in \mathbb{R}^{l \times n}$, and $l = l_{\mathrm{p}} + r$.

Next, we define the feedback control law as

$$u(t) = u_{\mathrm{n}}(t) + u_{\mathrm{a}}(t), \tag{11}$$

where $u_{\mathrm{n}}(t)$ is a nominal control law and $u_{\mathrm{a}}(t)$ is an adaptive control law. Using the output feedback adaptive control architecture documented in [33, 21, 34, 35], we consider the nominal controller given by

$$u_{\mathrm{n}}(t) = -K_x \hat{x}(t), \tag{12}$$

where $K_x \in \mathbb{R}^{m \times n}$ is a feedback matrix and $\hat{x}(t)$ is an estimate of the augmented system state vector $x(t)$ through a state observer to be defined later in this section. In order to determine the structure of the adaptive controller, we rewrite the augmented system dynamics

given by (8) and (9) as

$$\dot{x}(t) = Ax(t) + Bu_{\mathrm{n}}(t) + B\Lambda\left(u_{\mathrm{a}}(t) + W^{\mathrm{T}}\sigma\left(x_{\mathrm{p}}(t), u_{\mathrm{n}}(t)\right)\right) + B_{\mathrm{r}}r(t), \tag{13}$$

where $W \triangleq \left[W_o^{\mathrm{T}}, I_{m\times m} - \Lambda^{-1}\right]^{\mathrm{T}} \in \mathbb{R}^{(n+m)\times m}$ and $\sigma\left(x_{\mathrm{p}}(t), u_{\mathrm{n}}(t)\right) \triangleq \left[\sigma_o^{\mathrm{T}}(x_{\mathrm{p}}(t)), u_{\mathrm{n}}^{\mathrm{T}}(t)\right]^{\mathrm{T}} \in \mathbb{R}^{n+m}$. Motivating from the structure of the system uncertainties appearing in (13), consider the adaptive controller given by

$$u_{\mathrm{a}}(t) = -\hat{W}(t)^{\mathrm{T}}\sigma\left(\hat{x}_{\mathrm{p}}(t), u_{\mathrm{n}}(t)\right), \tag{14}$$

where $\sigma\left(\hat{x}_{\mathrm{p}}(t), u_{\mathrm{n}}(t)\right) \triangleq \left[\sigma_o^{\mathrm{T}}(\hat{x}_{\mathrm{p}}(t)), u_{\mathrm{n}}^{\mathrm{T}}(t)\right]^{\mathrm{T}} \in \mathbb{R}^{n+m}$ and $\hat{W}(t) \in \mathbb{R}^{(n+m)\times m}$ is the estimate of the unknown weight matrix W through the weight update law

$$\dot{\hat{W}}(t) = \Gamma\,\mathrm{Proj}_{\mathrm{m}}\left[\hat{W}(t), -\sigma\left(\hat{x}_{\mathrm{p}}(t), u_{\mathrm{n}}(t)\right)\tilde{y}^{\mathrm{T}}(t)R_0^{-\frac{1}{2}}ZS^{\mathrm{T}}\right], \tag{15}$$

where $\mathrm{Proj}_{\mathrm{m}}$ denotes the projection operator defined for matrices [44, 45, 21, 27], $\Gamma \in \mathbb{R}_+^{(s+m)\times(s+m)} \cap \mathbb{S}^{(s+m)\times(s+m)}$ is a learning rate matrix, $\tilde{y}(t) \in \mathbb{R}^l$ given by

$$\tilde{y}(t) \triangleq \hat{y}(t) - y(t) = C(\hat{x}(t) - x(t)), \tag{16}$$

is the measured output error, and $\hat{x}(t) \in \mathbb{R}^n$ is the estimated augmented system state obtained through the state observer given by

$$\dot{\hat{x}}(t) = A\hat{x}(t) + Bu_{\mathrm{n}}(t) + L_v\left(y(t) - \hat{y}(t)\right) + B_{\mathrm{r}}r(t), \tag{17}$$

$$\hat{y}(t) = C\hat{x}(t), \tag{18}$$

with $L_v \in \mathbb{R}^{n\times l}$ being the state observer gain matrix.

Following [33, 21], the state observer gain matrix is given by

$$L_v = P_v C^{\mathrm{T}} R_v^{-1}, \tag{19}$$

with $P_v \in \mathbb{R}_+^{n\times n}$ being the unique solution to the algebraic Riccati equation

$$0 = P_v \left(A + \eta I_{n\times n}\right)^{\mathrm{T}} + \left(A + \eta I_{n\times n}\right) P_v - P_v C^{\mathrm{T}} R_v^{-1} C P_v + Q_v, \quad \eta \in \mathbb{R}_+, \tag{20}$$

$$Q_v = Q_0 + \left(\frac{v+1}{v}\right) B_s B_s^{\mathrm{T}}, \quad Q_0 \in \mathbb{R}_+^{n\times n}, \quad v \in \mathbb{R}_+, \tag{21}$$

$$R_v = \left(\frac{v}{v+1}\right) R_0, \quad R_0 \in \mathbb{R}_+^{l\times l}. \tag{22}$$

In (21), $B_s = [B,\ B_2]$, where $B_2 \in \mathbb{R}^{n\times(l-m)}$ is a matrix such that $\det(CB_s) \neq 0$ and $C(sI_{n\times n} - A)^{-1}B_s$ is minimum phase. Note that $l > m$ is assumed in the above construction, where if $l = m$ then $B_2 = 0$. In addition, the observer closed-loop matrix given by

$$A_v = A - L_v C = A - P_v C^{\mathrm{T}} R_v^{-1} C \tag{23}$$

is Hurwitz for all $v \in \mathbb{R}_+$. Moreover, let $\tilde{P}_v = P_v^{-1}$ and $S = [I_{m\times m}\ ,\ 0_{m\times(l-m)}]$ to note [33, 21]

$$\tilde{P}_v B = C^{\mathrm{T}} R_0^{-\frac{1}{2}} Z S^{\mathrm{T}} + O(v), \tag{24}$$

and

$$A_v^{\mathrm{T}} \tilde{P}_v + \tilde{P}_v A_v = -C^{\mathrm{T}} R_v^{-1} C - \tilde{P}_v Q_v \tilde{P}_v - 2\eta \tilde{P}_v < 0. \tag{25}$$

In (15) and (24), $Z = (UV)^{\mathrm{T}}$, where two unitary matrices U and V result from the singular value decomposition $B_s^{\mathrm{T}} C^{\mathrm{T}} R_0^{-1/2} = U\Sigma V$ and Σ is the diagonal matrix of the corresponding singular values. In (24), "$O(\cdot)$" denotes the Bachmann-Lundau asymptotic order notation [46, 47]. For additional details on the output feedback adaptive control architecture overviewed in this section, we refer to [33, 21] as well as [34, 35]. To summarize, as

previously discussed, the considered architecture has the capability to achieve stringent performance specifications without causing high-frequency oscillations in the controller response, asymptotically satisfies a strictly positive real condition for the closed-loop dynamical system, and is less complex than other approaches to output feedback adaptive control.

Finally, for analysis purposes later in this chapter, we define the reference model capturing the ideal closed-loop dynamical system performance given by

$$\dot{x}_{\mathrm{m}} = A_{\mathrm{m}} x_{\mathrm{m}}(t) + B_{\mathrm{m}} r(t), \quad x_{\mathrm{m}}(0) = x_{\mathrm{m0}}, \tag{26}$$

$$y_{\mathrm{m}} = C_{\mathrm{Reg}} x_{\mathrm{m}}, \tag{27}$$

where $x_{\mathrm{m}}(t) \in \mathbb{R}^n$ is the reference model state, $A_{\mathrm{m}} = A - BK_x$ is Hurwitz, and $B_{\mathrm{m}} = B_{\mathrm{r}}$. In addition, let

$$\tilde{x}(t) \triangleq \hat{x}(t) - x(t), \tag{28}$$

$$\hat{e}(t) \triangleq \hat{x}(t) - x_{\mathrm{m}}(t), \tag{29}$$

$$\tilde{W}(t) \triangleq \hat{W}(t) - W. \tag{30}$$

be the state estimation error, the state tracking error, and the weight estimation error, respectively. Now, we can write

$$\dot{\hat{e}}(t) = A_{\mathrm{m}} \hat{e}(t) + L_v \left(y(t) - \hat{y}(t) \right), \tag{31}$$

using (17) and (26), and write

$$\begin{aligned} \dot{\tilde{x}}(t) &= \left(A - L_v C\right) \tilde{x}(t) + B\Lambda \left(\hat{W}^{\mathrm{T}}(t) \sigma \left(\hat{x}_{\mathrm{p}}(t), u_{\mathrm{n}}(t) \right) - W^{\mathrm{T}} \sigma \left(x_{\mathrm{p}}(t), u_{\mathrm{n}}(t) \right) \right) \\ &= A_v \tilde{x}(t) + B\Lambda \left(\tilde{W}^{\mathrm{T}}(t) \sigma \left(\hat{x}_{\mathrm{p}}(t), u_{\mathrm{n}}(t) \right) + g\left(\cdot\right) \right), \end{aligned} \tag{32}$$

using (13) and (17), where $g\left(\cdot\right) \triangleq W^{\mathrm{T}} \left(\sigma \left(\hat{x}_{\mathrm{p}}(t), u_{\mathrm{n}}(t) \right) - \sigma \left(x_{\mathrm{p}}(t), u_{\mathrm{n}}(t) \right) \right)$.

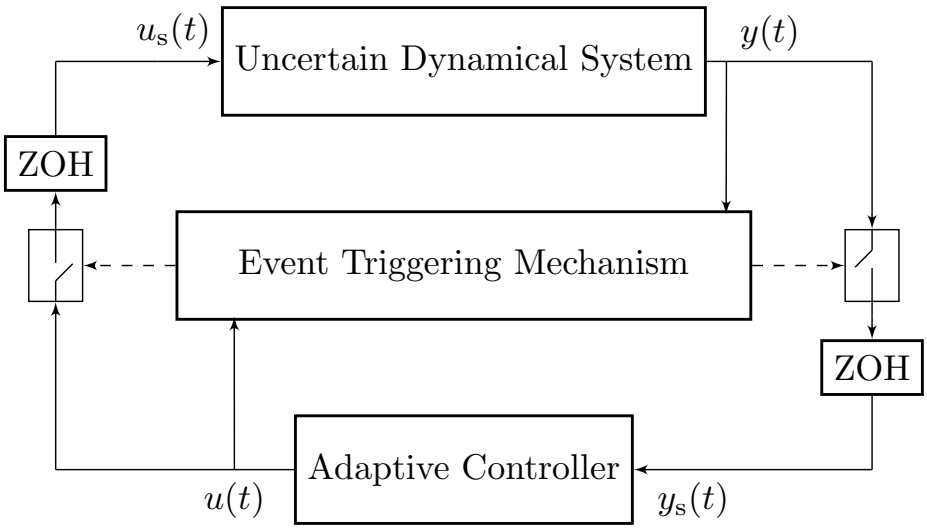

Figure 1. Event-triggered adaptive control system.

3. EVENT-TRIGGERED OUTPUT FEEDBACK ADAPTIVE CONTROL

In this section, we present the proposed event-triggered output feedback adaptive control architecture, which allows a desirable command following performance while the proposed controller exchanges data with the uncertain dynamical system through a wireless network. Mathematically speaking, the uncertain dynamical system sends its output signal to the adaptive controller only when a predefined event occurs. The kth time instants of the output transmission is represented by the monotonic sequence $\{s_k\}_{k=1}^{\infty}$, where $s_k \in \mathbb{R}_+$. The controller then uses this triggered system output signal to compute the control signal using the output feedback control architecture. Likewise, the updated feedback control input is transmitted to the uncertain dynamical system only when another predefined event occurs. The jth time instants of the feedback control transmission is then represented by the monotonic sequence $\left\{r_j\right\}_{j=1}^{\infty}$, where $r_j \in \mathbb{R}_+$. As depicted in Figure 1, each system output signal and control input is held by a zero-order-hold operator (ZOH) until the next triggering event for that signal takes place. In this chapter, we do not consider delay in sampling, data transmission, and computation.

3.1. Proposed Event-triggered Adaptive Control Algorithm. Based on the two-way data exchange structure depicted in Figure 1, consider the augmented uncertain dynamical system given by

$$\dot{x}(t) = Ax(t) + B\Lambda \left[u_{\mathrm{s}}(t) + \Delta(x_{\mathrm{p}}(t))\right] + B_{\mathrm{r}} r(t), \tag{33}$$

$$y_{\mathrm{reg}}(t) = C_{\mathrm{Reg}} x(t), \quad y(t) = Cx(t), \tag{34}$$

where $u_{\mathrm{s}}(t) \in \mathbb{R}^m$ is the sampled control input vector. Under the assumptions stated in Section 2 and considering the feedback control law given by (11) subject to the nominal controller given by (12) and the adaptive controller given by (14), the augmented uncertain dynamical system given by (33) and (34) can be equivalently written as

$$\dot{x}(t) = Ax(t) + Bu_{\mathrm{n}}(t) + B\Lambda \left(u_{\mathrm{a}}(t) + W^{\mathrm{T}} \sigma \left(x_{\mathrm{p}}(t), u_{\mathrm{n}}(t)\right)\right) + B\Lambda \left(u_{\mathrm{s}}(t) - u(t)\right) + B_{\mathrm{r}} r(t), \tag{35}$$

$$y_{\mathrm{reg}}(t) = C_{\mathrm{Reg}} x(t), \quad y(t) = Cx(t). \tag{36}$$

In addition, we consider

$$\dot{\hat{W}}(t) = \Gamma \, \mathrm{Proj}_{\mathrm{m}}\left[\hat{W}(t), -\sigma \left(\hat{x}_{\mathrm{p}}(t), u_{\mathrm{n}}(t)\right) \left(\hat{y}(t) - y_{\mathrm{s}}(t)\right)^{\mathrm{T}} R_0^{-\frac{1}{2}} Z S^{\mathrm{T}}\right], \tag{37}$$

for the estimated weight matrix $\hat{W}(t)$ in (14) and

$$\begin{aligned} \dot{\hat{x}}(t) &= A\hat{x}(t) + Bu_{\mathrm{n}}(t) + L_v \left(y_{\mathrm{s}}(t) - \hat{y}(t)\right) + B_{\mathrm{r}} r(t) \\ &= A_{\mathrm{m}} \hat{x}(t) + L_v \left(y_{\mathrm{s}}(t) - \hat{y}(t)\right) + B_{\mathrm{r}} r(t), \end{aligned} \tag{38}$$

$$\hat{y}(t) = C\hat{x}(t), \tag{39}$$

for the state observer, where $y_{\mathrm{s}}(t) \in \mathbb{R}^l$ in (37) and (38) denotes the sampled augmented measured output vector.

Table 1. Event-triggered output feedback adaptive control algorithm.

Augmented unc. dyn. sys.	$\dot{x}(t) = Ax(t) + B\Lambda \left[u_{\mathrm{s}}(t) + \Delta(x_{\mathrm{p}}(t))\right] + B_{\mathrm{r}} r(t),$ $y_{\mathrm{reg}}(t) = C_{\mathrm{Reg}} x(t),$ $y(t) = Cx(t)$
Feedback control law	$u(t) = u_{\mathrm{n}}(t) + u_{\mathrm{a}}(t)$
Nominal control law	$u_{\mathrm{n}}(t) = -K_x \hat{x}(t)$
Adaptive control law	$u_{\mathrm{a}}(t) = -\hat{W}(t)^{\mathrm{T}} \sigma\left(\hat{x}_{\mathrm{p}}(t), u_{\mathrm{n}}(t)\right),$ $\dot{\hat{W}}(t) = \Gamma \operatorname{Proj}_{\mathrm{m}}\Big[\hat{W}(t), -\sigma\left(\hat{x}_{\mathrm{p}}(t), u_{\mathrm{n}}(t)\right)(\hat{y}(t) - y_{\mathrm{s}}(t))^{\mathrm{T}}$ $\cdot R_0^{-\frac{1}{2}} Z S^{\mathrm{T}}\Big]$
State observer	$\dot{\hat{x}}(t) = A_{\mathrm{m}} \hat{x}(t) + L_v\left(y_{\mathrm{s}}(t) - \hat{y}(t)\right) + B_{\mathrm{r}} r(t),$ $\hat{y}(t) = C\hat{x}(t)$

The proposed event-triggered output feedback adaptive control algorithm is summarized in Table 1. Specifically, based on the two-way data exchange structure depicted in Figure 1, the controller generates $u(t)$ and the uncertain dynamical system is driven by the sampled version of this control signal $u_{\mathrm{s}}(t)$ depending on an event-triggering mechanism. Similarly, the controller utilizes $y_{\mathrm{s}}(t)$ that represents the sampled version of the uncertain dynamical system measured output $y(t)$ depending on an event-triggering mechanism. These event-triggering mechanisms are stated next.

3.2. Scheduling Two-way Data Exchange. Let $\epsilon_y \in \mathbb{R}_+$ be a given, user-defined sensing threshold to allow for data transmission from the uncertain dynamical system to the controller. In addition, let $\epsilon_u \in \mathbb{R}_+$ be a given, user-defined actuation threshold to allow for data transmission from the controller to the uncertain dynamical system. Similar in fashion

to [25, 27], we now define three logic rules for scheduling the two-way data exchange

$$E_1 : \quad \|y_{\rm s}(t) - y(t)\| \leq \epsilon_y, \tag{40}$$

$$E_2 : \quad \|u_{\rm s}(t) - u(t)\| \leq \epsilon_u, \tag{41}$$

$$E_3 : \quad \text{The controller receives } y_{\rm s}(t). \tag{42}$$

Specifically, when the inequality (40) is violated at the s_k moment of the kth time instant, the uncertain dynamical system triggers the measured output signal information such that $y_{\rm s}(t)$ is sent to the controller. Likewise, when (41) is violated or the controller receives a new transmitted system output from the uncertain dynamical system (i.e., when $\overline{E}_2 \vee E_3$ is true), then the feedback controller sends a new control input $u_{\rm s}(t)$ to the uncertain dynamical system at the r_j moment of the jth time instant.

Finally, using the definitions given by (28), (29), and (30), we write

$$\dot{\hat{e}}(t) = A_{\rm m}\hat{e}(t) + L_v\left(y_{\rm s}(t) - \hat{y}(t)\right), \quad \hat{e}(0) = \hat{e}_0, \tag{43}$$

$$\begin{aligned}\dot{\tilde{x}}(t) &= A_v\tilde{x}(t) + L_v\left(y_{\rm s}(t) - y(t)\right) + B\Lambda\left(\tilde{W}^{\rm T}(t)\sigma\left(\hat{x}_{\rm p}(t), u_{\rm n}(t)\right) + g\left(\cdot\right)\right) \\ &\quad -B\Lambda\left(u_{\rm s}(t) - u(t)\right), \quad \tilde{x}(0) = \tilde{x}_0.\end{aligned} \tag{44}$$

In the next section, we analyze the stability and performance of the proposed event-triggered output feedback adaptive control algorithm introduced in this section (see Table 1) using the error dynamics given by (43) and (44) well as the data exchange rules E_1, E_2, and E_3 respectively given by (40), (41), and (42).

4. STABILITY AND PERFORMANCE ANALYSIS

For organizational purposes, this section is divided into three subsections. Specifically, we analyze the uniform ultimate boundedness of the resulting closed-loop dynamical system in Section 4.1, compute the ultimate bound and highlight the effect of user-defined

thresholds and the adaptive controller design parameters to this ultimate bound in Section 4.2, and show that the proposed architecture does not yield to a Zeno behavior in Section 4.3.

4.1. Uniform Ultimate Boundedness Analysis. The following theorem presents the first result of this chapter.

Theorem 1. Consider the uncertain dynamical system given by (33) and (34), the reference model given by (26) and (27), the state observer given by (38) and (58) with the state observer gain matrix in (19) along with (20), (21), and (22), and the feedback control law given by (11), (12), (14), and (37). In addition, let the data transmission from the uncertain dynamical system to the controller occur when $\overline{E}_1$ is true and the data transmission from the controller to the uncertain dynamical system occur when $\overline{E}_2 \vee E_3$ is true. Then, the closed-loop solution $(\tilde{x}(t), \tilde{W}(t), \hat{e}(t))$ is uniformly ultimately bounded for all initial conditions.

Proof. Since the data transmission from the uncertain dynamical system to the controller and from the controller to the uncertain dynamical system occur when $\overline{E}_1$ and $\overline{E}_2 \vee E_3$ are true, respectively, note that $\|y_{\mathrm{s}}(t) - y(t)\| \leq \epsilon_y$ and $\|u_{\mathrm{s}}(t) - u(t)\| \leq \epsilon_u$ hold.

Consider the Lyapunov-like function given by

$$\mathcal{V}(\tilde{x}, \tilde{W}, \hat{e}) = \tilde{x}^{\mathrm{T}}(t)\tilde{P}_v\tilde{x} + \operatorname{tr}\left((\tilde{W}\Lambda^{\frac{1}{2}})^{\mathrm{T}}\Gamma^{-1}(\tilde{W}\Lambda^{\frac{1}{2}})\right) + \beta\hat{e}^{\mathrm{T}}P\hat{e}, \tag{45}$$

where $\tilde{P}_v \in \mathbb{R}_+^{n\times n}$ is a solution to (25) with $R_v \in \mathbb{R}_+^{l\times l}$ and $Q_v \in \mathbb{R}_+^{n\times n}$, $v \in \mathbb{R}_+$, $\eta \in \mathbb{R}_+$, $\beta \in \mathbb{R}_+$, and $P \in \mathbb{R}_+^{n\times n} \cap \mathbb{S}^{n\times n}$ is a solution to

$$0 = A_{\mathrm{m}}^{\mathrm{T}}P + PA_{\mathrm{m}} - PBR^{-1}B^{\mathrm{T}}P + Q, \tag{46}$$

with $R \in \mathbb{R}_+^{m\times m}$ and $Q \in \mathbb{R}_+^{n\times n}$. Note that $\mathcal{V}(0,0,0) = 0$ and $\mathcal{V}(\tilde{x}, \tilde{W}, \hat{e}) > 0$ for all $(\tilde{x}, \tilde{W}, \hat{e}) \neq (0,0,0)$. The time-derivative of (45) is given by

$$
\begin{aligned}
&\dot{\mathcal{V}}(\tilde{x}(t),\tilde{W}(t),\hat{e}(t)) \\
&\quad = \; 2\tilde{x}^{\mathrm{T}}(t)\tilde{P}_v\dot{\tilde{x}}(t) + 2\mathrm{tr}\left(\tilde{W}^{\mathrm{T}}(t)\Gamma^{-1}\dot{\tilde{W}}(t)\Lambda\right) + 2\beta\hat{e}^{\mathrm{T}}(t)P\dot{\hat{e}}(t) \\
&\quad = \; 2\tilde{x}^{\mathrm{T}}(t)\tilde{P}_v\Big(A_v\tilde{x}(t) + L_v\left(y_{\mathrm{s}}(t) - y(t)\right) + B\Lambda\Big(\tilde{W}^{\mathrm{T}}(t)\sigma\left(\hat{x}_{\mathrm{p}}(t),u_{\mathrm{n}}(t)\right) + g\left(\cdot\right)\Big) \\
&\qquad - B\Lambda\left(u_{\mathrm{s}}(t) - u(t)\right)\Big) + 2\mathrm{tr}\left(\tilde{W}^{\mathrm{T}}(t)\Gamma^{-1}\dot{\tilde{W}}(t)\Lambda\right) + 2\beta\hat{e}^{\mathrm{T}}(t)P\dot{\hat{e}}(t) \\
&\quad = \; -\tilde{x}^{\mathrm{T}}(t)\left(C^{\mathrm{T}}R_v^{-1}C + \tilde{P}_vQ_v\tilde{P}_v + 2\eta\tilde{P}_v\right)\tilde{x}(t) + 2\tilde{x}^{\mathrm{T}}(t)\tilde{P}_vL_v\left(y_{\mathrm{s}}(t) - y(t)\right) + 2\tilde{x}^{\mathrm{T}}(t) \\
&\qquad \cdot \tilde{P}_vB\Lambda\tilde{W}^{\mathrm{T}}(t)\sigma\left(\hat{x}_{\mathrm{p}}(t),u_{\mathrm{n}}(t)\right) + 2\tilde{x}^{\mathrm{T}}(t)\tilde{P}_vB\Lambda g\left(\cdot\right) - 2\tilde{x}^{\mathrm{T}}(t)\tilde{P}_vB\Lambda\left(u_{\mathrm{s}}(t) - u(t)\right) \\
&\qquad + 2\mathrm{tr}\left(\tilde{W}^{\mathrm{T}}(t)\Gamma^{-1}\dot{\tilde{W}}(t)\Lambda\right) + 2\beta\hat{e}^{\mathrm{T}}(t)P\dot{\hat{e}}(t) \\
&\quad = \; -\left(1+\frac{1}{v}\right)\tilde{x}^{\mathrm{T}}(t)C^{\mathrm{T}}R_0^{-1}C\tilde{x}(t) - \tilde{x}^{\mathrm{T}}(t)\tilde{P}_vQ_0\tilde{P}_v\tilde{x}(t) - \left(1+\frac{1}{v}\right)\tilde{x}^{\mathrm{T}}(t)\tilde{P}_vB_sB_s^{\mathrm{T}}\tilde{P}_v\tilde{x}(t) \\
&\qquad - 2\eta\tilde{x}(t)^{\mathrm{T}}(t)\tilde{P}_v\tilde{x}(t) + 2\tilde{x}^{\mathrm{T}}(t)\left(C^{\mathrm{T}}R_0^{-\frac{1}{2}}ZS^{\mathrm{T}} + O(v)\right)\Lambda\tilde{W}^{\mathrm{T}}(t)\sigma\left(\hat{x}_{\mathrm{p}}(t),u_{\mathrm{n}}(t)\right) \\
&\qquad + 2\tilde{x}^{\mathrm{T}}(t)\tilde{P}_vB\Lambda g\left(\cdot\right) + 2\tilde{x}^{\mathrm{T}}(t)\tilde{P}_vL_v\left(y_{\mathrm{s}}(t) - y(t)\right) - 2\tilde{x}^{\mathrm{T}}(t)\tilde{P}_vB\Lambda\left(u_{\mathrm{s}}(t) - u(t)\right) \\
&\qquad + 2\mathrm{tr}\left(\tilde{W}^{\mathrm{T}}(t)\Gamma^{-1}\dot{\tilde{W}}(t)\Lambda\right) + 2\beta\hat{e}^{\mathrm{T}}(t)P\dot{\hat{e}}(t) \\
&\quad = \; -\left(1+\frac{1}{v}\right)\tilde{x}^{\mathrm{T}}(t)C^{\mathrm{T}}R_0^{-1}C\tilde{x}(t) - \tilde{x}^{\mathrm{T}}(t)\tilde{P}_vQ_0\tilde{P}_v\tilde{x}(t) - \left(1+\frac{1}{v}\right)\tilde{x}^{\mathrm{T}}(t)\tilde{P}_vB_sB_s^{\mathrm{T}}\tilde{P}_v\tilde{x}(t) \\
&\qquad - 2\eta\tilde{x}^{\mathrm{T}}(t)\tilde{P}_v\tilde{x}(t) + 2\tilde{x}^{\mathrm{T}}(t)O(v)\Lambda\tilde{W}^{\mathrm{T}}(t)\sigma\left(\hat{x}_{\mathrm{p}}(t),u_{\mathrm{n}}(t)\right) + 2\tilde{x}^{\mathrm{T}}(t)\tilde{P}_vB\Lambda g\left(\cdot\right) \\
&\qquad + 2\tilde{x}^{\mathrm{T}}(t)\tilde{P}_vL_v\left(y_{\mathrm{s}}(t) - y(t)\right) - 2\tilde{x}^{\mathrm{T}}(t)\tilde{P}_vB\Lambda\left(u_{\mathrm{s}}(t) - u(t)\right) + 2\mathrm{tr}\Big(\tilde{W}^{\mathrm{T}}(t)\Big(\Gamma^{-1}\dot{\tilde{W}}(t) \\
&\qquad + \sigma\left(\hat{x}_{\mathrm{p}}(t),u_{\mathrm{n}}(t)\right)\tilde{y}^{\mathrm{T}}R_0^{-\frac{1}{2}}ZS^{\mathrm{T}}\Big)\Lambda\Big) + 2\beta\hat{e}^{\mathrm{T}}(t)P\left(A_{\mathrm{m}}\hat{e}(t) + L_v\left(y_{\mathrm{s}}(t) - \hat{y}(t)\right)\right). \quad (47)
\end{aligned}
$$

Now, noting $\|O(v)\| \leq vK$, $K \in \mathbb{R}_+$, and using (37) in (47) yields

$$
\begin{aligned}
&\dot{\mathcal{V}}(\tilde{x}(t)(t),\tilde{W}(t),\hat{e}(t)) \\
&\quad \leq \; -\left(1+\frac{1}{v}\right)\tilde{x}^{\mathrm{T}}(t)C^{\mathrm{T}}R_0^{-1}C\tilde{x}(t) - \tilde{x}^{\mathrm{T}}(t)\tilde{P}_vQ_0\tilde{P}_v\tilde{x}(t) - \left(1+\frac{1}{v}\right)\tilde{x}^{\mathrm{T}}(t)\tilde{P}_vB_sB_s^{\mathrm{T}}\tilde{P}_v\tilde{x}(t) \\
&\qquad - 2\eta\tilde{x}^{\mathrm{T}}(t)\tilde{P}_v\tilde{x}(t) + 2\tilde{x}^{\mathrm{T}}(t)O(v)\Lambda\tilde{W}^{\mathrm{T}}(t)\sigma\left(\hat{x}_{\mathrm{p}}(t),u_{\mathrm{n}}(t)\right) + 2\tilde{x}^{\mathrm{T}}(t)\tilde{P}_vB\Lambda g\left(\cdot\right) + 2\tilde{x}^{\mathrm{T}}(t) \\
&\qquad \cdot \tilde{P}_vL_v\left(y_{\mathrm{s}}(t) - y(t)\right) - 2\tilde{x}^{\mathrm{T}}(t)\tilde{P}_vB\Lambda\left(u_{\mathrm{s}}(t) - u(t)\right) + 2\left(y_{\mathrm{s}}(t) - y(t)\right)^{\mathrm{T}}R_0^{-\frac{1}{2}}ZS^{\mathrm{T}}\Lambda \\
&\qquad \cdot \tilde{W}^{\mathrm{T}}(t)\sigma\left(\hat{x}_{\mathrm{p}}(t),u_{\mathrm{n}}(t)\right) - \beta\hat{e}^{\mathrm{T}}(t)\left(-PBR^{-1}B^{\mathrm{T}}P + Q\right)\hat{e}(t) - 2\beta\hat{e}^{\mathrm{T}}(t)PL_vC\tilde{x}(t)
\end{aligned}
$$

$$
\begin{aligned}
&+ 2\beta\hat{e}^{\mathrm{T}}(t)PL_v\left(y_{\mathrm{s}}(t) - y(t)\right) \\
\leq\ & -\left(1+\frac{1}{v}\right)\lambda_{\min}(R_0^{-1})\|C\|_{\mathrm{F}}^2\,\|\tilde{x}(t)\|^2 - \lambda_{\min}(Q_0)\lambda_{\min}^2(\tilde{P}_v)\,\|\tilde{x}(t)\|^2 - \left(1+\frac{1}{v}\right) \\
&\cdot \lambda_{\min}^2(\tilde{P}_v)\,\|B_s\|_{\mathrm{F}}^2\,\|\tilde{x}(t)\|^2 - 2\eta\lambda_{\min}(\tilde{P}_v)\,\|\tilde{x}(t)\|^2 + 2Kv\,\|\Lambda\|_{\mathrm{F}}\left\|\tilde{W}(t)\right\|_{\mathrm{F}} \\
&\cdot \left\|\sigma\left(\hat{x}_{\mathrm{p}}(t), u_{\mathrm{n}}(t)\right)\right\|\|\tilde{x}(t)\| + 2\,\|\tilde{x}(t)\|\left\|\tilde{P}_v B\right\|_{\mathrm{F}}\|\Lambda\|_{\mathrm{F}}\,\|g\,(\cdot)\| + 2\,\|\tilde{x}(t)\|\left\|\tilde{P}_v\right\|_{\mathrm{F}}\|L_v\|_{\mathrm{F}}\,\epsilon_y \\
&+ 2\,\|\tilde{x}(t)\|\left\|\tilde{P}_v B\right\|_{\mathrm{F}}\|\Lambda\|_{\mathrm{F}}\,\epsilon_u + 2\epsilon_y\lambda_{\min}(R_0^{-\frac{1}{2}})\left\|ZS^{\mathrm{T}}\right\|_{\mathrm{F}}\|\Lambda\|_{\mathrm{F}}\left\|\tilde{W}(t)\right\|_{\mathrm{F}}\left\|\sigma\left(\hat{x}_{\mathrm{p}}(t), u_{\mathrm{n}}(t)\right)\right\| \\
&- \beta\Big(\lambda_{\min}(Q) - \lambda_{\max}(R^{-1})\,\|PB\|_{\mathrm{F}}^2\Big)\,\|\hat{e}(t)\|^2 + 2\beta\,\|\hat{e}(t)\|\,\|PL_vC\|_{\mathrm{F}}\,\|\tilde{x}(t)\| \\
&+ 2\beta\,\|\hat{e}(t)\|\,\|P\|_{\mathrm{F}}\,\|L_v\|_{\mathrm{F}}\,\epsilon_y. \qquad (48)
\end{aligned}
$$

Next, using (5), an upper bound for $\|g\,(\cdot)\|$ in (48) is given by

$$
\begin{aligned}
\|g\,(\cdot)\| &= \left\|W^{\mathrm{T}}\left(\sigma\left(\hat{x}_{\mathrm{p}}(t), u_{\mathrm{n}}(t)\right) - \sigma\left(x_{\mathrm{p}}(t), u_{\mathrm{n}}(t)\right)\right)\right\| \\
&\leq \underbrace{W_{\max}L_\sigma}_{K_g}\left\|\hat{x}_{\mathrm{p}}(t) - x_{\mathrm{p}}(t)\right\| \\
&\leq K_g\,\|\tilde{x}(t)\|, \qquad (49)
\end{aligned}
$$

where $K_g \in \mathbb{R}_+$ and $||W||_{\mathrm{F}} \leq W_{\max}$, $W_{\max} \in \mathbb{R}_+$. In addition, noting $\left\|\hat{x}_{\mathrm{p}}(t)\right\| \leq \|\hat{x}(t)\|$ and using (5), one can compute an upper bound for $\left\|\sigma\left(\hat{x}_{\mathrm{p}}(t), u_{\mathrm{n}}(t)\right)\right\|$ in (48) as

$$
\begin{aligned}
\left\|\sigma\left(\hat{x}_{\mathrm{p}}(t), u_{\mathrm{n}}(t)\right)\right\| &= \left\|\sigma\left(\hat{x}_{\mathrm{p}}(t), u_{\mathrm{n}}(t)\right) + \sigma(0) - \sigma(0)\right\| \\
&\leq \|\sigma(0)\| + \left\|\sigma\left(\hat{x}_{\mathrm{p}}(t), u_{\mathrm{n}}(t)\right) - \sigma(0)\right\| \\
&\leq b_\sigma + \left\|\begin{matrix}\sigma\left(\hat{x}_{\mathrm{p}}(t)\right) - \sigma(0) \\ u_{\mathrm{n}}(t)\end{matrix}\right\| \\
&\leq b_\sigma + \sqrt{\left\|\sigma\left(\hat{x}_{\mathrm{p}}(t)\right) - \sigma(0)\right\|^2 + \|K_x\|^2\,\|\hat{x}(t)\|^2} \\
&\leq b_\sigma + \sqrt{L_\sigma^2\,\|\hat{x}(t)\|^2 + \|K_x\|^2\,\|\hat{x}(t)\|^2} \\
&\leq b_\sigma + \sqrt{L_\sigma^2 + \|K_x\|^2}\,\|\hat{x}(t)\|. \qquad (50)
\end{aligned}
$$

Furthermore, since A_{m} is Hurwitz and $r(t)$ is bounded in (38), there exist constants ζ_1 and ζ_2 such that $\|\hat{x}(t)\| \leq \zeta_1 + \zeta_2 \|y_{\mathrm{s}}(t) - \hat{y}(t)\|$ holds [48], where this yields

$$\|\hat{x}(t)\| \leq \zeta_1 + \zeta_2 \epsilon_y + \zeta_2 \|C\|_{\mathrm{F}} \|\tilde{x}(t)\| . \tag{51}$$

Finally, using (51) in (50) gives

$$\begin{aligned} \left\|\sigma\left(\hat{x}_{\mathrm{p}}(t), u_{\mathrm{n}}(t)\right)\right\| &\leq b_\sigma + \sqrt{L_\sigma^2 + \|K_x\|^2}\left(\zeta_1 + \zeta_2 \epsilon_y + \zeta_2 \|C\|_{\mathrm{F}} \|\tilde{x}(t)\|\right) \\ &= b_1 + b_2 \epsilon_y + b_3 \|\tilde{x}(t)\| , \end{aligned} \tag{52}$$

where $b_1 \triangleq b_\sigma + \zeta_1 \sqrt{L_\sigma^2 + \|K_x\|^2}$, $b_2 \triangleq \zeta_2 \sqrt{L_\sigma^2 + \|K_x\|^2}$, and $b_3 \triangleq \zeta_2 \|C\|_{\mathrm{F}} \sqrt{L_\sigma^2 + \|K_x\|^2}$.

Noting that $\lambda_{\min}(\tilde{P}_v) \geq \lambda_{\min}(\tilde{P}_0) > 0$ [21] and using the bounds given by (49) and (52) in (48), one can write

$$\begin{aligned} &\dot{\mathcal{V}}(\tilde{x}(t), \tilde{W}(t), \hat{e}(t)) \\ &\leq -\left(1 + \frac{1}{v}\right) \lambda_{\min}(R_0^{-1}) \|C\|_{\mathrm{F}}^2 \|\tilde{x}(t)\|^2 - \lambda_{\min}(Q_0) \lambda_{\min}^2(\tilde{P}_0) \|\tilde{x}(t)\|^2 - \left(1 + \frac{1}{v}\right) \|B_s\|_{\mathrm{F}}^2 \\ &\quad \cdot \lambda_{\min}^2(\tilde{P}_0) \|\tilde{x}(t)\|^2 - 2\eta \lambda_{\min}(\tilde{P}_0) \|\tilde{x}(t)\|^2 + 2Kv \|\Lambda\|_{\mathrm{F}} \left\|\tilde{W}(t)\right\|_{\mathrm{F}} (b_1 + b_2 \epsilon_y \\ &\quad + b_3 \|\tilde{x}(t)\|) \|\tilde{x}(t)\| + 2 \left\|\tilde{P}_v B\right\|_{\mathrm{F}} \|\Lambda\|_{\mathrm{F}} K_g \|\tilde{x}(t)\|^2 + 2 \left\|\tilde{P}_v\right\|_{\mathrm{F}} \|L_v\|_{\mathrm{F}} \epsilon_y \|\tilde{x}(t)\| \\ &\quad + 2 \left\|\tilde{P}_v B\right\|_{\mathrm{F}} \|\Lambda\|_{\mathrm{F}} \epsilon_u \|\tilde{x}(t)\| + 2\epsilon_y \lambda_{\min}(R_0^{-\frac{1}{2}}) \left\|Z S^{\mathrm{T}}\right\|_{\mathrm{F}} \|\Lambda\|_{\mathrm{F}} \left\|\tilde{W}(t)\right\|_{\mathrm{F}} \left(b_1 + b_2 \epsilon_y \right. \\ &\quad \left. + b_3 \|\tilde{x}(t)\|\right) - \beta\left(\lambda_{\min}(Q) - \lambda_{\max}(R^{-1}) \|PB\|_{\mathrm{F}}^2\right) \|\hat{e}(t)\|_2^2 + 2\beta \|\hat{e}(t)\| \|PL_vC\|_{\mathrm{F}} \\ &\quad \cdot \|\tilde{x}(t)\| + 2\beta \|P\|_{\mathrm{F}} \|L_v\|_{\mathrm{F}} \epsilon_y \|\hat{e}(t)\| \\ &= -\left[\left(1 + \frac{1}{v}\right) \lambda_{\min}(R_0^{-1}) \|C\|_{\mathrm{F}}^2 + \lambda_{\min}(Q_0) \lambda_{\min}^2(\tilde{P}_0) + \left(1 + \frac{1}{v}\right) \|B_s\|_{\mathrm{F}}^2 \lambda_{\min}^2(\tilde{P}_0) \right. \\ &\quad \left. + 2\eta \lambda_{\min}(\tilde{P}_0) - 2Kv \|\Lambda\|_{\mathrm{F}} \left\|\tilde{W}(t)\right\|_{\mathrm{F}} b_3 - 2 \left\|\tilde{P}_v B\right\|_{\mathrm{F}} \|\Lambda\|_{\mathrm{F}} K_g\right] \|\tilde{x}(t)\|^2 + \left[2Kv \|\Lambda\|_{\mathrm{F}} \right. \\ &\quad \left. \cdot \left\|\tilde{W}(t)\right\|_{\mathrm{F}} \left(b_1 + b_2 \epsilon_y\right) + 2 \left\|\tilde{P}_v\right\|_{\mathrm{F}} \|L_v\|_{\mathrm{F}} \epsilon_y + 2 \left\|\tilde{P}_v B\right\|_{\mathrm{F}} \|\Lambda\|_{\mathrm{F}} \epsilon_u + 2\epsilon_y \lambda_{\min}(R_0^{-\frac{1}{2}}) \right. \\ &\quad \left. \cdot \left\|Z S^{\mathrm{T}}\right\|_{\mathrm{F}} \|\Lambda\|_{\mathrm{F}} \left\|\tilde{W}(t)\right\|_{\mathrm{F}} b_3\right] \|\tilde{x}(t)\| - \beta \left(\lambda_{\min}(Q) - \lambda_{\max}(R^{-1}) \|PB\|_{\mathrm{F}}^2\right) \|\hat{e}(t)\|_2^2 \\ &\quad + 2\beta \|\hat{e}(t)\| \|PL_vC\|_{\mathrm{F}} \|\tilde{x}(t)\| + 2\beta \|P\|_{\mathrm{F}} \|L_v\|_{\mathrm{F}} \epsilon_y \|\hat{e}(t)\| + 2\epsilon_y \lambda_{\min}(R_0^{-\frac{1}{2}}) \left\|Z S^{\mathrm{T}}\right\|_{\mathrm{F}} \end{aligned}$$

$$\cdot \|\Lambda\|_{\mathrm{F}} \left\|\tilde{W}(t)\right\|_{\mathrm{F}} \left(b_1 + b_2\epsilon_y\right). \tag{53}$$

Moreover, consider $2xy \leq \alpha x^2 + \frac{1}{\alpha}y^2$ that follows from Young's inequality [49] applied to scalars in $x \in \mathbb{R}$ and $y \in \mathbb{R}$, where $\alpha \in \mathbb{R}_+$. Using this inequality for the $2\beta \|\hat{e}(t)\| \|PL_vC\|_{\mathrm{F}} \|\tilde{x}(t)\|$ term in (53) yields

$$\begin{aligned}
&\dot{\mathcal{V}}(\tilde{x}(t), \tilde{W}(t), \hat{e}(t)) \\
&\leq -\Bigg[\left(1+\frac{1}{v}\right)\lambda_{\min}(R_0^{-1})\|C\|_{\mathrm{F}}^2 + \lambda_{\min}(Q_0)\lambda_{\min}^2(\tilde{P}_0) + \left(1+\frac{1}{v}\right)\|B_s\|_{\mathrm{F}}^2\,\lambda_{\min}^2(\tilde{P}_0) \\
&\quad + 2\eta\lambda_{\min}(\tilde{P}_0) - 2Kv\,\|\Lambda\|_{\mathrm{F}}\left\|\tilde{W}(t)\right\|_{\mathrm{F}} b_3 - 2\left\|\tilde{P}_vB\right\|_{\mathrm{F}}\|\Lambda\|_{\mathrm{F}}\,K_g\Bigg]\|\tilde{x}(t)\|^2 + \Bigg[2Kv\,\|\Lambda\|_{\mathrm{F}} \\
&\quad \cdot \left\|\tilde{W}(t)\right\|_{\mathrm{F}}\left(b_1 + b_2\epsilon_y\right) + 2\left\|\tilde{P}_v\right\|_{\mathrm{F}}\|L_v\|_{\mathrm{F}}\,\epsilon_y + 2\left\|\tilde{P}_vB\right\|_{\mathrm{F}}\|\Lambda\|_{\mathrm{F}}\,\epsilon_u + 2\epsilon_y\lambda_{\min}(R_0^{-\frac{1}{2}}) \\
&\quad \cdot \left\|ZS^{\mathrm{T}}\right\|_{\mathrm{F}}\|\Lambda\|_{\mathrm{F}}\left\|\tilde{W}(t)\right\|_{\mathrm{F}} b_3\Bigg]\|\tilde{x}(t)\| - \beta\left(\lambda_{\min}(Q) - \lambda_{\max}(R^{-1})\,\|PB\|_{\mathrm{F}}^2\right)\|\hat{e}(t)\|_2^2 \\
&\quad + \alpha\,\|PL_vC\|_{\mathrm{F}}^2\,\|\tilde{x}(t)\|_2^2 + \frac{\beta^2}{\alpha}\,\|\hat{e}(t)\|_2^2 + 2\beta\,\|P\|_{\mathrm{F}}\,\|L_v\|_{\mathrm{F}}\,\epsilon_y\,\|\hat{e}(t)\| + 2\epsilon_y\lambda_{\min}(R_0^{-\frac{1}{2}}) \\
&\quad \cdot \left\|ZS^{\mathrm{T}}\right\|_{\mathrm{F}}\|\Lambda\|_{\mathrm{F}}\left\|\tilde{W}(t)\right\|_{\mathrm{F}}(b_1 + b_2\epsilon_y) \\
&= -\Bigg[\left(1+\frac{1}{v}\right)\lambda_{\min}(R_0^{-1})\|C\|_{\mathrm{F}}^2 + \lambda_{\min}(Q_0)\lambda_{\min}^2(\tilde{P}_0) + \left(1+\frac{1}{v}\right)\|B_s\|_{\mathrm{F}}^2\,\lambda_{\min}^2(\tilde{P}_0) \\
&\quad + 2\eta\lambda_{\min}(\tilde{P}_0) - 2Kv\,\|\Lambda\|_{\mathrm{F}}\left\|\tilde{W}(t)\right\|_{\mathrm{F}} b_3 - 2\left\|\tilde{P}_vB\right\|_{\mathrm{F}}\|\Lambda\|_{\mathrm{F}}\,K_g - \alpha\,\|PL_vC\|_{\mathrm{F}}^2\Bigg]\|\tilde{x}(t)\|^2 \\
&\quad + \Bigg[2Kv\,\|\Lambda\|_{\mathrm{F}}\left\|\tilde{W}(t)\right\|_{\mathrm{F}}(b_1 + b_2\epsilon_y) + 2\left\|\tilde{P}_v\right\|_{\mathrm{F}}\|L_v\|_{\mathrm{F}}\,\epsilon_y + 2\left\|\tilde{P}_vB\right\|_{\mathrm{F}}\|\Lambda\|_{\mathrm{F}}\,\epsilon_u + 2\epsilon_y \\
&\quad \cdot \lambda_{\min}(R_0^{-\frac{1}{2}})\left\|ZS^{\mathrm{T}}\right\|_{\mathrm{F}}\|\Lambda\|_{\mathrm{F}}\left\|\tilde{W}(t)\right\|_{\mathrm{F}} b_3\Bigg]\|\tilde{x}(t)\| - \Bigg[\beta\left(\lambda_{\min}(Q) - \lambda_{\max}(R^{-1})\,\|PB\|_{\mathrm{F}}^2\right) \\
&\quad - \frac{\beta^2}{\alpha}\Bigg]\|\hat{e}(t)\|_2^2 + 2\beta\,\|P\|_{\mathrm{F}}\,\|L_v\|_{\mathrm{F}}\,\epsilon_y\,\|\hat{e}(t)\| + 2\epsilon_y\lambda_{\min}(R_0^{-\frac{1}{2}})\left\|ZS^{\mathrm{T}}\right\|_{\mathrm{F}}\|\Lambda\|_{\mathrm{F}}\left\|\tilde{W}(t)\right\|_{\mathrm{F}} \\
&\quad \cdot \left(b_1 + b_2\epsilon_y\right) \\
&\leq -d_1\,\|\tilde{x}(t)\|^2 - d_2\,\|\hat{e}(t)\|_2^2 + d_3\,\|\tilde{x}(t)\| + d_4\,\|\hat{e}(t)\| + d_5,
\end{aligned} \tag{54}$$

where $d_1 \triangleq \left(1+\frac{1}{v}\right)\lambda_{\min}(R_0^{-1})\|C\|_{\mathrm{F}}^2 + \lambda_{\min}(Q_0)\lambda_{\min}^2(\tilde{P}_0) + \left(1+\frac{1}{v}\right)\|B_s\|_{\mathrm{F}}^2\,\lambda_{\min}^2(\tilde{P}_0) + 2\eta\,\lambda_{\min}(\tilde{P}_0) - 2Kv\,\|\Lambda\|_{\mathrm{F}}\,\tilde{w}^* b_3 - 2\left\|\tilde{P}_v B\right\|_{\mathrm{F}}\|\Lambda\|_{\mathrm{F}}\,K_g - \alpha\,\|PL_vC\|_{\mathrm{F}}^2 \in \mathbb{R}_+$, $d_2 \triangleq \beta\Big(\lambda_{\min}(Q) - \lambda_{\max}(R^{-1})\,\|PB\|_{\mathrm{F}}^2\Big) - \frac{\beta^2}{\alpha} \in \mathbb{R}_+$, $d_3 \triangleq 2Kv\,\|\Lambda\|_{\mathrm{F}}\,\tilde{w}^*\left(b_1 + b_2\epsilon_y\right) + \left\|\tilde{P}_v\right\|_{\mathrm{F}}\|L_v\|_{\mathrm{F}}\,\epsilon_y + 2\left\|\tilde{P}_v B\right\|_{\mathrm{F}}\|\Lambda\|_{\mathrm{F}}\,\epsilon_u + 2\epsilon_y\lambda_{\min}(R_0^{-\frac{1}{2}})\left\|ZS^{\mathrm{T}}\right\|_{\mathrm{F}}\|\Lambda\|_{\mathrm{F}}\,\tilde{w}^* b_3$, $d_4 = 2\beta\,\|P\|_{\mathrm{F}}\,\|L_v\|_{\mathrm{F}}\,\epsilon_y$, and $d_5 \triangleq 2\epsilon_y\lambda_{\min}(R_0^{-\frac{1}{2}})\left\|ZS^{\mathrm{T}}\right\|_{\mathrm{F}}\|\Lambda\|_{\mathrm{F}}\,\tilde{w}^*\left(b_1 + b_2\epsilon_y\right)$ with $\left\|\tilde{W}(t)\right\|_{\mathrm{F}} \leq \tilde{w}^*$ due to utilizing the projection operator in the weight update law given by (37).

Finally, we rearrange (54) as

$$\dot{\mathcal{V}}(\tilde{x}(t),\tilde{W}(t),\hat{e}(t)) \leq -\left(\sqrt{d_1}\,\|\tilde{x}(t)\| - \frac{d_3}{2\sqrt{d_1}}\right)^2 - \left(\sqrt{d_2}\,\|\hat{e}(t)\| - \frac{d_4}{2\sqrt{d_2}}\right)^2 + \left(d_5 + \frac{d_3^2}{4d_1} + \frac{d_4^2}{4d_2}\right), \tag{55}$$

which shows that $\dot{\mathcal{V}}(\tilde{x}(t),\tilde{W}(t),\hat{e}(t)) \leq 0$ when $\|\tilde{x}(t)\| \geq \psi_1$ and $\|\hat{e}(t)\| \geq \psi_2$, where

$$\psi_1 \triangleq \frac{\frac{d_3}{2\sqrt{d_1}} + \sqrt{d_5 + \frac{d_3^2}{4d_1} + \frac{d_4^2}{4d_2}}}{\sqrt{d_1}}, \tag{56}$$

$$\psi_2 \triangleq \frac{\frac{d_4}{2\sqrt{d_2}} + \sqrt{d_5 + \frac{d_3^2}{4d_1} + \frac{d_4^2}{4d_2}}}{\sqrt{d_2}}. \tag{57}$$

This argument proves uniform ultimate boundedness of the closed-loop solution $(\tilde{x}(t),\tilde{W}(t),\hat{e}(t))$ for all initial conditions [50, 21]. ■

In the proof of Theorem 1, it is implicitly assumed that $d_1 \in \mathbb{R}_+$ and $d_2 \in \mathbb{R}_+$, which can be satisfied by suitable selection of the event-triggered output feedback adaptive controller design parameters. Although this theorem shows uniform ultimate boundedness of the closed-loop solution $(\tilde{x}(t),\tilde{W}(t),\hat{e}(t))$ for all initial conditions, it is of practical importance to compute the ultimate bound, which is given next.

4.2. Ultimate Bound Computation. For revealing the effect of user-defined thresholds and the event-triggered output feedback adaptive controller design parameters to the system performance, the next corollary presents a computation of the ultimate bound, which presents the second result of this chapter.

Corollary 1. Consider the uncertain dynamical system given by (33) and (34), the reference model given by (26) and (27), the state observer given by (38) and (58) with the state observer gain matrix in (19) along with (20), (21), and (22), and the feedback control law given by (11), (12), (14), and (37). In addition, let the data transmission from the uncertain dynamical system to the controller occur when $\overline{E}_1$ is true and the data transmission from the controller to the uncertain dynamical system occur when $\overline{E}_2 \vee E_3$ is true. Then, the ultimate bound of the system error between the uncertain dynamical system and the reference model is given by

$$||e(t)|| \;=\; ||x(t) - x_{\mathrm{m}}(t)|| \;\leq\; \tilde{\Phi}\left[\lambda_{\min}^{-1}(\tilde{P}_v) + \beta^{-1}\lambda_{\min}^{-1}(P)\right]^{\frac{1}{2}}, \quad t \geq T, \tag{58}$$

where $\tilde{\Phi} \triangleq \left[\lambda_{\max}(\tilde{P}_v)\psi_1^2 + \beta\lambda_{\max}(P)\psi_2^2 + \Gamma^{-1}\tilde{w}^{*2}\,\|\Lambda\|_{\mathrm{F}}\right]^{\frac{1}{2}}$.

Proof. It follows from the proof of Theorem 1 that $\dot{\mathcal{V}}(\tilde{x}(t), \tilde{W}(t), \hat{e}(t)) \leq 0$ outside the compact set given by $\mathcal{S} \triangleq \{(\tilde{x}(t), \hat{e}(t)) : \|\tilde{x}(t)\| \leq \psi_1\} \bigcap \{(\tilde{x}(t), \hat{e}(t)) : \|\hat{e}(t)\| \leq \psi_2\}$. That is, since $\mathcal{V}(\tilde{x}(t), \tilde{W}(t), \hat{e}(t))$ cannot grow outside $\mathcal{S}$, the evolution of $\mathcal{V}(\tilde{x}(t), \tilde{W}(t), \hat{e}(t))$ is upper bounded by

$$\begin{aligned}
\mathcal{V}(\tilde{x}(t), \tilde{W}(t), \hat{e}(t)) &\leq \max_{(\tilde{x}(t), \hat{e}(t)) \in \mathcal{S}} \mathcal{V}(\tilde{x}(t), \tilde{W}(t), \hat{e}(t)) \\
&= \lambda_{\max}(\tilde{P}_v)\psi_1^2 + \beta\lambda_{\max}(P)\psi_2^2 + \Gamma^{-1}\tilde{w}^{*2}\,\|\Lambda\|_{\mathrm{F}} \\
&= \tilde{\Phi}^2.
\end{aligned} \tag{59}$$

It follows from $\tilde{x}^{\mathrm{T}}(t)\tilde{P}_v\tilde{x} \leq \mathcal{V}(\tilde{x},\tilde{W},\hat{e})$ and $\beta\hat{e}^{\mathrm{T}}P\hat{e} \leq \mathcal{V}(\tilde{x},\tilde{W},\hat{e})$ that $\|\tilde{x}(t)\|^2 \leq \frac{\tilde{\Phi}^2}{\lambda_{\min}(\tilde{P}_v)}$ and $\|\hat{e}(t)\|^2 \leq \frac{\tilde{\Phi}^2}{\beta\lambda_{\min}(P)}$. Finally, since $e(t) = x(t) - \hat{x}(t) + \hat{x}(t) - x_{\mathrm{m}}(t)$, and hence, $\|e(t)\| \leq \|x(t) - \hat{x}(t)\| + \|\hat{x}(t) - x_{\mathrm{m}}(t)\| = \|\tilde{x}(t)\| + \|\hat{e}(t)\|$, the bound given by (58) follows. ■

To elucidate the effect of the user-defined thresholds and the event-triggered output feedback adaptive controller design parameters to the ultimate bound given by (58), let $A_{\mathrm{r}} = -5$, $B = 1$, $C = 1$, $W = 1$, $R_o = 1$, $R = 1$,$Q_o = 1$, $Q = 1$, $\Lambda = 1$, $\alpha = 0.5$, and $\beta = 0.25$. In this case, Figure 1 shows the effect of the variation in v and Γ on the system error bound for $\eta = 5$, $\epsilon_y = 0.1$ and $\epsilon_u = 0.1$. Specifically, one can conclude from this figure that increasing Γ reduces the ultimate bound and the minimum value of this bound is obtained for $v = 0.35$. Figure 4 shows the effect of the variation in v and η on the system error bound for $\Gamma = 100$ and the same previously defined parameters. It is evident from the figure, that increasing η increases the ultimate bound. This figure also shows that there exists an optimum value of v for each η value, which allows the selection of the best value of v to avoid increasing the ultimate bound.

Figures 3 and 7 show the effect of the variations in ϵ_y and ϵ_u, respectively. In particular, these figures show that the system error bound is more sensitive to the changes in the data transmission threshold from the physical system to the adaptive controller (sensing threshold, ϵ_y) than the data transmission threshold from the adaptive controller to the physical system (actuation threshold, ϵ_u), which implies that the actuation threshold can be chosen large enough to reduce wireless network utilization between the physical system and the adaptive controller without sacrificing closed-loop dynamical system performance.

4.3. Zeno Behavior Analysis. We now show that the proposed event-triggered output feedback adaptive control architecture does not yield to a Zeno behavior, which implies that it does not require a continuous two-way data exchange and reduces wireless network utilization. For the following corollary presenting the third result of this chapter,

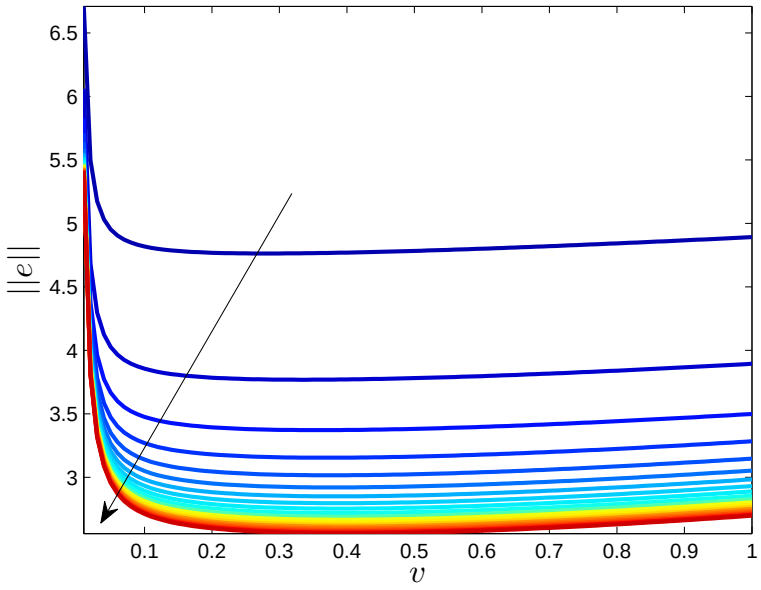

Figure 2. Effect of $\Gamma \in [5, 100]$ and $v \in [0.01, 1]$ to the ultimate bound (58) for $\eta = 5$, $\epsilon_y = 0.1$ and $\epsilon_u = 0.1$, where the arrow indicates the increase in Γ (dashed line denotes the case with $\Gamma = 100$).

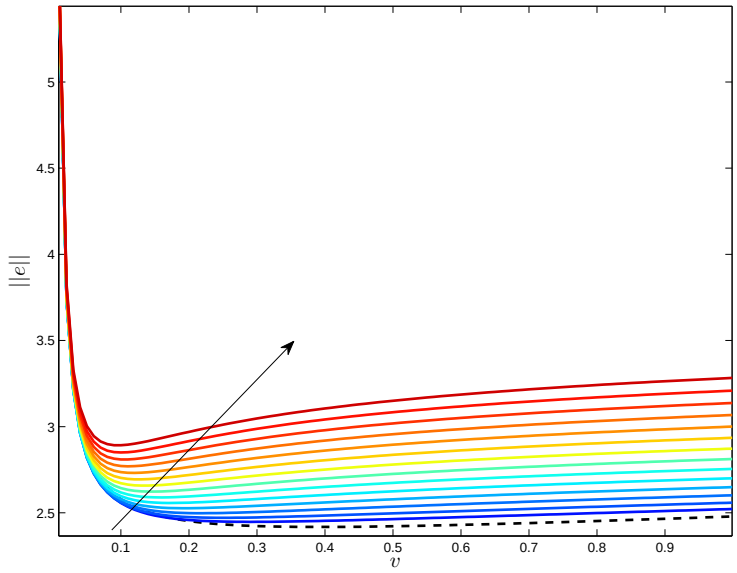

Figure 3. Effect of $\eta \in [5, 20]$ to the ultimate bound (58) for $\epsilon_y = 0.1$, $\epsilon_u = 0.1$, $v \in [0.01, 1]$, and $\Gamma = 100$, where the arrow indicates the increase in η (dashed line denotes the case with $\eta = 5$).

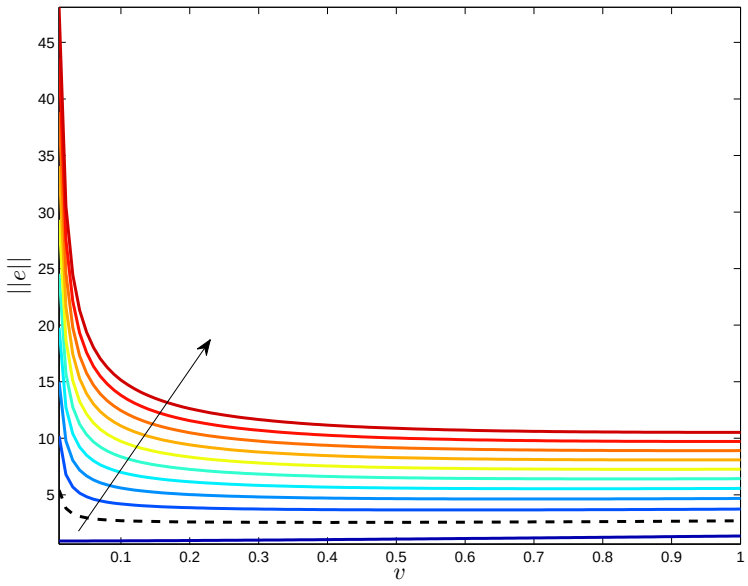

Figure 4. Effect of $\epsilon_y \in [0,1]$ to the ultimate bound (58) for $\eta = 5$, $\epsilon_u = 0.1$, $v \in [0.01,1]$, and $\Gamma = 100$, where the arrow indicates the increase in ϵ_y (dashed line denotes the case with $\epsilon_y = 0.1$ and blue bottom line denotes the case with $\epsilon_y = 0$).

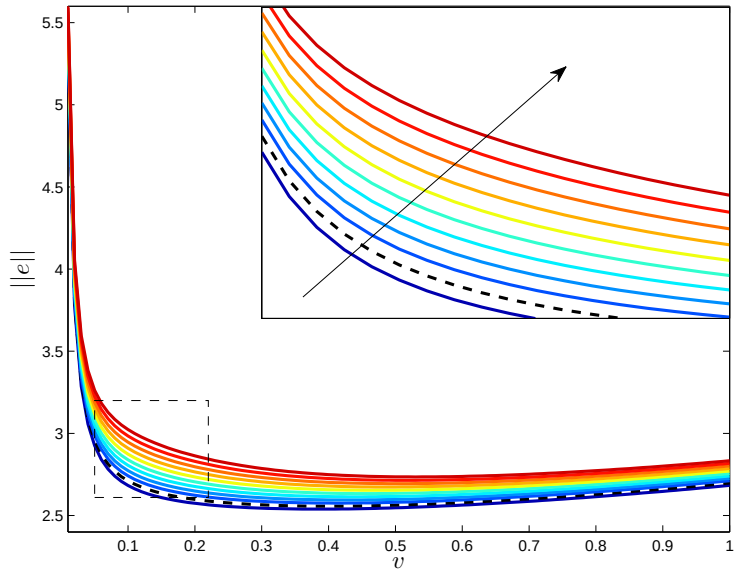

Figure 5. Effect of $\epsilon_u \in [0,1]$ to the ultimate bound (58) for $\eta = 5$, $\epsilon_y = 0.1$, $v \in [0.01,1]$, and $\Gamma = 100$, where the arrow indicates the increase in ϵ_u (dashed line denotes the case with $\epsilon_u = 0.1$).

we consider $r_i^k \in (s_k, s_{k+1})$ to be the ith time instant when E_2 is violated over (s_k, s_{k+1}), and since $\{s_k\}_{k=1}^{\infty}$ is a subsequence of $\left\{r_j\right\}_{j=1}^{\infty}$, it follows that $\left\{r_j\right\}_{j=1}^{\infty} = \{s_k\}_{k=1}^{\infty} \bigcup \left\{r_i^k\right\}_{k=1,i=1}^{\infty,m_k}$, where $m_k \in \mathbb{N}$ is the number of violation times of E_2 over (s_k, s_{k+1}).

Corollary 2. Consider the uncertain dynamical system given by (33) and (34), the reference model given by (26) and (27), the state observer given by (38) and (58) with the state observer gain matrix in (19) along with (20), (21), and (22), and the feedback control law given by (11), (12), (14), and (37). In addition, let the data transmission from the uncertain dynamical system to the controller occur when $\overline{E}_1$ is true and the data transmission from the controller to the uncertain dynamical system occur when $\overline{E}_2 \vee E_3$ is true. Then,

$$s_{k+1} - s_k > 0, \quad \forall k \in \mathbb{N}, \tag{60}$$

$$r_{i+1}^k - r_i^k > 0, \quad \forall i \in \{0, ..., m_k\}, \quad \forall k \in \mathbb{N}, \tag{61}$$

holds.

Proof. The time derivative of $\|x_{\mathrm{s}}(t) - x(t)\|$ over $t \in (s_k, s_{k+1})$, $\forall k \in \mathbb{N}$, is given by

$$\begin{aligned}\frac{d}{dt}\|y_{\mathrm{s}}(t) - y(t)\| \leq \|\dot{y}_{\mathrm{s}}(t) - \dot{y}(t)\| &= \|C\dot{x}(t)\| \leq \|C\|_{\mathrm{F}}\|\dot{x}(t)\| \\ &\leq \|C\|_{\mathrm{F}}\Big[\,\|A\|_{\mathrm{F}}\,\|x(t)\| + \|B\|_{\mathrm{F}}\,\|\Lambda\|_{\mathrm{F}}\,\|u_{\mathrm{s}}(t)\| + \|B\|_{\mathrm{F}}\,\|\Lambda\|_{\mathrm{F}}\,\|W\|_{\mathrm{F}} \\ &\quad \cdot \|\sigma\left(x_{\mathrm{p}}(t)\right)\| + \|B_{\mathrm{r}}\|_{\mathrm{F}}\|r(t)\|\Big].\end{aligned} \tag{62}$$

Now, we determine an upper bound for $\|x(t)\|$ in (62) as

$$\begin{aligned}\|x(t)\| = \|\tilde{x}(t) + \hat{x}(t)\| &\leq \|\tilde{x}(t)\| + \zeta_1 + \zeta_2\epsilon_y + \zeta_2\|C\|_{\mathrm{F}}\,\|\tilde{x}(t)\| \\ &= \zeta_1 + \zeta_2\epsilon_y + (1 + \zeta_2\|C\|_{\mathrm{F}})\,\|\tilde{x}(t)\|\,.\end{aligned} \tag{63}$$

In addition, we determine an upper bound for $\|\sigma\left(x_{\mathrm{p}}(t)\right)\|$ in (62) as

$$\begin{aligned}
\|\sigma\left(x_{\mathrm{p}}(t)\right)\| =& \|\sigma\left(x_{\mathrm{p}}(t)\right)-\sigma\left(\hat{x}_{\mathrm{p}}(t)\right)+\sigma\left(\hat{x}_{\mathrm{p}}(t)\right)\| \\
&\leq L_{\sigma}\|\tilde{x}_{\mathrm{p}}(t)\|+\|\sigma\left(\hat{x}_{\mathrm{p}}(t)\right)\| \\
&\leq L_{\sigma}\|\tilde{x}_{\mathrm{p}}(t)\|+\|\sigma\left(\hat{x}_{\mathrm{p}}(t)\right)-\sigma(0)\|+\|\sigma(0)\| \\
&\leq L_{\sigma}\underbrace{\|\tilde{x}_{\mathrm{p}}(t)\|}_{\leq\|\tilde{x}(t)\|}+L_{\sigma}\underbrace{\|\hat{x}_{\mathrm{p}}(t)\|}_{\leq\|\hat{x}(t)\|}+b_{\sigma} \\
&\leq L_{\sigma}\|\tilde{x}(t)\|+L_{\sigma}\left(\zeta_{1}+\zeta_{2}\epsilon_{y}+\zeta_{2}\|C\|_{\mathrm{F}}\|\tilde{x}(t)\|\right)+b_{\sigma} \\
&= L_{\sigma}\left(1+\zeta_{2}\|C\|_{\mathrm{F}}\right)\|\tilde{x}(t)\|+L_{\sigma}\left(\zeta_{1}+\zeta_{2}\epsilon_{y}\right)+b_{\sigma}. \qquad (64)
\end{aligned}$$

Substituting (63) and (64) into (62), gives

$$\begin{aligned}
\frac{d}{dt}\|y_{\mathrm{s}}(t)-y(t)\| \leq& \|C\|_{\mathrm{F}}\|A\|_{\mathrm{F}}\left[\zeta_{1}+\zeta_{2}\epsilon_{y}+\left(1+\zeta_{2}\|C\|_{\mathrm{F}}\right)\|\tilde{x}(t)\|\right]+\|C\|_{\mathrm{F}}\|B\|_{\mathrm{F}}\|\Lambda\|_{\mathrm{F}} \\
&\cdot\|u_{\mathrm{s}}(t)\|+\|C\|_{\mathrm{F}}\|B\|_{\mathrm{F}}\|\Lambda\|_{\mathrm{F}}W_{\max}\left[L_{\sigma}\left(1+\zeta_{2}\|C\|_{\mathrm{F}}\right)\|\tilde{x}(t)\|\right. \\
&\left.+L_{\sigma}\left(\zeta_{1}+\zeta_{2}\epsilon_{y}\right)+b_{\sigma}\right]+\|C\|_{\mathrm{F}}\|B_{\mathrm{r}}\|_{\mathrm{F}}r(t). \qquad (65)
\end{aligned}$$

Since the closed-loop dynamical system is uniformly ultimately bounded by Theorem 1, there exists an upper bound to (65). Letting Φ_1 denote this upper bound and with the initial condition satisfying $\lim_{t\to s_k^+}||y_{\mathrm{s}}(t)-y(t)||=0$, it follows from (65) that

$$\|y_{\mathrm{s}}(t)-y(t)\|\leq\Phi_{1}(t-s_{k}),\quad\forall t\in(s_{k},s_{k+1}). \qquad (66)$$

Therefore, when $\overline{E}_1$ is true, then $\lim_{t\to s_{k+1}^-}\|y_{\mathrm{s}}(t)-y(t)\|=\epsilon_y$ and it then follows from (66) that $s_{k+1}-s_k\geq\dfrac{\epsilon_y}{\Phi_1}$.

Similarly, the time derivative of $\|u_{\mathrm{s}}(t) - u(t)\|$ over $t \in \left(r_i^k, r_{i+1}^k\right), \forall i \in \mathbb{N}$, is given by

$$\frac{d}{dt}\|u_{\mathrm{s}}(t) - u(t)\| \leq \|\dot{u}_{\mathrm{s}}(t) - \dot{u}(t)\| = \|\dot{u}(t)\| \leq \|\dot{u}_{\mathrm{n}}(t)\| + \|\dot{u}_{\mathrm{a}}(t)\|. \tag{67}$$

Now, we determine an upper bound for $\|\dot{u}_{\mathrm{n}}(t)\|$ in (67) as

$$\begin{aligned}
\|\dot{u}_{\mathrm{n}}(t)\| &= \|K_x\dot{\hat{x}}(t)\| \\
&\leq \|K_x\|_{\mathrm{F}}\|\dot{\hat{x}}(t)\| \\
&\leq \|K_x\|_{\mathrm{F}}\left[\|A\|_{\mathrm{F}}\|\hat{x}(t)\| + \|B\|_{\mathrm{F}}\|u_{\mathrm{n}}(t)\| + \|L_v\|_{\mathrm{F}}\|y_{\mathrm{s}}(t) - \hat{y}(t)\| + \|B_{\mathrm{r}}\|_{\mathrm{F}}\|r(t)\|\right] \\
&\leq \|K_x\|_{\mathrm{F}}\Bigg[\|A\|_{\mathrm{F}}\left[\zeta_1 + \zeta_2\epsilon_y + \zeta_2\|C\|_{\mathrm{F}}\,\|\tilde{x}(t)\|\right] + \|B\|_{\mathrm{F}}\|u_{\mathrm{n}}(t)\| + \|L_v\|_{\mathrm{F}}\|C\|_{\mathrm{F}}\|\tilde{x}(t)\| \\
&\quad + \|L_v\|_{\mathrm{F}}\epsilon_y + \|B_{\mathrm{r}}\|_{\mathrm{F}}\|r(t)\|\Bigg].
\end{aligned} \tag{68}$$

Letting β_1 to denote the upper bound of $\|\dot{u}_{\mathrm{n}}(t)\|$, we determine the upper bound of $\|\dot{u}_{\mathrm{a}}(t)\|$ in (67) as

$$\begin{aligned}
\|\dot{u}_{\mathrm{a}}(t)\| &= \|\dot{\hat{W}}^{\mathrm{T}}(t)\sigma\left(\hat{x}_{\mathrm{p}}(t), u_{\mathrm{n}}(t)\right) + \hat{W}^{\mathrm{T}}(t)\dot{\sigma}\left(\hat{x}_{\mathrm{p}}(t), u_{\mathrm{n}}(t)\right)\| \\
&\leq \|SZ^{\mathrm{T}}R_0^{\frac{-1}{2}}(\hat{y}(t) - y_{\mathrm{s}}(t))\sigma^{\mathrm{T}}\left(\hat{x}_{\mathrm{p}}(t), u_{\mathrm{n}}(t)\right)\Gamma\sigma\left(\hat{x}_{\mathrm{p}}(t), u_{\mathrm{n}}(t)\right)\| \\
&\quad + \|\hat{W}(t)\|_{\mathrm{F}}\left[\|\dot{\sigma}_0\left(\hat{x}_{\mathrm{p}}(t)\right)\| + \|\dot{u}_{\mathrm{n}}(t)\|\right] \\
&\leq \lambda_{\max}(\Gamma)\|SZ^{\mathrm{T}}R_0^{\frac{-1}{2}}\|_{\mathrm{F}}\|\sigma\left(\hat{x}_{\mathrm{p}}(t), u_{\mathrm{n}}(t)\right)\|^2\Phi_1 + \|\hat{W}(t)\|_{\mathrm{F}}\left[\sigma^* + \beta_1\right],
\end{aligned} \tag{69}$$

where $\|\dot{\sigma}\left(\hat{x}_{\mathrm{p}}(t)\right)\| \leq \sigma^*$. Substituting (68) and (69) into (67), gives

$$\frac{d}{dt}\|u_{\mathrm{s}}(t) - u(t)\| \leq \lambda_{\max}(\Gamma)\|SZ^{\mathrm{T}}R_0^{\frac{-1}{2}}\|_{\mathrm{F}}\|\sigma\left(\hat{x}_{\mathrm{p}}(t), u_{\mathrm{n}}(t)\right)\|^2\Phi_1 + \|\hat{W}(t)\|_{\mathrm{F}}\left[\sigma^* + \beta_1\right] + \beta_1. \tag{70}$$

Once again, since the closed-loop dynamical system is uniformly ultimately bounded by Theorem 1, there exists an upper bound to (70). Letting Φ_2 denote this upper bound and with the initial condition satisfying $\lim_{t\to r_i^{k+}} \|u_{\rm s}(t) - u(t)\| = 0$, it follows from (70) that

$$\|u_{\rm s}(t) - u(t)\| \leq \Phi_2(t - r_i^k), \quad \forall t \in \left(r_i^k, r_{i+1}^k\right). \tag{71}$$

Therefore, when $\overline{E}_2 \vee E_3$ is true, then $\lim_{t\to r_{i+1}^{k-}} \|u_{\rm s}(t) - u(t)\| = \epsilon_u$ and it then follows from (71) that $r_{i+1}^k - r_i^k \geq \dfrac{\epsilon_u}{\Phi_2}$. ■

Corollary 2 shows that the intersample times for the system output vector and feedback control vector are bounded away from zero, and hence, the proposed event-triggered adaptive control approach does not yield to a Zeno behavior.

5. ILLUSTRATIVE NUMERICAL EXAMPLE

In this section, the efficacy of the proposed event-triggered output feedback adaptive control approach is demonstrated in an illustrative numerical example. For this purpose, we consider the uncertain dynamical system given by

$$\begin{aligned}
\begin{bmatrix} \dot{x}_{\rm p1}(t) \\ \dot{x}_{\rm p2}(t) \end{bmatrix} &= \begin{bmatrix} 0 & 1 \\ 0 & 0 \end{bmatrix} \begin{bmatrix} x_{\rm p1}(t) \\ x_{\rm p2}(t) \end{bmatrix} + \begin{bmatrix} 0 \\ 1 \end{bmatrix} \Lambda \left[u_{\rm s}(t) + \Delta(x_{\rm p}(t))\right], \\
y_{\rm p}(t) &= \begin{bmatrix} 1 & 0 \\ 0.5 & 0.5 \end{bmatrix} \begin{bmatrix} x_{\rm p1}(t) \\ x_{\rm p2}(t) \end{bmatrix}, \quad y_{\rm reg}(t) = \begin{bmatrix} 1 & 0 \end{bmatrix} \begin{bmatrix} x_{\rm p1}(t) \\ x_{\rm p2}(t) \end{bmatrix}.
\end{aligned} \tag{72}$$

For this study, let the uncertain parameters be $\Lambda = 0.5$ and $W = [-2\ ,\ 3]^{\rm T}$, and we choose $\sigma(x_{\rm p}(t)) = x_{\rm p}(t)$ as the basis function.

For the nominal control design, we note

$$A = \begin{bmatrix} 0 & 1 & 0 \\ 0 & 0 & 0 \\ -1 & 0 & 0 \end{bmatrix}, \quad B = \begin{bmatrix} 0 \\ 1 \\ 0 \end{bmatrix}, \quad B_{\mathrm{r}} = \begin{bmatrix} 0 \\ 0 \\ 1 \end{bmatrix},$$
$$C = \begin{bmatrix} 1 & 0 & 0 \\ 0.5 & 0.5 & 0 \\ 0 & 0 & 1 \end{bmatrix}, \quad C_{\mathrm{Reg}} = \begin{bmatrix} 1 & 0 & 0 \end{bmatrix}. \tag{73}$$

for (33) and (34). In particular, a linear quadratic regulator formulation is used to choose K_x of the nominal controller as

$$K_x = R_{\mathrm{lqr}}^{-1} B^{\mathrm{T}} P_{\mathrm{lqr}}, \tag{74}$$
$$0 = \left(A + \eta_{\mathrm{lqr}} I_{n\times n}\right)^{\mathrm{T}} P_{\mathrm{lqr}} + P_{\mathrm{lqr}} \left(A + \eta_{\mathrm{lqr}} I_{n\times n}\right) - P_{\mathrm{lqr}} B R_{\mathrm{lqr}}^{-1} B^{\mathrm{T}} P_{\mathrm{lqr}} + Q_{\mathrm{lqr}}, \tag{75}$$

where $Q_{\mathrm{lqr}} = \mathrm{diag}([20, 3, 1])$, $R_{\mathrm{lqr}} = 0.5$, and $\eta_{\mathrm{lqr}} = 0.2$ is considered, which yields $K_x = [9.6, 5.2, -3.6]$. Next, for the adaptive control design, we choose

$$B_2 = \begin{bmatrix} 1 & 0 \\ 1 & 0 \\ 0 & 1 \end{bmatrix}, \tag{76}$$

to square up the dynamical system [21], which results in

$$B_s = \begin{bmatrix} 0 & 1 & 0 \\ 1 & 1 & 0 \\ 0 & 0 & 1 \end{bmatrix}. \tag{77}$$

In particular, with (77), $\det(CB_s)$ is nonzero and $G(s) = C(sI_{n\times n} - A)^{-1}B_s$ is minimum phase. To calculate the observer gain L_v given by (19), we set $Q_0 = I$, $R_0 = 30I$, $\eta = 10$, and $v = 0.1$ for (20), (21), and (22), which yields

$$L_v = \begin{bmatrix} 20.24 & -18.79 & -0.97 \\ 0.72 & 39.84 & -0.48 \\ -0.97 & 0.01 & 20.16 \end{bmatrix} \tag{78}$$

Finally, note that $d_1 \in \mathbb{R}_+$ and $d_2 \in \mathbb{R}_+$ for $\alpha = 1$ and $\beta = 1$.

Figure 6 presents the results with the proposed event-triggered output feedback adaptive control approach when $\epsilon_y = 0.3$, and $\epsilon_u = 0.3$ are chosen, where the output of the uncertain dynamical system achieves a good command following performance. In Figures 7 and 8, we fix ϵ_y to 0.3 and change ϵ_u to 0.1 and 0.5, respectively. As expected from the proposed theory, the variation on ϵ_u does not alter the command following performance significantly. In addition, in Figures 9 and 10, we fix ϵ_u to 0.3 and change ϵ_y to 0.1 and 0.5, respectively, where it can be seen that the variation on ϵ_y alters the command following performance more than the variation in ϵ_u, as discussed earlier in this chapter. Finally, output and control event triggers for the cases in Figures 6-10 are given in Figure 11, where it can be seen that increasing ϵ_y (respectively, ϵ_u) yields less output event triggers when ϵ_u (respectively, less control event triggers when ϵ_y) is fixed, which reduces network utilization.

6. CONCLUSION

A critical task in the design and implementation of networked control systems is to guarantee system stability while reducing wireless network utilization and achieving a given system performance in the presence of system uncertainties. Motivating from this standpoint, design and analysis of an event-triggered output feedback adaptive control methodology is presented for a class of uncertain dynamical systems in the presence

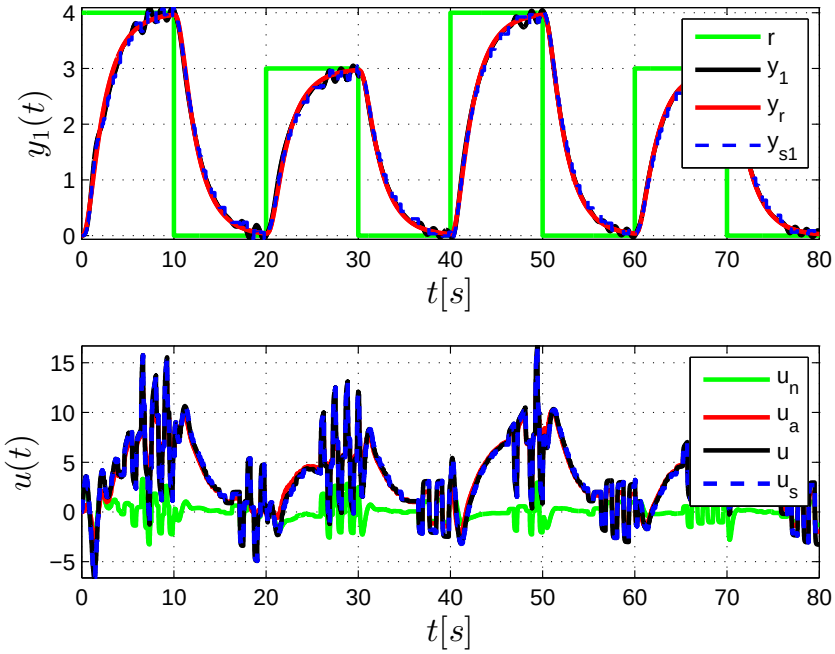

Figure 6. Command following performance for the proposed event-triggered output feedback adaptive control approach with $\Gamma = 50I$, $\epsilon_y = 0.3$, and $\epsilon_u = 0.3$.

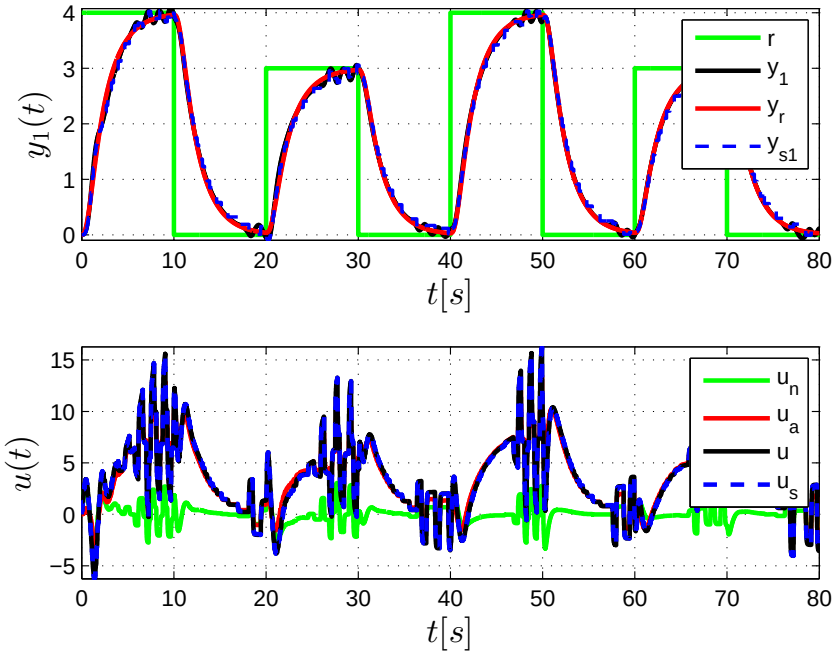

Figure 7. Command following performance for the proposed event-triggered output feedback adaptive control approach with $\Gamma = 50I$, $\epsilon_y = 0.3$, and $\epsilon_u = 0.1$.

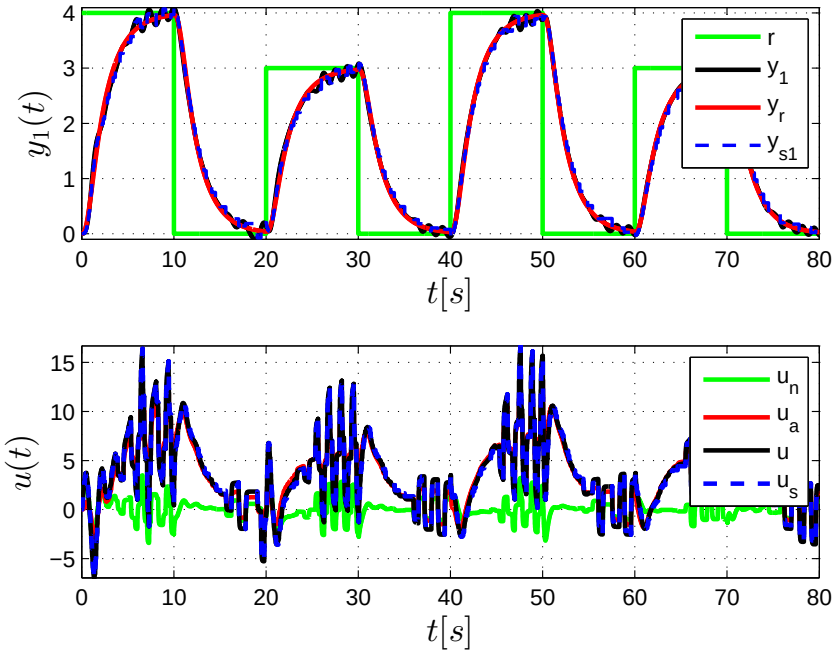

Figure 8. Command following performance for the proposed event-triggered output feedback adaptive control approach with $\Gamma = 50I$, $\epsilon_y = 0.3$, and $\epsilon_u = 0.5$.

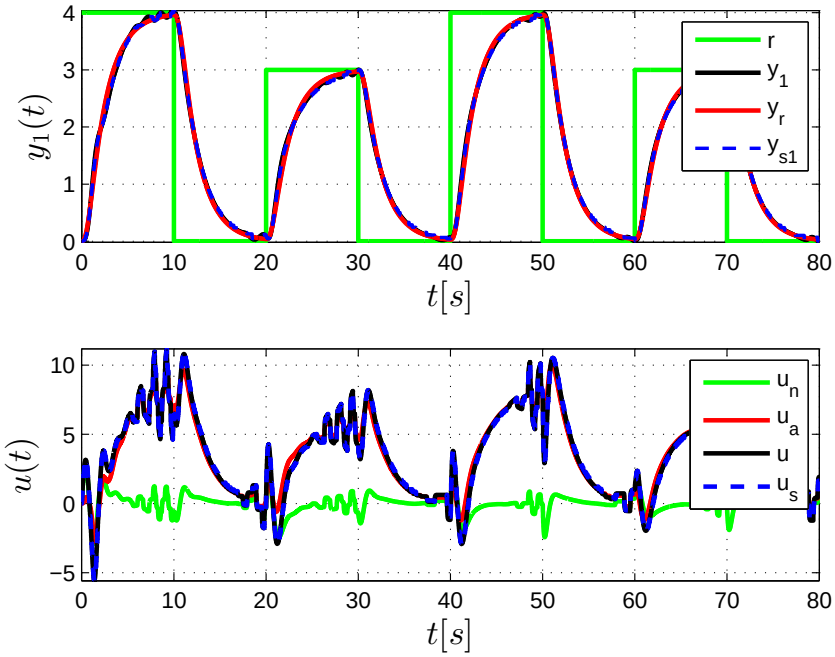

Figure 9. Command following performance for the proposed event-triggered output feedback adaptive control approach with $\Gamma = 50I$, $\epsilon_y = 0.1$, and $\epsilon_u = 0.3$.

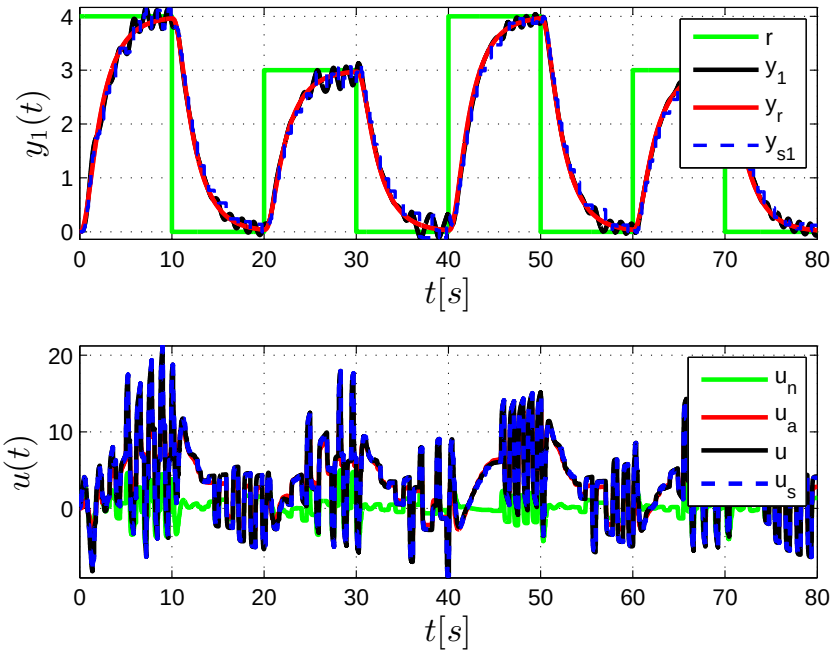

Figure 10. Command following performance for the proposed event-triggered output feedback adaptive control approach with $\Gamma = 50I$, $\epsilon_y = 0.5$, and $\epsilon_u = 0.3$.

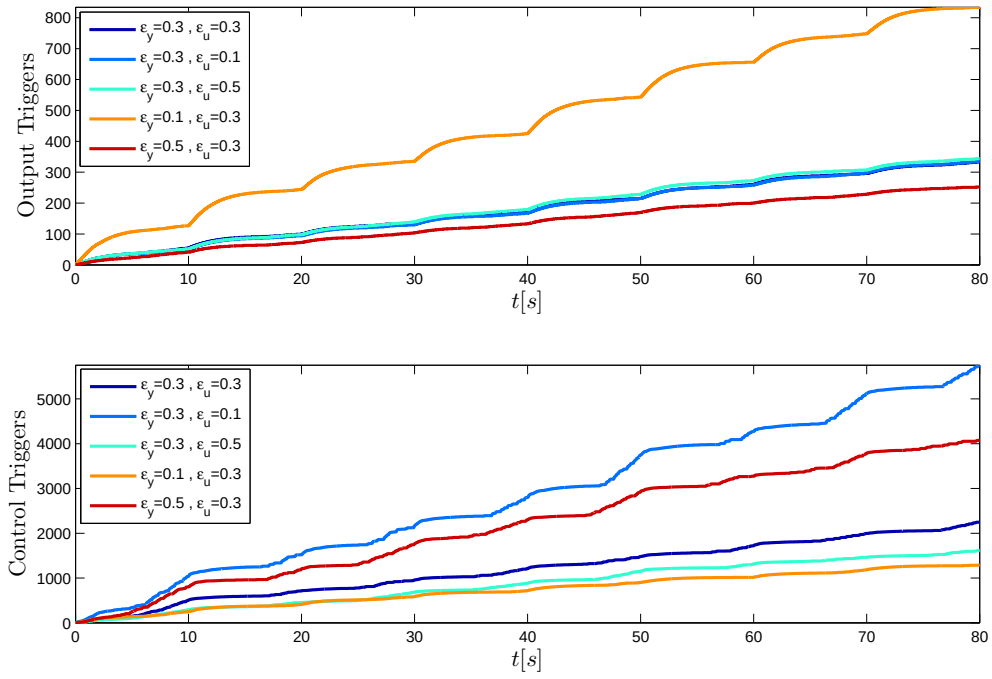

Figure 11. Output and control event triggers for the cases in Figures 7–10.

of two-way data exchange between the physical system and the proposed controller over a wireless network. Specifically, we showed using tools and methods from nonlinear systems theory and Lyapunov stability in particular that the proposed feedback control approach guarantees system stability in the presence of system uncertainties. In addition, we characterized and discussed the effect of user-defined thresholds and output feedback adaptive controller design parameters to the system performance and showed that the proposed methodology does not yield to a Zeno behavior. Finally, we illustrated the efficacy of the proposed adaptive control approach in a numerical example.

REFERENCES

[1] W. Zhang, M. S. Branicky, and S. M. Phillips, "Stability of networked control systems," *IEEE Control Systems Magazine*, vol. 21, no. 1, pp. 84–99, 2001.

[2] G. C. Walsh and H. Ye, "Scheduling of networked control systems," *Control Systems, IEEE*, vol. 21, no. 1, pp. 57–65, 2001.

[3] Y. Tipsuwan and M.-Y. Chow, "Control methodologies in networked control systems," *Control engineering practice*, vol. 11, no. 10, pp. 1099–1111, 2003.

[4] L. Zhang and D. Hristu-Varsakelis, "Communication and control co-design for networked control systems," *Automatica*, vol. 42, no. 6, pp. 953–958, 2006.

[5] J. P. Hespanha, P. Naghshtabrizi, and Y. Xu, "A survey of recent results in networked control systems," *Proceedings of the IEEE*, vol. 95, no. 1, pp. 138–162, 2007.

[6] R. Alur, K.-E. Arzen, J. Baillieul, T. Henzinger, D. Hristu-Varsakelis, and W. S. Levine, *Handbook of networked and embedded control systems*. Springer Science & Business Media, 2007.

[7] F.-Y. Wang and D. Liu, *Networked Control Systems*. Springer, 2008.

[8] A. Bemporad, M. Heemels, and M. Johansson, *Networked Control Systems*. Springer, 2010.

[9] P. Tabuada, "Event-triggered real-time scheduling of stabilizing control tasks," *IEEE Transactions on Automatic Control*, vol. 52, no. 9, pp. 1680–1685, 2007.

[10] M. Mazo Jr and P. Tabuada, "On event-triggered and self-triggered control over sensor/actuator networks," in *IEEE Conference on Decision and Control*, pp. 435–440, 2008.

[11] M. Mazo Jr, A. Anta, and P. Tabuada, "On self-triggered control for linear systems: Guarantees and complexity," in *IEEE European Control Conference*, pp. 3767–3772, 2009.

[12] J. Lunze and D. Lehmann, "A state-feedback approach to event-based control," *Automatica*, vol. 46, no. 1, pp. 211–215, 2010.

[13] R. Postoyan, A. Anta, D. Nesic, and P. Tabuada, "A unifying Lyapunov-based framework for the event-triggered control of nonlinear systems," in *IEEE Conference on Decision and Control and European Control Conference*, pp. 2559–2564, 2011.

[14] W. Heemels, K. H. Johansson, and P. Tabuada, "An introduction to event-triggered and self-triggered control," in *IEEE Annual Conference on Decision and Control*, pp. 3270–3285, 2012.

[15] J.-J. E. Slotine and W. Li, "On the adaptive control of robot manipulators," *The international journal of robotics research*, vol. 6, no. 3, pp. 49–59, 1987.

[16] M. Krstic, P. V. Kokotovic, and I. Kanellakopoulos, *Nonlinear and adaptive control design*. John Wiley & Sons, Inc., 1995.

[17] K. Zhou, J. C. Doyle, and K. Glover, *Robust and optimal control*, vol. 40. Prentice hall New Jersey, 1996.

[18] K. Zhou and J. C. Doyle, *Essentials of Robust Control*. Upper Saddle River, NJ: Prentice Hall, 1998.

[19] K. S. Narendra and A. M. Annaswamy, *Stable Adaptive Systems*. Courier Corporation, 2012.

[20] P. A. Ioannou and J. Sun, *Robust Adaptive Control*. Courier Corporation, 2012.

[21] E. Lavretsky and K. Wise, *Robust and Adaptive Control: With Aerospace Applications*. Springer, 2012.

[22] K. J. Åström and B. Wittenmark, *Adaptive Control*. Courier Corporation, 2013.

[23] A. Sahoo, H. Xu, and S. Jagannathan, "Neural network-based adaptive event-triggered control of nonlinear continuous-time systems," *IEEE International Symposium on Intelligent Control*, pp. 35–40, 2013.

[24] A. Sahoo, H. Xu, and S. Jagannathan, "Neural network approximation-based event-triggered control of uncertain mimo nonlinear discrete time systems," *IEEE American Control Conference*, pp. 2017–2022, 2014.

[25] X. Wang and N. Hovakimyan, "$\mathcal{L}_1$ adaptive control of event-triggered networked systems," *IEEE American Control Conference*, pp. 2458–2463, 2010.

[26] X. Wang, E. Kharisov, and N. Hovakimyan, "Real-time $\mathcal{L}_1$ adaptive control for uncertain networked control systems," *IEEE Transactions on Automatic Control*, vol. 60, no. 9, pp. 2500–2505, 2015.

[27] A. Albattat, B. C. Gruenwald, and T. Yucelen, "Event-triggered adaptive control," in *ASME 2015 Dynamic Systems and Control Conference*, American Society of Mechanical Engineers, 2015.

[28] H. K. Khalil, "Adaptive output feedback control of nonlinear systems represented by input-output models," *Automatic Control, IEEE Transactions on*, vol. 41, no. 2, pp. 177–188, 1996.

[29] A. J. Calise, N. Hovakimyan, and M. Idan, "Adaptive output feedback control of nonlinear systems using neural networks," *Automatica*, vol. 37, no. 8, pp. 1201–1211, 2001.

[30] N. Hovakimyan, F. Nardi, A. Calise, and N. Kim, "Adaptive output feedback control of uncertain nonlinear systems using single-hidden-layer neural networks," *Neural Networks, IEEE Transactions on*, vol. 13, no. 6, pp. 1420–1431, 2002.

[31] K. Y. Volyanskyy, W. M. Haddad, and A. J. Calise, "A new neuroadaptive control architecture for nonlinear uncertain dynamical systems: Beyond-and-modifications," *IEEE Transactions on Neural Networks*, vol. 20, no. 11, pp. 1707–1723, 2009.

[32] T. Yucelen and W. M. Haddad, "Output feedback adaptive stabilization and command following for minimum phase dynamical systems with unmatched uncertainties and disturbances," *International Journal of Control*, vol. 85, no. 6, pp. 706–721, 2012.

[33] E. Lavretsky, "Adaptive output feedback design using asymptotic properties of LQG/LTR controllers," *Automatic Control, IEEE Transactions on*, vol. 57, no. 6, pp. 1587–1591, 2012.

[34] T. E. Gibson, Z. Qu, A. M. Annaswamy, and E. Lavretsky, "Adaptive output feedback based on closed-loop reference models," *arXiv preprint arXiv:1410.1944*, 2014.

[35] E. Lavretsky, "Transients in output feedback adaptive systems with observer-like reference models," *International Journal of Adaptive Control and Signal Processing*, vol. 29, no. 12, pp. 1515–1525, 2015.

[36] K. Kaneko and R. Horowitz, "Repetitive and adaptive control of robot manipulators with velocity estimation," *Robotics and Automation, IEEE Transactions on*, vol. 13, no. 2, pp. 204–217, 1997.

[37] T. Burg, D. Dawson, and P. Vedagarbha, "A redesigned dcal controller without velocity measurements: theory and demonstration," *Robotica*, vol. 15, no. 03, pp. 337–346, 1997.

[38] E. Zergeroglu, W. Dixon, D. Haste, and D. Dawson, "A composite adaptive output feedback tracking controller for robotic manipulators," *Robotica*, vol. 17, no. 06, pp. 591–600, 1999.

[39] F. Zhang, D. M. Dawson, M. S. de Queiroz, W. E. Dixon, *et al.*, "Global adaptive output feedback tracking control of robot manipulators," *IEEE Transactions on Automatic Control*, vol. 45, no. 6, pp. 1203–1208, 2000.

[40] K. Kim, T. Yucelen, and A. J. Calise, "A parameter dependent riccati equation approach to output feedback adaptive control," in *AIAA Guidance, Navigation, and Control Conference*, 2011.

[41] K. Kim, A. J. Calise, T. Yucelen, and N. Nguyen, "Adaptive output feedback control for an aeroelastic generic transport model: A parameter dependent riccati equation approach," in *AIAA Guidance, Navigation, and Control Conference*, 2011.

[42] A. Yeşildirek and F. L. Lewis, "Feedback linearization using neural networks," *Automatica*, vol. 31, no. 11, pp. 1659–1664, 1995.

[43] Y. H. Kim and F. L. Lewis, "Neural network output feedback control of robot manipulators," *Robotics and Automation, IEEE Transactions on*, vol. 15, no. 2, pp. 301–309, 1999.

[44] J.-B. Pomet and L. Praly, "Adaptive nonlinear regulation: estimation from the Lyapunov equation," *IEEE Transactions on Automatic Control*, vol. 37, no. 6, pp. 729–740, 1992.

[45] T. E. Lavretsky, Eugene and and A. M. Annaswamy, "Projection operator in adaptive systems," 2011.

[46] J. Kevorkian and J. D. Cole, *Multiple Scale and Singular Perturbation Methods*. Springer-Verlag New York, 1996.

[47] J. D. Murray, *Asymptotic Analysis*. Springer-Verlag New York, 1984.

[48] E. Lavretsky, "Adaptive output feedback design using asymptotic properties of lqg/ltr controllers," *AIAA Guidance, Navigation, and Control Conference*, 2010.

[49] D. S. Bernstein, *Matrix mathematics: Theory, Facts, and Formulas*. Princeton University Press, 2009.

[50] H. K. Khalil, *Nonlinear Systems*. Upper Saddle River, NJ: PrenticeHall, 1996.

III. ON EVENT-TRIGGERED ADAPTIVE ARCHITECTURES FOR DECENTRALIZED AND DISTRIBUTED CONTROL OF LARGE-SCALE MODULAR SYSTEMS

Ali Albattat[1], Benjamin C. Gruenwald[2] ,and Tansel Yucelen[2]

[1] Department of Mechanical & Aerospace Engineering

Missouri University of Science and Technology

[2] Department of Mechanical Engineering

University of South Florida

ABSTRACT

The last decade has witnessed an increased interest in physical systems controlled over wireless networks (networked control systems). These systems allow the computation of control signals via processors that are not attached to the physical systems, and the feedback loops are closed over wireless networks. The contribution of this paper is to design and analyze event-triggered decentralized and distributed adaptive control architectures for uncertain networked large-scale modular systems; that is, systems consist of physically-interconnected modules controlled over wireless networks. Specifically, the proposed adaptive architectures guarantee overall system stability while reducing wireless network utilization and achieving a given system performance in the presence of system uncertainties that can result from modeling and degraded modes of operation of the modules and their interconnections between each other. In addition to the theoretical findings including rigorous system stability and the boundedness analysis of the closed-loop dynamical system, as well as the characterization of the effect of user-defined event-triggering

thresholds and the design parameters of the proposed adaptive architectures on the overall system performance, an illustrative numerical example is further provided to demonstrate the efficacy of the proposed decentralized and distributed control approaches.

Keywords: large-scale modular systems; networked control systems; uncertain dynamical systems; event-triggered control; decentralized control; distributed control; system stability and performance

1. INTRODUCTION

The design and implementation of decentralized and distributed architectures for controlling complex, large-scale systems is a nontrivial control engineering task involving the consideration of components interacting with the physical processes to be controlled. In particular, large-scale systems are characterized by a large number of highly coupled components exchanging matter, energy or information and have become ubiquitous given the recent advances in embedded sensor and computation technologies. Examples of such systems include, but are not limited to, multi-vehicle systems, communication systems, power systems, process control systems and water systems (see, for example, [1, 2, 3, 4, 5, 6] and the references therein). This paper concentrates on an important class of large-scale systems; namely, large-scale modular systems that consist of physically-interconnected and generally heterogeneous modules.

1.1. Motivation and Literature Review. Two sweeping generalizations can be made about large-scale modular systems. The first is that their complex structure and large-scale nature yield to inaccurate mathematical module models, since it is a challenge to precisely model each module of a large-scale system and the interconnections between these modules. As a consequence, the discrepancies between the modules and their mathematical models, that is system uncertainties, result in the degradation of overall system stability and the performance of the large-scale modular systems. To this end, adaptive control methodologies [7, 8, 9, 10, 11, 12, 13] offer an important capability for this class of

dynamical systems to learn and suppress the effect of system uncertainties resulting from modeling and degraded modes of operation, and hence, they offer system stability and desirable closed-loop system performance in the presence of system uncertainties without excessively relying on mathematical models.

The second generalization about large-scale modular systems is that these systems are often controlled over wireless networks, and hence, the communication costs between the modules and their remote processors increase proportionally with the increase in the number of modules and often the interconnection between these modules. To this end, event-triggered control methodologies [14, 15, 16] offer new control execution paradigms that relax the fixed periodic demand of computational resources and allow for the aperiodic exchange of sensor and actuator information with the remote processor to reduce overall communication cost over a wireless network. Note that adaptive control methodologies and event-triggered control methodologies are often studied separately in the literature, where it is of practical importance to theoretically integrate these two approaches to guarantee system stability and the desirable closed-loop system performance of uncertain large-scale modular systems with reduced communication costs over wireless networks, which is the main focus of this paper.

More specifically, the authors of [17, 18, 19, 20, 21, 22, 23, 6] proposed decentralized and distributed adaptive control architectures for large-scale systems; however, these approaches do not make any attempts to reduce the overall communication cost over wireless networks using, for example, event-triggered control methodologies. In addition, the authors of [24, 25, 26, 27, 28, 29, 30] present decentralized and distributed control architectures with event triggering; however, these approaches do not consider adaptive control architectures and assume perfect models of the processes to be controlled; hence, they are not practical for large-scale modular systems with significant system uncertainties. Only the authors of [31, 32, 33, 34, 35, 36] present event-triggered adaptive control approaches for uncertain dynamical systems. In particular, the authors of [31, 32] consider data transmission from a physical system to the controller, but not vice versa, while de-

veloping their adaptive control approaches to deal with system uncertainties. On the other hand, the adaptive control architectures of the authors in [33, 34, 35, 36] consider two-way data transmission over wireless networks; that is, from a physical system to the controller and from the controller to this physical system. However, none of these approaches can be directly applied to large-scale modular systems. This is due to the fact that large-scale modular systems require decentralized and distributed architectures, and direct application of the results in [31, 32, 33, 34, 35, 36] to this class of systems can result in centralized architectures, which is not practically desired due to the large-scale nature of modular systems. To summarize, there do not exist resilient adaptive control architectures for large-scale systems in the literature to deal with system uncertainties while reducing the communication costs between the models and their remote processors.

1.2. Contribution. The contribution of this paper is to design and analyze event-triggered decentralized and distributed adaptive control architectures for uncertain large-scale systems controlled over wireless networks. Specifically, the proposed decentralized and distributed adaptive architectures of this paper guarantee overall system stability while reducing wireless network utilization and achieving a given system performance in the presence of system uncertainties that can result from modeling and degraded modes of operation of the modules and their interconnections between each other. From a theoretical viewpoint, the proposed event-triggered adaptive architectures here can be viewed as a significant generalization of our prior work documented in [35, 36] to large-scale modular systems, which consider a state emulator-based adaptive control methodology with robustness against high-frequency oscillations in the controller response [10, 37, 38, 39, 40, 41, 13, 42]. In this generalization, we also adopt necessary tools and methods from [23, 6] on decentralized and distributed adaptive controller construction for large-scale modular systems. In addition to the theoretical findings including rigorous system stability and boundedness analysis of the closed-loop dynamical system and the characterization of the effect of user-defined event-triggering thresholds, as well as the design parameters of the

proposed adaptive architectures on the overall system performance, an illustrative numerical example is further provided to demonstrate the efficacy of the proposed decentralized and distributed control approaches.

1.3. Organization. The contents of the paper are as follows. In Section 2, we consider an event-triggered decentralized adaptive control approach for large-scale modular systems, where the considered approach assumes that physically-interconnected modules cannot communicate with each other for exchanging their state information. Specifically, Theorem 1 and Corollaries 1–4 show the main results of Section 2 subject to some structural conditions on the parameters of the large-scale modular systems and the proposed event-triggered decentralized control architecture (see Assumptions 4 and 5). In Section 3, we consider an event-triggered distributed adaptive control approach in Theorem 2 and Corollaries 5–7 for getting rid of such structural conditions, where the considered approach assumes that physically-interconnected modules can locally communicate with each other for exchanging their state information. Finally, the illustrative numerical example is presented in Section 4, and conclusions are summarized in Section 5.

1.4. Notation. The notation used in this paper is fairly standard. Specifically, $\mathbb{R}$ denotes the set of real numbers, $\mathbb{R}^n$ denotes the set of $n \times 1$ real column vectors, $\mathbb{R}^{n\times m}$ denotes the set of $n \times m$ real matrices, $\mathbb{R}_+$ denotes the set of positive real numbers, $\mathbb{R}_+^{n\times n}$ denotes the set of $n \times n$ positive-definite real matrices, $\mathbb{S}^{n\times n}$ denotes the set of $n \times n$ symmetric real matrices, $\mathbb{D}^{n\times n}$ denotes the set of $n \times n$ real matrices with diagonal scalar entries, $(\cdot)^{\mathrm{T}}$ denotes transpose, $(\cdot)^{-1}$ denotes inverse, $\mathrm{tr}(\cdot)$ denotes the trace operator, $\mathrm{diag}(a)$ denotes diagonal matrix with the vector a on its diagonal, and "$\triangleq$" denotes equality by definition. In addition, we write $\lambda_{\min}(A)$ (respectively, $\lambda_{\max}(A)$) for the minimum and respectively maximum eigenvalue of the Hermitian matrix A, $\|\cdot\|$ for the Euclidean norm, and $\|\cdot\|_{\mathrm{F}}$ for the Frobenius matrix norm. Furthermore, we use "$\vee$" for the "or" logic operator and "$\overline{(\cdot)}$" for the "not" logic operator.

We adopt graphs [43] to encode physical interactions and communications between modules. In particular, an undirected graph $\mathcal{G}$ is defined by $\mathcal{V}_\mathcal{G} = \{1, \cdots, N\}$ of nodes and a set $\mathcal{E}_\mathcal{G} \in \mathcal{V}_\mathcal{G} \times \mathcal{V}_\mathcal{G}$, of edges. If $(i, j) \in \mathcal{E}_\mathcal{G}$, then the nodes i and j are neighbors and the neighboring relation is indicated with $i \sim j$. The degree of a node is given by the number of its neighbors, where d_i denotes the degree of node i. Lastly, the adjacency matrix of a graph $\mathcal{G}$, $\mathcal{A}(\mathcal{G}) \in \mathbb{R}^{N\times N}$, is given by

$$[\mathcal{A}(\mathcal{G})]_{ij} \triangleq \begin{cases} 1, & \text{if } (i,j) \in \mathcal{E}_\mathcal{G}, \\ 0, & \text{otherwise.} \end{cases} \tag{1}$$

2. EVENT-TRIGGERED DECENTRALIZED ADAPTIVE CONTROL

In this section, we introduce an event-triggered decentralized adaptive control architecture, where it is assumed that physically-interconnected modules cannot communicate with each other. For organizational purposes, this section is broken up into two subsections. Specifically, we first briefly overview a standard decentralized adaptive control architecture without event-triggering and then present the proposed event-triggered decentralized adaptive control approach, which includes rigorous stability and performance analyses with no Zeno behavior and generalizations to the state emulator case for suppressing the effect of possible high-frequency oscillations in the controller response.

2.1. Overview of a Standard Decentralized Adaptive Control Architecture Without Event-triggering. Consider an uncertain large-scale modular system $\mathcal{S}$ consisting of N interconnected modules $\mathcal{S}_i$, $i \in \mathcal{V}_\mathcal{G}$, given by:

$$\mathcal{S}_i : \qquad \dot{x}_i(t) = A_i x_i(t) + B_i \left[\Lambda_i u_i(t) + \Delta_i \left(x_i(t) \right) + \sum_{i\sim j} \delta_{ij}(x_j(t)) \right], \quad x_i(0) = x_{i0}, \tag{2}$$

where $x_i(t) \in \mathbb{R}^{n_i}$ is the state of $\mathcal{S}_i$, $u_i(t) \in \mathbb{R}^{m_i}$ is the control input applied to $\mathcal{S}_i$, $A_i \in \mathbb{R}^{n_i \times n_i}$, $B_i(t) \in \mathbb{R}^{n_i \times m_i}$ are known matrices and the pair (A_i, B_i) is controllable. In addition, $\Lambda_i \in \mathbb{R}_+^{m_i \times m_i} \cap \mathbb{D}^{m_i \times m_i}$ is an unknown module control effectiveness matrix; $\Delta_i : \mathbb{R}^{n_i} \to \mathbb{R}^{m_i}$ represents matched module bounded uncertainties; and $\delta_{ij} : \mathbb{R}^{n_j} \to \mathbb{R}^{m_i}$ represents matched unknown physical interconnections with respect to module j, $j \in \mathcal{V}_\mathcal{G}$, such that $(i, j) \in \mathcal{E}_\mathcal{G}$.

Assumption 1. The unknown module uncertainty is parameterized as:

$$\Delta_i(x_i(t)) = W_{\mathrm{o}i}^{\mathrm{T}} \beta_i(x_i(t)), \quad x_i \in \mathbb{R}^{n_i}, \tag{3}$$

where $W_{\mathrm{o}i} \in \mathbb{R}^{g_i \times m_i}$ is an unknown weight matrix, which satisfies $\|W_{\mathrm{o}i}\|_{\mathrm{F}} \leq \omega_i^*$, $\omega_i^* \in \mathbb{R}_+$, and $\beta_i(x_i(t)) : \mathbb{R}^{n_i} \to \mathbb{R}^{g_i}$ is a known Lipschitz continuous basis function vector satisfying:

$$\|\beta_i(x_{1i}) - \beta_i(x_{2i})\| \leq L_{\beta i} \|x_{1i} - x_{2i}\|, \tag{4}$$

with $L_{\beta i} \in \mathbb{R}_+$.

Assumption 2. The function $\delta_{ij}(x_j(t))$ in Equation (2) satisfies:

$$\|\delta_{ij}(x_j(t))\| \leq \alpha_{ij} \|x_j(t)\|, \quad \alpha_{ij} > 0, \quad x_j \in \mathbb{R}^{n_j}. \tag{5}$$

Next, consider the reference model $\mathcal{S}_{\mathrm{r}i}$ capturing a desired closed-loop performance for module i, $i \in \mathcal{V}_\mathcal{G}$ given by:

$$\mathcal{S}_{\mathrm{r}i} : \qquad \dot{x}_{\mathrm{r}i}(t) = A_{\mathrm{r}i} x_{\mathrm{r}i}(t) + B_{\mathrm{r}i} c_i(t), \quad x_{\mathrm{r}i}(0) = x_{\mathrm{r}i0}, \tag{6}$$

where $x_{\mathrm{r}i}(t) \in \mathbb{R}^{n_i}$ is the reference state vector of $\mathcal{S}_{\mathrm{r}i}$, $c_i(t) \in \mathbb{R}^{m_i}$ is a given bounded command of $\mathcal{S}_{\mathrm{r}i}$, $A_{\mathrm{r}i} \in \mathbb{R}^{n_i \times n_i}$ is the reference system matrix and $B_{\mathrm{r}i} \in \mathbb{R}^{n_i \times m_i}$ is the command input matrix.

Assumption 3. There exist $K_{1i} \in \mathbb{R}^{m_i \times n_i}$ and $K_{2i} \in \mathbb{R}^{m_i \times m_i}$, such that $A_{\mathrm{r}i} = A_i - B_i K_{1i}$ and $B_{\mathrm{r}i} = B_i K_{2i}$ hold with $A_{\mathrm{r}i}$ being Hurwitz.

Using Assumptions 1 and 3, Equation (2) can be equivalently written as:

$$\dot{x}_i(t) = A_{\mathrm{r}i}x_i(t) + B_{\mathrm{r}i}c_i(t) + B_i\Lambda_i\left[u_i(t) + W_i^{\mathrm{T}}\sigma_i\left(x_i(t), c_i(t)\right)\right] + B_i\sum_{i\sim j}\delta_{ij}(x_j(t)), \quad (7)$$

where $W_i \triangleq \left[\Lambda_i^{-1}W_{\mathrm{o}i}^{\mathrm{T}}\,,\,\Lambda_i^{-1}K_{1i}^{\mathrm{T}}\,,\,\Lambda_i^{-1}K_{2i}^{\mathrm{T}}\right]^{\mathrm{T}} \in \mathbb{R}^{(g_i+n_i+m_i)\times m_i}$ is the unknown weight matrix and $\sigma_i\big(x_i(t), c_i(t)\big) \triangleq \left[\beta_i^{\mathrm{T}}(x_i(t))\,,\,x_i^{\mathrm{T}}(t)\,,\,c_i^{\mathrm{T}}(t)\right]^{\mathrm{T}} \in \mathbb{R}^{g_i+n_i+m_i}$. Motivated from the structure of the uncertain terms appearing in Equation (7), let the decentralized adaptive feedback controller of $\mathcal{S}_i$, $i \in \mathcal{V}_{\mathcal{G}}$, be given by:

$$\mathcal{C}_i: \qquad u_i(t) \triangleq -\hat{W}_i(t)^{\mathrm{T}}\sigma_i\left(x_i(t), c_i(t)\right), \quad (8)$$

where $\hat{W}_i(t)$ is an estimate of W_i satisfying the update law:

$$\dot{\hat{W}}_i(t) \triangleq \gamma_i\mathrm{Proj}_{\mathrm{m}}\Big[\hat{W}_i(t)\,,\,\sigma_i\left(x_i(t), c_i(t)\right)\left(x_i(t) - x_{ri}(t)\right)^{\mathrm{T}}P_iB_i\Big], \quad \hat{W}_i(0) = \hat{W}_{i0}, \quad (9)$$

where $\mathrm{Proj}_{\mathrm{m}}$ denotes the projection operator defined for matrices [44, 45, 10, 35], $\gamma_i \in \mathbb{R}_+$ being the learning rate and $P_i \in \mathbb{R}_+^{n_i\times n_i} \cap \mathbb{S}^{n_i\times n_i}$ being a solution of the Lyapunov equation:

$$0 = A_{\mathrm{r}i}^{\mathrm{T}}P_i + P_iA_{\mathrm{r}i} + R_i, \quad (10)$$

with $R_i \in \mathbb{R}_+^{n_i\times n_i} \cap \mathbb{S}^{n_i\times n_i}$. Now, letting:

$$e_i(t) \triangleq x_i(t) - x_{\mathrm{r}i}(t), \quad (11)$$

$$\tilde{W}_i(t) \triangleq \hat{W}_i(t) - W_i, \quad (12)$$

and using Equations (6) and (7), the module-level closed-loop error dynamics are given by:

$$\dot{e}_i(t) = A_{\mathrm{r}i}e_i(t) - B_i\Lambda_i\tilde{W}_i^{\mathrm{T}}(t)\sigma_i\left(x_i(t), c_i(t)\right) + B_i\sum_{i\sim j}\delta_{ij}(x_j(t)), \quad e_i(t) = e_{i0}. \quad (13)$$

2.2. Proposed Event-triggered Decentralized Adaptive Control Architecture.

We now present the proposed event-triggered decentralized adaptive control architecture for large-scale modular systems, which reduces wireless network utilization and allows a desirable command tracking performance during the two-way data exchange between the module $\mathcal{S}_i$, $i \in \mathcal{V}_{\mathcal{G}}$, and its local controller $\mathcal{C}_i$, over a wireless network. For this objective, we utilize event-triggering control theory to schedule the data exchange dependent on errors exceeding user-defined thresholds. Specifically, the module sends its state signal to its local adaptive controller only when a predefined event occurs. The k_i-th time instants of the state transmission of the module are represented by the monotonic sequence $\{s_{k_i}\}_{k_i=1}^{\infty}$, where $s_{k_i} \in \mathbb{R}_+$. The local controller uses this triggered module state signal to compute the control signal using adaptive control architecture. In addition, the local controller sends the updated feedback control input to the module only when another predefined event occurs. The j_i-th time instants of the feedback control transmission are then represented by the monotonic sequence $\left\{r_{j_i}\right\}_{j_i=1}^{\infty}$, where $r_{j_i} \in \mathbb{R}_+$. As depicted in Figure 1, each module state signal and its local control input are held by a zero-order-hold operator (ZOH) until the next triggering event for the corresponding signal takes place. The delay in sampling, data transmission and computation is not considered in this paper. Consider the uncertain dynamical module i given by:

$$\mathcal{S}_i: \qquad \dot{x}_i(t) = A_i x_i(t) + B_i \left[\Lambda_i u_{\mathrm{s}i}(t) + \Delta_i\left(x_i(t)\right) + \sum_{i\sim j} \delta_{ij}(x_j(t))\right], \quad x_i(0) = x_{i0}, \tag{14}$$

where $u_{\mathrm{s}i}(t) \in \mathbb{R}^{m_i}$ is the sampled control input vector. Using Assumptions 1 and 3, Equation (14) can be equivalently written as:

$$\begin{aligned}\dot{x}_i(t) \;=\; & A_{\mathrm{r}i}x_i(t) + B_{\mathrm{r}i}c_i(t) + B_i\Lambda_i\left[u_{\mathrm{s}i}(t) + W_i^{\mathrm{T}}\sigma_i\left(x_i(t), x_{\mathrm{s}i}(t), c_i(t)\right)\right] + B_i\sum_{i\sim j}\delta_{ij}(x_j(t)) \\ & + B_i\Lambda_i(u_{\mathrm{s}i}(t) - u_i(t)) + B_iK_{1i}(x_{\mathrm{s}i}(t) - x_i(t)),\end{aligned} \tag{15}$$

where $x_{si}(t) \in \mathbb{R}^{n_i}$ is the sampled state vector, $\sigma_i\left(x_i(t), x_{si}(t), c_i(t)\right) \triangleq \left[\beta_i^{\mathrm{T}}(x_i(t))\ ,\ x_{si}^{\mathrm{T}}(t)\right.$ $\left.,\ c_i^{\mathrm{T}}(t)\right]^{\mathrm{T}} \in \mathbb{R}^{g_i+n_i+m_i}$. Now, let the adaptive feedback control law be given by:

$$C_i: \qquad u_i(t) = -\hat{W}_i(t)^{\mathrm{T}}\sigma_i\left(x_{si}(t), c_i(t)\right), \tag{16}$$

where $\sigma_i\left(x_{si}(t), c_i(t)\right) = \left[\beta_i^{\mathrm{T}}(x_{si}(t))\ ,\ x_{si}^{\mathrm{T}}(t)\ ,\ c_i^{\mathrm{T}}(t)\right]^{\mathrm{T}} \in \mathbb{R}^{g_i+n_i+m_i}$, and $\hat{W}_i(t)$ satisfies the weight update law:

$$\dot{\hat{W}}_i(t) = \gamma_i \mathrm{Proj}_{\mathrm{m}}\Big[\hat{W}_i(t)\ ,\ \sigma_i\left(x_{si}(t), c_i(t)\right) e_{si}^{\mathrm{T}}(t) P_i B_i\Big], \quad \hat{W}_i(0) = \hat{W}_{i0}, \tag{17}$$

with $e_{si}(t) \triangleq x_{si}(t) - x_{ri}(t) \in \mathbb{R}^{n_i}$ being the error of the triggered module state vector. Note that using Equation (16), Equation (15) can be rewritten as:

$$\begin{aligned}\dot{x}_i(t) =& A_{ri}x_i(t) + B_{ri}c_i(t) - B_i\Lambda_i\tilde{W}_i^{\mathrm{T}}(t)\sigma_i\left(x_{si}(t), c_i(t)\right) - B_i\Lambda_i g_i(\cdot) + B_i\sum_{i\sim j}\delta_{ij}(x_j(t)) \\ &+ B_i\Lambda_i(u_{si}(t) - u_i(t)) + B_iK_{1i}(x_{si}(t) - x_i(t)),\end{aligned} \tag{18}$$

where $g_i(\cdot) \triangleq W_i^{\mathrm{T}}\left[\sigma_i\left(x_{si}(t), c_i(t)\right) - \sigma_i\left(x_i(t), x_{si}(t), c_i(t)\right)\right]$, and using Equations (18) and (6), we can write the module error dynamics as:

$$\begin{aligned}\dot{e}_i(t) =& A_{ri}e_i(t) - B_i\Lambda_i\tilde{W}_i^{\mathrm{T}}(t)\sigma_i\left(x_{si}(t), c_i(t)\right) - B_i\Lambda_i g_i(\cdot) + B_i\sum_{i\sim j}\delta_{ij}(x_j(t)) \\ &+ B_i\Lambda_i(u_{si}(t) - u_i(t)) + B_iK_{1i}(x_{si}(t) - x_i(t))\end{aligned} \tag{19}$$

The proposed event-triggered decentralized adaptive control algorithm is based on the two-way data exchange structure depicted in Figure 1, where the local controller generates $u_i(t)$ and the uncertain dynamical module is driven by the sampled version of its local control signal $u_{si}(t)$ depending on an event-triggering mechanism. Similarly, the local controller utilizes $x_{si}(t)$ that represents the sampled version of the uncertain dynamical module state $x_i(t)$ depending on an event-triggering mechanism. For this purpose, let $\epsilon_{xi} \in \mathbb{R}_+$ be a

given, user-defined sensing threshold to allow for data transmission from the uncertain dynamical system to the controller. In addition, let $\epsilon_{ui} \in \mathbb{R}_+$ be a given, user-defined actuation threshold to allow for data transmission from the local controller to the uncertain dynamical module. Similar in fashion to [33, 35], we now define three logic rules for scheduling the two-way data exchange:

$$E_{1i}: \quad \|x_{si}(t) - x_i(t)\| \leq \epsilon_{xi}, \tag{20}$$

$$E_{2i}: \quad \|u_{si}(t) - u_i(t)\| \leq \epsilon_{ui}, \tag{21}$$

$$E_{3i}: \quad \text{The controller receives } x_{si}(t). \tag{22}$$

Specifically, when the inequality in Equation (20) is violated at the s_{k_i} moment of the k_i-th time instant, the uncertain module triggers the measured state signal information, such that $x_{si}(t)$ is sent to its local controller. Likewise, when Equation (21) is violated or the local controller receives a new transmitted module state from the uncertain dynamical system (i.e., when $\overline{E}_{2i} \vee E_{3i}$ is true), then the local controller sends a new control input $u_{si}(t)$ to the uncertain dynamical module at the r_{j_i} moment of the j_i-th time instant.

We now analyze the system stability and performance of the proposed event-triggered decentralized adaptive control algorithm introduced in this section using the error dynamics given by Equation (19), as well as the data exchange rules E_{1i}, E_{2i}, and E_{3i} respectively given by Equations (20)–(22). For organizational purposes, the rest of this section, is divided into four subsections. Specifically, we analyze the uniform ultimate boundedness of the resulting closed-loop dynamical system in Section 2.2.1, compute the ultimate bound and highlight the effect of user-defined thresholds and the adaptive controller design parameters on this ultimate bound in Section 2.2.2, show that the proposed architecture does not yield to a Zeno behavior in Section 2.2.3 and generalize the decentralized event-triggered adaptive control algorithm using a state emulator-based framework in Section 2.2.4.

2.2.1. Stability analysis and uniform ultimate boundedness. We now present the first result of this paper, where the following assumption is needed.

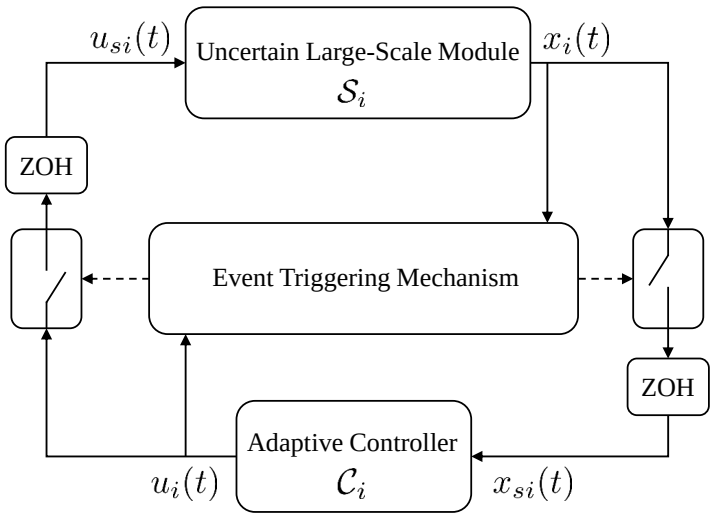

Figure 1. Event-triggered adaptive control for large-scale modular systems.

Assumption 4. $D_{1i} \triangleq \lambda_{\min}(R_i) - 2\lambda_{\max}(P_i)\|B_i\|_{\mathrm{F}} \sum_{i\sim j} \alpha_{ij} - \sum_{i\sim j} \lambda_{\max}(P_j)\|B_j\|_{\mathrm{F}}\alpha_{ji}$ is positive by suitable selection of the design parameters.

Theorem 1. Consider the uncertain large-scale modular system $\mathcal{S}$ consisting of N interconnected modules $\mathcal{S}_i$ described by Equation (14) subject to Assumptions 1–4. Consider, in addition, the reference model given by Equation (6), and the module feedback control law given by Equations (16) and (17). Moreover, let the data transmission from the uncertain dynamical module to the local controller occur when $\overline{E}_{1i}$ is true and the data transmission from the controller to the uncertain dynamical system occur when $\overline{E}_{2i} \vee E_{3i}$ is true. Then, the closed-loop solution $(e_i(t), \tilde{W}_i(t))$ is uniformly ultimately bounded for all $i = 1, 2, ..., N$.

Proof. Since the data transmission from the uncertain modules to their local controllers and from the local controllers to the uncertain modules occur when $\overline{E}_{1i}$ and $\overline{E}_{2i} \vee E_{3i}$ are true, respectively, note that $\|x_{si}(t) - x_i(t)\| \leq \epsilon_{xi}$ and $\|u_{si}(t) - u_i(t)\| \leq \epsilon_{ui}$ hold. Consider now the Lyapunov-like function given by:

$$\mathcal{V}_i(e_i, \tilde{W}_i) = e_i^{\mathrm{T}} P_i e_i + \gamma_i^{-1} \mathrm{tr}\left((\tilde{W}_i \Lambda_i^{\frac{1}{2}})^{\mathrm{T}} (\tilde{W}_i \Lambda_i^{\frac{1}{2}})\right). \tag{23}$$

Note that $\mathcal{V}_i(0,0) = 0$ and $\mathcal{V}_i(e_i, \tilde{W}_i) > 0$ for all $(e_i, \tilde{W}_i) \neq (0,0)$. The time-derivative of Equation (23) is given by:

$$
\begin{aligned}
&\dot{\mathcal{V}}_i(e_i(t), \tilde{W}_i(t)) \\
&= 2e_i^{\mathrm{T}}(t)P\dot{e}_i(t) + 2\gamma_i^{-1}\mathrm{tr}\left(\tilde{W}_i^{\mathrm{T}}(t)\dot{\tilde{W}}_i(t)\Lambda_i\right) \\
&\leq 2e_i^{\mathrm{T}}(t)P_i\Bigg(A_{\mathrm{r}i}e_i(t) - B_i\Lambda_i\tilde{W}_i^{\mathrm{T}}(t)\sigma_i\left(x_{\mathrm{s}i}(t), c_i(t)\right) - B_i\Lambda_i g_i(\cdot) + B_i\sum_{i\sim j}\delta_{ij}(x_j(t)) \\
&\quad + B_i\Lambda_i(u_{\mathrm{s}i}(t) - u_i(t)) + B_iK_{1i}(x_{\mathrm{s}i}(t) - x_i(t))\Bigg) + 2\mathrm{tr}\big(\tilde{W}_i^{\mathrm{T}}(t)\Lambda_i\sigma_i\left(x_{\mathrm{s}i}(t), c_i(t)\right)e_{\mathrm{s}i}^{\mathrm{T}}(t) \\
&\quad \cdot P_iB_i\big) \\
&\leq -e_i^{\mathrm{T}}(t)R_ie_i(t) - 2e_i^{\mathrm{T}}(t)P_iB_i\Lambda_ig_i(\cdot) + 2e_i^{\mathrm{T}}(t)P_iB_i\sum_{i\sim j}\delta_{ij}(x_j(t)) + 2e_i^{\mathrm{T}}(t)P_iB_i\Lambda_i \\
&\quad \cdot(u_{\mathrm{s}i}(t) - u_i(t)) + 2e_i^{\mathrm{T}}(t)P_iB_iK_{1i}(x_{\mathrm{s}i}(t) - x_i(t)) + 2\mathrm{tr}\Big(\tilde{W}_i^{\mathrm{T}}(t)\Lambda_i\sigma_i\left(x_{\mathrm{s}i}(t), c_i(t)\right) \\
&\quad \cdot(x_{\mathrm{s}i}(t) - x_i(t))^{\mathrm{T}}P_iB_i\Big) \\
&\leq -\lambda_{\min}(R_i)\|e_i(t)\|^2 + 2\|e_i(t)\|\lambda_{\max}(P_i)\|B_i\|_{\mathrm{F}}\|\Lambda_i\|_{\mathrm{F}}\|g_i(\cdot)\| \\
&\quad + \|2e_i(t)P_iB_i\sum_{i\sim j}\delta_{ij}(x_j(t))\| + 2\|e_i(t)\|\lambda_{\max}(P_i)\|B_i\|_{\mathrm{F}}\|\Lambda_i\|_{\mathrm{F}}\epsilon_{ui} + 2\|e_i(t)\|\lambda_{\max}(P_i) \\
&\quad \cdot\|B_i\|_{\mathrm{F}}\|K_{1i}\|_{\mathrm{F}}\epsilon_{xi} + 2\|\tilde{W}_i(t)\|_{\mathrm{F}}\|\Lambda_i\|_{\mathrm{F}}\|\sigma_i\left(x_{\mathrm{s}i}(t), c_i(t)\right)\|\epsilon_{xi}\lambda_{\max}(P_i)\|B_i\|_{\mathrm{F}}. \qquad (24)
\end{aligned}
$$

It follows from Assumption 1 that an upper bound for $\|g_i(\cdot)\|$ in Equation (24) can be given by:

$$
\begin{aligned}
\|g_i(\cdot)\| &= \left\|W_i^{\mathrm{T}}\left[\sigma_i\left(x_{\mathrm{s}i}(t), c_i(t)\right) - \sigma_i\left(x_i(t), x_{\mathrm{s}i}(t), c_i(t)\right)\right]\right\| \\
&\leq \underbrace{\|\Lambda_i^{-1}\|_{\mathrm{F}}\omega_i^*L_{\beta i}}_{K_{gi}}\|x_{\mathrm{s}i}(t) - x_i(t)\| \leq K_{gi}\epsilon_{xi}, \qquad (25)
\end{aligned}
$$

where $K_{gi} \in \mathbb{R}_+$. In addition, one can compute an upper bound for $\|\sigma_i\left(x_{\mathrm{s}i}(t), c_i(t)\right)\|$ in Equation (24) as:

$$
\begin{aligned}
\|\sigma_i\left(x_{\mathrm{s}i}(t), c_i(t)\right)\| &\leq \|\beta_i(x_{\mathrm{s}i}(t))\| + \|x_{\mathrm{s}i}(t)\| + \|c_i(t)\| \\
&\leq L_{\beta i}\|x_{\mathrm{s}i}(t)\| + \|x_{\mathrm{s}i}(t)\| + \|c_i(t)\|
\end{aligned}
$$

$$= (L_{\beta i} + 1)\epsilon_{xi} + (L_{\beta i} + 1)\|e_i(t)\| + (L_{\beta i} + 1)x^*_{\mathrm{r}i} + \|c_i(t)\|, \tag{26}$$

where $\|x_{\mathrm{r}i}(t)\| \leq x^*_{\mathrm{r}i}$. Then, using the bounds given by Equations (25) and (26) in Equation (24), one can write:

$$\begin{aligned}
&\dot{\mathcal{V}}_i(e_i(t), \tilde{W}_i(t)) \\
&\leq -\lambda_{\min}(R_i)\|e_i(t)\|^2 + \Big(2\lambda_{\max}(P_i)\|B_i\|_{\mathrm{F}}\|\Lambda_i\|_{\mathrm{F}}K_{gi}\epsilon_{xi} + 2\lambda_{\max}(P_i)\|B_i\|_{\mathrm{F}}\|\Lambda_i\|_{\mathrm{F}}\epsilon_{ui} \\
&\quad +2\lambda_{\max}(P_i)\|B_i\|_{\mathrm{F}}\|K_{1i}\|_{\mathrm{F}}\epsilon_{xi} + 2\|\tilde{W}_i(t)\|_{\mathrm{F}}\|\Lambda_i\|_{\mathrm{F}}(L_{\beta i} + 1)\lambda_{\max}(P_i)\|B_i\|_{\mathrm{F}}\epsilon_{xi}\Big)\|e_i(t)\| \\
&\quad +2\|\tilde{W}_i(t)\|_{\mathrm{F}}\|\Lambda_i\|_{\mathrm{F}}\left((L_{\beta i} + 1)\epsilon_{xi} + (L_{\beta i} + 1)x^*_{\mathrm{r}i} + \|c_i(t)\|\right)\lambda_{\max}(P_i)\|B_i\|_{\mathrm{F}}\epsilon_{xi} \\
&\quad +\|2e_i(t)P_iB_i\sum_{i\sim j}\delta_{ij}(x_j(t))\| \\
&= -c_{1i}\|e_i(t)\|^2 + c_{2i}\|e_i(t)\| + c_{3i} + \|2e_i(t)P_iB_i\delta_{ij}(x_j(t))\|,
\end{aligned} \tag{27}$$

where $c_{1i} \triangleq \lambda_{\min}(R_i)$, $c_{2i} \triangleq 2\lambda_{\max}(P_i)\|B_i\|_{\mathrm{F}}\|\Lambda_i\|_{\mathrm{F}}K_{gi}\epsilon_{xi} + 2\lambda_{\max}(P_i)\|B_i\|_{\mathrm{F}}\|\Lambda_i\|_{\mathrm{F}}\epsilon_{ui} + 2\lambda_{\max}(P_i)\|B_i\|_{\mathrm{F}}\|K_{1i}\|_{\mathrm{F}}\cdot\epsilon_{xi} + 2\tilde{w}^*_i\|\Lambda_i\|_{\mathrm{F}}(L_{\beta i}+1)\lambda_{\max}(P_i)\|B_i\|_{\mathrm{F}}\epsilon_{xi}$ and $c_{3i} \triangleq 2\tilde{w}^*_i\|\Lambda_i\|_{\mathrm{F}}((L_{\beta i}+1)\epsilon_{xi} + (L_{\beta i} + 1)x^*_{\mathrm{r}i} + \|c_i(t)\|)\lambda_{\max}(P_i)\|B_i\|_{\mathrm{F}}\epsilon_{xi}$ with $||\tilde{W}_i(t)||_{\mathrm{F}} \leq \tilde{w}^*_i$ due to utilizing the projection operator in the weight update law given by Equation (9).

Since $x_j(t) = e_j(t) + x_{\mathrm{r}j}(t)$ with $\|x_{\mathrm{r}j}(t)\| \leq x^*_{\mathrm{r}j}$, it follows from Assumption 2 that:

$$\|\sum_{i\sim j}\delta_{ij}(x_j(t))\| \leq \sum_{i\sim j}\alpha_{ij}\Big[\|e_j(t)\| + x^*_{\mathrm{r}j}\Big]. \tag{28}$$

Furthermore, using Equation (28) in the last term of Equation (27) results in:

$$\begin{aligned}
\|2e_i(t)P_iB_i\sum_{i\sim j}\delta_{ij}(x_j(t))\| &\leq 2\lambda_{\max}(P_i)\|e_i(t)\|\|B_i\|_{\mathrm{F}}\|\sum_{i\sim j}\delta_{ij}(x_j(t))\| \\
&\leq 2\lambda_{\max}(P_i)\|e_i(t)\|\|B_i\|_{\mathrm{F}}\sum_{i\sim j}\alpha_{ij}\Big[\|e_j(t)\| + x^*_{\mathrm{r}j}\Big] \\
&\leq \lambda_{\max}(P_i)\|B_i\|_{\mathrm{F}}\sum_{i\sim j}\alpha_{ij}\Big[2\|e_i(t)\|\|e_j(t)\| + 2\|e_i(t)\|x^*_{\mathrm{r}j}\Big]
\end{aligned}$$

$$\leq \lambda_{\max}(P_i)\|B_i\|_{\mathrm{F}} \sum_{i\sim j} \alpha_{ij}\Big[2\|e_i(t)\|^2 + \|e_j(t)\|^2 + {x^*_{\mathrm{r}j}}^2\Big], \quad (29)$$

where Young's inequality [46] is considered in the scalar form of $2xy \leq \nu x^2 + y^2/\nu$, where $x, y \in \mathbb{R}$ and $\nu > 0$, and applied to terms $\|e_i(t)\|\|e_j(t)\|$ and $\|e_i(t)\|x^*_{\mathrm{r}j}$ with $\nu = 1$. Hence, Equation (27) becomes:

$$\begin{aligned}\dot{\mathcal{V}}_i(e_i(t), \tilde{W}_i(t)) \leq\ & -\Big[\underbrace{c_{1i} - 2\lambda_{\max}(P_i)\|B_i\|_{\mathrm{F}} \sum_{i\sim j} \alpha_{ij}}_{d_{1i}}\Big]\|e_i(t)\|^2 \\ & + \underbrace{\lambda_{\max}(P_i)\|B_i\|_{\mathrm{F}}}_{f_i} \sum_{i\sim j} \alpha_{ij}\|e_j(t)\|^2 + c_{2i}\|e_i(t)\| + \varphi_i, \end{aligned} \quad (30)$$

where $\varphi_i \triangleq c_{3i} + \lambda_{\max}(P_i)\|B_i\|_{\mathrm{F}} \sum_{i\sim j} \alpha_{ij} {x^*_{\mathrm{r}j}}^2$.

Introducing:

$$\mathcal{V}(\cdot) = \sum_{i=1}^{N} \mathcal{V}_i(e_i(t), \tilde{W}_i(t)), \quad (31)$$

for the uncertain system $\mathcal{S}$ results in:

$$\begin{aligned}\dot{\mathcal{V}}(\cdot) \leq\ & \sum_{i=1}^{N}\Big[- d_{1i}\|e_i(t)\|^2 + f_i \sum_{i\sim j} \alpha_{ij}\|e_j(t)\|^2 + c_{2i}\|e_i(t)\| + \varphi_i\Big] \\ =\ & \sum_{i=1}^{N}\Big[- \underbrace{\Big(d_{1i} - \sum_{i\sim j} f_j\alpha_{ji}\Big)}_{D_{1i}}\|e_i(t)\|^2 + c_{2i}\|e_i(t)\| + \varphi_i\Big], \end{aligned} \quad (32)$$

where $D_{1i} > 0$ is defined in Assumption 4. Letting $e_a(t) \triangleq [\|e_1(t)\|, \ldots, \|e_N(t)\|]^{\mathrm{T}}$, $D_1 \triangleq \mathrm{diag}([D_{11}, \ldots, D_{1N}])$, $C_2 \triangleq \mathrm{diag}([c_{21}, \ldots, c_{2N}])$ and $\varphi_a \triangleq \sum_{i=1}^{N} \varphi_i$, Equation (32) can equivalently be written as:

$$\begin{aligned}\dot{\mathcal{V}}(\cdot) &\leq -e_a^{\mathrm{T}}(t)D_1e_a(t) + C_2e_a(t) + \varphi_a \\ &\leq -\lambda_{\min}(D_1)\|e_a(t)\|^2 + \lambda_{\max}(C_2)\|e_a(t)\| + \varphi_a, \end{aligned} \quad (33)$$

When $\|e_a(t)\| > \psi$, this renders $\dot{\mathcal{V}}(\cdot) < 0$, where $\psi \triangleq \frac{\frac{\lambda_{\max}(C_2)}{2\sqrt{\lambda_{\min}(D_1)}} + \sqrt{\frac{\lambda^2_{\max}(C_2)}{4\lambda_{\min}(D_1)} + \varphi_a}}{\sqrt{\lambda_{\min}(D_1)}}$. Hence, $e_i(t)$ and $\tilde{W}_i(t)$ are uniformly ultimate bounded for all $i = 1, 2, \ldots, N$. ■

2.2.2. Computation of the ultimate bound for system performance assessment. For revealing the effect of user-defined thresholds and the event-triggered feedback adaptive controller design parameters to the system performance, the next corollary presents a computation of the ultimate bound for the system $\mathcal{S}$. For this purpose, we define the following, $P_{\min} \triangleq \operatorname{diag}([\lambda_{\min}(P_1), \ldots, \lambda_{\min}(P_N)])$, $P_{\max} \triangleq \operatorname{diag}([\lambda_{\max}(P_1), \ldots, \lambda_{\max}(P_N)])$, $\gamma_a \triangleq \operatorname{diag}\left(\left[\gamma_1^{-1}, \ldots, \gamma_N^{-1}\right]\right)$, $\Lambda_a \triangleq \operatorname{diag}([\|\Lambda_1\|_{\mathrm{F}}, \ldots, \|\Lambda_N\|_{\mathrm{F}}])$, $\tilde{W}_a(t) \triangleq [\|\tilde{W}_1(t)\|_{\mathrm{F}}, \ldots, \|\tilde{W}_N(t)\|_{\mathrm{F}}]^{\mathrm{T}}$.

Corollary 1. Consider the uncertain dynamical system $\mathcal{S}$ consisting of N interconnected modules $\mathcal{S}_i$ described by Equation (14) subject to Assumptions 1–4. Consider, in addition, the reference model given by Equation (6), and the module feedback control law given by Equations (16) and (17). Moreover, let the data transmission from the uncertain modules to their local controllers occur when $\overline{E}_{1i}$ is true and the data transmission from the controllers to the uncertain modules occur when $\overline{E}_{2i} \vee E_{3i}$ is true. Then, the ultimate bound of the system error between the uncertain dynamical system and the reference model is given by:

$$||e_a(t)|| \leq \tilde{\Phi} \lambda_{\min}^{-\frac{1}{2}}(P_{\min}), \quad t \geq T, \tag{34}$$

where:

$$\tilde{\Phi} \triangleq [\lambda_{\max}(P_{\max})\psi^2 + \lambda_{\max}(\gamma_a)\lambda_{\max}(\Lambda_a)\|\tilde{W}_a(t)\|^2]^{\frac{1}{2}}. \tag{35}$$

Proof. It follows from the proof of Theorem 1 that $\dot{\mathcal{V}}(e_a(t), \tilde{W}_a(t)) \leq 0$ outside the compact set given by:

$$\mathcal{S} \triangleq \{e_a(t) : \|e_a(t)\| \leq \psi\}. \tag{36}$$

That is, since $\mathcal{V}(e_a(t), \tilde{W}_a(t))$ cannot grow outside $\mathcal{S}$, the evolution of $\mathcal{V}(e_a(t), \tilde{W}_a(t))$ is upper bounded by:

$$\begin{aligned} \mathcal{V}(e_a(t), \tilde{W}_a(t)) &\leq \max_{e_a(t)\in\mathcal{S}} \mathcal{V}(e_a(t), \tilde{W}_a(t)) \\ &= \lambda_{\max}(P_{\max})\psi^2 + \lambda_{\max}(\gamma_a)\lambda_{\max}(\Lambda_a)\|\tilde{W}_a(t)\|^2 \\ &= \tilde{\Phi}^2 \end{aligned} \tag{37}$$

It follows from $e_a^{\mathrm{T}} P_{\min} e_a \leq \mathcal{V}(e_a, \tilde{W}_a)$ that $\|e_a(t)\|^2 \leq \frac{\tilde{\Phi}^2}{\lambda_{\min}(P_{\min})}$, and Equation (34) is immediate. ■

2.2.3. Computation of the event-triggered inter-sample time lower bound. We now show that the proposed event-triggered decentralized adaptive control architecture does not yield to a Zeno behavior, which implies that it does not require a continuous two-way data exchange and reduces wireless network utilization. For the following corollary presenting the result of this subsection, we consider $r_{q_i}^{k_i} \in (s_{k_i}, s_{k_i+1})$ to be the q_i-th time instant when E_{2i} is violated over (s_{k_i}, s_{k_i+1}), and since $\{s_{k_i}\}_{k_i=1}^{\infty}$ is a subsequence of $\left\{r_{j_i}\right\}_{j_i=1}^{\infty}$, it follows that $\left\{r_{j_i}\right\}_{j_i=1}^{\infty} = \{s_{k_i}\}_{k_i=1}^{\infty} \bigcup \left\{r_{q_i}^{k_i}\right\}_{k_i=1,q_i=1}^{\infty,m_{k_i}}$, where $m_{k_i} \in \mathbb{N}$ is the number of violation times of E_{2i} over (s_{k_i}, s_{k_i+1}).

Corollary 2. Consider the uncertain dynamical system $\mathcal{S}$ consisting of N interconnected modules $\mathcal{S}_i$ described by Equation (14) subject to Assumptions 1–4. Consider, in addition, the reference model given by Equation (6), and the module feedback control law given by Equations (16) and (17). Moreover, let the data transmission from the uncertain dynamical module to the local controller occur when $\overline{E}_{1i}$ is true and the data transmission from the controller to the uncertain dynamical system occur when $\overline{E}_{2i} \vee E_{3i}$ is true. Then, there exist positive scalars $\alpha_{xi} \triangleq \frac{\epsilon_{xi}}{\Phi_{1i}}$ and $\alpha_{ui} \triangleq \frac{\epsilon_{ui}}{\Phi_{2i}}$ such that:

$$s_{k_i+1} - s_{k_i} > \alpha_{xi}, \quad \forall k_i \in \mathbb{N}, \tag{38}$$

$$r_{q_i+1}^{k_i} - r_{q_i}^{k_i} > \alpha_{ui}, \quad \forall q_i \in \{0, \ldots, m_{k_i}\}, \quad \forall k_i \in \mathbb{N}. \tag{39}$$

Proof. The time derivative of $\|x_{\mathrm{s}i}(t) - x_i(t)\|$ over $t \in (s_{k_i}, s_{k_i+1})$, $\forall k_i \in \mathbb{N}$, is

given by:

$$
\begin{aligned}
&\frac{d}{dt}\left\|x_{si}(t)-x_i(t)\right\| \\
&\quad\leq \left\|\dot{x}_{si}(t)-\dot{x}_i(t)\right\| = \left\|\dot{x}_i(t)\right\| \\
&\quad\leq \left\|A_{ri}\right\|_{\mathrm{F}}\left[\left\|e_i(t)\right\|+x_{ri}^{*}\right]+\left\|B_{ri}\right\|_{\mathrm{F}}\left\|c_i(t)\right\|+\left\|B_i\right\|_{\mathrm{F}}\left\|\Lambda_i\right\|_{\mathrm{F}}\tilde{w}_i^{*}\Big[L_{\beta i}(\epsilon_{xi}+\left\|e_i(t)\right\| \\
&\qquad+x_{ri}^{*})+\left\|K_{1i}\right\|_{\mathrm{F}}\left(\epsilon_{xi}+\left\|e_i(t)\right\|+x_{ri}^{*}\right)+\left\|K_{2i}\right\|_{\mathrm{F}}\left\|c_i(t)\right\|\Big]+\left\|B_i\right\|_{\mathrm{F}}\left\|\Lambda_i\right\|_{\mathrm{F}}K_{gi}\epsilon_{xi} \\
&\qquad+\left\|B_i\right\|_{\mathrm{F}}\sum_{i\sim j}\alpha_{ij}\left(\left\|e_j(t)\right\|+x_{rj}^{*}\right)+\left\|B_i\right\|_{\mathrm{F}}\left\|\Lambda_i\right\|_{\mathrm{F}}\epsilon_{ui}+\left\|B_i\right\|_{\mathrm{F}}\left\|K_{1i}\right\|_{\mathrm{F}}\epsilon_{xi}. \qquad (40)
\end{aligned}
$$

Since the closed-loop dynamical system is uniformly ultimately bounded by Theorem 1, there exists an upper bound to Equation (40). Letting Φ_{1i} denote this upper bound and with the initial condition satisfying $\lim_{t\to s_{k_i}^{+}}\left\|x_{si}(t)-x_i(t)\right\|=0$, it follows from Equation (40) that:

$$
\left\|x_{si}(t)-x_i(t)\right\|\leq\Phi_{1i}(t-s_{k_i}),\quad\forall t\in(s_{k_i},s_{k_i+1}). \qquad (41)
$$

Therefore, when $\overline{E}_{1i}$ is true, then $\lim_{t\to s_{k_i+1}^{-}}\left\|x_{si}(t)-x_i(t)\right\|=\epsilon_{xi}$, and it then follows from Equation (41) that $s_{k_i+1}-s_{k_i}\geq\alpha_{xi}$.

Similarly, the time derivative of $\left\|u_{si}(t)-u_i(t)\right\|$ over $t\in\left(r_{q_i}^{k_i},r_{q_i+1}^{k_i}\right),\forall q_i\in\mathbb{N}$, is given by:

$$
\begin{aligned}
&\frac{d}{dt}\left\|u_{si}(t)-u_i(t)\right\| \\
&\quad\leq \left\|\dot{u}_{si}(t)-\dot{u}_i(t)\right\| = \left\|\dot{u}_i(t)\right\| \\
&\quad= \left\|\hat{\dot{W}}_i^{\mathrm{T}}(t)\sigma_i\left(x_{si}(t),c_i(t)\right)+\hat{W}_i^{\mathrm{T}}(t)\dot{\sigma}_i\left(x_{si}(t),c_i(t)\right)\right\| \\
&\quad\leq \gamma_i\left\|B_i\right\|_{\mathrm{F}}\lambda_{\max}(P_i)\left\|e_{si}(t)\right\|\left\|\sigma_i\left(x_{si}(t),c_i(t)\right)\right\|^2+\left\|\Lambda_i^{-1}\right\|_{\mathrm{F}}\left\|K_{2i}\right\|_{\mathrm{F}}\left\|\dot{c}_i(t)\right\| \\
&\quad\leq \gamma_i\left\|B_i\right\|_{\mathrm{F}}\lambda_{\max}(P_i)\left(\left\|e_i(t)\right\|+\epsilon_{xi}\right)\Big[L_{\beta i}(\epsilon_{xi}+\left\|e_i(t)\right\|+x_{ri}^{*})+\left\|K_{1i}\right\|_{\mathrm{F}}(\epsilon_{xi} \\
&\qquad+\left\|e_i(t)\right\|+x_{ri}^{*})+\left\|K_{2i}\right\|_{\mathrm{F}}\left\|c_i(t)\right\|\Big]^2+\left\|\Lambda_i^{-1}\right\|_{\mathrm{F}}\left\|K_{2i}\right\|_{\mathrm{F}}\left\|\dot{c}_i(t)\right\|. \qquad (42)
\end{aligned}
$$

Once again, since the closed-loop dynamical system is uniformly ultimately bounded by Theorem 1, there exists an upper bound to Equation (42). Letting Φ_{2i} denote this upper bound, and with the initial condition satisfying $\lim_{t\to r_{q_i}^{k_i+}} \|u_{\mathrm{s}i}(t) - u_i(t)\| = 0$, it follows from Equation (42) that:

$$\|u_{\mathrm{s}i}(t) - u_i(t)\| \leq \Phi_{2i}(t - r_{q_i}^{k_i}), \quad \forall t \in \left(r_{q_i}^{k_i}, r_{q_i+1}^{k_i}\right). \tag{43}$$

Therefore, when $\bar{E}_{2i} \vee E_{3i}$ is true, then $\lim_{t\to r_{q_i+1}^{k_i-}} \|u_{\mathrm{s}i}(t) - u_i(t)\| = \epsilon_{ui}$, and it then follows from Equation (43) that $r_{q_i+1}^{k_i} - r_{q_i}^{k_i} \geq \alpha_{ui}$. ■

Corollary 2 shows that the inter-sample times for the module state vector and decentralized feedback control vector are bounded away from zero, and hence, the proposed event-triggered adaptive control approach does not yield to a Zeno behavior. As discussed earlier, this implies that the proposed event-triggered decentralized adaptive control methodology does not require a continuous two-way data exchange, and it reduces wireless network utilization.

2.2.4. Generalizations to the event-triggered decentralized adaptive control with state emulator. We now generalize our framework to a state emulator-based design, since this framework has the capability to suppress possible high-frequency oscillation in the control signal of the uncertain module $\mathcal{S}_i$ [37, 38, 39, 40, 41, 13, 42, 10]. Consider the (modified) reference system, so-called the state emulator of $\mathcal{S}_i$, given by:

$$\dot{\hat{x}}_i(t) = A_{\mathrm{r}i}\hat{x}_i(t) + B_{\mathrm{r}i}c_i(t) + L_i\left(x_{\mathrm{s}i}(t) - \hat{x}_i(t)\right), \quad \hat{x}_i(0) = \hat{x}_{i0}, \tag{44}$$

where $L_i \in \mathbb{R}_+^{n_i\times n_i} \cap \mathbb{D}^{n_i\times n_i}$ is the state emulator gain. Letting $\hat{e}_i(t) \triangleq \hat{x}_i(t) - x_{\mathrm{r}i}(t) \in \mathbb{R}^{n_i}$, the reference model error dynamics capturing the difference between the ideal reference model in Equation (6) and the state emulator-based (modified) reference model in Equation (44) is given by:

$$\dot{\hat{e}}_i(t) = A_{\mathrm{r}i}\hat{e}_i(t) + L_i\left(x_{\mathrm{s}i}(t) - \hat{x}_i(t)\right). \tag{45}$$

In addition, letting $\tilde{x}_i(t) \triangleq x_i(t) - \hat{x}_i(t) \in \mathbb{R}^{n_i}$ to denote the system state error vector, the (state emulator-based) system error dynamics follows from Equations (18) and (44) as:

$$\begin{aligned}\dot{\tilde{x}}_i(t) &= A_{Li}\tilde{x}_i(t) - B_i\Lambda_i\tilde{W}_i^{\mathrm{T}}(t)\sigma_i\left(x_{\mathrm{s}i}(t), c_i(t)\right) - B_i\Lambda_i g_i(\cdot) + B_i\sum_{i\sim j}\delta_{ij}(x_j(t)) \\ &\quad + B_i\Lambda_i(u_{\mathrm{s}i}(t) - u_i(t)) + (B_iK_{1i} - L_i)(x_{\mathrm{s}i}(t) - x_i(t)), \quad \tilde{x}_i(0) = \tilde{x}_{i0}, \end{aligned} \tag{46}$$

where $A_{Li} \triangleq A_{\mathrm{r}i} - L_i \in \mathbb{R}^{n_i\times n_i}$ is Hurwitz by a suitable selection of the state emulator gain L_i (e.g., A_{Li} is Hurwitz with $L_i = \kappa_i I$, $\kappa_i \in \mathbb{R}_+$, since $A_{\mathrm{r}i}$ is Hurwitz). To maintain system stability, we utilize the adaptive controller given by Equation (16) with the update law described by:

$$\dot{\hat{W}}_i(t) \triangleq \gamma_i \mathrm{Proj}_{\mathrm{m}}\Big[\hat{W}_i(t)\ ,\ \sigma_i\left(x_{\mathrm{s}i}(t), c_i(t)\right)\left(x_{\mathrm{s}i}(t) - \hat{x}_i(t)\right)^{\mathrm{T}}P_iB_i\Big], \quad \hat{W}_i(0) = \hat{W}_{i0}, \tag{47}$$

where $P_i \in \mathbb{R}_+^{n_i\times n_i} \cap \mathbb{S}^{n_i\times n_i}$ is the unique solution of the algebraic Riccati equation:

$$0 = A_{Li}^{\mathrm{T}}P_i + P_iA_{Li} - P_iB_iR_i^{-1}B_i^{\mathrm{T}}P_i + Q_i, \tag{48}$$

with $R_i \in \mathbb{R}_+^{m_i\times m_i} \cap \mathbb{S}^{n_i\times n_i}$ and $Q_i \in \mathbb{R}_+^{n_i\times n_i} \cap \mathbb{S}^{n_i\times n_i}$.

Note from [42, 10] that the state emulator-based adaptive control framework achieves stringent transient and steady-state system performance specifications by judiciously choosing the learning rate γ_i and the state emulator gain L_i without causing high-frequency oscillations in the controller response, unlike standard model reference adaptive controllers overviewed earlier in this section. We also note that if one selects $L_i = 0$, then the results of this paper hold for standard model reference adaptive controllers, and hence, there is no loss in generality in using a state emulator-based adaptive control framework for the main results of this paper.

Consider a parameter-dependent Riccati equation [23, 47] given by:

$$0 = A_{\mathrm{r}i}^{\mathrm{T}}\tilde{P}_i + \tilde{P}_iA_{\mathrm{r}i} + \tilde{Q}_i, \tag{49}$$

$$\tilde{Q}_i = \mu_i\tilde{P}_iL_iL_i^{\mathrm{T}}\tilde{P}_i + \tilde{Q}_{oi}, \tag{50}$$

where $\tilde{P}_i \in \mathbb{R}_+^{n_i \times n_i}$ is a unique solution with $\tilde{Q}_{oi} \in \mathbb{R}_+^{n_i \times n_i}$ and $\mu_i > 0$.

Remark 1 [23]. Let $0 < \mu_i < \bar{\mu}_i$ define the largest set within which there is a positive-definite solution for $\tilde{P}_i$. Since $\tilde{P}_i > 0$ for $\mu_i = 0$ and $\tilde{P}_i > 0$ depends continuously on μ_i, the existence of $\tilde{P}_i(\mu_i) > 0$ for $0 < \mu_i < \bar{\mu}_i$ is assured.

The next lemma shows that for $\mu_i < \bar{\mu}_i$, Equations (49) and (50) can reliably be solved for $\tilde{P}_i > 0$ using the Potter approach given in [48]. This also implies that $\bar{\mu}_i$ can be determined by searching for the boundary value, $\bar{\mu}_i$. We employ notation $\mathrm{ric}(\cdot)$ and $\mathrm{dom}(\cdot)$ as defined in [48].

Lemma 1 [23, 48]. Let $\tilde{P}_i > 0$ satisfy the parameter dependent Riccati equation given by Equations (49) and (50), and let the modified Hamiltonian be given by:

$$H_i = \begin{bmatrix} A_{\mathrm{r}i} & \mu_i L_i L_i^{\mathrm{T}} \\ -\tilde{Q}_{oi} & -A_{\mathrm{r}i}^{\mathrm{T}} \end{bmatrix}. \tag{51}$$

Then, for all $0 < \mu_i < \bar{\mu}_i$, $H_i \in \mathrm{dom}(\mathrm{ric})$ and $\tilde{P}_i = \mathrm{ric}(H_i)$.

Assumption 5. $D_{1i} \triangleq \lambda_{\min}(Q_i) - \lambda_{\min}(R_i^{-1})\lambda_{\max}^2(P_i)\|B_i\|_{\mathrm{F}}^2 - \frac{l_i}{\mu_i} - 3\lambda_{\max}(P_i)\|B_i\|_{\mathrm{F}} \cdot \sum_{i\sim j} \alpha_{ij} - \sum_{i\sim j} \lambda_{\max}(P_j)\|B_j\|_{\mathrm{F}}\alpha_{ji}$ and $D_{2i} \triangleq l_i\lambda_{\min}(\tilde{Q}_{oi}) - \sum_{i\sim j} \lambda_{\max}(P_j)\|B_j\|_{\mathrm{F}}\alpha_{ji}$, $l_i > 0$, are positive by suitable selection of the design parameters.

Corollary 3. Consider the uncertain dynamical system $\mathcal{S}$ consisting of N interconnected modules $\mathcal{S}_i$ described by Equation (14) subject to Assumptions 1–3 and 5. Consider in addition, the ideal reference model given by Equation (6), the state emulator given by Equation (44) and the module feedback control law given by Equations (16) and (47). Moreover, let the data transmission from the uncertain dynamical module to the local controller occur when $\overline{E}_{1i}$ is true and the data transmission from the controller to the uncertain dynamical system occur when $\overline{E}_{2i} \vee E_{3i}$ is true. Then, the closed-loop solution $(\tilde{x}_i(t), \tilde{W}_i(t), \hat{e}_i(t))$ is uniformly ultimately bounded for all $i = 1, 2, ..., N$.

Proof. Consider the Lyapunov-like function given by:

$$\mathcal{V}_i(\tilde{x}_i, \tilde{W}_i, \hat{e}_i) = \tilde{x}_i^{\mathrm{T}} P_i \tilde{x}_i + \gamma_i^{-1}\mathrm{tr}(\tilde{W}_i\Lambda_i^{\frac{1}{2}})^{\mathrm{T}}(\tilde{W}_i\Lambda_i^{\frac{1}{2}}) + l_i\hat{e}_i^{\mathrm{T}}\tilde{P}_i\hat{e}_i, \tag{52}$$

where $l_i > 0$ and $\tilde{P}_i > 0$ satisfies the parameter dependent Riccati equation in Equations (49) and (50). Note that $\mathcal{V}_i(0,0,0) = 0$ and $\mathcal{V}_i(\tilde{x}_i, \tilde{W}_i, \hat{e}_i) > 0$ for all $(\tilde{x}_i, \tilde{W}_i, \hat{e}_i) \neq (0,0,0)$. The time-derivative of Equation (52) is given by:

$$
\begin{aligned}
&\dot{\mathcal{V}}_i(\tilde{x}_i(t), \tilde{W}_i(t), \hat{e}_i(t)) \\
&= 2\tilde{x}_i^{\mathrm{T}}(t) P_i \dot{\tilde{x}}_i(t) + 2\gamma_i^{-1} \mathrm{tr}(\tilde{W}_i(t) \Lambda_i^{\frac{1}{2}})^{\mathrm{T}} (\dot{\tilde{W}}_i(t) \Lambda_i^{\frac{1}{2}}) + 2 l_i \hat{e}_i^{\mathrm{T}}(t) \tilde{P}_i \dot{\hat{e}}_i(t) \\
&\leq 2\tilde{x}_i^{\mathrm{T}}(t) P_i \Big[A_{L_i} \tilde{x}_i(t) - B_i \Lambda_i \tilde{W}_i^{\mathrm{T}}(t) \sigma_i\left(x_{si}(t), c_i(t)\right) - B_i \Lambda_i g_i(\cdot) + B_i \sum_{i \sim j} \delta_{ij}(x_j(t)) \\
&\quad + B_i \Lambda_i \big(u_{si}(t) - u_i(t)\big) + (B_i K_{1i} - L_i)(x_{si}(t) - x_i(t)) \Big] + 2\mathrm{tr} \tilde{W}_i^{\mathrm{T}}(t) \sigma_i\left(x_{si}(t), c_i(t)\right) \\
&\quad \cdot \left(x_{si}(t) - \hat{x}_i(t)\right)^{\mathrm{T}} P_i B_i \Lambda_i + 2 l_i \hat{e}_i^{\mathrm{T}}(t) \tilde{P}_i \left[A_{ri} \hat{e}_i(t) + L_i \left(x_{si}(t) - \hat{x}_i(t)\right) \right] \\
&\leq -\tilde{x}_i^{\mathrm{T}}(t) Q_i \tilde{x}_i(t) + \tilde{x}_i^{\mathrm{T}}(t) P_i B_i R_i^{-1} B_i^{\mathrm{T}} P_i \tilde{x}_i(t) - 2\tilde{x}_i^{\mathrm{T}}(t) P_i B_i \Lambda_i g_i(\cdot) + 2\tilde{x}_i^{\mathrm{T}}(t) P_i B_i \\
&\quad \cdot \sum_{i \sim j} \delta_{ij}(x_j(t)) + 2\tilde{x}_i^{\mathrm{T}}(t) P_i B_i \Lambda_i \big(u_{si}(t) - u_i(t)\big) + 2\tilde{x}_i^{\mathrm{T}}(t) P_i (B_i K_{1i} - L_i)(x_{si}(t) \\
&\quad - x_i(t)) + 2\mathrm{tr} \tilde{W}_i(t)^{\mathrm{T}} \sigma_i\left(x_{si}(t), c_i(t)\right) \left(x_{si}(t) - x_i(t)\right)^{\mathrm{T}} P_i B_i \Lambda_i - l_i \hat{e}_i^{\mathrm{T}}(t) \tilde{Q}_{oi} \hat{e}_i(t) \\
&\quad - l_i \hat{e}_i^{\mathrm{T}}(t) \mu_i \tilde{P}_i L_i L_i^{\mathrm{T}} \tilde{P}_i \hat{e}_i(t) + 2 l_i \hat{e}_i^{\mathrm{T}}(t) \tilde{P}_i L_i (x_{si}(t) - x_i(t)) + 2 l_i \hat{e}_i^{\mathrm{T}}(t) \tilde{P}_i L_i \tilde{x}_i(t). \qquad (53)
\end{aligned}
$$

Young's inequality [46] applied to the last term in Equation (53) produces:

$$
2 l_i \hat{e}_i^{\mathrm{T}}(t) \tilde{P}_i L_i \tilde{x}_i(t) \leq \mu_i l_i \hat{e}_i^{\mathrm{T}}(t) \tilde{P}_i L_i L_i^{\mathrm{T}} \tilde{P}_i \hat{e}_i(t) + \frac{l_i}{\mu_i} \tilde{x}_i^{\mathrm{T}}(t) \tilde{x}_i(t). \qquad (54)
$$

Using Equation (54) in Equation (53) yields:

$$
\begin{aligned}
&\dot{\mathcal{V}}_i(\tilde{x}_i(t), \tilde{W}_i(t), \hat{e}_i(t)) \\
&\leq -\tilde{x}_i^{\mathrm{T}}(t) Q_i \tilde{x}_i(t) + \tilde{x}_i^{\mathrm{T}}(t) P_i B_i R_i^{-1} B_i^{\mathrm{T}} P_i \tilde{x}_i(t) - 2\tilde{x}_i^{\mathrm{T}}(t) P_i B_i \Lambda_i g_i(\cdot) + 2\tilde{x}_i^{\mathrm{T}}(t) P_i B_i \\
&\quad \cdot \sum_{i \sim j} \delta_{ij}(x_j(t)) + 2\tilde{x}_i^{\mathrm{T}}(t) P_i B_i \Lambda_i \big(u_{si}(t) - u_i(t)\big) + 2\tilde{x}_i^{\mathrm{T}}(t) P_i (B_i K_{1i} - L_i)(x_{si}(t) - x_i(t)) \\
&\quad + 2\mathrm{tr} \tilde{W}_i^{\mathrm{T}}(t) (x_{si}(t) - x_i(t))^{\mathrm{T}} P_i B_i \Lambda_i - l_i \hat{e}_i^{\mathrm{T}}(t) \tilde{Q}_{oi} \hat{e}_i(t) + 2 l_i \hat{e}_i^{\mathrm{T}}(t) \tilde{P}_i L_i (x_{si}(t) - x_i(t)) \\
&\quad + \frac{l_i}{\mu_i} \tilde{x}_i^{\mathrm{T}}(t) \tilde{x}_i(t)
\end{aligned}
$$

$$\leq -\lambda_{\min}(R_i)\|\tilde{x}_i(t)\|^2 + \lambda_{\min}(R_i^{-1})\lambda_{\max}^2(P_i)\|B_i\|_{\mathrm{F}}^2\|\tilde{x}_i(t)\|^2 + 2\lambda_{\max}(P_i)\|B_i\|_{\mathrm{F}}\|\Lambda_i\|_{\mathrm{F}}\|g_i(\cdot)\|$$
$$\cdot \|\tilde{x}_i(t)\| + \|2\tilde{x}_i(t)P_iB_i\sum_{i\sim j}\delta_{ij}(x_j(t))\| + 2\|\tilde{x}_i(t)\|\lambda_{\max}(P_i)\|B_i\|_{\mathrm{F}}\|\Lambda_i\|_{\mathrm{F}}\epsilon_{ui} + 2\|\tilde{x}_i(t)\|$$
$$\cdot \lambda_{\max}(P_i)\big(\|B_iK_{1i}\|_{\mathrm{F}} + \|L_i\|_{\mathrm{F}}\big)\epsilon_{xi} + 2\|\tilde{W}_i(t)\|_{\mathrm{F}}\|\sigma_i\left(x_{si}(t), c_i(t)\right)\|\epsilon_{xi}\lambda_{\max}(P_i)\|B_i\|_{\mathrm{F}}\|\Lambda_i\|_{\mathrm{F}}$$
$$- l_i\lambda_{\min}(\tilde{Q}_{oi})\|\hat{e}_i(t)\|^2 + 2l_i\|\hat{e}_i(t)\|\lambda_{\max}(\tilde{P}_i)\|L_i\|_{\mathrm{F}}\epsilon_{xi} + \frac{l_i}{\mu_i}\|\tilde{x}_i(t)\|^2. \tag{55}$$

Using Equations (25) and (26), Equation (55) can be written:

$$\dot{\mathcal{V}}_i(\tilde{x}_i(t), \tilde{W}_i(t), \hat{e}_i(t))$$
$$\leq -\left(\lambda_{\min}(Q_i) - \lambda_{\min}(R_i^{-1})\lambda_{\max}^2(P_i)\|B_i\|_{\mathrm{F}}^2 - \frac{l_i}{\mu_i}\right)\|\tilde{x}_i(t)\|^2 - l_i\lambda_{\min}(\tilde{Q}_{oi})\|\hat{e}_i(t)\|^2$$
$$+ \Big(2\lambda_{\max}(P_i)\|B_i\|_{\mathrm{F}}\|\Lambda_i\|_{\mathrm{F}}K_{gi}\epsilon_{xi} + 2\lambda_{\max}(P_i)\|B_i\|_{\mathrm{F}}\|\Lambda_i\|_{\mathrm{F}}\epsilon_{ui} + 2\lambda_{\max}(P_i)\|B_i\|_{\mathrm{F}}\|K_{1i}\|_{\mathrm{F}}\epsilon_{xi}$$
$$+ 2\|\tilde{W}_i(t)\|_{\mathrm{F}}\|\Lambda_i\|_{\mathrm{F}}(L_{\beta i}+1)\lambda_{\max}(P_i)\|B_i\|_{\mathrm{F}}\epsilon_{xi}\Big)\|\tilde{x}_i(t)\| + 2\|\tilde{W}_i(t)\|_{\mathrm{F}}\|\Lambda_i\|_{\mathrm{F}}\big((L_{\beta i}+1)\epsilon_{xi}$$
$$+ (L_{\beta i}+1)x_{\mathrm{r}i}^* + \|c_i(t)\|\big)\lambda_{\max}(P_i)\|B_i\|_{\mathrm{F}}\epsilon_{xi} + \|2\tilde{x}_i(t)P_iB_i\sum_{i\sim j}\delta_{ij}(x_j(t))\| + 2l_i\lambda_{\max}(\tilde{P}_i)$$
$$\cdot \|L_i\|_{\mathrm{F}}\epsilon_{xi}\|\hat{e}_i(t)\|$$
$$= -c_{1i}\|\tilde{x}_i(t)\|^2 - c_{2i}\|\hat{e}_i(t)\|^2 + c_{3i}\|\tilde{x}_i(t)\| + c_{4i}\|\hat{e}_i(t)\| + c_{5i} + \|2\tilde{x}_i(t)P_iB_i\sum_{i\sim j}\delta_{ij}(x_j(t))\|, \tag{56}$$

where $c_{1i} \triangleq \lambda_{\min}(Q_i) - \lambda_{\min}(R_i^{-1})\lambda_{\max}^2(P_i)\|B_i\|_{\mathrm{F}}^2 - \frac{l_i}{\mu_i}$, $c_{2i} \triangleq l_i\lambda_{\min}(\tilde{Q}_{oi})$, $c_{3i} \triangleq 2\lambda_{\max}(P_i)\|B_i\|_{\mathrm{F}}\|\Lambda_i\|_{\mathrm{F}}K_{gi}\epsilon_{xi} + 2\lambda_{\max}(P_i)\|B_i\|_{\mathrm{F}}\|\Lambda_i\|_{\mathrm{F}}\epsilon_{ui} + 2\lambda_{\max}(P_i)\|B_i\|_{\mathrm{F}}\|K_{1i}\|_{\mathrm{F}}\epsilon_{xi} + 2\tilde{w}_i^*\|\Lambda_i\|(L_{\beta i}+1)\lambda_{\max}(P_i)\|B_i\|_{\mathrm{F}}\epsilon_{xi}$, $c_{4i} \triangleq 2l_i\lambda_{\max}(\tilde{P}_i)\|L_i\|_{\mathrm{F}}\epsilon_{xi}$ and $c_{5i} \triangleq 2\tilde{w}_i^*\|\Lambda_i\|_{\mathrm{F}}\Big((L_{\beta i}+1)\epsilon_{xi} + (L_{\beta i}+1)x_{\mathrm{r}i}^* + \|c_i(t)\|\Big)\lambda_{\max}(P_i)\|B_i\|_{\mathrm{F}}\epsilon_{xi}$.

Since $x_j(t) = \tilde{x}_j(t) + \hat{e}_j(t) + x_{\mathrm{r}j}(t)$, it follows from Assumption 2 that:

$$\|\sum_{i\sim j}\delta_{ij}(x_j(t))\| \leq \sum_{i\sim j}\alpha_{ij}\Big[\|\tilde{x}_j(t)\| + \|\hat{e}_j(t)\| + x_{\mathrm{r}j}^*\Big]. \tag{57}$$

Furthermore, using Equation (57) in the last term of Equation (56) results in:

$$
\begin{aligned}
&\|2\tilde{x}_i(t)P_iB_i\sum_{i\sim j}\delta_{ij}(x_j(t))\| \\
&\quad\le 2\lambda_{\max}(P_i)\|\tilde{x}_i(t)\|\|B_i\|_{\mathrm{F}}\|\sum_{i\sim j}\delta_{ij}(x_j(t))\| \\
&\quad\le 2\lambda_{\max}(P_i)\|\tilde{x}_i(t)\|\|B_i\|_{\mathrm{F}}\sum_{i\sim j}\alpha_{ij}\Big[\|\tilde{x}_j(t)\|+\|\hat{e}_j(t)\|+x^*_{\mathrm{r}j}\Big] \\
&\quad\le \lambda_{\max}(P_i)\|B_i\|_{\mathrm{F}}\sum_{i\sim j}\alpha_{ij}\Big[2\|\tilde{x}_i(t)\|\|\tilde{x}_j(t)\|+2\|\tilde{x}_i(t)\|\|\hat{e}_j(t)\|+2\|\tilde{x}_i(t)\|x^*_{\mathrm{r}j}\Big] \\
&\quad\le \lambda_{\max}(P_i)\|B_i\|_{\mathrm{F}}\sum_{i\sim j}\alpha_{ij}\Big[3\|\tilde{x}_i(t)\|^2+\|\tilde{x}_j(t)\|^2+\|\hat{e}_j(t)\|^2+{x^*_{\mathrm{r}j}}^2\Big],
\end{aligned}
\tag{58}
$$

where Young's inequality [46] is considered in the scalar form of $2xy \le \nu x^2 + y^2/\nu$, with $x, y \in \mathbb{R}$ and $\nu > 0$, and applied to terms $\|\tilde{x}_i(t)\|\|\tilde{x}_j(t)\|$, $\|\tilde{x}_i(t)\|\|\hat{e}_j(t)\|$ and $\|\tilde{x}_i(t)\|x^*_{\mathrm{r}j}$ with $\nu = 1$. Hence, Equation (56) becomes:

$$
\begin{aligned}
&\dot{\mathcal{V}}_i(\tilde{x}_i(t),\tilde{W}_i(t),\hat{e}_i(t)) \\
&\le -\Big[\underbrace{c_{1i}-3\lambda_{\max}(P_i)\|B_i\|_{\mathrm{F}}\sum_{i\sim j}\alpha_{ij}}_{d_{1i}}\Big]\|\tilde{x}_i(t)\|^2-c_{2i}\|\hat{e}_i(t)\|^2+c_{3i}\|\tilde{x}_i(t)\|+c_{4i}\|\hat{e}_i(t)\| \\
&\quad+\underbrace{\lambda_{\max}(P_i)\|B_i\|_{\mathrm{F}}}_{f_i}\sum_{i\sim j}\alpha_{ij}\|\tilde{x}_j(t)\|^2+\underbrace{\lambda_{\max}(P_i)\|B_i\|_{\mathrm{F}}}_{f_i}\sum_{i\sim j}\alpha_{ij}\|\hat{e}_j(t)\|^2+\varphi_i,
\end{aligned}
\tag{59}
$$

where $\varphi_i \triangleq c_{5i} + \lambda_{\max}(P_i)\|B_i\|_{\mathrm{F}}\sum_{i\sim j}\alpha_{ij}{x^*_{\mathrm{r}j}}^2$. Introducing:

$$
\mathcal{V}(\cdot)=\sum_{i=1}^{N}\mathcal{V}_i(\tilde{x}_i(t),\tilde{W}_i(t)\hat{e}_i(t)),
\tag{60}
$$

for the uncertain system $\mathcal{S}$ results in:

$$
\begin{aligned}
\dot{\mathcal{V}}(\cdot)\le\ &\sum_{i=1}^{N}\Big[-d_{1i}\|\tilde{x}_i(t)\|^2-c_{2i}\|\hat{e}_i(t)\|^2+c_{3i}\|\tilde{x}_i(t)\| \\
&+c_{4i}\|\hat{e}_i(t)\|+f_i\sum_{i\sim j}\alpha_{ij}\|\tilde{x}_j(t)\|^2+f_i\sum_{i\sim j}\alpha_{ij}\|\hat{e}_j(t)\|^2+\varphi_i\Big]
\end{aligned}
$$

$$= \sum_{i=1}^{N} \Big[- \underbrace{\Big(d_{1i} - \sum_{i\sim j} f_j \alpha_{ji} \Big)}_{D_{1i}} \|\tilde{x}_i(t)\|^2 - \underbrace{\Big(c_{2i} - \sum_{i\sim j} f_j \alpha_{ji} \Big)}_{D_{2i}} \|\hat{e}_i(t)\|^2$$

$$+ c_{3i}\|\tilde{x}_i(t)\| + c_{4i}\|\hat{e}_i(t)\| + \varphi_i \Big], \tag{61}$$

where $D_{1i} > 0$ and $D_{2i} > 0$ are defined in Assumption 5. Letting $\tilde{x}_a(t) \triangleq [\, \|\tilde{x}_1(t)\|, \ldots, \|\tilde{x}_N(t)\|]^{\mathrm{T}}$, $\hat{e}_a(t) \triangleq [\|\hat{e}_1(t)\|, \ldots, \|\hat{e}_N(t)\|]^{\mathrm{T}}$, $D_1 \triangleq \mathrm{diag}([D_{11}, \ldots, D_{1N}])$, $D_2 \triangleq \mathrm{diag}([D_{21}, \ldots, D_{2N}])$, $C_3 \triangleq \mathrm{diag}([c_{31}, \ldots, c_{3N}])$, $C_4 \triangleq \mathrm{diag}([c_{41}, \ldots, c_{4N}])$ and $\varphi_a \triangleq \sum_{i=1}^{N} \varphi_i$, then Equation (61) can equivalently be written as:

$$\begin{aligned} \dot{\mathcal{V}}(\cdot) &\leq -\tilde{x}_a^{\mathrm{T}}(t) D_1 \tilde{x}_a(t) - \hat{e}_a^{\mathrm{T}}(t) D_2 \hat{e}_a(t) + C_3 \tilde{x}_a(t) + C_4 \hat{e}_a(t) + \varphi_a \\ &\leq -\lambda_{\min}(D_1)\|\tilde{x}_a(t)\|^2 - \lambda_{\min}(D_2)\|\hat{e}_a(t)\|^2 + \lambda_{\max}(C_3)\|\tilde{x}_a(t)\| \\ &\quad + \lambda_{\max}(C_4)\|\hat{e}_a(t)\| + \varphi_a. \end{aligned} \tag{62}$$

Either $\|\tilde{x}_a(t)\| > \psi_1$ or $\|\hat{e}_a(t)\| > \psi_2$ renders $\dot{\mathcal{V}}(\cdot) < 0$, where $\psi_1 \triangleq \frac{\frac{\lambda_{\max}(C_3)}{2\sqrt{\lambda_{\min}(D_1)}} + \sqrt{\frac{\lambda_{\max}^2(C_3)}{4\lambda_{\min}(D_1)} + \frac{\lambda_{\max}^2(C_4)}{4\lambda_{\min}(D_2)} + \varphi_a}}{\sqrt{\lambda_{\min}(D_1)}}$ and $\psi_2 \triangleq \frac{\frac{\lambda_{\max}(C_4)}{2\sqrt{\lambda_{\min}(D_2)}} + \sqrt{\frac{\lambda_{\max}^2(C_3)}{4\lambda_{\min}(D_1)} + \frac{\lambda_{\max}^2(C_4)}{4\lambda_{\min}(D_2)} + \varphi_a}}{\sqrt{\lambda_{\min}(D_2)}}$, and hence, $\tilde{x}_i(t)$, $\hat{e}_i(t)$ and $\tilde{W}_i(t)$ are uniformly ultimate bounded for all $i = 1, 2, \ldots, N$. ■

Corollary 4. Under the conditions of Corollary 3, we can show that $e_i(t)$ is bounded for all $i = 1, 2, \ldots, N$.

Proof. It readily follows from:

$$\begin{aligned} \|e_i(t)\| &= \|x_i(t) - \hat{x}(t) + \hat{x}(t) - x_r(t)\| \\ &\leq \|x_i(t) - \hat{x}(t)\| + \|\hat{x}(t) - x_r(t)\| \\ &\leq \|\tilde{x}_i(t)\| + \|\hat{e}_i(t)\|, \end{aligned} \tag{63}$$

and Corollary 3 that $e_i(t)$ is bounded for all $i = 1, 2, \ldots, N$. ■

Remark 2. In order to obtain the closed-loop system error ultimate bound value for Equation (63) and the no Zeno behavior characterization, we can follow the same steps highlighted in Corollaries 1 and 2, respectively.

3. EVENT-TRIGGERED DISTRIBUTED ADAPTIVE CONTROL

We now introduce an event-triggered distributed adaptive control architecture in this section, where it is assumed that physically-interconnected modules can locally communicate with each other for exchanging their state information. For organizational purposes, this section is broken up into two subsections. Specifically, we first briefly overview a standard distributed adaptive control architecture without event-triggering and then present the proposed event-triggered decentralized adaptive control approach, which includes rigorous stability and performance analyses with no Zeno behavior and generalizations to the state emulator case for suppressing the effect of possible high-frequency oscillations in the controller response. As shown, the benefit of using the proposed distributed adaptive control architecture versus the decentralized architecture of the previous section is that there is no need for any structural assumptions; that is, Assumptions 4 and 5, in the distributed case to guarantee overall system stability (for applications where modules are allowed to locally communicate with each other).

3.1. Overview of a Standard Distributed Adaptive Control Architecture Without Event-triggering.

The standard distributed adaptive control architecture overviewed in this section builds on the problem formulation stated in Section 2.1 with an important difference that the physically-interconnected modules can locally communicate with each other for exchanging their state information, as discussed above. For this purpose, we first replace Assumption 2 of Section 2.1 with the following assumption.

Assumption 6. The function $\delta_{ij}(x_j(t))$ in Equation (2) satisfies:

$$\delta_{ij}(x_j(t)) = Q_{ij}^{\mathrm{T}}\phi_{ij}(x_j(t)), \tag{64}$$

where $Q_{ij} \in \mathbb{R}^{g_j \times m_i}$ is an unknown weight matrix and $\phi_{ij} : \mathbb{R}^{n_j} \to \mathbb{R}^{g_j}$ is a known Lipschitz continuous basis function vector satisfying:

$$\|\phi_{ij}(x_{1j}) - \phi_{ij}(x_{2j})\| \leq L_{\phi ij}\|x_{1j} - x_{2j}\|, \tag{65}$$

with $L_{\phi ij} \in \mathbb{R}_+$.

Remark 3. We can equivalently represent Equation (64) as:

$$\sum_{i\sim j} Q_{ij}^{\mathrm{T}}\phi_{ij}(x_j(t)) \triangleq G_{ij}^{\mathrm{T}}F_{ij}(x_j(t)), \tag{66}$$

where $G_{ij} \in \mathbb{R}^{g_{ij} \times m_i}$ is the matrix combination for the ideal weight matrices of the connected graph, $F_{ij}(x_j(t)) : \mathbb{R}^{n_{ij}} \to \mathbb{R}^{g_{ij}}$ is the vector combination for basis function vectors of the connected graph, $g_{ij} = \sum_{i\sim j} g_j$, and $n_{ij} = \sum_{i\sim j} n_j$. The right hand side of Equation (66) can be given as:

$$G_{ij}^{\mathrm{T}}F_{ij}(x_j(t)) = G_i^{\mathrm{T}}\mathcal{A}_{ai}F_i(x_j(t)), \tag{67}$$

where

$$\mathcal{A}_{ai} = \begin{bmatrix} [\mathcal{A}(\mathcal{G})]_{i1}\, I_{g_1} & \cdots & 0 \\ \vdots & \ddots & \vdots \\ 0 & \cdots & [\mathcal{A}(\mathcal{G})]_{iN}\, I_{g_N} \end{bmatrix} \in \mathbb{R}^{g_a \times g_a}, \tag{68}$$

$G_i \in \mathbb{R}^{g_a \times m_i}$ is the matrix combination for all modules' ideal weight matrices of the system toward $\mathcal{S}_i$, $F_i(x_j(t)) : \mathbb{R}^{n_a} \to \mathbb{R}^{g_a}$ is the vector combination for all basis function vectors of the system toward $\mathcal{S}_i$, $g_a = \sum_{j=1}^{N} g_j$, and $n_a = \sum_{j=1}^{N} n_j$.

Next, using Assumptions 1, 3 and 6, Equation (2) can be equivalently written as:

$$\dot{x}_i(t) = A_{ri}x_i(t) + B_{ri}c_i(t) + B_i\Lambda_i\left[u_i(t) + W_i^{\mathrm{T}}\sigma_i\left(x_i(t), c_i(t), x_j(t)\right)\right], \tag{69}$$

where $W_i \triangleq \left[\Lambda_i^{-1}W_{oi}^{\mathrm{T}}\,,\,\Lambda_i^{-1}K_{1i}^{\mathrm{T}}\,,\,\Lambda_i^{-1}K_{2i}^{\mathrm{T}}\,,\,\Lambda_i^{-1}G_{ij}^{\mathrm{T}}\right]^{\mathrm{T}} \in \mathbb{R}^{(g_i+n_i+m_i+g_{ij})\times m_i}$ is an unknown weight matrix and $\sigma_i\left(x_i(t),c_i(t),x_j(t)\right) \triangleq \left[\beta_i^{\mathrm{T}}(x_i(t))\,,\,x_i^{\mathrm{T}}(t)\,,\,c_i^{\mathrm{T}}(t)\,,\,F_{ij}^{\mathrm{T}}(x_j(t))\right]^{\mathrm{T}} \in \mathbb{R}^{g_i+n_i+m_i+g_{ij}}$. Motivated from the structure of the uncertain terms appearing in Equation (69), let the distributed adaptive feedback controller of $\mathcal{S}_i$, $i \in \mathcal{V}_{\mathcal{G}}$, be given by:

$$\mathcal{C}_i: \qquad u_i(t) = -\hat{W}_i(t)^{\mathrm{T}}\sigma_i\left(x_i(t),c_i(t),x_j(t)\right) \tag{70}$$

where $\hat{W}_i(t)$ is an estimate of W_i satisfying the update law:

$$\dot{\hat{W}}_i(t) = \gamma_i \mathrm{Proj}_{\mathrm{m}}\left[\hat{W}_i(t)\,,\,\sigma_i\left(x_i(t),c_i(t),x_j(t)\right)e_i^{\mathrm{T}}(t)P_iB_i\right], \quad \hat{W}_i(0) = \hat{W}_{i0}, \tag{71}$$

where $P_i \in \mathbb{R}_+^{n_i\times n_i} \cap \mathbb{S}^{n_i\times n_i}$ is a solution of the Lyapunov Equation (10). Now, from Equations (6) and (69), the module-level closed-loop error dynamics can be given by:

$$\dot{e}_i(t) = A_{ri}e_i(t) - B_i\Lambda_i\tilde{W}_i^{\mathrm{T}}(t)\sigma_i\left(x_i(t),c_i(t),x_j(t)\right), \quad e_i(t) = e_{i0}. \tag{72}$$

3.2. Proposed Event-triggered Distributed Adaptive Control Architecture. We now present the proposed event-triggered distributed adaptive control architecture for modular systems, where each uncertain module can exchange its state information with its interconnected neighboring modules.

Consider the uncertain dynamical module i given by:

$$\mathcal{S}_i: \qquad \dot{x}_i(t) = A_ix_i(t) + B_i\left[\Lambda_iu_{si}(t) + \Delta_i\left(x_i(t)\right) + \sum_{i\sim j}\delta_{ij}(x_{sj}(t))\right], \quad x_i(0) = x_{i0}, \tag{73}$$

where $\delta_{ij}(x_{sj}(t)) \triangleq Q_{ij}^{\mathrm{T}}\phi_{ij}(x_{sj}(t))$ and $x_{sj}(t) \in \mathbb{R}^{n_j}$. Using Assumptions 1, 3 and 6, Equation (73) can be equivalently written as:

$$\begin{aligned}\dot{x}_i(t) =& A_{ri}x_i(t) + B_{ri}c_i(t) + B_i\Lambda_i\left[u_{si}(t) + W_i^{\mathrm{T}}\sigma_i\left(x_i(t),x_{si}(t),c_i(t),x_{sj}(t)\right)\right]\\ &+ B_i\Lambda_i(u_{si}(t) - u_i(t)) + B_iK_{1i}(x_{si}(t) - x_i(t)),\end{aligned} \tag{74}$$

where $\sigma_i\left(x_i(t), x_{\mathrm{s}i}(t), c_i(t), x_{\mathrm{s}j}(t)\right) \triangleq \left[\beta_i^{\mathrm{T}}(x_i(t))\ ,\ x_{\mathrm{s}i}^{\mathrm{T}}(t)\ ,\ c_i^{\mathrm{T}}(t)\ ,\ F_{ij}^{\mathrm{T}}(x_{\mathrm{s}j}(t))\right]^{\mathrm{T}} \in \mathbb{R}^{g_i+n_i+m_i+g_{ij}}$, and the distributed adaptive feedback control is given by:

$$C_i: \qquad u_i(t) = -\hat{W}_i(t)^{\mathrm{T}}\sigma_i\left(x_{\mathrm{s}i}(t), c_i(t), x_{\mathrm{s}j}(t)\right), \tag{75}$$

where $\sigma_i\left(x_{\mathrm{s}i}(t), c_i(t), x_{\mathrm{s}j}(t)\right) \triangleq \left[\beta_i^{\mathrm{T}}(x_{\mathrm{s}i}(t))\ ,\ x_{\mathrm{s}i}^{\mathrm{T}}(t)\ ,\ c_i^{\mathrm{T}}(t)\ ,\ F_{ij}^{\mathrm{T}}(x_{\mathrm{s}j}(t))\right]^{\mathrm{T}} \in \mathbb{R}^{g_i+n_i+m_i+g_i\cdot d_i}$, and $\hat{W}_i(t)$ satisfies the weight update law:

$$\dot{\hat{W}}_i(t) = \gamma_i \mathrm{Proj}_{\mathrm{m}}\left[\hat{W}_i(t)\ ,\ \sigma_i\left(x_{\mathrm{s}i}(t), c_i(t), x_{\mathrm{s}j}(t)\right) e_{\mathrm{s}i}^{\mathrm{T}}(t) P_i B_i\right], \quad \hat{W}_i(0) = \hat{W}_{i0}, \tag{76}$$

Now, using Equation (75) in Equation (74) yields:

$$\begin{aligned}\dot{x}_i(t) =& A_{\mathrm{r}i}x_i(t) + B_{\mathrm{r}i}c_i(t) - B_i\Lambda_i\tilde{W}_i^{\mathrm{T}}(t)\sigma_i\left(x_{\mathrm{s}i}(t), c_i(t), x_{\mathrm{s}j}(t)\right) - B_i\Lambda_i g_i(\cdot) \\ &+ B_i\Lambda_i(u_{\mathrm{s}i}(t) - u_i(t)) + B_i K_{1i}(x_{\mathrm{s}i}(t) - x_i(t)),\end{aligned} \tag{77}$$

where $g_i(\cdot) \triangleq W_i^{\mathrm{T}}\left[\sigma_i\left(x_{\mathrm{s}i}(t), c_i(t), x_{\mathrm{s}j}(t)\right) - \sigma_i\left(x_i(t), x_{\mathrm{s}i}(t), c_i(t), x_{\mathrm{s}j}(t)\right)\right]$, and using Equations (77) and (6), we can write the module error dynamics as:

$$\begin{aligned}\dot{e}_i(t) =& A_{\mathrm{r}i}e_i(t) - B_i\Lambda_i\tilde{W}_i^{\mathrm{T}}(t)\sigma_i\left(x_{\mathrm{s}i}(t), c_i(t), x_{\mathrm{s}j}(t)\right) - B_i\Lambda_i g_i(\cdot) + B_i\Lambda_i(u_{\mathrm{s}i}(t) - u_i(t)) \\ &+ B_i K_{1i}(x_{\mathrm{s}i}(t) - x_i(t)).\end{aligned} \tag{78}$$

For organizational purposes, we now divide this section into four sections. Specifically, we analyze the uniform ultimate boundedness of the resulting closed-loop dynamical system in Section 3.2.1, compute the ultimate bound in Section 3.2.2, show that the proposed architecture does not yield to a Zeno behavior in Section 3.2.3 and generalize the distributed event-triggered adaptive control algorithm using the state emulator-based framework in Section 3.2.4.

3.2.1. Stability analysis and uniform ultimate boundedness. Theorem 2. Consider the uncertain dynamical system $\mathcal{S}$ consisting of N interconnected modules $\mathcal{S}_i$ described by Equation (73) subject to Assumptions 1, 3 and 6. Consider, in addition, the

reference model given by Equation (6) and the module feedback control law given by Equations (75) and (76). Moreover, let the data transmission from the uncertain dynamical module to the local controller occur when $\overline{E}_{1i}$ is true and the data transmission from the controller to the uncertain dynamical system occur when $\overline{E}_{2i} \vee E_{3i}$ is true. Then, the closed-loop solution $(e_i(t), \tilde{W}_i(t))$ is uniformly ultimately bounded for all $i = 1, 2, ..., N$.

Proof. Since the data transmission from the uncertain dynamical module to the local controller and from the local controller to the uncertain dynamical module occur when $\overline{E}_{1i}$ and $\overline{E}_{2i} \vee E_{3i}$ are true, respectively, note that $\|x_{si}(t) - x_i(t)\| \leq \epsilon_{yi}$ and $\|u_{si}(t) - u_i(t)\| \leq \epsilon_{ui}$ hold. Consider the Lyapunov-like function given by:

$$\mathcal{V}_i(e_i, \tilde{W}_i) = e_i^{\mathrm{T}} P_i e_i + \gamma_i^{-1} \mathrm{tr}\left((\tilde{W}_i \Lambda_i^{\frac{1}{2}})^{\mathrm{T}} (\tilde{W}_i \Lambda_i^{\frac{1}{2}})\right). \tag{79}$$

Note that $\mathcal{V}_i(0,0) = 0$ and $\mathcal{V}_i(e_i, \tilde{W}_i) > 0$ for all $(e_i, \tilde{W}_i) \neq (0,0)$. The time derivative of Equation (79) is given by:

$$\begin{aligned}
&\dot{\mathcal{V}}_i(e_i(t), \tilde{W}_i(t)) \\
&= 2e_i^{\mathrm{T}}(t) P \dot{e}_i(t) + \gamma_i^{-1} 2\mathrm{tr}\left(\tilde{W}_i^{\mathrm{T}}(t) \dot{\tilde{W}}_i(t) \Lambda_i\right) \\
&\leq 2e_i^{\mathrm{T}}(t) P_i \Big(A_{ri} e_i(t) - B_i \Lambda_i \tilde{W}_i^{\mathrm{T}}(t) \sigma_i\left(x_{si}(t), c_i(t), x_{sj}(t)\right) - B_i \Lambda_i g_i(\cdot) + B_i \Lambda_i (u_{si}(t) \\
&\quad - u_i(t)) + B_i K_{1i}(x_{si}(t) - x_i(t)) \Big) + 2\mathrm{tr}\left(\tilde{W}_i^{\mathrm{T}}(t) \Lambda_i \sigma_i\left(x_{si}(t), c_i(t), x_{sj}(t)\right) e_{si}^{\mathrm{T}}(t) P_i B_i\right) \\
&\leq -e_i^{\mathrm{T}}(t) R_i e_i(t) - 2e_i^{\mathrm{T}}(t) P_i B_i \Lambda_i g_i(\cdot) + 2e_i^{\mathrm{T}}(t) P_i B_i \Lambda_i (u_{si}(t) - u_i(t)) + 2e_i^{\mathrm{T}}(t) P_i B_i K_{1i} \\
&\quad \cdot (x_{si}(t) - x_i(t)) + 2\mathrm{tr}\left(\tilde{W}_i^{\mathrm{T}}(t) \Lambda_i \sigma_i\left(x_{si}(t), c_i(t), x_{sj}(t)\right) (x_{si}(t) - x_i(t))^{\mathrm{T}} P_i B_i\right) \\
&\leq -\lambda_{\min}(R_i) \|e_i(t)\|^2 + 2\|e_i(t)\| \lambda_{\max}(P_i) \|B_i\|_{\mathrm{F}} \|\Lambda_i\|_{\mathrm{F}} \|g_i(\cdot)\| + 2\|e_i(t)\| \lambda_{\max}(P_i) \|B_i\|_{\mathrm{F}} \\
&\quad \cdot \|\Lambda_i\|_{\mathrm{F}} \epsilon_{ui} + 2\|e_i(t)\| \lambda_{\max}(P_i) \|B_i\|_{\mathrm{F}} \|K_{1i}\|_{\mathrm{F}} \epsilon_{xi} + 2\|\tilde{W}_i(t)\|_{\mathrm{F}} \|\Lambda_i\|_{\mathrm{F}} \\
&\quad \cdot \|\sigma_i\left(x_{si}(t), c_i(t), x_{sj}(t)\right)\| \epsilon_{xi} \lambda_{\max}(P_i) \|B_i\|_{\mathrm{F}},
\end{aligned} \tag{80}$$

where the same upper bound $\|g_i(\cdot)\|$ has the same result of Equation (25). In addition, one can compute an upper bound for $\|\sigma_i\left(x_{si}(t), c_i(t), x_{sj}(t)\right)\|$ in Equation (80) as:

$$\begin{aligned}\|\sigma_i\left(x_{si}(t), c_i(t), x_{sj}(t)\right)\| &\leq \|\beta_i(x_{si}(t))\| + \|x_{si}(t)\| + \|c_i(t)\| + \|F_{ij}(x_{sj}(t))\| \\ &\leq L_{\beta i}\|x_{si}(t)\| + \|x_{si}(t)\| + \|c_i(t)\| + \sum_{i\sim j}\|\phi_{ij}(x_j(t))\| \\ &= (L_{\beta i}+1)\epsilon_{xi} + (L_{\beta i}+1)\|e_i(t)\| + (L_{\beta i}+1)x_{ri}^* + \|c_i(t)\| \\ &\quad + \sum_{i\sim j} L_{\phi ij}\left(\epsilon_{xj} + \|e_j(t)\| + x_{rj}^*\right), \end{aligned} \tag{81}$$

where $\|x_{ri}(t)\| \leq x_{ri}^*$ and $\|x_{rj}(t)\| \leq x_{rj}^*$. Then, using the bounds given by Equations (25) and (81) in Equation (80) yields:

$$\begin{aligned}&\dot{\mathcal{V}}_i(e_i(t), \tilde{W}_i(t)) \\ &\leq -\lambda_{\min}(R_i)\|e_i(t)\|^2 + 2\|e_i(t)\|\lambda_{\max}(P_i)\|B_i\|_F\|\Lambda_i\|_F K_{gi}\epsilon_{xi} + 2\|e_i(t)\|\lambda_{\max}(P_i)\|B_i\|_F \\ &\quad \cdot \|\Lambda_i\|_F\epsilon_{ui} + 2\|e_i(t)\|\lambda_{\max}(P_i)\|B_i\|_F\|K_{1i}\|_F\epsilon_{xi} + 2\|\tilde{W}_i(t)\|_F\|\Lambda_i\|_F\Big((L_{\beta i}+1)\epsilon_{xi} \\ &\quad + (L_{\beta i}+1)\|e_i(t)\| + (L_{\beta i}+1)x_{ri}^* + \|c_i(t)\| + \sum_{i\sim j} L_{\phi ij}\left(\epsilon_{xj} + \|e_j(t)\| + x_{rj}^*\right)\Big)\epsilon_{xi} \\ &\quad \cdot \lambda_{\max}(P_i)\|B_i\|_F \\ &\leq -\lambda_{\min}(R_i)\|e_i(t)\|^2 + \Big(2\lambda_{\max}(P_i)\|B_i\|_F\|\Lambda_i\|_F K_{gi}\epsilon_{xi} + 2\lambda_{\max}(P_i)\|B_i\|_F\|\Lambda_i\|_F\epsilon_{ui} \\ &\quad + 2\lambda_{\max}(P_i)\|B_i\|_F\|K_{1i}\|_F\epsilon_{xi} + 2\tilde{w}_i^*\|\Lambda_i\|_F(L_{\beta i}+1)\epsilon_{xi}\lambda_{\max}(P_i)\|B_i\|_F\Big)\|e_i(t)\| \\ &\quad + 2\tilde{w}_i^*\|\Lambda_i\|_F\Big((L_{\beta i}+1)\epsilon_{xi} + (L_{\beta i}+1)x_{ri}^* + \|c_i(t)\| + \sum_{i\sim j} L_{\phi ij}\left(\epsilon_{xj} + x_{rj}^*\right)\Big)\epsilon_{xi} \\ &\quad \cdot \lambda_{\max}(P_i)\|B_i\|_F + 2\tilde{w}_i^*\|\Lambda_i\|_F\epsilon_{xi}\lambda_{\max}(P_i)\|B_i\|_F\sum_{i\sim j} L_{\phi ij}\|e_j(t)\| \\ &\leq -d_{1i}\|e_i(t)\|^2 + d_{2i}\|e_i(t)\| + d_{3i} + f_i\sum_{i\sim j} L_{\phi ij}\|e_j(t)\|, \end{aligned} \tag{82}$$

where $d_{1i} \triangleq \lambda_{\min}(R_i)$, $d_{2i} \triangleq 2\lambda_{\max}(P_i)\|B_i\|_{\mathrm{F}}\|\Lambda_i\|_{\mathrm{F}}K_{gi}\epsilon_{xi} + 2\lambda_{\max}(P_i)\|B_i\|_{\mathrm{F}}\|\Lambda_i\|_{\mathrm{F}}\epsilon_{ui} + 2\lambda_{\max}(P_i)\|B_i\|_{\mathrm{F}}\|K_{1i}\|_{\mathrm{F}}\epsilon_{xi} + 2\tilde{w}_i^*\|\Lambda_i\|_{\mathrm{F}}(L_{\beta i}+1)\epsilon_{xi}\lambda_{\max}(P_i)\|B_i\|_{\mathrm{F}}$, $d_{3i} \triangleq 2\tilde{w}_i^*\|\Lambda_i\|_{\mathrm{F}}\Big((L_{\beta i}+1)\epsilon_{xi} + (L_{\beta i}+1)x_{\mathrm{r}i}^* + \|c_i(t)\| + \sum_{i\sim j} L_{\phi ij}\left(\epsilon_{xj} + x_{\mathrm{r}j}^*\right)\Big)\epsilon_{xi}\lambda_{\max}(P_i)\|B_i\|_{\mathrm{F}}$ and $f_i \triangleq 2\tilde{w}_i^*\|\Lambda_i\|_{\mathrm{F}}\epsilon_{xi}\lambda_{\max}(P_i)\|B_i\|_{\mathrm{F}}$.

Introducing:

$$\mathcal{V}(\cdot) = \sum_{i=1}^{N} \mathcal{V}_i(e_i(t), \tilde{W}_i(t)), \tag{83}$$

for the uncertain system $\mathcal{S}$ results in:

$$\begin{aligned}\dot{\mathcal{V}}(\cdot) \leq & \sum_{i=1}^{N}\Big[-d_{1i}\|e_i(t)\|^2 + d_{2i}\|e_i(t)\| + f_i\sum_{i\sim j} L_{\phi ij}\|e_j(t)\| + d_{3i}\Big] \\ = & \sum_{i=1}^{N}\Big[-d_{1i}\|e_i(t)\|^2 + \underbrace{\Big(d_{2i} + \sum_{i\sim j} f_j L_{\phi ji}\Big)}_{D_{2i}}\|e_i(t)\| + d_{3i}\Big],\end{aligned} \tag{84}$$

where $D_{1i} > 0$. Letting $e_a(t) \triangleq [\|e_1(t)\|, \ldots, \|e_N(t)\|]^{\mathrm{T}}$, $D_1 \triangleq \mathrm{diag}([d_{11}, \ldots, d_{1N}])$, $D_2 \triangleq \mathrm{diag}([D_{21}, \ldots, D_{2N}])$, and $D_3 \triangleq \sum_{i=1}^{N} d_{3i}$, then Equation (32) can equivalently be written as:

$$\begin{aligned}\dot{\mathcal{V}}(\cdot) &\leq -e_a^{\mathrm{T}}(t)D_1 e_a(t) + D_2 e_a(t) + D_3 \\ &\leq -\lambda_{\min}(D_1)\|e_a(t)\|^2 + \lambda_{\max}(D_2)\|e_a(t)\| + D_3.\end{aligned} \tag{85}$$

When $\|e_a(t)\| > \psi$, this renders $\dot{\mathcal{V}}(\cdot) < 0$, where $\psi \triangleq \frac{\frac{\lambda_{\max}(D_2)}{2\sqrt{\lambda_{\min}(D_1)}} + \sqrt{\frac{\lambda_{\max}^2(D_2)}{4\lambda_{\min}(D_1)} + D_3}}{\sqrt{\lambda_{\min}(D_1)}}$, and hence, $e_i(t)$ and $\tilde{W}_i(t)$ are uniformly ultimate bounded for all $i = 1, 2, \ldots, N$. ■

3.2.2. Computation of the ultimate bound for system performance assessment. For revealing the effect of user-defined thresholds and the event-triggered output feedback adaptive controller design parameters to the system performance, the next corollary presents a computation of the ultimate bound.

Corollary 5. Consider the uncertain dynamical system $\mathcal{S}$ consisting of N interconnected modules $\mathcal{S}_i$ described by Equation (73) subject to Assumptions 1, 3 and 6. Consider, in addition, the reference model given by Equation (6) and the module feedback control law given by Equations (75) and (76). Moreover, let the data transmission from the uncertain dynamical module to the local controller occur when $\overline{E}_{1i}$ is true and the data transmission from the controller to the uncertain dynamical system occur when $\overline{E}_{2i} \vee E_{3i}$ is true. Then, the ultimate bound of the system error between the uncertain dynamical system and the reference model is given by:

$$||e_a(t)|| \quad \leq \quad \tilde{\Phi}\lambda_{\min}^{-\frac{1}{2}}(P_{\min}), \quad t \geq T, \tag{86}$$

where

$$\tilde{\Phi} \triangleq \left[\lambda_{\max}(P_{\max})\psi^2 + \lambda_{\max}(\gamma_a)\lambda_{\max}(\Lambda_a)\|\tilde{W}_a(t)\|^2\right]^{\frac{1}{2}}. \tag{87}$$

Proof. The proof is similar to the proof of Corollary 1, and hence, omitted. ■

3.2.3. Computation of the event-triggered inter-sample time lower bound. In this subsection, we show that the proposed event-triggered distributed adaptive control architecture does not yield to a Zeno behavior, which implies that it does not require a continuous two-way data exchange and reduces wireless network utilization. For this purpose, we use the same mathematical notations introduced in Section 2.2.2 and make the following assumption.

Assumption 7. Each module $\mathcal{S}_i$ holds the received triggered state information $\delta_{ij}(x_{sj}(t))$ from its interconnected neighboring modules $\mathcal{S}_j$ and sends this information to its local controller C_i when the condition E_{1i} in Equation (20) is violated.

Corollary 6. Consider the uncertain dynamical system $\mathcal{S}$ consisting of N interconnected modules $\mathcal{S}_i$ described by Equation (73) subject to Assumptions 1, 3, 6 and 7. Consider, in addition, the reference model given by Equation (6) and the module feedback control law given by Equations (75) and (76). Moreover, let the data transmission from

the uncertain dynamical module to the local controller occur when $\overline{E}_{1i}$ is true and the data transmission from the controller to the uncertain dynamical system occur when $\overline{E}_{2i} \vee E_{3i}$ is true. Then, there exist positive scalars $\alpha_{xi} \triangleq \frac{\epsilon_{xi}}{\Phi_{1i}}$ and $\alpha_{ui} \triangleq \frac{\epsilon_{ui}}{\Phi_{2i}}$, such that:

$$s_{k_i+1} - s_{k_i} > \alpha_{xi}, \quad \forall k_i \in \mathbb{N}, \tag{88}$$

$$r^{k_i}_{q_i+1} - r^{k}_{q_i} > \alpha_{ui}, \quad \forall q_i \in \{0, ..., m_{k_i}\}, \quad \forall k_i \in \mathbb{N}. \tag{89}$$

Proof. The proof is similar to the proof of Corollary 2, and hence, omitted. ■

Corollary 6 also shows that the inter-sample times for the module state vector and distributed feedback control vector are bounded away from zero, and hence, the proposed event-triggered distributed adaptive control approach does not yield to a Zeno behavior.

3.2.4. Generalizations to the event-triggered distributed adaptive control with state emulator. Similar to Section 2.2.4, consider the (modified) reference model, so-called the state emulator, given by Equation (44) and the reference model error dynamics capturing the difference between the ideal reference model Equation (6), and the state emulator-based (modified) reference model Equation (44) is given by Equation (45). In addition, the (state emulator-based) system error dynamics follow from Equations (77) and (44) as:

$$\begin{aligned} \dot{\tilde{x}}_i(t) &= A_{\mathrm{r}i}\tilde{x}_i(t) - B_i\Lambda_i\tilde{W}_i^{\mathrm{T}}(t)\sigma_i\left(x_{\mathrm{s}i}(t), c_i(t), x_{\mathrm{s}j}(t)\right) - B_i\Lambda_i g_i(\cdot) + B_i\Lambda_i(u_{\mathrm{s}i}(t) - u_i(t)) \\ &\quad + (B_iK_{1i} - L_i)(x_{\mathrm{s}i}(t) - x_i(t)) - L_i\tilde{x}_i(t) \quad \tilde{x}_i(0) = \tilde{x}_{i0}, \end{aligned} \tag{90}$$

where the adaptive controller Equation (75) is used and the weight update law is given by:

$$\dot{\hat{W}}_i(t) = \gamma_i \mathrm{Proj}_{\mathrm{m}}\left[\hat{W}_i(t)\ ,\ \sigma_i\left(x_{\mathrm{s}i}(t), c_i(t), x_{\mathrm{s}j}(t)\right)(x_{\mathrm{s}i}(t) - \hat{x}_i(t))^{\mathrm{T}}P_iB_i\right],\ \ \hat{W}_i(0) = \hat{W}_{i0}, \tag{91}$$

with $P_i \in \mathbb{R}_+^{n_i \times n_i} \cap \mathbb{S}^{n_i \times n_i}$ being a solution to the Lyapunov Equation (10).

Corollary 7. Consider the uncertain dynamical system $\mathcal{S}$ consisting of N interconnected modules $\mathcal{S}_i$ described by Equation (73) subject to Assumptions 1, 3 and 6. Consider, in addition, the ideal reference model given by Equation (6), the state emulator given by Equation (44) and the module feedback control law given by Equations (75) and (91). Moreover, let the data transmission from the uncertain dynamical module to the local controller occur when $\overline{E}_{1i}$ is true and the data transmission from the controller to the uncertain dynamical system occur when $\overline{E}_{2i} \vee E_{3i}$ is true. Then, the closed-loop solution $(\tilde{x}_i(t), \tilde{W}_i(t), \hat{e}_i(t))$ is uniformly ultimately bounded for all $i = 1, 2, ..., N$.

Proof. Consider the Lyapunov-like function given by:

$$\mathcal{V}_i(\tilde{x}_i, \tilde{W}_i, \hat{e}_i) = \tilde{x}_i^{\mathrm{T}} P_i \tilde{x}_i + \gamma_i^{-1} \mathrm{tr}(\tilde{W}_i \Lambda_i^{\frac{1}{2}})^{\mathrm{T}} (\tilde{W}_i \Lambda_i^{\frac{1}{2}}) + 2 l_i \|L_i\|_{\mathrm{F}}^{-1} \lambda_{\max}(P_i) \lambda_{\max}(R_i) \hat{e}_i^{\mathrm{T}} P_i \hat{e}_i. \quad (92)$$

Note that $\mathcal{V}_i(0,0,0) = 0$ and $\mathcal{V}_i(\tilde{x}_i, \tilde{W}_i, \hat{e}_i) > 0$ for all $(\tilde{x}_i, \tilde{W}_i, \hat{e}_i) \neq (0,0,0)$. The time-derivative of Equation (92) is given by:

$$\begin{aligned}
&\dot{\mathcal{V}}_i(\tilde{x}_i(t), \tilde{W}_i(t), \hat{e}_i(t)) \\
&= 2\tilde{x}_i^{\mathrm{T}}(t) P_i \dot{\tilde{x}}_i(t) + 2\gamma_i^{-1} \mathrm{tr}(\tilde{W}_i(t) \Lambda_i^{\frac{1}{2}})^{\mathrm{T}} (\dot{\tilde{W}}_i(t) \Lambda_i^{\frac{1}{2}}) + 4 l_i \|L_i\|_{\mathrm{F}}^{-1} \lambda_{\max}(P_i) \lambda_{\min}(R_i) \hat{e}_i^{\mathrm{T}} P_i \dot{\hat{e}}_i(t) \\
&\leq 2\tilde{x}_i^{\mathrm{T}}(t) P_i \Big[A_{\mathrm{r}i} \tilde{x}_i(t) - B_i \Lambda_i \tilde{W}_i^{\mathrm{T}}(t) \sigma_i \left(x_{\mathrm{s}i}(t), c_i(t), x_{\mathrm{s}j}(t) \right) - B_i \Lambda_i g_i(\cdot) + B_i \Lambda_i \big(u_{\mathrm{s}i}(t) \\
&\quad - u_i(t) \big) + (B_i K_{1i} - L_i)(x_{\mathrm{s}i}(t) - x_i(t)) - L_i \tilde{x}_i(t) \Big] + 2\mathrm{tr} \tilde{W}_i^{\mathrm{T}}(t) \sigma_i \left(x_{\mathrm{s}i}(t), c_i(t), x_{\mathrm{s}j}(t) \right) \\
&\quad \cdot (x_{\mathrm{s}i}(t) - \hat{x}_i(t))^{\mathrm{T}} P_i B_i \Lambda_i + 4 l_i \|L_i\|_{\mathrm{F}}^{-1} \lambda_{\max}(P_i) \lambda_{\min}(R_i) \hat{e}_i^{\mathrm{T}}(t) P_i \big[A_{\mathrm{r}i} \hat{e}_i(t) + L_i \tilde{x}_i(t)) \\
&\quad + L_i (x_{\mathrm{s}i}(t) - x_i(t)) \big] \\
&\leq -\tilde{x}_i^{\mathrm{T}}(t) R_i \tilde{x}_i(t) - 2\tilde{x}_i^{\mathrm{T}}(t) P_i B_i \Lambda_i g_i(\cdot) + 2\tilde{x}_i^{\mathrm{T}}(t) P_i B_i \Lambda_i \big(u_{\mathrm{s}i}(t) - u_i(t) \big) + 2\tilde{x}_i^{\mathrm{T}}(t) P_i (B_i K_{1i} \\
&\quad - L_i)(x_{\mathrm{s}i}(t) - x_i(t)) - 2\tilde{x}_i^{\mathrm{T}}(t) P_i L_i \tilde{x}_i(t) + 2\mathrm{tr} \tilde{W}_i(t)^{\mathrm{T}} \sigma_i \left(x_{\mathrm{s}i}(t), c_i(t), x_{\mathrm{s}j}(t) \right) (x_{\mathrm{s}i}(t) \\
&\quad - x_i(t))^{\mathrm{T}} P_i B_i \Lambda_i - 2 l_i \|L_i\|_{\mathrm{F}}^{-1} \lambda_{\max}(P_i) \lambda_{\min}(R_i) \hat{e}_i^{\mathrm{T}}(t) R_i \hat{e}_i(t) + 4 l_i \|L_i\|_{\mathrm{F}}^{-1} \lambda_{\max}(P_i) \\
&\quad \cdot \lambda_{\min}(R_i) \hat{e}_i^{\mathrm{T}}(t) P_i L_i (x_{\mathrm{s}i}(t) - x_i(t)) + 4 l_i \|L_i\|_{\mathrm{F}}^{-1} \lambda_{\max}(P_i) \lambda_{\min}(R_i) \hat{e}_i^{\mathrm{T}}(t) P_i L_i \tilde{x}_i(t) \\
&\leq -\lambda_{\min}(R_i) \|\tilde{x}_i(t)\|^2 + 2\lambda_{\max}(P_i) \|B_i\|_{\mathrm{F}} \|\Lambda_i\|_{\mathrm{F}} \|g_i(\cdot)\| \|\tilde{x}_i(t)\| + 2\|\tilde{x}_i(t)\| \lambda_{\max}(P_i) \|B_i\|_{\mathrm{F}}
\end{aligned}$$

$$\cdot \|\Lambda_i\|_{\mathrm{F}}\epsilon_{ui} + 2\|\tilde{x}_i(t)\|\lambda_{\max}(P_i)\big(\|B_iK_{1i}\|_{\mathrm{F}} + \|L_i\|_{\mathrm{F}}\big)\epsilon_{xi} - 2\lambda_{\max}(P_i)\|L_i\|\|\tilde{x}_i(t)\|^2$$
$$+ 2\|\tilde{W}_i(t)\|_{\mathrm{F}}\|\sigma_i\left(x_{\mathrm{s}i}(t), c_i(t), x_{\mathrm{s}j}(t)\right)\|\lambda_{\max}(P_i)\|B_i\|_{\mathrm{F}}\|\Lambda_i\|_{\mathrm{F}}\epsilon_{xi} - 2l_i\|L_i\|_{\mathrm{F}}^{-1}\lambda_{\max}^{-1}(P_i)$$
$$\cdot \lambda_{\min}^2(R_i)\|\hat{e}_i(t)\|^2 + 4l_i\lambda_{\min}(R_i)\epsilon_{xi}\|\hat{e}_i(t)\| + 4l_i\lambda_{\min}(R_i)\|\hat{e}_i(t)\|\|\tilde{x}_i(t)\|. \tag{93}$$

Now, using Young's inequality [46] for the last term in Equation (93), with $\mu_i \in \mathbb{R}_+$, yields:

$$\dot{\mathcal{V}}_i(\tilde{x}_i(t), \tilde{W}_i(t), \hat{e}_i(t))$$
$$\leq -\lambda_{\min}(R_i)\|\tilde{x}_i(t)\|^2 + 2\lambda_{\max}(P_i)\|B_i\|_{\mathrm{F}}\|\Lambda_i\|_{\mathrm{F}}\|g_i(\cdot)\|\|\tilde{x}_i(t)\| + 2\|\tilde{x}_i(t)\|\lambda_{\max}(P_i)\|B_i\|_{\mathrm{F}}$$
$$\cdot \|\Lambda_i\|_{\mathrm{F}}\epsilon_{ui} + 2\|\tilde{x}_i(t)\|\lambda_{\max}(P_i)\big(\|B_iK_{1i}\|_{\mathrm{F}} + \|L_i\|_{\mathrm{F}}\big)\epsilon_{xi} - 2\lambda_{\max}(P_i)\|L_i\|\|\tilde{x}_i(t)\|^2$$
$$+ 2\|\tilde{W}_i(t)\|_{\mathrm{F}}\|\sigma_i\left(x_{\mathrm{s}i}(t), c_i(t), x_{\mathrm{s}j}(t)\right)\|\lambda_{\max}(P_i)\|B_i\|_{\mathrm{F}}\|\Lambda_i\|_{\mathrm{F}}\epsilon_{xi} - 2l_i\|L_i\|_{\mathrm{F}}^{-1}\lambda_{\max}^{-1}(P_i)$$
$$\cdot \lambda_{\min}^2(R_i)\|\hat{e}_i(t)\|^2 + 4l_i\lambda_{\min}(R_i)\epsilon_{xi}\|\hat{e}_i(t)\| + 2l_i\mu_i\lambda_{\min}(R_i)\|\hat{e}_i(t)\|^2$$
$$+ 2\frac{l_i}{\mu_i}\lambda_{\min}(R_i)\|\tilde{x}_i(t)\|^2. \tag{94}$$

Using Equations (25) and (80), Equation (94) can be written by:

$$\dot{\mathcal{V}}_i(\tilde{x}_i(t), \tilde{W}_i(t), \hat{e}_i(t))$$
$$\leq -\left[\lambda_{\min}(R_i) - 2\lambda_{\max}(P_i)\|L_i\|_{\mathrm{F}} - 2\frac{l_i}{\mu_i}\lambda_{\min}(R_i)\right]\|\tilde{x}_i(t)\|^2 - 2\Big[l_i\|L_i\|_{\mathrm{F}}^{-1}\lambda_{\max}^{-1}(P_i)\lambda_{\min}^2(R_i)$$
$$- l_i\mu_i\lambda_{\min}(R_i)\Big]\|\hat{e}_i(t)\|^2 + \Big[2\lambda_{\max}(P_i)\|B_i\|_{\mathrm{F}}\|\Lambda_i\|_{\mathrm{F}}K_{gi}\epsilon_{xi} + 2\lambda_{\max}(P_i)\|B_i\|_{\mathrm{F}}\|\Lambda_i\|_{\mathrm{F}}\epsilon_{ui}$$
$$+ 2\lambda_{\max}(P_i)\big(\|B_iK_{1i}\|_{\mathrm{F}} + \|L_i\|_{\mathrm{F}}\big)\epsilon_{xi}\Big]\|\tilde{x}_i(t)\| + 4l_i\lambda_{\min}(R_i)\epsilon_{xi}\|\hat{e}_i(t)\|$$
$$+ 2\tilde{w}_i^*\Big[(L_{\beta i}+1)\epsilon_{xi} + (L_{\beta i}+1)\|\tilde{x}_i(t) + \hat{e}_i(t)\| + (L_{\beta i}+1)x_{\mathrm{r}i}^* + \|c_i(t)\| + \sum_{i\sim j}L_{\phi ij}\big(\epsilon_{xj}$$
$$+ \|\tilde{x}_j(t) + \hat{e}_j(t)\| + x_{\mathrm{r}j}^*\big)\Big]\lambda_{\max}(P_i)\|B_i\|_{\mathrm{F}}\|\Lambda_i\|_{\mathrm{F}}\epsilon_{xi}$$
$$\leq -\left[\lambda_{\min}(R_i) - 2\lambda_{\max}(P_i)\|L_i\|_{\mathrm{F}} - 2\frac{l_i}{\mu_i}\lambda_{\min}(R_i)\right]\|\tilde{x}_i(t)\|^2 - 2\Big[l_i\|L_i\|_{\mathrm{F}}^{-1}\lambda_{\max}^{-1}(P_i)\lambda_{\min}^2(R_i)$$
$$- l_i\mu_i\lambda_{\min}(R_i)\Big]\|\hat{e}_i(t)\|^2 + \Big[2\lambda_{\max}(P_i)\|B_i\|_{\mathrm{F}}\|\Lambda_i\|_{\mathrm{F}}K_{gi}\epsilon_{xi} + 2\lambda_{\max}(P_i)\|B_i\|_{\mathrm{F}}\|\Lambda_i\|_{\mathrm{F}}\epsilon_{ui}$$
$$+ 2\lambda_{\max}(P_i)\big(\|B_iK_{1i}\|_{\mathrm{F}} + \|L_i\|_{\mathrm{F}}\big)\epsilon_{xi} + 2\tilde{w}_i^*\lambda_{\max}(P_i)\|B_i\|_{\mathrm{F}}\|\Lambda_i\|_{\mathrm{F}}\epsilon_{xi}\Big]\|\tilde{x}_i(t)\|$$
$$+ \Big[4l_i\lambda_{\min}(R_i)\epsilon_{xi} + 2\tilde{w}_i^*\lambda_{\max}(P_i)\|B_i\|_{\mathrm{F}}\|\Lambda_i\|_{\mathrm{F}}\epsilon_{xi}\Big]\|\hat{e}_i(t)\|$$

$$+ 2\tilde{w}_i^* \lambda_{\max}(P_i)\|B_i\|_{\mathrm{F}}\|\Lambda_i\|_{\mathrm{F}}\epsilon_{xi}\Big((L_{\beta i}+1)(\epsilon_{xi}+x_{\mathrm{r}i}^*) + \|c_i(t)\| + \sum_{i\sim j} L_{\phi ij}(\epsilon_{xj}+x_{\mathrm{r}j}^*)\Big)$$

$$+ 2\tilde{w}_i^* \lambda_{\max}(P_i)\|B_i\|_{\mathrm{F}}\|\Lambda_i\|_{\mathrm{F}}\epsilon_{xi}\sum_{i\sim j} L_{\phi ij}(\|\tilde{x}_j(t)\| + \|\hat{e}_j(t)\|). \tag{95}$$

then setting $\mu_i = l_i \lambda_{\min}(R_i)\lambda_{\max}^{-1}(P_i)\|L_i\|_{\mathrm{F}}^{-1}$ in Equation (95) yields:

$$\begin{aligned}
&\dot{\mathcal{V}}_i(\tilde{x}_i(t), \tilde{W}_i(t), \hat{e}_i(t)) \\
&\leq -\lambda_{\min}(R_i)\|\tilde{x}_i(t)\|^2 - 2l_i\|L_i\|_{\mathrm{F}}^{-1}\lambda_{\max}^{-1}(P_i)\lambda_{\min}(R_i)\Big[\lambda_{\min}(R_i) - l_i\Big]\|\hat{e}_i(t)\|^2 \\
&\quad + \Big[2\lambda_{\max}(P_i)\|B_i\|_{\mathrm{F}}\|\Lambda_i\|_{\mathrm{F}}K_{gi}\epsilon_{xi} + 2\lambda_{\max}(P_i)\|B_i\|_{\mathrm{F}}\|\Lambda_i\|_{\mathrm{F}}\epsilon_{ui} + 2\lambda_{\max}(P_i)\big(\|B_iK_{1i}\|_{\mathrm{F}} \\
&\quad + \|L_i\|_{\mathrm{F}}\big)\epsilon_{xi} + 2\tilde{w}_i^*\lambda_{\max}(P_i)\|B_i\|_{\mathrm{F}}\|\Lambda_i\|_{\mathrm{F}}\epsilon_{xi}\Big]\|\tilde{x}_i(t)\| + \Big[4l_i\lambda_{\min}(R_i)\epsilon_{xi} + 2\tilde{w}_i^*\lambda_{\max}(P_i) \\
&\quad \cdot \|B_i\|_{\mathrm{F}}\|\Lambda_i\|_{\mathrm{F}}\epsilon_{xi}\Big]\|\hat{e}_i(t)\| + 2\tilde{w}_i^*\lambda_{\max}(P_i)\|B_i\|_{\mathrm{F}}\|\Lambda_i\|_{\mathrm{F}}\epsilon_{xi}\Big((L_{\beta i}+1)(\epsilon_{xi}+x_{\mathrm{r}i}^*) + \|c_i(t)\| \\
&\quad + \sum_{i\sim j} L_{\phi ij}(\epsilon_{xj}+x_{\mathrm{r}j}^*)\Big) + 2\tilde{w}_i^*\lambda_{\max}(P_i)\|B_i\|_{\mathrm{F}}\|\Lambda_i\|_{\mathrm{F}}\epsilon_{xi}\sum_{i\sim j} L_{\phi ij}(\|\tilde{x}_j(t)\| + \|\hat{e}_j(t)\|).
\end{aligned} \tag{96}$$

It then follows that Equation (96) can be given by:

$$\begin{aligned}
\dot{\mathcal{V}}_i(\tilde{x}_i(t), \tilde{W}_i(t), \hat{e}_i(t)) \leq -d_{1i}\|\tilde{x}_i(t)\|^2 - d_{2i}\|\hat{e}_i(t)\|^2 + d_{3i}\|\tilde{x}_i(t)\| + d_{4i}\|\hat{e}_i(t)\| + d_{5i} \\
+ f_i\sum_{i\sim j} L_{\phi ij}\|\tilde{x}_j(t)\| + f_i\sum_{i\sim j} L_{\phi ij}\|\hat{e}_j(t)\|,
\end{aligned} \tag{97}$$

where $d_{1i} \triangleq \lambda_{\min}(R_i)$, $d_{2i} \triangleq 2l_i\|L_i\|_{\mathrm{F}}^{-1}\lambda_{\max}^{-1}(P_i)\lambda_{\min}(R_i)\Big[\lambda_{\min}(R_i) - l_i\Big]$, $d_{3i} \triangleq 2\lambda_{\max}(P_i)$ $\cdot \|B_i\|_{\mathrm{F}}\|\Lambda_i\|_{\mathrm{F}}K_{gi}\epsilon_{xi} + 2\lambda_{\max}(P_i)\|B_i\|_{\mathrm{F}}\|\Lambda_i\|_{\mathrm{F}}\epsilon_{ui} + 2\lambda_{\max}(P_i)\big(\|B_iK_{1i}\|_{\mathrm{F}} + \|L_i\|_{\mathrm{F}}\big)\epsilon_{xi} + 2\tilde{w}_i^*$ $\cdot \lambda_{\max}(P_i)\|B_i\|_{\mathrm{F}}\|\Lambda_i\|_{\mathrm{F}}\epsilon_{xi}$, $d_{4i} \triangleq 4l_i\lambda_{\min}(R_i)\epsilon_{xi} + 2\tilde{w}_i^*\lambda_{\max}(P_i)\|B_i\|_{\mathrm{F}}\|\Lambda_i\|_{\mathrm{F}}\epsilon_{xi}$, $d_{5i} \triangleq 2\tilde{w}_i^*$ $\cdot \lambda_{\max}(P_i)\|B_i\|_{\mathrm{F}}\|\Lambda_i\|_{\mathrm{F}}\epsilon_{xi}\Big((L_{\beta i}+1)(\epsilon_{xi}+x_{\mathrm{r}i}^*) + \|c_i(t)\| + \sum_{i\sim j} L_{\phi ij}(\epsilon_{xj}+x_{\mathrm{r}j}^*)\Big)$ and f_i $\triangleq 2\tilde{w}_i^*\lambda_{\max}(P_i)\|B_i\|_{\mathrm{F}}\|\Lambda_i\|_{\mathrm{F}}\epsilon_{xi}$. To ensure that d_{2i} is positive definite, we consider $l_i = \theta_i$ $\cdot \lambda_{\min}(R_i)$ and $\theta_i \in (0,1)$.

Introducing:

$$\mathcal{V}(\cdot) = \sum_{i=1}^{N} \mathcal{V}_i(\tilde{x}_i(t), \tilde{W}_i(t)\hat{e}_i(t)), \tag{98}$$

for the uncertain system $\mathcal{S}$ results in:

$$\begin{aligned}\dot{\mathcal{V}}_i(\cdot) \leq & \sum_{i=1}^{N}\Big[- d_{1i}\|\tilde{x}_i(t)\|^2 - d_{2i}\|\hat{e}_i(t)\|^2 + d_{3i}\|\tilde{x}_i(t)\| + d_{4i}\|\hat{e}_i(t)\| + d_{5i} \\ & + f_i\sum_{i\sim j} L_{\phi ij}\|\tilde{x}_j(t)\| + f_i\sum_{i\sim j} L_{\phi ij}\|\hat{e}_j(t)\|\Big] \\ = & \sum_{i=1}^{N}\Big[- d_{1i}\|\tilde{x}_i(t)\|^2 - d_{2i}\|\hat{e}_i(t)\|^2 + \underbrace{\Big(d_{3i} + \sum_{i\sim j} f_j L_{\phi ji}\Big)}_{D_{3i}}\|\tilde{x}_i(t)\| \\ & + \underbrace{\Big(d_{4i} + \sum_{i\sim j} f_j L_{\phi ji}\Big)}_{D_{4i}}\|\hat{e}_i(t)\| + d_{5i}\Big]. \end{aligned} \tag{99}$$

Letting $\tilde{x}_a(t) \triangleq [\|\tilde{x}_1(t)\|,\ldots,\|\tilde{x}_N(t)\|]^{\mathrm{T}}$, $\hat{e}_a(t) \triangleq [\|\hat{e}_1(t)\|,\ldots,\|\hat{e}_N(t)\|]^{\mathrm{T}}$, $D_1 \triangleq \mathrm{diag}([d_{11},\ldots,d_{1N}])$,$D_2 \triangleq \mathrm{diag}([d_{21},\ldots,d_{2N}])$, $D_3 \triangleq \mathrm{diag}([D_{31},\ldots,D_{3N}])$, $D_4 \triangleq \mathrm{diag}([D_{41},\ldots,D_{4N}])$, and $D_5 \triangleq \sum_{i=1}^{N} d_{5i}$, then Equation (99) can equivalently be written as:

$$\begin{aligned}\dot{\mathcal{V}}(\cdot) &\leq -\tilde{x}_a^{\mathrm{T}}(t)D_1\tilde{x}_a(t) - \hat{e}_a^{\mathrm{T}}(t)D_2\hat{e}_a(t) + D_3\tilde{x}_a(t) + D_4 e_a(t) + D_5 \\ &\leq -\lambda_{\min}(D_1)\|\tilde{x}_a(t)\|^2 - \lambda_{\min}(D_2)\|\hat{e}_a(t)\|^2 + \lambda_{\max}(D_3)\|\tilde{x}_a(t)\| \\ &\quad + \lambda_{\max}(D_4)\|\hat{e}_a(t)\| + D_5. \end{aligned} \tag{100}$$

Either $\|\tilde{x}_a(t)\| > \psi_1$ or $\|\hat{e}_a(t)\| > \psi_2$, renders $\dot{\mathcal{V}}(\cdot) < 0$, where $\psi_1 \triangleq \frac{\lambda_{\max}(D_3)}{2\lambda_{\min}(D_1)} + \frac{\sqrt{\frac{\lambda_{\max}^2(D_3)}{4\lambda_{\min}(D_1)} + \frac{\lambda_{\max}^2(D_4)}{4\lambda_{\min}(D_2)} + D_5}}{\sqrt{\lambda_{\min}(D_1)}}$ and $\psi_2 \triangleq \frac{\lambda_{\max}(D_4)}{2\lambda_{\min}(D_2)} + \frac{\sqrt{\frac{\lambda_{\max}^2(D_3)}{4\lambda_{\min}(D_1)} + \frac{\lambda_{\max}^2(D_4)}{4\lambda_{\min}(D_2)} + D_5}}{\sqrt{\lambda_{\min}(D_2)}}$, and hence, $\tilde{x}_i(t)$, $\hat{e}_i(t)$, and $\tilde{W}_i(t)$ are uniformly ultimate bounded for all $i = 1,2,\ldots,N$. ■

Remark 4. To show that $e_i(t)$ is bounded for all $i = 1,2,\ldots,N$ under the condition of Corollary 7, we can follow Corollary 4 to show the boundedness of $e_i(t)$ for all $i = 1,\ldots,N$ using:

$$\|e_i(t)\| \leq \|\tilde{x}_i(t)\| + \|\hat{e}_i(t)\|. \tag{101}$$

Furthermore, in order to obtain the closed-loop system error ultimate bound value for Equation (101) and the no Zeno characterization proof, we can follow the same steps highlighted in Corollaries 5 and 6, respectively.

4. ILLUSTRATIVE NUMERICAL EXAMPLE

In this section, the efficacy of the proposed event-triggered decentralized adaptive control approach is demonstrated in an illustrative numerical example. For this purpose, we consider the uncertain dynamical system, which consists of five masses connected serially by springs and dampers as depicted in Figure 2. We use the following equations of motion for the i-th mass:

$$\begin{bmatrix} \dot{x}_1(t) \\ \ddot{x}_1(t) \end{bmatrix} = \begin{bmatrix} 0 & 1 \\ \frac{-k_1}{m_1} & \frac{-b_1}{m_1} \end{bmatrix} \begin{bmatrix} x_1(t) \\ \dot{x}_1(t) \end{bmatrix} + \begin{bmatrix} 0 \\ \frac{1}{m_1} \end{bmatrix} \left[\Lambda_1 u_1(t) + \Delta_1\left(x_1(t)\right) + \delta_{12}(x_2(t))\right], \tag{102}$$

$$\begin{bmatrix} \dot{x}_i(t) \\ \ddot{x}_i(t) \end{bmatrix} = \begin{bmatrix} 0 & 1 \\ \frac{-(k_{i-1}+k_i)}{m_i} & \frac{-(b_{i-1}+b_i)}{m_i} \end{bmatrix} \begin{bmatrix} x_i(t) \\ \dot{x}_i(t) \end{bmatrix} + \begin{bmatrix} 0 \\ \frac{1}{m_i} \end{bmatrix} \Big[\Lambda_i u_i(t) + \Delta_i\left(x_i(t)\right) + \delta_{ij}(x_j(t))\Big],$$

$$i = \{2,3,4\}, \tag{103}$$

$$\begin{bmatrix} \dot{x}_5(t) \\ \ddot{x}_5(t) \end{bmatrix} = \begin{bmatrix} 0 & 1 \\ \frac{-k_4}{m_5} & \frac{-b_4}{m_5} \end{bmatrix} \begin{bmatrix} x_5(t) \\ \dot{x}_5(t) \end{bmatrix} + \begin{bmatrix} 0 \\ \frac{1}{m_5} \end{bmatrix} \left[\Lambda_5 u_i(t) + \Delta_5\left(x_5(t)\right) + \delta_{54}(x_4(t))\right], \tag{104}$$

where $m_i = 1\text{Kg}$, $k_i = 1.5\ \text{N}\cdot\text{m}^{-1}$, $b_i = 0.4\ \text{N}\cdot\text{sec}\cdot\text{m}^{-1}$, $\Lambda_i = 0.7$, $W_{oi} = [3\ ,\ 1]^{\text{T}}$, and we set the basis function as $\beta_i(x_i(t)) = x_i(t)$. In addition, $\delta_{12}(x_2(t))$, $\delta_{ij}(x_j(t))$ and $\delta_{54}(x_4(t))$, which represent the effect of the system interconnections, are given by:

$$\delta_{12}(x_2(t)) = \begin{bmatrix} k_1 & b_1 \end{bmatrix} \begin{bmatrix} x_2(t) \\ \dot{x}_2(t) \end{bmatrix}, \tag{105}$$

$$\delta_{ij}(x_j(t)) = \begin{bmatrix} k_{j=i-1} & b_{j=i-1} \end{bmatrix} \begin{bmatrix} x_{j=i-1}(t) \\ \dot{x}_{j=i-1}(t) \end{bmatrix} + \begin{bmatrix} k_{j=i} & b_{j=i} \end{bmatrix} \begin{bmatrix} x_{j=i+1}(t) \\ \dot{x}_{j=i+1}(t) \end{bmatrix},$$
$$i = \{2,3,4\}, \tag{106}$$

$$\delta_{54}(x_4(t))) = \begin{bmatrix} k_4 & b_4 \end{bmatrix} \begin{bmatrix} x_4(t) \\ \dot{x}_4(t) \end{bmatrix}. \tag{107}$$

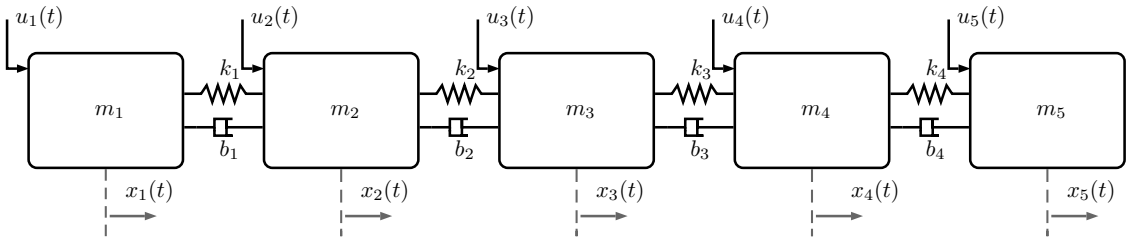

Figure 2. Connected mass-damper-spring system.

The control objective of each module is to enforce $x_i(t)$ to track a filtered square reference input $c_i(t)$ under the effect of uncertainties and disturbances with reduced communication effort by event-triggering architecture. For our example, we choose a second-order ideal reference model that has a natural frequency of 2 rad/s and a damping ratio of 0.707 for all $\mathcal{S}_i, i = 1,\ldots,5$. In addition, we use a state emulator gain $L_i = 9I_2$ and set all initial conditions to zero for all $\mathcal{S}_i, i = 1,\ldots,5$.

For the event-triggered decentralized model reference adaptive control (which is equivalent to $L_i = 0$), we set $Q_i = I_2$ in order to compute P_i in Equation (10). The condition in Assumption 4 holds when $\alpha_{ij} \leq 0.26$ for $i = \{1,5\}$ and $\alpha_{ij} \leq 0.13$ for $i = \{2,3,4\}$. In this case, Assumption 2 is satisfied for the coupling terms given in Equations (105)–(107). For the purpose of event-triggered state emulator-based decentralized adaptive control, we set $R_i = 3$ and $Q_i = I_{2\times 2}$ in order to compute P_i in Equation (48). For $l_i = 0.001$ and $\tilde{Q}_{0i} = 250I_2$, the condition in Assumption 5 holds when $\alpha_{ij} \leq 4.2$ for $i = \{1,5\}$ and $\alpha_{ij} \leq 2.1$ for $i = \{2,3,4\}$. In addition, Assumption 2 is satisfied for coupling terms given by Equations (105)–(107).

For the proposed event-triggered distributed adaptive control, we set $Q_i = I_2$ in order to compute P_i in Equation (10). Note that there are no fundamental stability conditions for the case of distributed adaptive control. Lastly, for the event-triggering thresholds, we choose $\epsilon_{xi} = 0.2$ and $\epsilon_{ui} = 0.2$ for $i = \{1,3,5\}$ and $\epsilon_{xi} = 0.07$ and $\epsilon_{ui} = 0.07$ for $i = \{2,4\}$.

For the proposed event-triggered decentralized adaptive control design of Theorem 1 and Corollary 1, Figures 3–5 represent the results for various γ_i and L_i. In particular, we first set $\gamma_i = 50$ and $L_i = 0$ in Figure 3, which results in a control response with high-frequency oscillations. In order to suppress these undesired oscillations, we set $L_i = 9I_2$ as seen in Figure 4. In this figure, even though such oscillations are reduced, the command tracking performance becomes worse as we increase L_i compared to the response in Figure 3. In addition to increasing L_i, we also increase γ_i in Figure 5, to improve command tracking performance without causing high-frequency oscillations. In general, if one picks L_i to be greater than nine, then it may also be necessary to increase γ_i further to obtain a similar closed-loop system performance. It should also be mentioned that choosing L_i and γ_i to produce both a control response without any significant high-frequency oscillations, and a small uniform ultimate bound can be cast as an optimization problem, as well.

Figures 6–8 represent the results of the proposed event-triggered distributed adaptive control of Theorem 2 and Corollary 7 for the same γ_i and L_i values. Specifically, we see high frequency content in the control signal in Figure 6 when $\gamma_i = 50$ and $L_i = 0$, which is mitigated by increasing the state emulator gain to $L_i = 9I_2$, as seen in Figure 7. In order to enhance the command tracking, which is degraded by increasing the state emulator gain, we increase γ_i as seen in Figure 8.

From these results, we observe from the decentralized adaptive control case that the state emulator-based approach not only gives stringent performance without causing high frequencies in the controller response, but also tolerates the interconnection uncertainties of the modules. In addition, the performance of the distributed adaptive controller is better than the decentralized adaptive controller with the corresponding design parameter setting. The total number of the state and control event triggers of the whole system for the cases

in Figures 3–8 is given in Figure 9A,B, respectively. Figure 9 shows the drastic decrement of the triggering number using the event-triggering approach and also the further triggering number decrement due to utilizing the state emulator-based approach.

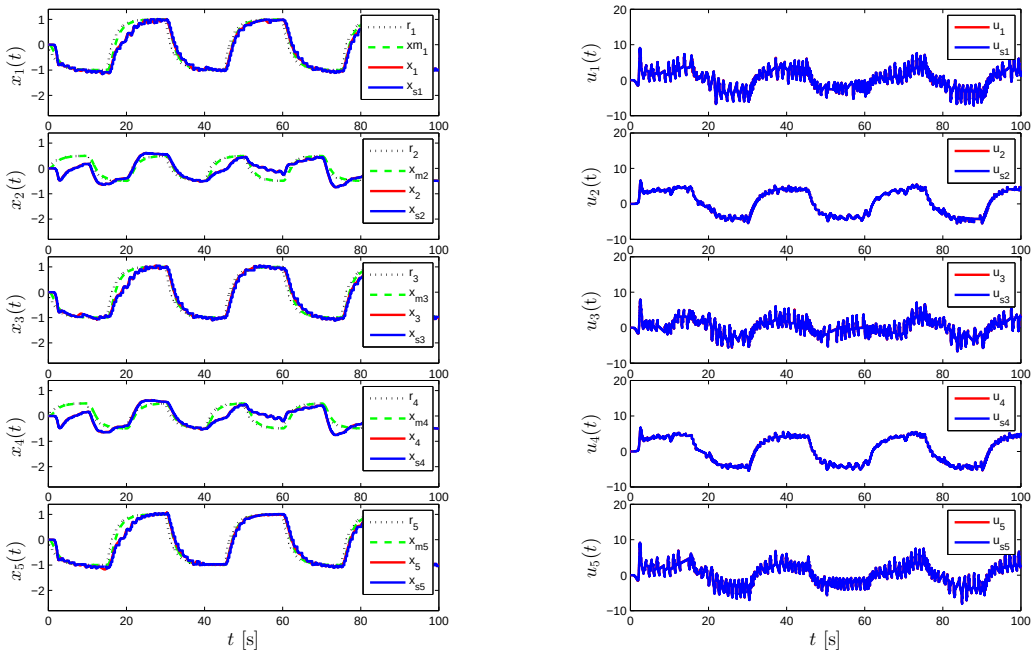

(**A**) State signals (**B**) Control signals

Figure 3. Command following performance for the proposed event-triggered decentralized adaptive control approach with $\gamma_i = 50$ and $L_i = 0$.

5. CONCLUSIONS

The design and analysis of event-triggered decentralized and distributed adaptive control architectures for uncertain networked large-scale modular systems were presented. For the decentralized case, it is shown in Section 2 that the proposed event-triggered adaptive control architecture guarantees system stability and performance with no Zeno behavior under some structural conditions stated in Assumptions 4 and 5 that depend on the parameters of the large-scale modular systems and the proposed architecture. For the distributed case, it is shown in Section 3 that the proposed event-triggered adaptive control architecture guarantees the same system stability and performance with no Zeno behavior without such structural conditions under the assumption that physically-interconnected

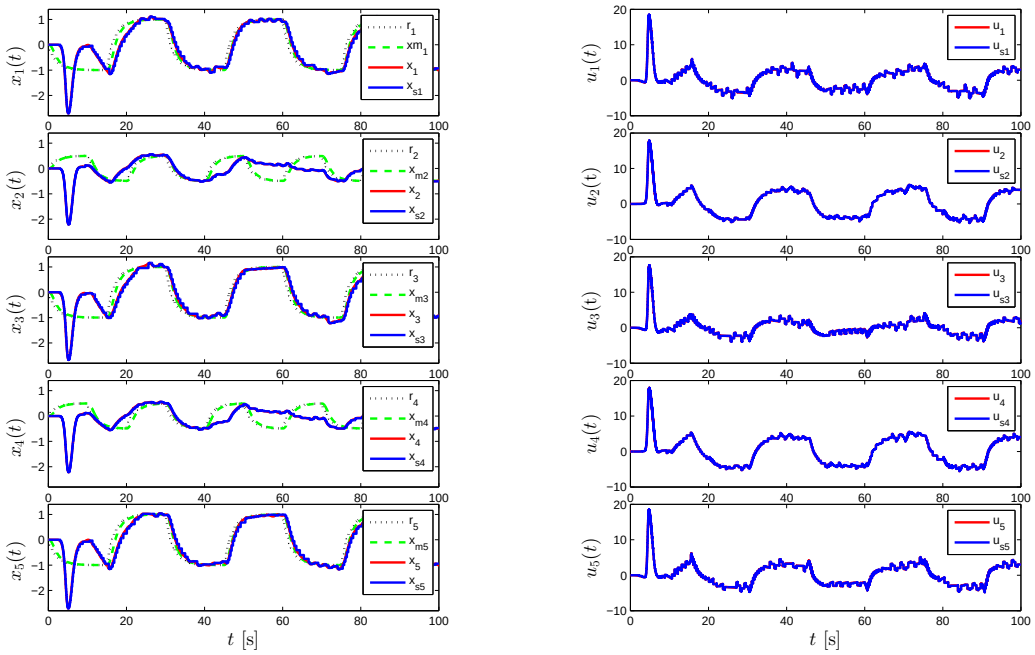

(**A**) State signals (**B**) Control signals

Figure 4. Command following performance for the proposed event-triggered decentralized adaptive control approach with $\gamma_i = 50$ and $L_i = 9$.

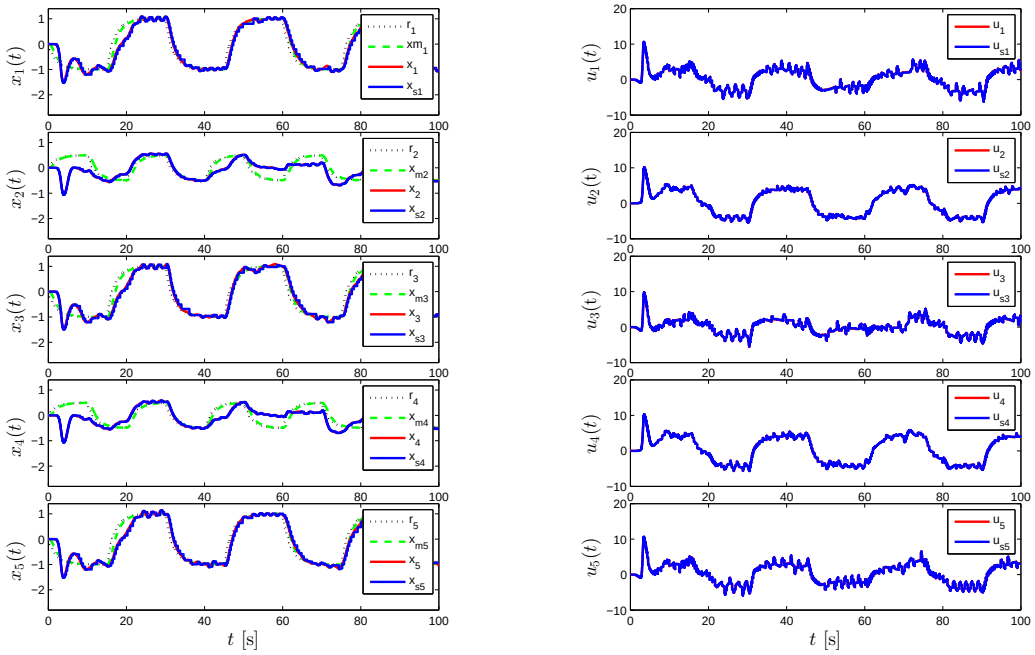

(**A**) State signals (**B**) Control signals

Figure 5. Command following performance for the proposed event-triggered decentralized adaptive control approach with $\gamma_i = 200$ and $L_i = 9$.

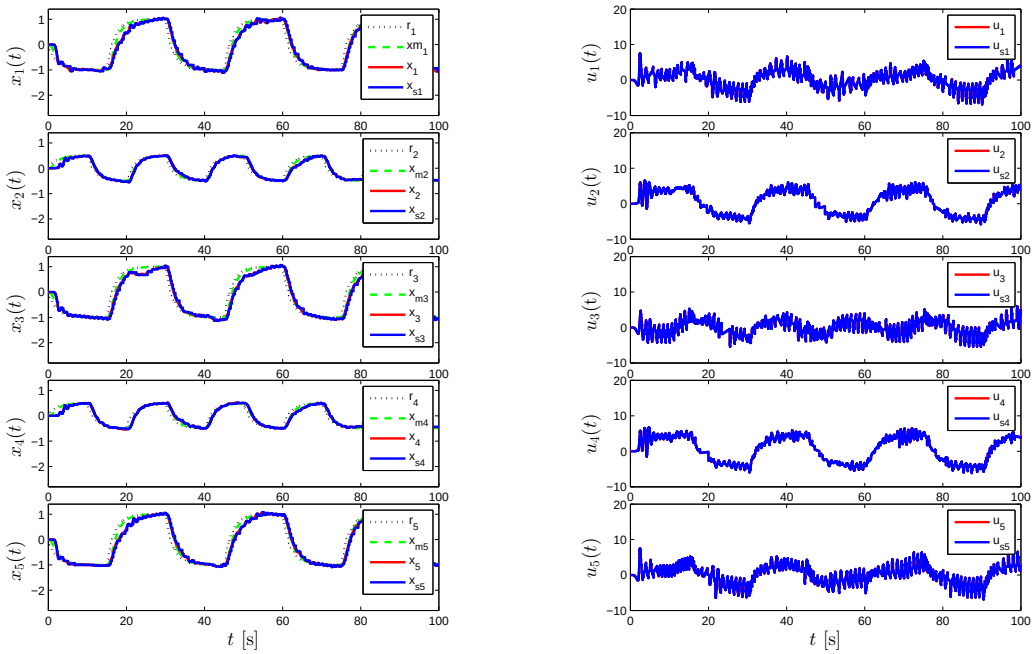

(**A**) State signals (**B**) Control signals

Figure 6. Command following performance for the proposed event-triggered distributed adaptive control approach with $\gamma_i = 50$ and $L_i = 0$.

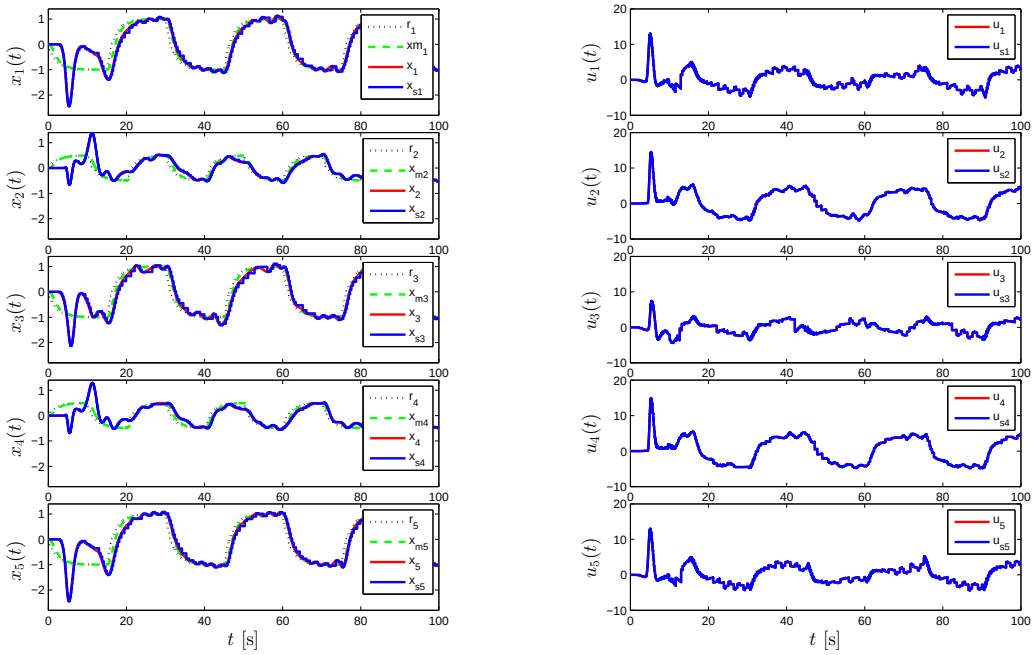

(**A**) State signals (**B**) Control signals

Figure 7. Command following performance for the proposed event-triggered distributed adaptive control approach with $\gamma_i = 50$ and $L_i = 9$.

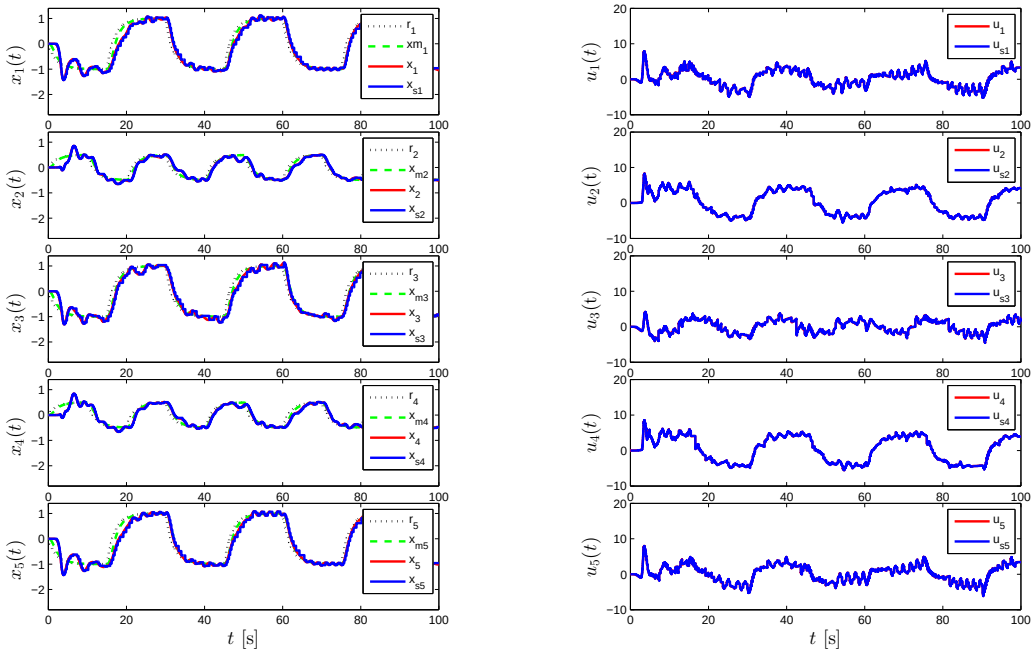

(**A**) State signals (**B**) Control signals

Figure 8. Command following performance for the proposed event-triggered distributed adaptive control approach with $\gamma_i = 200$ and $L_i = 9$.

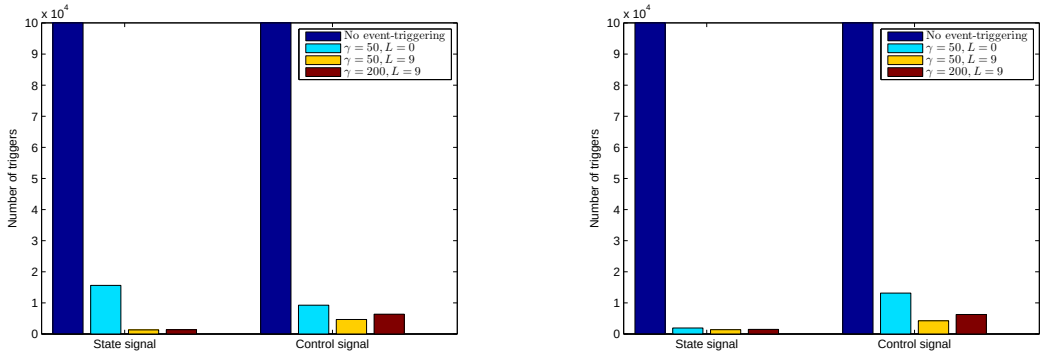

(**A**) Decentralized adaptive control (**B**) Distributed adaptive control

Figure 9. Number of triggers with respect to the controller design parameters.

modules can locally communicate with each other for exchanging their state information. In addition to the presented theoretical findings, the efficacy of the proposed event-triggered decentralized and distributed adaptive control approaches is demonstrated on an illustrative numerical example in Section 4, where significant reduction on the overall communication cost is obtained for large-scale modular systems in the presence of system uncertainties

resulting from modeling and degraded modes of operation of the modules and their interconnections between each other. For the future work, sampling, data transmission and computation delays will be considered along with the proposed results of this paper, since they also play an important role in the performance of networked control systems. Furthermore, we will also consider the cases when a set of diagonal elements of the control effectiveness matrix is zero and generalize the results of this paper to cover these so-called loss of control cases.

REFERENCES

[1] F. Bullo, J. Cortes, and S. Martinez, *Distributed control of robotic networks: A mathematical approach to motion coordination algorithms*. Princeton University Press, 2009.

[2] M. Mesbahi and M. Egerstedt, *Graph theoretic methods in multiagent networks*. Princeton University Press, 2010.

[3] D. D. Siljak, *Decentralized control of complex systems*. Courier Corporation, 2011.

[4] T. Yucelen and E. N. Johnson, "Control of multivehicle systems in the presence of uncertain dynamics," *International Journal of Control*, vol. 86, no. 9, pp. 1540–1553, 2013.

[5] E. J. Davison and A. G. Aghdam, *Decentralized control of large-scale systems*. Springer Publishing Company, Incorporated, 2014.

[6] T. Yucelen and J. S. Shamma, "Adaptive architectures for distributed control of modular systems," in *American Control Conference*, pp. 1328–1333, 2014.

[7] P. A. Ioannou and J. Sun, *Robust Adaptive Control*. Courier Corporation, 2012.

[8] T. Yucelen and W. M. Haddad, "A robust adaptive control architecture for disturbance rejection and uncertainty suppression with $\mathcal{L}_\infty$ transient and steady-state performance guarantees," *International Journal of Adaptive Control and Signal Processing*, vol. 26, no. 11, pp. 1024–1055, 2012.

[9] K. J. Åström and B. Wittenmark, *Adaptive Control*. Courier Corporation, 2013.

[10] E. Lavretsky and K. A. Wise, "Robust adaptive control," in *Robust and Adaptive Control*, Springer, 2013.

[11] K. S. Narendra and A. M. Annaswamy, *Stable Adaptive Systems*. Courier Corporation, 2012.

[12] T. Yucelen and W. M. Haddad, "Low-frequency learning and fast adaptation in model reference adaptive control," *IEEE Transactions on Automatic Control*, vol. 58, no. 4, pp. 1080–1085, 2013.

[13] T. Yucelen, G. De La Torre, and E. N. Johnson, "Improving transient performance of adaptive control architectures using frequency-limited system error dynamics," *International Journal of Control*, vol. 87, no. 11, pp. 2383–2397, 2014.

[14] K. J. Åström and B. Bernhardsson, "Comparison of riemann and lebesque sampling for first order stochastic systems," in *Proceedings of the 41st IEEE Conference on Decision and Control*, vol. 2, pp. 2011–2016, 2002.

[15] P. Tabuada, "Event-triggered real-time scheduling of stabilizing control tasks," *IEEE Transactions on Automatic Control*, vol. 52, no. 9, pp. 1680–1685, 2007.

[16] W. Heemels, M. Donkers, and A. R. Teel, "Periodic event-triggered control for linear systems," *IEEE Transactions on Automatic Control*, vol. 58, no. 4, pp. 847–861, 2013.

[17] P. Ioannou, "Decentralized adaptive control of interconnected systems," *IEEE Transactions on Automatic Control*, vol. 31, no. 4, pp. 291–298, 1986.

[18] D. T. Gavel and D. Siljak, "Decentralized adaptive control: structural conditions for stability," *IEEE Transactions on Automatic Control*, vol. 34, no. 4, pp. 413–426, 1989.

[19] L. Shi and S. K. Singh, "Decentralized adaptive controller design for large-scale systems with higher order interconnections," *IEEE Transactions on Automatic Control*, vol. 37, no. 8, pp. 1106–1118, 1992.

[20] J. T. Spooner and K. M. Passino, "Decentralized adaptive control of nonlinear systems using radial basis neural networks," *IEEE transactions on automatic control*, vol. 44, no. 11, pp. 2050–2057, 1999.

[21] B. M. Mirkin, "Decentralized adaptive controller with zero residual tracking errors," in *Proceedings of the 7th Mediterranean Conference on Control and Automation (MED99)*, pp. 28–30, 1999.

[22] K. S. Narendra and N. O. Oleng, "Exact output tracking in decentralized adaptive control systems," *IEEE Transactions on Automatic Control*, vol. 47, no. 2, pp. 390–395, 2002.

[23] T. Yucelen and A. J. Calise, "Derivative-free model reference adaptive control," *Journal of Guidance, Control, and Dynamics*, vol. 34, no. 4, pp. 933–950, 2011.

[24] M. Mazo and P. Tabuada, "Decentralized event-triggered control over wireless sensor/actuator networks," *IEEE Transactions on Automatic Control*, vol. 56, no. 10, pp. 2456–2461, 2011.

[25] A. Molin and S. Hirche, "Optimal design of decentralized event-triggered controllers for large-scale systems with contention-based communication," in *IEEE Conference on Decision and Control and European Control*, pp. 4710–4716, 2011.

[26] D. V. Dimarogonas, E. Frazzoli, and K. H. Johansson, "Distributed event-triggered control for multi-agent systems," *IEEE Transactions on Automatic Control*, vol. 57, no. 5, pp. 1291–1297, 2012.

[27] M. Donkers and W. Heemels, "Output-based event-triggered control with guaranteed-gain and improved and decentralized event-triggering," *IEEE Transactions on Automatic Control*, vol. 57, no. 6, pp. 1362–1376, 2012.

[28] E. Garcia, Y. Cao, H. Yu, P. Antsaklis, and D. Casbeer, "Decentralised event-triggered cooperative control with limited communication," *International Journal of Control*, vol. 86, no. 9, pp. 1479–1488, 2013.

[29] Y. Fan, G. Feng, Y. Wang, and C. Song, "Distributed event-triggered control of multi-agent systems with combinational measurements," *Automatica*, vol. 49, no. 2, pp. 671–675, 2013.

[30] E. Garcia, Y. Cao, and D. W. Casbeer, "Cooperative control with general linear dynamics and limited communication: centralized and decentralized event-triggered control strategies," in *IEEE American Control Conference*, pp. 159–164, 2014.

[31] A. Sahoo, H. Xu, and S. Jagannathan, "Neural network-based adaptive event-triggered control of nonlinear continuous-time systems," *IEEE International Symposium on Intelligent Control*, pp. 35–40, 2013.

[32] A. Sahoo, H. Xu, and S. Jagannathan, "Neural network approximation-based event-triggered control of uncertain mimo nonlinear discrete time systems," *IEEE American Control Conference*, pp. 2017–2022, 2014.

[33] X. Wang and N. Hovakimyan, "$\mathcal{L}_1$ adaptive control of event-triggered networked systems," *IEEE American Control Conference*, pp. 2458–2463, 2010.

[34] X. Wang, E. Kharisov, and N. Hovakimyan, "Real-time $\mathcal{L}_1$ adaptive control for uncertain networked control systems," *IEEE Transactions on Automatic Control*, vol. 60, no. 9, pp. 2500–2505, 2015.

[35] A. Albattat, B. C. Gruenwald, and T. Yucelen, "Event-triggered adaptive control," in *ASME 2015 Dynamic Systems and Control Conference*, American Society of Mechanical Engineers, 2015.

[36] A. Albattat, B. C. Gruenwald, and T. Yucelen, *Adaptive Control for Robotic Manipulators*, ch. Output Feedback Adaptive Control of Uncertain Dynamical Systems with Event-Triggering. CRC Press/Taylor & Francis Group: Boca Raton, FL, USA, 2016.

[37] E. Lavretsky, R. Gadient, and I. M. Gregory, "Predictor-based model reference adaptive control," *Journal of Guidance, Control, and Dynamics*, vol. 33, no. 4, pp. 1195–1201, 2010.

[38] J. A. Muse and A. J. Calise, "H_∞ adaptive flight control of the generic transport model," *AIAA Infotech@Aerospace*, 2010.

[39] V. Stepanyan and K. Krishnakumar, "MRAC revisited: guaranteed performance with reference model modification," *IEEE American Control Conference*, pp. 93–98, 2010.

[40] V. Stepanyan and K. Krishnakumar, "M-MRAC for nonlinear systems with bounded disturbances," *IEEE Decision and Control and European Control Conference*, pp. 5419–5424, 2011.

[41] T. E. Gibson, A. M. Annaswamy, and E. Lavretsky, "Improved transient response in adaptive control using projection algorithms and closed loop reference models," *AIAA Guidance Navigation and Control Conference*, 2012.

[42] T. E. Gibson, A. M. Annaswamy, and E. Lavretsky, "Adaptive systems with closed-loop reference models: Stability, robustness and transient performance," *arXiv preprint arXiv:1201.4897*, 2012.

[43] C. Godsil and G. Royle, *Algebraic graph theory*. New York, NY: Springer, 2001.

[44] J.-B. Pomet and L. Praly, "Adaptive nonlinear regulation: estimation from the Lyapunov equation," *IEEE Transactions on Automatic Control*, vol. 37, no. 6, pp. 729–740, 1992.

[45] T. E. Lavretsky, Eugene and and A. M. Annaswamy, "Projection operator in adaptive systems," 2011.

[46] D. S. Bernstein, *Matrix mathematics: Theory, Facts, and Formulas*. Princeton University Press, 2009.

[47] K. Kim, T. Yucelen, and A. J. Calise, "A parameter dependent riccati equation approach to output feedback adaptive control," in *AIAA Guidance, Navigation, and Control Conference*, 2011.

[48] K. Glover, J. Doyle, P. P. Khargonekar, and B. A. Francis, "State space solutions to standard H_2 and H_∞ control problems," *IEEE transactions on automatic control*, vol. 34, no. 8, 1989.

IV. AN OBSERVER-FREE OUTPUT FEEDBACK COOPERATIVE CONTROL ARCHITECTURE FOR MULTIVEHICLE SYSTEMS

Ali Albattat[1], Tansel Yucelen[2], Benjamin C. Gruenwald[2], and Sarangapani Jagannathan[1]

[1] Department of Mechanical & Aerospace Engineering

Missouri University of Science and Technology

[2] Department of Mechanical Engineering

University of South Florida

ABSTRACT

The contribution of this paper is a new, observer-free output feedback cooperative control architecture for continuous-time, minimum phase, and high-order multivehicle systems in the context of a containment problem (i.e., outputs of the follower vehicles convergence to the convex hull spanned by those of the leader vehicles). The proposed architecture is predicated on a nonminimal state-space realization that generates an expanded set of states only using the filtered input and filtered output and their derivatives for each follower vehicle, without the need for designing an observer for each vehicle. Specifically, the proposed observer-free output feedback control law consists of a vehicle-level controller and a local cooperative controller for each vehicle, where the former addresses internal stability of vehicles and the latter addresses the containment problem. Two illustrative numerical examples complement the proposed theoretical contribution.

1. INTRODUCTION

Owing to the ever-increasing advances in embedded systems technologies, we are rapidly moving toward a future in which squadrons of vehicles (henceforth, referred as multivehicle systems) will autonomously perform a broad spectrum of tasks in both military

and civilian domains. Examples of such tasks include but are not limited to collaborative exploration; search and rescue; nuclear, biological, and chemical attack detection; and target tracking. Motivated from this standpoint, cooperative control enabling multivehicle systems to work in coherence through local information exchange between vehicles has been the focus of high research activity during the last two decades (e.g., see books [1, 2, 3, 4] for a thorough coverage of the recent progress).

In this paper, we focus on the output feedback cooperative control problem in the context of a containment problem (i.e., outputs of the follower vehicles convergence to the convex hull spanned by those of the leader vehicles). While full state feedback designs lead to computationally simpler cooperative control laws, output feedback designs are required for most applications that involve high-dimensional vehicle models with inaccessible states. To this end, several output feedback cooperative control approaches are proposed in the literature for multivehicle systems (e.g., see [5, 6, 7, 8, 9, 10, 11, 12] and references therein), where the common denominator of these approaches is that they utilize an observer in their cooperative control laws.

Unlike the existing literature, the contribution of this paper is a new, observer-free output feedback cooperative control architecture for continuous-time, minimum phase, and high-order multivehicle systems. The proposed architecture is predicated on a nonminimal state-space realization originally proposed in [13, 14] that generates an expanded set of states only using the filtered input and filtered output and their derivatives for each follower vehicle, without the need for designing an observer for each vehicle. Specifically, the proposed observer-free output feedback control law consists of a vehicle-level controller and a local cooperative controller for each vehicle as in [15], where the former addresses internal stability of vehicles and the latter addresses the containment problem. An illustrative numerical example complements the proposed theoretical contribution.

The organization of this paper is as follows. Section 3 presents the nonminimal state space realization architecture of [13, 14] in the context of the multivehicle system setup of this paper. The proposed output feedback cooperative control architecture is then given in Section 4. An analysis of the proposed architecture is presented in 5, where two illustrative numerical examples are included in Section 6. Finally, conclusions are summarized in Section 7. Note that the results of this paper can be viewed as a generalization of some of the state feedback cooperative control results in [15] to the output feedback one by resorting to the nominimal state-space realization method presented in [13, 14].

2. MATHEMATICAL PRELIMINARIES

The notation used in this paper is fairly standard. Specifically, $\mathbb{R}$ denotes the set of real numbers; $\mathbb{R}^n$ denotes the set of $n \times 1$ real column vectors; $\mathbb{R}^{n\times m}$ denotes the set of $n \times m$ real matrices; $\mathbb{R}_+$ denotes the set of positive real numbers; $\mathbb{R}_+^{n\times n}$ denotes the set of $n \times n$ positive-definite real matrices; $\mathbb{S}^{n\times n}$ denotes the set of $n \times n$ symmetric real matrices; $\mathbb{D}^{n\times n}$ denotes the set of $n \times n$ real matrices with diagonal scalar entries; $(\cdot)^{\mathrm{T}}$ denotes transpose; $(\cdot)^{-1}$ denotes inverse; $\mathrm{diag}(a)$ denotes the diagonal matrix with the vector a on its diagonal; and "$\triangleq$" denotes equality by definition. In addition, we write $\lambda_{\min}(A)$ (respectively, $\lambda_{\max}(A)$) for the minimum and respectively maximum eigenvalue of the Hermitian matrix A and $\|\cdot\|$ for the Euclidean norm.

In addition, we adopt graph theoretical notation (e.g., see [16, 2]) to encode interactions between vehicles. In particular, an undirected graph $\mathcal{G}$ is defined by $\mathcal{V}_{\mathcal{G}} = \{1, \cdots, N\}$ of nodes and a set $\mathcal{E}_{\mathcal{G}} \in \mathcal{V}_{\mathcal{G}} \times \mathcal{V}_{\mathcal{G}}$ of edges. If $(i, j) \in \mathcal{E}_{\mathcal{G}}$, then the nodes i and j are neighbors, and the neighboring relation is indicated with $i \sim j$. The degree d_i of node i is defined by the number of its neighbors and the degree matrix of graph $\mathcal{G}$ is then given by $\mathcal{D}(\mathcal{G}) \triangleq \mathrm{diag}(d) \in \mathbb{R}^{N\times N}$, $d = [d_1, \cdots, d_N]^{\mathrm{T}}$. A path $i_0 i_1 \cdots i_L$ is a finite sequence of nodes such that $i_{k-1} \sim i_k$, $k = 1, \cdots, L$, and if any pair of district nodes has a path, then a graph $\mathcal{G}$ is connected. Furthermore, we write $\mathcal{A}(\mathcal{G}) \in \mathbb{R}^{N\times N}$ for adjacency matrix of a

graph $\mathcal{G}$ defined by

$$[\mathcal{A}(\mathcal{G})]_{ij} \triangleq \begin{cases} 1, & \text{if } (i,j) \in \mathcal{E}_{\mathcal{G}} \\ 0, & \text{otherwise,} \end{cases} \tag{1}$$

and $\mathcal{B}(\mathcal{G}) \in \mathbb{R}^{N\times M}$ for the (node-edge) incidence matrix of the graph $\mathcal{G}$ defined by

$$[\mathcal{B}(\mathcal{G})]_{ij} \triangleq \begin{cases} 1, & \text{if node } i \text{ is the head of the edge} j, \\ -1, & \text{if node } i \text{ is the tail of the edge} j, \\ 0, & \text{otherwise,} \end{cases} \tag{2}$$

where M is the number of edges, i is an index for the node set, and j is an index for the edge set. Finally, the graph Laplacian matrix, $\mathcal{L}(\mathcal{G}) \in \overline{\mathbb{R}}_{+}^{N\times N} \cap \mathbb{S}^{N\times N}$, is defined by

$$\mathcal{L}(\mathcal{G}) \triangleq \mathcal{D}(\mathcal{G}) - \mathcal{A}(\mathcal{G}), \tag{3}$$

or equivalently,

$$\mathcal{L}(\mathcal{G}) = \mathcal{B}(\mathcal{G})\mathcal{B}(\mathcal{G})^{\mathrm{T}}. \tag{4}$$

We next recall some of the basic results for (scalar) multivehicle systems [2]. For this purpose, let nodes and edges represent vehicles and information exchange links between vehicles, respectively. Then, we can model a given multivehicle system by a graph $\mathcal{G}$. For example, let $x_i(t) \in \mathbb{R}$ be the state of node i, $i = 1, ..., N$, satisfying

$$\dot{x}_i(t) = u_i(t), \quad x_i(0) = x_{i0}, \tag{5}$$

where $u_i(t) \in \mathbb{R}$ is the control input. If each vehicle receives the relative state information with respect to its neighbors, then

$$u_i(t) = -\sum_{i\sim j} \left(x_i(t) - x_j(t)\right), \tag{6}$$

solves the rendezvous problem, where (5) subject to (6) can be written at the multivehicle system level as

$$\dot{x}(t) = -\mathcal{L}(\mathcal{G})x(t), \quad x_i(0) = x_{i0}, \tag{7}$$

with $x(t) = \left[x_1^{\mathrm{T}}(t), \cdots, x_N^{\mathrm{T}}(t)\right]$ denoting the aggregated state vector. Note that the spectrum of $\mathcal{L}(\mathcal{G})$ has one zero eigenvalue and $N-1$ positive real eigenvalues if and only if the graph $\mathcal{G}$ is connected and undirected. In this case, the solution of the multivehicle system given by (7) evolves as $x(t) \to (\mathbf{1}_N \mathbf{1}_N^{\mathrm{T}}/N)x_0$ as $t \to \infty$.

Finally, we recall some results on leader-follower multivehicle system frameworks. For this purpose, let the incidence matrix (2) be partitioned as

$$\mathcal{B}(\mathcal{G}) = \left[\begin{array}{c} \mathcal{B}_{\mathrm{L}}(\mathcal{G}) \\ \mathcal{B}_{\mathrm{F}}(\mathcal{G}) \end{array}\right], \tag{8}$$

where $\mathcal{B}_{\mathrm{L}}(\mathcal{G}) \in \mathbb{R}^{N_{\mathrm{L}} \times M}$ and $\mathcal{B}_{\mathrm{F}}(\mathcal{G}) \in \mathbb{R}^{N_{\mathrm{F}} \times M}$ with N_{L} and N_{F} denoting cardinalities of the leader and follower groups, respectively, such that $N = N_{\mathrm{L}} + N_{\mathrm{F}}$. Then, using (4) and (8) the partitioned graph Laplacian matrix $\mathcal{L}(\mathcal{G})$ is given by

$$\mathcal{L}(\mathcal{G}) = \left[\begin{array}{cc} L(\mathcal{G}) & G(\mathcal{G})^{\mathrm{T}} \\ G(\mathcal{G}) & F(\mathcal{G}) \end{array}\right], \tag{9}$$

where $L(\mathcal{G}) \triangleq \mathcal{B}_{\mathrm{L}}(\mathcal{G})\mathcal{B}_{\mathrm{L}}(\mathcal{G})^{\mathrm{T}}$, $G(\mathcal{G}) = \mathcal{B}_{\mathrm{F}}(\mathcal{G})\mathcal{B}_{\mathrm{L}}(\mathcal{G})^{\mathrm{T}}$ and $F(\mathcal{G}) = \mathcal{B}_{\mathrm{F}}(\mathcal{G})\mathcal{B}_{\mathrm{F}}(\mathcal{G})^{\mathrm{T}}$. Note that $F(\mathcal{G}) \in \mathbb{R}_+^{N_{\mathrm{F}} \times N_{\mathrm{F}}} \cap \mathbb{S}^{N_{\mathrm{F}} \times N_{\mathrm{F}}}$, and hence, $F(\mathcal{G})$ is nonsingular since $\det(F(\mathcal{G})) \neq 0$. Furthermore $F(\mathcal{G})\mathbf{1}_{N_{\mathrm{F}}} = -G(\mathcal{G})\mathbf{1}_{N_{\mathrm{L}}}$, or equivalently, each row of $-F(\mathcal{G})^{-1}G(\mathcal{G})$ has a sum equal to 1. Now, we can model a given multivehicle system on a leader-follower framework. In particular, let $x_{\mathrm{L}}(t) \in \mathbb{R}^{N_{\mathrm{L}}}$ and $x_{\mathrm{F}}(t) \in \mathbb{R}^{N_{\mathrm{F}}}$ be the aggregated state vector of the leaders and followers, respectively. Then, the followers evolve through the Laplacian-based dynamics as

$$\dot{x}_{\mathrm{F}}(t) = -F(\mathcal{G})x_{\mathrm{F}}(t) - G(\mathcal{G})x_{\mathrm{L}}(t), \quad x_{\mathrm{F}}(0) = x_{\mathrm{F}0}. \tag{10}$$

Throughout this paper, we consider leaders as command generators for the neighboring followers and that a connected, undirected graph $\mathcal{G}$ represents the interaction topology between the vehicles.

3. NONMINIMAL STATE SPACE REALIZATION FOR FOLLOWER VEHICLES

Consider controllable and observable minimum phase linear dynamical follower vehicle system $i, i = 1, \cdots, N_{\mathrm{F}}$, given by

$$\dot{x}_i(t) = Ax_i(t) + Bu_i(t), \quad x_i(0) = x_{0i}, \quad t \geq 0, \tag{11}$$

$$y_i(t) = Cx_i(t), \tag{12}$$

where $x_i(t) \in \mathbb{R}^n$, $t \geq 0$ is the unknown state vector, $u_i(t) \in \mathbb{R}^m$, $t \geq 0$ is the known control input, $y_i(t) \in \mathbb{R}^l$, $t \geq 0$ is the known system output. In addition, $A \in \mathbb{R}^{n \times n}$, $B \in \mathbb{R}^{n \times m}$, $C \in \mathbb{R}^{l \times n}$, are known follower system matrices and are minimal.

We use a nonminimal state-space representation method employed in [13, 14], for the follower vehicle dynamics $i, i = 1, \cdots, N_{\mathrm{F}}$, such that an input-output equivalent (from control inputs $u_i(t)$, $t \geq 0$, to system outputs $y_i(t)$, $t \geq 0$) nonminimal observer canonical state-space model [17] of (11) and (12) for $l > 1$ is obtained. For this purpose, consider

$$\dot{x}_{oi}(t) = A_o x_{oi}(t) + B_o u_i(t), \quad x_{oi}(0) = x_{o0i}, \; t \geq 0, \tag{13}$$

$$y_i(t) = C_o x_{oi}(t), \tag{14}$$

where $x_{oi}(t) \in \mathbb{R}^{ln}$, $t \geq 0$ is the state vector,

$$A_o = \begin{bmatrix} 0 & I_l & \cdots & 0 \\ \vdots & \ddots & \ddots & \vdots \\ 0 & \cdots & 0 & I_l \\ -a_0 I_l & -a_1 I_l & \cdots & -a_{n-1} I_l \end{bmatrix} \in \mathbb{R}^{ln \times ln}, \tag{15}$$

$$B_o = \begin{bmatrix} CB \\ CAB \\ \vdots \\ CA^{n-1}B \end{bmatrix} \in \mathbb{R}^{ln \times m}, \tag{16}$$

$$C_o = \begin{bmatrix} 0 & I_l & \cdots & 0 \end{bmatrix} \in \mathbb{R}^{l \times ln}. \tag{17}$$

with a_k, $k = 0, 1, \cdots, n-1$, in (15) being the coefficients of the characteristic polynomial of A in (11). Defining

$$\bar{B}_0 \triangleq C_o(a_1 I_{ln} + a_2 A_o + \cdots + a_{n-2} A_o^{n-3} + a_{n-1} A_o^{n-2} + A_o^{n-1}) B_o, \tag{18}$$

$$\bar{B}_1 \triangleq C_o(a_2 I_{ln} + a_3 A_o + \cdots + a_{n-1} A_o^{n-3} + A_o^{n-2}) B_o, \tag{19}$$

$$\vdots$$

$$\bar{B}_{n-1} \triangleq C_o B_o, \tag{20}$$

and using a known filtered expanded state vector $x_{\mathrm{f}i}(t) \in \mathbb{R}^{n_{\mathrm{f}}}$, $t \geq 0$, $n_{\mathrm{f}} \triangleq (m+l)n$, given by

$$x_{\mathrm{f}i}(t) = \left[q_{1i}^{\mathrm{T}}(t), \cdots, q_{ni}^{\mathrm{T}}(t), \nu_{1i}^{\mathrm{T}}, \cdots, \nu_{ni}^{\mathrm{T}} \right]^{\mathrm{T}}, \tag{21}$$

where $q_{ki}(t) \triangleq y_{\mathrm{f}i}^{k-1}(t)$, $\nu_{ki} = u_{\mathrm{f}i}^{k-1}(t)$, $k = 1, 2, \cdots, n$, $z^{(n)} \triangleq \mathrm{d}^n z(t)/\mathrm{d}t^n$, and where $x_{\mathrm{f}i}(t)$ is obtained by filtering $u_i(t)$ and $y_i(t)$ though the filter $\lambda^n/\Lambda(s)$, where

$$\begin{aligned} \Lambda(s) = (s+\lambda)^n &= \sum_{p=0}^{n} \binom{n}{p} s^{n-p} \lambda^p \\ &= s^n + n\lambda s^{n-1} + \cdots + \lambda^n, \end{aligned} \tag{22}$$

is a monic Hurwitz polynomial of degree n with $\lambda > 0$, an alternative input-output equivalent nonminimal controllable state-space realization of (11) and (12) is given by

$$\dot{x}_{\mathrm{f}i}(t) = A_{\mathrm{f}}x_{\mathrm{f}i}(t) + B_{\mathrm{f}}u_i(t), \quad x_{\mathrm{f}i}(0) = x_{\mathrm{f}0i}, \ t \geq 0, \tag{23}$$

$$y_i(t) = C_{\mathrm{f}}x_{\mathrm{f}i}(t), \tag{24}$$

with

$$A_{\mathrm{f}} = \begin{bmatrix} 0 & I_l & 0 & \cdots & & & \cdots & 0 \\ \vdots & & \ddots & & & & & \vdots \\ 0 & \cdots & 0 & I_l & 0 & \cdots & \cdots & 0 \\ -a_0 I_l & \cdots & \cdots & -a_{n-1} I_l & \bar{B}_0 & \cdots & \cdots & \bar{B}_{n-1} \\ 0 & \cdots & & \cdots & 0 & I_m & 0 & 0 \\ \vdots & & & & & & \ddots & \vdots \\ \vdots & & & & & \cdots & 0 & I_m \\ 0 & \cdots & \cdots & 0 & -\lambda^n I_m & \cdots & \cdots & -n\lambda I_m \end{bmatrix} \in \mathbb{R}^{n_{\mathrm{f}} \times n_{\mathrm{f}}}, \tag{25}$$

$$B_{\mathrm{f}} = \begin{bmatrix} 0 & 0 & \cdots & \lambda^n I_m \end{bmatrix}^{\mathrm{T}} \in \mathbb{R}^{n_{\mathrm{f}} \times m}, \tag{26}$$

$$C_{\mathrm{f}} = [\, -\lambda^{-n}(a_0 I_l + \lambda^n I_l) \cdots \ \cdots -\lambda^{-n}(a_{n-1} I_l + n\lambda^n I_l)$$

$$\lambda^{-n}\bar{B}_0 \cdots \ \cdots \ \lambda^{-n}\bar{B}_{n-1}] \in \mathbb{R}^{l \times n_{\mathrm{f}}}. \tag{27}$$

Now, following the results documented in [13, 14], the ith follower vehicle dynamics (11) and (12) are input-output equivalent to the dynamics given by (23) and (24).

4. COOPERATIVE CONTROL DESIGN BASED ON NONMINIMAL STATE SPACE REALIZATION

Before constructing the system controller architecture, we present the leader system dynamics that are necessary for the considered containment problem. For this purpose, consider the dynamics of the leader i, $i = 1, \cdots, N_{\mathrm{L}}$, given by

$$\dot{x}_{\mathrm{L}i}(t) = A_{\mathrm{L}i}x_{\mathrm{L}i}(t) + B_{\mathrm{L}i}c_i(t), \ x_{\mathrm{L}i}(0) = x_{\mathrm{L}0i}, \ t \geq 0, \tag{28}$$

$$y_{\mathrm{L}i}(t) = C_{\mathrm{L}i}x_{\mathrm{L}i}(t), \tag{29}$$

where $x_{\mathrm{L}i}(t) \in \mathbb{R}^{n_i}$ is the leader state vector, $c_i(t) \in \mathbb{R}^{m_i}$ is a vehicle bounded input command (i.e., $\|c_i(t)\| \leq c_i^*$) with bounded time rate change (i.e., $\|\dot{c}_i(t)\| \leq \dot{c}_i^*$), $y_{\mathrm{L}i}(t) \in \mathbb{R}^l$ is the leader output, $A_{\mathrm{L}i} \in \mathbb{R}^{n_i \times n_i}$ is the leader system matrix, $B_{\mathrm{L}i} \in \mathbb{R}^{n_i \times m_i}$ is the leader command input matrix, $C_{\mathrm{L}i} \in \mathbb{R}^{l \times n_i}$ is the leader output matrix, $(A_{\mathrm{L}i}, B_{\mathrm{L}i}, C_{\mathrm{L}i})$ is minimal, and $A_{\mathrm{L}i}$ is Hurwitz.

To achieve the control objective of driving the follower vehicles to the convex hull spanned by the leaders, we design a two level output feedback cooperative control for the nonminimal state-space realization follower vehicle $i, i = 1, \cdots, N_{\mathrm{F}}$ as

$$u_i(t) = u_{\mathrm{c}i}(t) + u_{\mathrm{v}i}(t). \tag{30}$$

Here, $u_{\mathrm{c}i}(t) \in \mathbb{R}^m$ is the local cooperative controller that receives the relative output measurements of the neighboring vehicles in terms of $y_{\mathrm{f}i}(t)$ and $y_{\mathrm{L}i}(t)$ and $u_{\mathrm{v}i}(t) \in \mathbb{R}^m$ is the vehicle level controller that receives the internal nonminimal state-space realization based state measurements, i.e., $x_{\mathrm{f}i}(t)$.

4.1. Vehicle-level Control Law. We consider the vehicle-level control law given by

$$u_{\mathrm{v}i}(t) \triangleq -kx_{\mathrm{f}i}(t), \tag{31}$$

in order to make $A_{\mathrm{fr}} \triangleq A_{\mathrm{f}} - B_{\mathrm{f}}k \in \mathbb{R}^{n_{\mathrm{f}} \times n_{\mathrm{f}}}$ Hurwitz (i.e., internal stability), where $k \in \mathbb{R}^{m_{\mathrm{f}} \times n_{\mathrm{f}}}$ is a feedback matrix designed using pole placement. Since A_{fr} is Hurwitz, it follows from converse Lyapunov theory [18] that there is exists a unique $P \in \mathbb{R}_+^{n_{\mathrm{f}} \times n_{\mathrm{f}}} \bigcap \mathbb{S}_+^{n_{\mathrm{f}} \times n_{\mathrm{f}}}$ satisfying

$$0 = A_{\mathrm{fr}}^{\mathrm{T}}P + PA_{\mathrm{fr}} + R, \tag{32}$$

where $R \in \mathbb{R}_+^{n_{\mathrm{f}} \times n_{\mathrm{f}}} \bigcap \mathbb{S}_+^{n_{\mathrm{f}} \times n_{\mathrm{f}}}$. Then, the follower vehicle dynamics in (23) become

$$\dot{x}_{\mathrm{f}i}(t) = A_{\mathrm{fr}}x_{\mathrm{f}i}(t) + B_{\mathrm{f}}u_{ci}(t), \quad x_{\mathrm{f}i}(0) = x_{\mathrm{f}0i}, \ t \geq 0. \tag{33}$$

Now that the internal stability of the vehicles has been addressed using the above vehicle-level control law, we can now design the cooperative control law for the containment problem.

4.2. Local Cooperative Control Law. In order to present the cooperative control, we consider the approach in [15] and let $\tilde{y}(t) \triangleq \left[y_{\mathrm{L}}^{\mathrm{T}}(t), y_{\mathrm{f}}^{\mathrm{T}}(t)\right]^{\mathrm{T}} \in \mathbb{R}^{(N_{\mathrm{L}}\times N_{\mathrm{F}})l}$ be the vector associated with the graph $\mathcal{G}$, where $y_{\mathrm{L}}^{\mathrm{T}}(t) \triangleq [y_{\mathrm{L}1}^{\mathrm{T}}(t), \cdots, y_{\mathrm{L}N_{\mathrm{L}}}^{\mathrm{T}}(t)]^{\mathrm{T}} \in \mathbb{R}^{N_{\mathrm{L}}l}$ denotes the first N_{L} nodes representing the aggregated output vector of the leaders and $y_{\mathrm{f}}^{\mathrm{T}}(t) \triangleq [y_{\mathrm{f}1}^{\mathrm{T}}(t), \cdots, y_{\mathrm{f}N_{\mathrm{F}}}^{\mathrm{T}}(t)]^{\mathrm{T}} \in \mathbb{R}^{N_{\mathrm{F}}l}$ denotes the last N_{F} nodes representing the aggregated filtered output vector of the follower vehicles. Note that $F(\mathcal{G}) \in \mathbb{R}^{(N_{\mathrm{F}}\times N_{\mathrm{F}})}$ and $G(\mathcal{G}) \in \mathbb{R}^{(N_{\mathrm{F}}\times N_{\mathrm{L}})}$ are given in (9). For each vehicle $i, i = 1, \cdots, N_{\mathrm{F}}$, consider the local cooperative controller receiving the relative output measurements of the neighboring vehicles in terms of $y_{\mathrm{f}i}(t), i = 1, \cdots, N_{\mathrm{F}}$, and $y_{\mathrm{L}i}(t), i = 1, \cdots, N_{\mathrm{L}}$ as [15]

$$u_{ci}(t) = K_c\Big[-\sum_{i\sim j}\Big(\tilde{y}_i(t) - \tilde{y}_j(t)\Big) + \theta_i(t)\Big], \tag{34}$$

$$\dot{\theta}_i(t) = \delta\Big[-\sum_{i\sim j}\Big(\tilde{y}_i(t) - \tilde{y}_j(t)\Big) - \zeta\left(\theta_i(t) - \nu_i(t)\right)\Big], \quad \theta_i(0) = \theta_{i0}, \tag{35}$$

$$\dot{\nu}_i(t) = \eta\left(\theta_i(t) - \nu_i(t)\right), \quad \nu_i(0) = \nu_{i0}, \tag{36}$$

where $K_c \in \mathbb{R}^{m\times l}$ is a gain matrix, $\theta_i(t) \in \mathbb{R}^l$ is the integrator state, $\nu_i(t) \in \mathbb{R}^l$ is the filter state, $\delta \in \mathbb{R}_+$ is the integrator gain, $\zeta \in \mathbb{R}_+$ is the modification gain, and $\eta \in \mathbb{R}_+$ is the filter gain. Next, applying the local cooperative controller (34), (35), and (36) to the follower vehicle dynamics given by (33) yields

$$\dot{x}_{\mathrm{f}i}(t) = A_{\mathrm{fr}}x_{\mathrm{f}i}(t) - B_{\mathrm{f}}K_c\sum_{i\sim j}\Big(\tilde{y}_i(t) - \tilde{y}_j(t)\Big) + B_{\mathrm{f}}K_c\theta_i(t). \tag{37}$$

Letting $x_{\mathrm{f}}(t) \triangleq [x_{\mathrm{f}1}^{\mathrm{T}}(t), \cdots, x_{\mathrm{f}N_{\mathrm{F}}}^{\mathrm{T}}(t)]^{\mathrm{T}} \in \mathbb{R}^{N_{\mathrm{F}}n_{\mathrm{f}}}$, $\theta(t) \triangleq [\theta_1^{\mathrm{T}}(t), \cdots, \theta_{N_{\mathrm{F}}}^{\mathrm{T}}(t)]^{\mathrm{T}} \in \mathbb{R}^{N_{\mathrm{F}}l}$, and $\nu(t) \triangleq [\nu_1^{\mathrm{T}}(t), \cdots, \nu_{N_{\mathrm{F}}}^{\mathrm{T}}(t)]^{\mathrm{T}} \in \mathbb{R}^{N_{\mathrm{F}}l}$, and $y_{\mathrm{f}i}(t) = C_o x_{\mathrm{f}i}(t)$ where $C_o \triangleq [I_l, \cdots, 0] \in \mathbb{R}^{l \times n_{\mathrm{f}}}$, the follower vehicle dynamics (33) subject to the local cooperative controller (34), (35), and (36) can be written at the multivehicle system level as

$$\begin{aligned}
\dot{x}_{\mathrm{f}}(t) &= (I_{N_{\mathrm{F}}} \otimes A_{\mathrm{fr}})x_{\mathrm{f}}(t) - (F(\mathcal{G}) \otimes B_{\mathrm{f}}K_c)y_{\mathrm{f}}(t) - (G(\mathcal{G}) \otimes B_{\mathrm{f}}K_c)y_{\mathrm{L}}(t) \\
&\quad + (I_{N_{\mathrm{F}}} \otimes B_{\mathrm{f}}K_c)\theta(t) \\
&= [I_{N_{\mathrm{F}}} \otimes A_{\mathrm{fr}} - F(\mathcal{G}) \otimes B_{\mathrm{f}}K_cC_o]x_{\mathrm{f}}(t) - (G(\mathcal{G}) \otimes B_{\mathrm{f}}K_c)y_{\mathrm{L}}(t) \\
&\quad + (I_{N_{\mathrm{F}}} \otimes B_{\mathrm{f}}K_c)\theta(t), \quad x_{\mathrm{f}}(0) = x_{\mathrm{f}0}, \qquad (38) \\
\dot{\theta}(t) &= -\delta(F(\mathcal{G}) \otimes I_l)y_{\mathrm{f}}(t) - \delta(G(\mathcal{G}) \otimes I_l)y_{\mathrm{L}}(t) - \delta\zeta\,(\theta(t) - \nu(t)) \\
&= -\delta(F(\mathcal{G}) \otimes C_o)x_{\mathrm{f}}(t) - \delta(G(\mathcal{G}) \otimes I_l)y_{\mathrm{L}}(t) - \delta\zeta\,(\theta(t) - \nu(t)), \quad \theta(0) = \theta_0, \qquad (39) \\
\dot{\nu}(t) &= \eta\,(\theta(t) - \nu(t)), \quad \nu(0) = \nu_0. \qquad (40)
\end{aligned}$$

This can further be written compactly as

$$\dot{\xi}(t) = \mathcal{A}(\mathcal{G})\xi(t) + \mathcal{B}(\mathcal{G})y_{\mathrm{L}}(t), \quad \xi(0) = \xi_0. \qquad (41)$$

where $\xi \triangleq [x_{\mathrm{f}}^{\mathrm{T}}(t),\ \theta^{\mathrm{T}}(t),\ \nu^{\mathrm{T}}(t)]^{\mathrm{T}} \in \mathbb{R}^{n_\xi}$, $n_\xi \triangleq N_{\mathrm{F}}(n_{\mathrm{f}} + 2l)$, $A_\xi(\mathcal{G}) \triangleq I_{N_{\mathrm{F}}} \otimes A_{\mathrm{fr}} - F(\mathcal{G}) \otimes B_{\mathrm{f}}K_cC_o \in \mathbb{R}^{N_{\mathrm{F}}n_{\mathrm{f}} \times N_{\mathrm{F}}n_{\mathrm{f}}}$, and

$$\mathcal{A}(\mathcal{G}) = \begin{bmatrix} A_\xi(\mathcal{G}) & I_{N_{\mathrm{F}}} \otimes B_{\mathrm{f}}K_c & 0 \\ -\delta(F(\mathcal{G}) \otimes C_o) & -\delta\zeta I_{N_{\mathrm{F}}l} & \delta\zeta I_{N_{\mathrm{F}}l} \\ 0 & \eta I_{N_{\mathrm{F}}l} & -\eta I_{N_{\mathrm{F}}l} \end{bmatrix} \in \mathbb{R}^{n_\xi \times n_\xi}, \qquad (42)$$

$$\mathcal{B}(\mathcal{G}) = \begin{bmatrix} -G(\mathcal{G}) \otimes B_{\mathrm{f}}K_c \\ -\delta(G(\mathcal{G}) \otimes I_l) \\ 0 \end{bmatrix} \in \mathbb{R}^{n_\xi \times N_{\mathrm{F}}l}. \qquad (43)$$

The objective of the proposed observer-free vehicle-level controller given in the previous section is to stabilize the follower vehicle dynamics. Furthermore, the objective of the local cooperative controller given in this section based on [15] is to solve the containment problem. For this purpose, we first need to ensure that the solution $\xi(t)$ to (41) is $\mathcal{L}_\infty$ stable [19], that is for every bounded $y_{\rm L}(t)$, and $\xi(t)$ is bounded. So, we know that $y_{\rm L}(t)$ is bounded, since every $A_{{\rm L}i}, i = 1, \cdots, N_{\rm L}$, are Hurwitz. Therefore, in order to conclude that (41) is $\mathcal{L}_\infty$ stable, $\mathcal{A}(\mathcal{G})$ needs to be Hurwitz. A necessary and sufficient condition satisfying this requirement is given in the following remarks.

Remark 1 *Similar to the results in [20, 21, 15], let $\mu_i \in spec(F(\mathcal{G})), i = 1, \cdots, N_F$. If*

$$\mathcal{U}_{\mathcal{A}(\mathcal{G})i} = \begin{bmatrix} A_{fr} - \mu_i B_f K_c C_o & B_f K_c & 0 \\ -\mu_i \delta C_o & -\delta\zeta I_l & \delta\zeta I_l \\ 0 & \eta I_l & \eta I_l \end{bmatrix} \in \mathbb{R}^{(n_f+2l)\times(n_f+2l)}, \tag{44}$$

is Hurwitz for $i = 1, \cdots, N_F$, then $\mathcal{A}(\mathcal{G})$ in (42) is Hurwitz. This shows that (44) can be made Hurwitz for $i = 1, \cdots, N_L$ by arbitrarily choosing the design parameters K_c, δ, ζ, and η. This further implies that the system (41) with the leader dynamical given by (28) and (29) is $\mathcal{L}_\infty$ stable (e.g., see Corollary 6.1 of [15]).

5. ANALYSIS

In this section, we state the main result of the this paper in the following theorem which shows that the proposed control architecture solves the containment problem. For this purpose, we first let $\xi \triangleq [x_{\rm f}^{\rm T}(t),\ \theta^{\rm T}(t),\ \nu^{\rm T}(t)]^{\rm T} \in \mathbb{R}^{n_\xi}$, with $x_{\rm f}(t) \in \mathbb{R}^{N_{\rm F} n_{\rm f}}$, $\theta(t) \in \mathbb{R}^{N_{\rm F} l}$, and $\nu(t) \in \mathbb{R}^{N_{\rm F} l}$. In addition, let $A_{\rm L} \triangleq$ block-diag$(A_{\rm L1}, \cdots, A_{{\rm L}N_{\rm L}}) \in \mathbb{R}^{n_{\rm L}\times n_{\rm L}}$, $B_{\rm L} \triangleq$ block-diag$(B_{\rm L1}, \cdots, B_{{\rm L}N_{\rm L}}) \in \mathbb{R}^{n_{\rm L}\times m_{\rm L}}$, $C_{\rm L} \triangleq$ block-diag$(C_{\rm L1}^{\rm T}, \cdots, C_{{\rm L}N_{\rm L}}^{\rm T})^{\rm T} \in \mathbb{R}^{N_{\rm L} l \times n_{\rm L}}$, and $c(t) \triangleq [c_1^{\rm T}(t), \cdots, c_{N_{\rm L}}^{\rm T}(t)]^{\rm T} \in \mathbb{R}^{m_{\rm L}}$, with $\|c(t)\| \leq c^*$, where $n_{\rm L} = \sum_{i=1}^{N_{\rm L}} n_i$, and $m_{\rm L} = \sum_{i=1}^{N_{\rm L}} m_i$.

Theorem 1 *Consider the follower vehicle dynamics given compactly by (41) with (42) being Hurwitz and the leader dynamics given by (28) and (29) for* $i = 1, \cdots, N_L$. *First, if the reference command is constant, then* $y_f(t) \to (M(\mathcal{G}) \otimes I_l) y_L(t)$ *as* $t \to \infty$; *that is,* $y_{fi}(t)$, $i = 1, \cdots, N_F$, *asymptotically converge to the convex hull formed by the leaders. If, in addition,* $N_L = 1$, *then* $y_f(t) \to \mathbf{1}_{N_F} \otimes y_{L1}(t)$ *as* $t \to \infty$; *that is ,* $y_{fi}(t), i = 1, \cdots, N_F$, *asymptotically converge to the output of the leader. Second, if the reference command is time varying with bounded time rate of change, then* $y_f(t)$ *converge to the neighborhood of the convex hull formed by* $(M(\mathcal{G}) \otimes I_l) y_L(t)$ *as* $t \to \infty$. *If, in addition,* $N_L = 1$, *then* $y_f(t)$ *converge to the neighborhood of* $\mathbf{1}_{N_F} \otimes y_{L1}(t)$ *as* $t \to \infty$; *that is* $y_{fi}(t), i = 1, \cdots, N_F$, *converge to the neighborhood of the output of the leader.*

Proof. Considering the augmented state vector given by

$$\mathcal{Z}(t) \triangleq [x_{\mathrm{L}}^{\mathrm{T}}(t), \xi^{\mathrm{T}}(t)]^{\mathrm{T}} \in \mathbb{R}^{n_{\mathrm{L}}+n_\xi}, \tag{45}$$

(28) and (41) can be written in a compact form as

$$\dot{\mathcal{Z}}(t) = \mathcal{A}_z(\mathcal{G})\mathcal{Z}(t) + \mathcal{B}_z c(t), \quad \mathcal{Z}(0) = \mathcal{Z}_0, \quad t \geq 0 \tag{46}$$

where

$$\mathcal{A}_z(\mathcal{G}) = \begin{bmatrix} A_{\mathrm{L}} & 0 \\ B(\mathcal{G})C_{\mathrm{L}} & A(\mathcal{G}) \end{bmatrix} \in \mathbb{R}^{(n_{\mathrm{L}}+n_\xi)\times(n_{\mathrm{L}}+n_\xi)}, \tag{47}$$

$$\mathcal{B}_z = \begin{bmatrix} B_{\mathrm{L}} \\ 0 \end{bmatrix} \in \mathbb{R}^{(n_{\mathrm{L}}+n_\xi)\times m_{\mathrm{L}}}. \tag{48}$$

Since $\mathcal{A}(\mathcal{G})$ is Hurwitz as shown in Remark 4 and A_{L} is Hurwitz, it follows from the upper triangle structure of (47) that $\mathcal{A}_z(\mathcal{G})$ is Hurwitz, and hence, there exists a unique positive definite matrix P_z such that

$$0 = \mathcal{A}(\mathcal{G})^{\mathrm{T}}\mathcal{P}_z + \mathcal{P}_z\mathcal{A}(\mathcal{G}) + \mathcal{R}_z, \tag{49}$$

holds for a positive-definite matrix $\mathcal{R}_z$.

Now, similar to the proposed analysis in [22], consider

$$\mathcal{H}(t) \triangleq \mathcal{Z}(t) + \mathcal{A}_z(\mathcal{G})^{-1}\mathcal{B}_z c(t), \tag{50}$$

where $\mathcal{A}_z(\mathcal{G})$ is invertible since it has a nonzero determinant. In addition, consider the Lyapunov function candidate given by

$$\mathcal{V}(\mathcal{H}(t)) = \mathcal{H}^{\mathrm{T}}(t)\mathcal{P}_z\mathcal{H}(t), \tag{51}$$

where $\mathcal{V}(0) = 0$, $\mathcal{V}(\mathcal{H}(t)) > 0$ for all $\mathcal{H}(t) \neq 0$, and $\mathcal{V}(\mathcal{H}(t))$ is radially unbounded. The time derivative of (51) along the trajectory of (46) and (50) is given by

$$\begin{aligned}\dot{\mathcal{V}}(\mathcal{H}(t)) = \;& 2\mathcal{H}^{\mathrm{T}}(t)\mathcal{P}_z\left(\dot{\mathcal{Z}}(t) + \mathcal{A}_z(\mathcal{G})^{-1}\mathcal{B}_z\dot{c}(t)\right)\\ =\;& 2\mathcal{H}^{\mathrm{T}}(t)\mathcal{P}_z\left(\mathcal{A}_z(\mathcal{G})\mathcal{Z}(t) + \mathcal{B}_z c(t)\right)\\ &+ 2\mathcal{H}^{\mathrm{T}}(t)\mathcal{P}_z\mathcal{A}_z(\mathcal{G})^{-1}\mathcal{B}_z\dot{c}(t).\end{aligned} \tag{52}$$

In the remainder of this proof, we consider two cases.

Case 1: For $\dot{c}(t) = 0$, it follows from (49) and (52) that

$$\lim_{t\to\infty}\mathcal{H}(t) = 0. \tag{53}$$

Next, similar to [15], since (53) implies $\dot{\mathcal{Z}}(t) \to 0$ as $t \to \infty$, (46) can be written as

$$\mathcal{A}_z(\mathcal{G})\mathcal{Z}(\infty) + \mathcal{B}_z c(\infty) = 0, \tag{54}$$

where $\mathcal{Z}(\infty) = \lim_{t\to\infty} \mathcal{Z}(t)$ and $c(\infty) = \lim_{t\to\infty} c(t)$. In addition, letting $x_{\mathrm{L}}(\infty) = \lim_{t\to\infty} x_{\mathrm{L}}(t)$, $x_{\mathrm{f}}(\infty) = \lim_{t\to\infty} x_{\mathrm{f}}(t)$, $\theta(\infty) = \lim_{t\to\infty} \theta(t)$, $\nu(\infty) = \lim_{t\to\infty} \nu(t)$, and using the definition of $\mathcal{A}_z(\mathcal{G})$ and $\mathcal{B}_z$ given by (47) and (48), respectively, in (54) we have

$$0 = A_{\mathrm{L}} x_{\mathrm{L}}(\infty) + B_{\mathrm{L}} c(\infty), \tag{55}$$

$$\begin{aligned} 0 = {} & [I_{N_{\mathrm{F}}} \otimes A_{\mathrm{fr}} - F(\mathcal{G}) \otimes B_{\mathrm{f}} K_c C_o] x_{\mathrm{f}}(\infty) - (G(\mathcal{G}) \otimes B_{\mathrm{f}} K_c) y_{\mathrm{L}}(\infty) \\ & + (I_{N_{\mathrm{F}}} \otimes B_{\mathrm{f}} K_c)\theta(\infty), \end{aligned} \tag{56}$$

$$0 = -\delta(F(\mathcal{G}) \otimes C_o) x_{\mathrm{f}}(\infty) - \delta(G(\mathcal{G}) \otimes I_l) y_{\mathrm{L}}(\infty) - \delta\zeta\left(\theta(\infty) - \nu(\infty)\right), \tag{57}$$

$$0 = \eta\left(\theta(\infty) - \nu(\infty)\right). \tag{58}$$

Since, $\theta(\infty) = \nu(\infty)$ in (58), (57) implies

$$y_{\mathrm{f}}(\infty) = -(F(\mathcal{G})^{-1} G(\mathcal{G}) \otimes I_l) y_{\mathrm{L}}(\infty), \tag{59}$$

and hence, $y_{\mathrm{f}i}(t)$, $i = 1, \cdots, N_{\mathrm{F}}$, asymptotically converge to the convex hull formed by the leaders. In addition, if $N_{\mathrm{L}} = 1$, then $-F(\mathcal{G})^{-1} G(\mathcal{G}) = \mathbf{1}_{N_{\mathrm{F}}}$ and as a direct consequence of (59) we have

$$\begin{aligned} y_{\mathrm{f}}(\infty) &= (\mathbf{1}_{N_{\mathrm{F}}} \otimes I_l) y_{\mathrm{L}1}(\infty) \\ &= \mathbf{1}_{N_{\mathrm{F}}} \otimes y_{\mathrm{L}1}(\infty), \end{aligned} \tag{60}$$

and hence, $y_{\mathrm{f}i}(t)$, $i = 1, \cdots, N_{\mathrm{F}}$, asymptotically converge to the output of the leader. ***Case 2***: We now consider $\|\dot{c}(t)\| \leq \dot{c}^*$, where $\dot{c}^* > 0$. For this purpose, (52) can be rewritten as

$$\begin{aligned}\dot{\mathcal{V}}(\mathcal{H}(t)) &= -\mathcal{H}^{\mathrm{T}}(t)\mathcal{R}_z\mathcal{H}(t) + 2\mathcal{H}^{\mathrm{T}}(t)\mathcal{P}_z\mathcal{A}_z(\mathcal{G})^{-1}\mathcal{B}_z\dot{c}(t)\\ &\leq -\lambda_{\min}(\mathcal{R}_z)\|\mathcal{H}(t)\|^2 + \Psi\|\mathcal{H}(t)\|,\\ &= -\lambda_{\min}(\mathcal{R}_z)\|\mathcal{H}(t)\|\left(\|\mathcal{H}(t)\| - \frac{\Psi}{\lambda_{\min}(\mathcal{R}_z)}\right). \end{aligned} \tag{61}$$

where $\Psi \triangleq 2\|\mathcal{P}_z\mathcal{A}_z(\mathcal{G})^{-1}\mathcal{B}_z\|_{\mathrm{F}}\dot{c}^*$. It follows from (61) that $\dot{\mathcal{V}}(\mathcal{H}(t)) < 0$ outside the compact set

$$\Omega \triangleq \left\{\mathcal{H}(t) : \mathcal{H}(t) \geq \frac{\Psi}{\lambda_{\min}(\mathcal{R}_z)}\right\}, \tag{62}$$

which proves uniform ultimate boundedness of the closed-loop solution $\mathcal{Z}(t)+\mathcal{A}_z(\mathcal{G})^{-1}\mathcal{B}_z c(t)$ for all initial conditions[19]. Since $\dot{\mathcal{V}}(\mathcal{H}(t)) < 0$ outside the compact set (62), then an ultimate bound for the distance of $\mathcal{H}(t) \triangleq \mathcal{Z}(t) + \mathcal{A}_z(\mathcal{G})^{-1}\mathcal{B}_z c(t)$ can be computed as

$$\|\mathcal{H}(t)\| \leq \sqrt{\frac{\lambda_{\max}(\mathcal{P}_z)}{\lambda_{\min}(\mathcal{P}_z)}}\frac{\Psi}{\lambda_{\min}(\mathcal{R}_z)}, \quad t \geq T. \tag{63}$$

Note that if the right side of (63) is small, then the distance of $\mathcal{Z}(t) + \mathcal{A}_z(\mathcal{G})^{-1}\mathcal{B}_z c(t)$ is small for $t \geq 0$. Therefore, a small $\mathcal{Z}(t) + \mathcal{A}_z(\mathcal{G})^{-1}\mathcal{B}_z c(t)$ implies $y_{\mathrm{f}i}(t)$, $i = 1, \cdots, N_{\mathrm{F}}$ to stay at the neighborhood of the convex hull formed by those of the leaders. In addition, if $N_{\mathrm{L}} = 1$, then $-F(\mathcal{G})^{-1}G(\mathcal{G}) = \mathbf{1}_{N_{\mathrm{F}}}$, implies $y_{\mathrm{f}i}(t)$, $i = 1, \cdots, N_{\mathrm{F}}$ stay close to the output of the leader.

This concludes the entire proof. ■

6. ILLUSTRATIVE NUMERICAL EXAMPLES

In this section, we present two numerical examples to demonstrate the efficacy of the proposed output feedback control architecture for multivehicle systems. For this purpose, we consider a line graph of leader and follower vehicles. For the follower vehicle

dynamics we consider system matrices given by

$$A = \begin{bmatrix} 0 & 1 \\ 1 & 1 \end{bmatrix}, \quad B = \begin{bmatrix} 0 \\ 1 \end{bmatrix}, \quad C = \begin{bmatrix} 1 & 0 \end{bmatrix}, \tag{64}$$

with zero initial conditions. In addition, for the leader vehicle dynamics we consider $A_{\mathrm{L}} = -0.5$, $B_{\mathrm{L}} = 0.5$, $C_{\mathrm{L}} = 1$, with $x_{\mathrm{L}1}(0) = 0$. We let $\lambda = 0.8$, and

$$A_{\mathrm{fr}} = \begin{bmatrix} 0 & 1 & 0 & 0 \\ -6.25 & -3.535 & 1 & 0 \\ 0 & 0 & 0 & 1 \\ 0 & 0 & -0.64 & -1.6 \end{bmatrix}, \tag{65}$$

to create the nominal feedback gain $k = [37, 59.5, 29.75, 7.09]$ and choose $K_{\mathrm{c}} = 1.5$, $\zeta = 1.5$, $\eta = 2$, $\delta = 5$ for the cooperative control design.

Throughout the simulation, in order to show efficacy of the proposed control architecture regarding the stability and convergence, we consider two types of reference command for the leader system, constant and time varying reference commands.

Example 1. For the first example, we consider a line graph with four follower vehicles and a single leader and our aim is to track a given reference command $c_1(t)$, $t \geq 0$. This is first done for a unit step reference command as shown in Figure 1 where it is clear the the follower vehicles asymptotically converge to the output of the leader. We then apply a time varying reference command given by $c_1(t) = 0.5 \sin(0.02t)$ as shown in Figure 4. In this case, the outputs of the follower vehicles converge asymptotically to a neighborhood of the leader vehicle which is consistent with the proposed approach.

Example 2. For the second example, we consider four follower vehicles and two leaders with different reference commands. In this way, the leaders create a convex hull for the followers to converge to. First, for a constant reference command, we consider

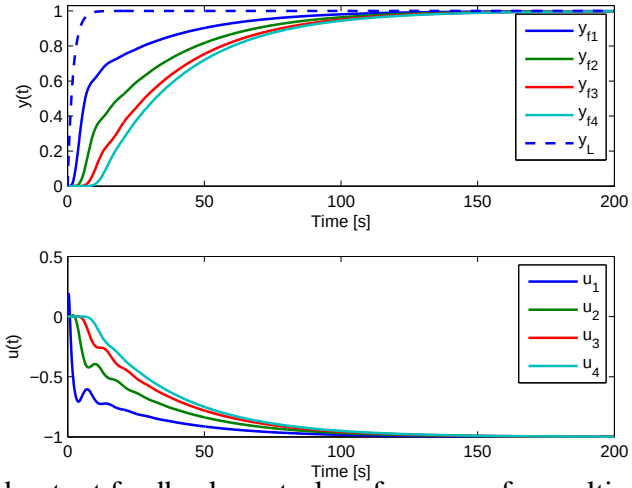

Figure 1. Proposed output feedback control performance for multivehicle system with one leader following a constant command.

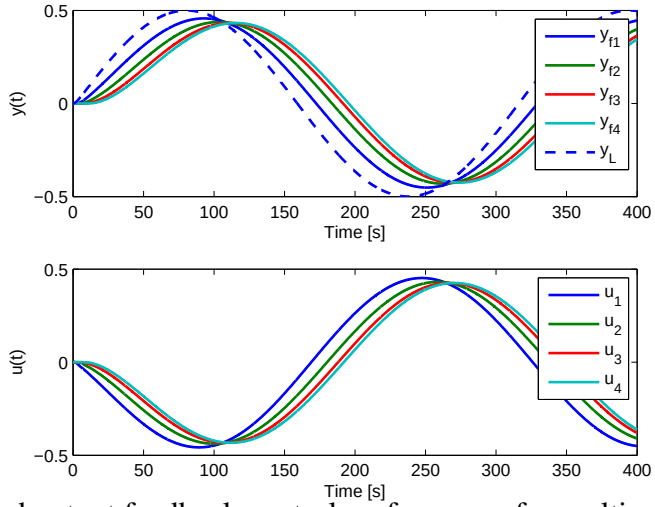

Figure 2. Proposed output feedback control performance for multivehicle system with one leader following a time varying command.

$c(t) = [1\ ,\ 0.8]^{\mathrm{T}}$ as shown in Figure 3. In Figure 7, we use the time varying commands given by $c_i(t) = (-1)^{i+1}0.8 + (-1)^{i+1}0.5\sin((0.02 * i)t)$, $i = 1,2$. In both cases, follower vehicles converge to the convex hull of leader outputs.

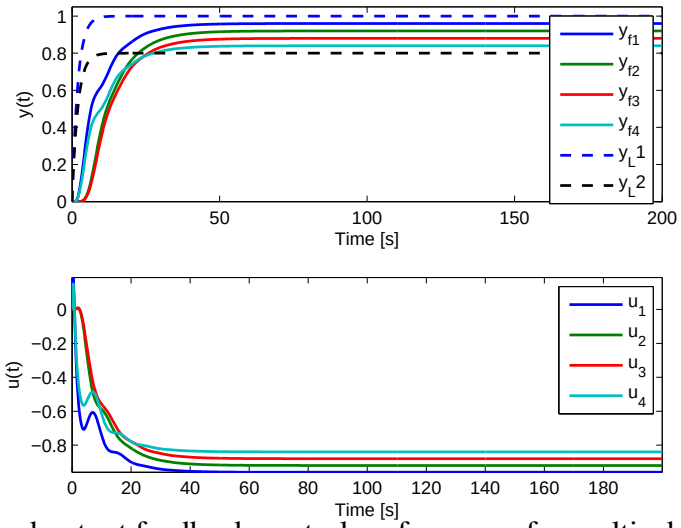

Figure 3. Proposed output feedback control performance for multivehicle system with two leaders creating a constant convex hull.

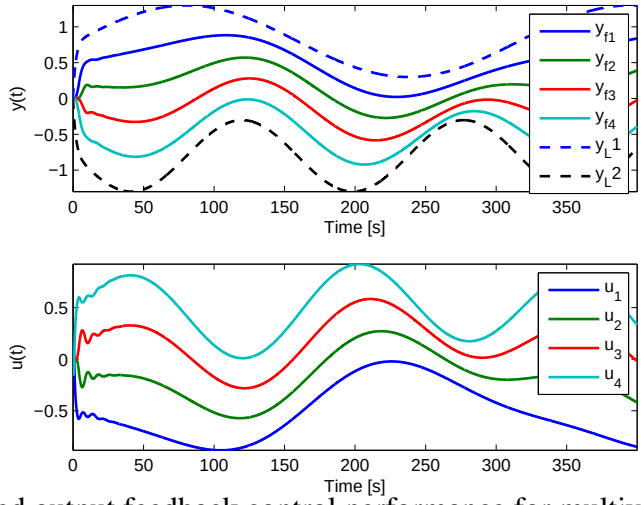

Figure 4. Proposed output feedback control performance for multivehicle system with two leaders creating a time varying convex hull.

7. CONCLUSIONS

A new, observer-free output feedback cooperative control architecture was presented for continuous-time, minimum phase, and high-order multivehicle systems. In particular, a nonminimal state-space realization method was utilized to generate an expanded set of states for each vehicle, where these nonminimal states were then utilized to design

a cooperative control architecture to address the containment problem. In addition to rigorous analyses on the stability and convergence, two illustrative numerical examples were further included to demonstrate the efficacy of the proposed approach. Future research will include comparison of the proposed observer-free cooperative control architecture with other observer-based cooperative control methods.

ACKNOWLEDGMENT

This research has been supported by the Dynamic Data-Driven Applications Systems Program of the Air Force Office of Scientific Research.

REFERENCES

[1] F. Bullo, J. Cortes, and S. Martinez, *Distributed control of robotic networks: A mathematical approach to motion coordination algorithms*. Princeton University Press, 2009.

[2] M. Mesbahi and M. Egerstedt, *Graph theoretic methods in multiagent networks*. Princeton University Press, 2010.

[3] W. Ren and Y. Cao, *Distributed coordination of multi-agent networks: Emergent problems, models, and issues*. Springer Science & Business Media, 2010.

[4] F. L. Lewis, H. Zhang, K. Hengster-Movric, and A. Das, *Cooperative control of multi-agent systems: optimal and adaptive design approaches*. Springer Science & Business Media, 2013.

[5] J. Xiang, W. Wei, and Y. Li, "Synchronized output regulation of linear networked systems," *IEEE Transactions on Automatic Control*, vol. 54, no. 6, pp. 1336–1341, 2009.

[6] H. Zhang, F. L. Lewis, and A. Das, "Optimal design for synchronization of cooperative systems: state feedback, observer and output feedback," *IEEE Transactions on Automatic Control*, vol. 56, no. 8, pp. 1948–1952, 2011.

[7] Y. Su and J. Huang, "Cooperative output regulation of linear multi-agent systems," *IEEE Transactions on Automatic Control*, vol. 57, no. 4, pp. 1062–1066, 2012.

[8] R. Cui, B. Ren, and S. Ge, "Synchronised tracking control of multi-agent system with high-order dynamics," *IET Control Theory & Applications*, vol. 6, no. 5, pp. 603–614, 2012.

[9] T. Liu and Z.-P. Jiang, "Distributed output-feedback control of nonlinear multi-agent systems," *IEEE Transactions on Automatic Control*, vol. 58, no. 11, pp. 2912–2917, 2013.

[10] H. Zhang, G. Feng, H. Yan, and Q. Chen, "Observer-based output feedback event-triggered control for consensus of multi-agent systems," *IEEE Transactions on Industrial Electronics*, vol. 61, no. 9, pp. 4885–4894, 2014.

[11] B. Zhou, C. Xu, and G. Duan, "Distributed and truncated reduced-order observer based output feedback consensus of multi-agent systems," *IEEE Transactions on Automatic Control*, vol. 59, no. 8, pp. 2264–2270, 2014.

[12] C. P. Chen, G.-X. Wen, Y.-J. Liu, and Z. Liu, "Observer-based adaptive backstepping consensus tracking control for high-order nonlinear semi-strict-feedback multiagent systems," *IEEE transactions on cybernetics*, vol. 46, no. 7, pp. 1591–1601, 2016.

[13] T. Yucelen and F. Pourboghrat, "Active noise blocking: Non-minimal modeling, robust control, and implementation," in *American Control Conference, 2009. ACC'09.*, pp. 5492–5497, IEEE, 2009.

[14] T. Yucelen and W. M. Haddad, "Output feedback adaptive stabilization and command following for minimum phase dynamical systems with unmatched uncertainties and disturbances," *International Journal of Control*, vol. 85, no. 6, pp. 706–721, 2012.

[15] T. Yucelen and E. N. Johnson, "Control of multivehicle systems in the presence of uncertain dynamics," *International Journal of Control*, vol. 86, no. 9, pp. 1540–1553, 2013.

[16] C. Godsil and G. Royle, *Algebraic graph theory*. New York, NY: Springer, 2001.

[17] P. J. Antsaklis and A. N. Michel, *Linear systems*. Bosten, MA: Birkhäuser, 2006.

[18] W. M. Haddad and V. Chellaboina, *Nonlinear Dynamical Systems and Control:* A L*yapunov-Based Approach*. Princeton University Press, 2008.

[19] H. K. Khalil, *Nonlinear Systems*. Upper Saddle River, NJ: PrenticeHall, 1996.

[20] J. A. Fax and R. M. Murray, "Information flow and cooperative control of vehicle formations," *IEEE transactions on automatic control*, vol. 49, no. 9, pp. 1465–1476, 2004.

[21] C.-Q. Ma and J.-F. Zhang, "Necessary and sufficient conditions for consensusability of linear multi-agent systems," *IEEE Transactions on Automatic Control*, vol. 55, no. 5, pp. 1263–1268, 2010.

[22] D. Tran and T. Yucelen, "On control of multiagent formations through local interactions," in *IEEE Conference on Decision and Control*, 2016.

V. AN OBSERVER-FREE OUTPUT FEEDBACK COOPERATIVE CONTROL ARCHITECTURE FOR LINEAR MULTIAGENT SYSTEMS WITH EVENT-TRIGGERING

Ali Albattat[1], Tansel Yucelen[2], and Sarangapani Jagannathan[1]

[1] Department of Mechanical & Aerospace Engineering

Missouri University of Science and Technology

[2] Department of Mechanical Engineering

University of South Florida

ABSTRACT

An event-triggering methodology is proposed on an observer-free output feedback cooperative control scheme for linear multiagent systems in order to schedule the exchanged information between the agents depending upon error exceeding user-defined thresholds for reducing wireless network utilization. Specifically, the cooperative control scheme is designed for continuous-time, minimum phase, and high-order linear multiagent systems in the context of a containment problem (i.e., outputs of the follower agents convergence to the convex hull spanned by those of the leader agents). The proposed observer-free output feedback cooperative control scheme with event-triggering guarantees follower agents' system stability and performance, and also does not yield to a Zeno behavior. Two illustrative numerical examples complement the proposed theoretical contribution.

1. INTRODUCTION

During the past few decades, cooperative control of multiagent systems has attracted increased attention in the control engineering community owing to its diverse and influential application in areas of science and engineering such as formation flight of un-

manned air, land, and underwater vehicles, as well as the control of clusters of satellites and telescopes (e.g., see [1, 2, 3, 4]). Since cooperative control enables the multiagent systems to work coherently utilizing local information exchange between agents, a challenge in the design and implementation of networked control systems is to reduce wireless network utilization. To this end, the last decade has witnessed an increased interest in event-triggering control theory [5, 6, 7, 8, 9].

In this paper, we propose an event-triggering methodology for the output feedback cooperative control to schedule the exchanged output measurements information between the agents in order to reduce wireless network utilization. The utilized output feedback cooperative control architecture is in the context of a containment problem (i.e., outputs of the follower agents convergence to the convex hull spanned by those of the leader agents). While full state feedback designs lead to computationally simpler cooperative control laws [10, 11], output feedback designs are required for most applications that involve high-dimensional agent models with inaccessible states. To this end, several output feedback cooperative control with event triggering approaches are proposed in the literature for multiagent systems (e.g., see [12, 13] and references therein), where the common denominator of these approaches is that they utilize an observer in their cooperative control laws.

Unlike the aforementioned existing literature, the contribution of this paper is an event-triggering mechanism on the exchanged output measurements between agents that are controlled by an observer-free output feedback cooperative control architecture for continuous-time, minimum phase, and high-order linear multiagent systems, where the results reported here can be viewed as a generalization of our recent papers in [14, 15], where they do not consider event-triggering. The key feature of our adopted controller scheme is that it is predicated on a nonminimal state-space realization originally proposed in [16, 17] that generates an expanded set of states only using the filtered input and filtered output and their derivatives for each follower agent, without the need for designing an observer for each agent.

Specifically, the adopted observer-free output feedback control law consists of a agent-level controller and a local cooperative controller for each agent as in [18], where the former addresses internal stability of agents and the latter addresses the containment problem. In addition, the proposed event-triggering methodology is applied on the relative output measurements of the agents, where each agent has its own event-triggering threshold to transmit its own output measurements to the neighbor agents asynchronously. Since the information exchanged happening in the event-triggering manner, additional terms in the Laplacian matrices are observed, and these additional terms are utilized in the controller scheme design. Note that our cooperative controller scheme operates in a periodic sampling instances and it uses event-triggered output measurements transmitted from the neighboring agents. Two illustrative numerical examples complement the proposed theoretical contribution.

This paper's organization is as follows. Section 2 recalls necessary basic results from the multiagent systems literature. Section 3 presents an over view of the nonminimal state space realization architecture of [14, 15, 16, 17] in the context of the multiagent system setup of this paper. The proposed output feedback cooperative control architecture with event-triggering is then given in Section 4. User-defined event-triggering rules are given in Section 5. A performance analysis of the proposed architecture is presented in 6. Computing the lower bound for event-triggering intersampling time by Zeno analysis is presented in 7, where two illustrative numerical examples are included in Section 8. Finally, conclusions are summarized in Section 9.

2. NECESSARY PRELIMINARIES

The notation used in this paper is fairly standard (e.g see [14, 15]). In addition, we adopt graph-theoretical notation (e.g., see [19, 2]) to encode interactions between agents. In particular, an undirected graph $\mathcal{G}$ is defined by $\mathcal{V}_{\mathcal{G}} = \{1, \cdots, N\}$ of nodes and a set $\mathcal{E}_{\mathcal{G}} \in \mathcal{V}_{\mathcal{G}} \times \mathcal{V}_{\mathcal{G}}$ of edges. If $(i, j) \in \mathcal{E}_{\mathcal{G}}$, then the nodes i and j are neighbors, and

the neighboring relation is indicated with $i \sim j$. The degree d_i of node i is defined by the number of its neighbors and the degree matrix of graph $\mathcal{G}$ is then given by $\mathcal{D}(\mathcal{G}) \triangleq \operatorname{diag}(d) \in \mathbb{R}^{N\times N}$, $d = [d_2, \cdots, d_N]^{\mathrm{T}}$. A path $i_0 i_1 \cdots i_L$ is a finite sequence of nodes such that $i_{k-1} \sim i_k$, $k = 1, \cdots, L$, and if any pair of district nodes has a path, then a graph $\mathcal{G}$ is connected. Furthermore, we write $\mathcal{A}(\mathcal{G}) \in \mathbb{R}^{N\times N}$ for adjacency matrix of a graph $\mathcal{G}$ defined by $[\mathcal{A}(\mathcal{G})]_{ij} \triangleq 1$ if $(i, j) \in \mathcal{E}_{\mathcal{G}}$ and $[\mathcal{A}(\mathcal{G})]_{ij} \triangleq 0$ otherwise, and $\mathcal{B}(\mathcal{G}) \in \mathbb{R}^{N\times M}$ for the (node-edge) incidence matrix of the graph $\mathcal{G}$, defined by $[\mathcal{B}(\mathcal{G})]_{ij} \triangleq 1$ if node i is the head of the edge j, $[\mathcal{B}(\mathcal{G})]_{ij} \triangleq -1$ if node i is the tail of the edge j, and $[\mathcal{B}(\mathcal{G})]_{ij} \triangleq 0$ otherwise, where M is the number of edges, i is an index for the node set, and j is an index for the edge set. Finally, the graph Laplacian matrix, $\mathcal{L}(\mathcal{G}) \in \overline{\mathbb{R}}_{+}^{N\times N} \cap \mathbb{S}^{N\times N}$, is defined by $\mathcal{L}(\mathcal{G}) \triangleq \mathcal{D}(\mathcal{G}) - \mathcal{A}(\mathcal{G})$, or equivalently, $\mathcal{L}(\mathcal{G}) = \mathcal{B}(\mathcal{G})\mathcal{B}(\mathcal{G})^{\mathrm{T}}$. We next recall some of the basic results for (scalar) multiagent systems [2]. For this purpose, let nodes and edges represent agents and information exchange links between agents, respectively. Then, we can model a given multiagent system by a graph $\mathcal{G}$. For example, let $x_i(t) \in \mathbb{R}$ be the state of node i, $i = 1, \ldots, N$, satisfying

$$\dot{x}_i(t) = u_i(t), \quad x_i(0) = x_{i0}, \tag{1}$$

where $u_i(t) \in \mathbb{R}$ is the control input. If each agent receives the relative state information with respect to its neighbors, then

$$u_i(t) = -\sum_{i\sim j} \big(x_i(t) - x_j(t)\big), \tag{2}$$

solves the rendezvous problem, where (1) subject to (2) can be written at the multiagent system level as

$$\dot{x}(t) = -\mathcal{L}(\mathcal{G})x(t), \quad x_i(0) = x_{i0}, \tag{3}$$

with $x(t) = \left[x_1^{\mathrm{T}}(t), \cdots, x_N^{\mathrm{T}}(t)\right]^{\mathrm{T}}$ denoting the aggregated state vector. Note that the spectrum of $\mathcal{L}(\mathcal{G})$ has one zero eigenvalue and $N-1$ positive real eigenvalues if and only if the graph $\mathcal{G}$ is connected and undirected. In this case, the solution of the multiagent system given by (3) evolves as $x(t) \to (\mathbf{1}_N \mathbf{1}_N^{\mathrm{T}}/N)x_0$ as $t \to \infty$.

Finally, we recall some results on leader-follower multiagent system frameworks. For this purpose, let the incidence matrix be partitioned as $\mathcal{B}(\mathcal{G}) = [\mathcal{B}_{\mathrm{L}}(\mathcal{G})^{\mathrm{T}}, \mathcal{B}_{\mathrm{F}}(\mathcal{G})^{\mathrm{T}}]^{\mathrm{T}}$, where $\mathcal{B}_{\mathrm{L}}(\mathcal{G}) \in \mathbb{R}^{N_{\mathrm{L}} \times M}$ and $\mathcal{B}_{\mathrm{F}}(\mathcal{G}) \in \mathbb{R}^{N_{\mathrm{F}} \times M}$ with N_{L} and N_{F} denoting cardinalities of the leader and follower groups, respectively, such that $N = N_{\mathrm{L}} + N_{\mathrm{F}}$. Then, using $\mathcal{L}(\mathcal{G}) = \mathcal{B}(\mathcal{G})\mathcal{B}(\mathcal{G})^{\mathrm{T}}$ and the partitioned incidence matrix the partitioned graph Laplacian matrix $\mathcal{L}(\mathcal{G})$ is given by

$$\mathcal{L}(\mathcal{G}) = \begin{bmatrix} L(\mathcal{G}) & G(\mathcal{G})^{\mathrm{T}} \\ G(\mathcal{G}) & F(\mathcal{G}) \end{bmatrix}, \tag{4}$$

where $L(\mathcal{G}) \triangleq \mathcal{B}_{\mathrm{L}}(\mathcal{G})\mathcal{B}_{\mathrm{L}}(\mathcal{G})^{\mathrm{T}}$, $G(\mathcal{G}) = \mathcal{B}_{\mathrm{F}}(\mathcal{G})\mathcal{B}_{\mathrm{L}}(\mathcal{G})^{\mathrm{T}}$ and $F(\mathcal{G}) = \mathcal{B}_{\mathrm{F}}(\mathcal{G})\mathcal{B}_{\mathrm{F}}(\mathcal{G})^{\mathrm{T}}$.

Note that $F(\mathcal{G}) \in \mathbb{R}_+^{N_{\mathrm{F}} \times N_{\mathrm{F}}} \cap \mathbb{S}^{N_{\mathrm{F}} \times N_{\mathrm{F}}}$, and hence, $F(\mathcal{G})$ is nonsingular since $\det(F(\mathcal{G})) \neq 0$. Furthermore $F(\mathcal{G})\mathbf{1}_{N_{\mathrm{F}}} = -G(\mathcal{G})\mathbf{1}_{N_{\mathrm{L}}}$, or equivalently, each row of $-F(\mathcal{G})^{-1}G(\mathcal{G})$ has a sum equal to 1. Now, we can model a given multiagent system on a leader-follower framework. In particular, let $x_{\mathrm{L}}(t) \in \mathbb{R}^{N_{\mathrm{L}}}$ and $x_{\mathrm{F}}(t) \in \mathbb{R}^{N_{\mathrm{F}}}$ be the aggregated state vector of the leaders and followers, respectively. Then, the followers evolve through the Laplacian-based dynamics as

$$\dot{x}_{\mathrm{F}}(t) = -F(\mathcal{G})x_{\mathrm{F}}(t) - G(\mathcal{G})x_{\mathrm{L}}(t), \quad x_{\mathrm{F}}(0) = x_{\mathrm{F}0}. \tag{5}$$

Throughout this paper, we consider leaders as command generators for the neighboring followers and that a connected, undirected graph $\mathcal{G}$ represents the interaction topology between the agents.

Remark 2 *In the case of event-triggering for the exchanged information between the agents, (2) can be given by*

$$u_i(t) = -\sum_{i\sim j}\Big(x_i(t) - x_{sj}(t)\Big), \tag{6}$$

where $x_{sj}(t)$ is the event-triggered state vector of the neighboring agent. Then, (1) subject to (6) can be written at the multiagent system level as

$$\dot{x}(t) = -\mathcal{L}_p(\mathcal{G})x(t) - \mathcal{L}_s(\mathcal{G})x_s(t), \quad x_i(0) = x_{i0}, \tag{7}$$

where $x_s(t) = \left[x_{s1}^{\mathrm{T}}(t), \cdots, x_{sN}^{\mathrm{T}}(t)\right]^{\mathrm{T}}$ is the aggregated event-triggered state vector, $\mathcal{L}_p(\mathcal{G})$ is graph Laplacian matrix corresponds to the periodic state vector owing to utilizing event-triggering, $\mathcal{L}_s(\mathcal{G})$ is graph Laplacian matrix corresponds to the event-trigged state vector. Note that the partitioned resulting Laplacian matrices are given by

$$\mathcal{L}_p(\mathcal{G}) = \begin{bmatrix} L_p(\mathcal{G}) & G_p(\mathcal{G})^{\mathrm{T}} \\ G_p(\mathcal{G}) & F_p(\mathcal{G}) \end{bmatrix}, \tag{8}$$

$$\mathcal{L}_s(\mathcal{G}) = \begin{bmatrix} L_s(\mathcal{G}) & G_s(\mathcal{G})^{\mathrm{T}} \\ G_s(\mathcal{G}) & F_s(\mathcal{G}) \end{bmatrix}, \tag{9}$$

where $\mathcal{L}(\mathcal{G}) \triangleq \mathcal{L}_p(\mathcal{G}) + \mathcal{L}_s(\mathcal{G})$, $G_p(\mathcal{G}) = 0$, $L_s(\mathcal{G}) = 0$, $G_s(\mathcal{G}) \triangleq G(\mathcal{G})$, $L_p(\mathcal{G}) \triangleq L(\mathcal{G})$, and $F(\mathcal{G}) \triangleq F_p(\mathcal{G}) + F_s(\mathcal{G})$. Now, we can model a given multiagent system on a leader-follower framework with event-triggered state vectors that exchanged between the multiagent systems. Then, the Laplacian-based dynamics in (5) can be given as

$$\dot{x}_F(t) = -F_p(\mathcal{G})x_F(t) - G_s(\mathcal{G})x_{Ls}(t) - F_s(\mathcal{G})x_{Fs}(t), \quad x_F(0) = x_{F0}. \tag{10}$$

Owing to proposing event-triggering methodology on the exchanged information between the agents, we have additional different Laplacian matrices here in this paper. In addition, it will be shown in the sequel how these additional Laplacian matrices affect on the followers agents' performance analysis.

3. AN OVERVIEW OF THE NONMINIMAL STATE SPACE REALIZATION

Consider controllable and observable minimum phase linear dynamical follower agent system i, $i = 1, \cdots, N_{\mathrm{F}}$, given by

$$\dot{x}_i(t) = Ax_i(t) + Bu_i(t), \;\; x_i(0) = x_{0i}, \;\; t \geq 0, \tag{11}$$

$$y_i(t) = Cx_i(t), \tag{12}$$

where $x_i(t) \in \mathbb{R}^n$, $t \geq 0$ is the unknown state vector, $u_i(t) \in \mathbb{R}^m$, $t \geq 0$ is the known control input, $y_i(t) \in \mathbb{R}^l$, $t \geq 0$ is the known system output. In addition, $A \in \mathbb{R}^{n\times n}$, $B \in \mathbb{R}^{n\times m}$, $C \in \mathbb{R}^{l\times n}$, are known follower system matrices and the triple (A,B,C) is minimal. We use a nonminimal state-space representation method utilized in [14, 15, 16, 17] for the follower agent dynamics $i, i = 1, \cdots, N_{\mathrm{F}}$, such that an input-output equivalent (from control inputs $u_i(t)$, $t \geq 0$, to system outputs $y_i(t)$, $t \geq 0$) nonminimal observer canonical state-space model [20] of (11) and (12) for $l > 1$ is obtained. An input-output equivalent nonminimal controllable state-space realization of (11) and (12) is now given by

$$\dot{x}_{\mathrm{f}i}(t) = A_{\mathrm{f}}x_{\mathrm{f}i}(t) + B_{\mathrm{f}}u_i(t), \quad x_{\mathrm{f}i}(0) = x_{\mathrm{f}0i}, \;\; t \geq 0, \tag{13}$$

$$y_i(t) = C_{\mathrm{f}}x_{\mathrm{f}i}(t), \tag{14}$$

with

$$A_{\mathrm{f}} = \begin{bmatrix} 0 & I_l & 0 & \cdots & & & \cdots & 0 \\ \vdots & & \ddots & & & & & \vdots \\ 0 & \cdots & 0 & I_l & 0 & \cdots\cdots & & 0 \\ -a_0 I_l & \cdots\cdots & & -a_{n-1} I_l & \bar{B}_0 & \cdots\cdots & & \bar{B}_{n-1} \\ 0 & \cdots & & \cdots & 0 & I_m & 0 & 0 \\ \vdots & & & & & & \ddots & \vdots \\ \vdots & & & & & & \cdots\ 0 & I_m \\ 0 & \cdots\cdots & & 0 & -\lambda^n I_m & \cdots\cdots & & -n\lambda I_m \end{bmatrix} \in \mathbb{R}^{n_{\mathrm{f}} \times n_{\mathrm{f}}}, \tag{15}$$

$$B_{\mathrm{f}} = \begin{bmatrix} 0 & 0 \cdots \lambda^n I_m \end{bmatrix}^{\mathrm{T}} \in \mathbb{R}^{n_{\mathrm{f}} \times m}, \tag{16}$$

$$C_{\mathrm{f}} = [-\lambda^{-n}(a_0 I_l + \lambda^n I_l) \cdots\cdots -\lambda^{-n}(a_{n-1} I_l + n\lambda^n I_l) \ \ \lambda^{-n}\bar{B}_0 \cdots\cdots \lambda^{-n}\bar{B}_{n-1}] \in \mathbb{R}^{l \times n_{\mathrm{f}}}, \tag{17}$$

where $x_{\mathrm{f}i}(t) = \left[q_{1i}^{\mathrm{T}}(t), \cdots, q_{ni}^{\mathrm{T}}(t), v_{1i}^{\mathrm{T}}, \cdots, v_{ni}^{\mathrm{T}}\right]^{\mathrm{T}} \in \mathbb{R}^{n_{\mathrm{f}}}$, $i = 1, \cdots, N_{\mathrm{F}}$, with $n_{\mathrm{f}} \triangleq (m+l)n$, is the known expanded state vector that contains the filtered input and filtered output and their derivatives given by $q_{ki}(t) \triangleq y_{\mathrm{f}i}^{k-1}(t)$, $v_{ki} = u_{\mathrm{f}i}^{k-1}(t)$, $k = 1,2,\cdots,n$, $z^{(n)} \triangleq \mathrm{d}^n z(t)/\mathrm{d}t^n$, $a_k, k = 0,\ldots,n-1$, is the coefficients of the characteristic polynomial of system matrix for the nonmimimal observer canonical state space model of (11) and (12) for $l > 1$, λ is the filter gain of the transfer function $\Lambda(s) = \lambda^n/(s+\lambda)^n$ for the known expanded state vector $x_{\mathrm{f}i}(t)$ in (13), and $\bar{B}_k, k = 0,\ldots,n-1$ is the combination matrix of the nonminimal observer canonical state-space form matrices of (11) and (12). The nonminimal state space realization steps are omitted here due to the page limit restrictions, and the details are available in [14].

4. COOPERATIVE CONTROL DESIGN BASED ON NONMINIMAL STATE SPACE REALIZATION

In order to construct the system controller architecture, we need first to introduce the leader system dynamics that are necessary for the considered containment problem. For this purpose, consider the dynamics of the leader i, $i = 1, \cdots, N_{\mathrm{L}}$, given by

$$\dot{x}_{\mathrm{L}i}(t) = A_{\mathrm{L}i}x_{\mathrm{L}i}(t) + B_{\mathrm{L}i}c_i(t),\ x_{\mathrm{L}i}(0) = x_{\mathrm{L}0i},\ t \geq 0, \tag{18}$$

$$y_{\mathrm{L}i}(t) = C_{\mathrm{L}i}x_{\mathrm{L}i}(t), \tag{19}$$

where $x_{\mathrm{L}i}(t) \in \mathbb{R}^{n_i}$ is the leader state vector, $c_i(t) \in \mathbb{R}^{m_i}$ is a agent bounded input command (i.e., $\|c_i(t)\| \leq c_i^*$) with bounded time rate change (i.e., $\|\dot{c}_i(t)\| \leq \dot{c}_i^*$), $y_{\mathrm{L}i}(t) \in \mathbb{R}^l$ is the leader output, $A_{\mathrm{L}i} \in \mathbb{R}^{n_i \times n_i}$ is the leader system matrix, $B_{\mathrm{L}i} \in \mathbb{R}^{n_i \times m_i}$ is the leader command input matrix, $C_{\mathrm{L}i} \in \mathbb{R}^{l \times n_i}$ is the leader output matrix, $(A_{\mathrm{L}i}, B_{\mathrm{L}i}, C_{\mathrm{L}i})$ is minimal, and $A_{\mathrm{L}i}$ is Hurwitz.

To achieve the control objective of driving the follower agents to the convex hull spanned by the leaders, we utilize the control architecture presented in [14], where a two-level output feedback control for the nonminimal state-space realization follower agent $i, i = 1, \cdots, N_{\mathrm{F}}$ given as

$$u_i(t) = u_{\mathrm{c}i}(t) + u_{\mathrm{v}i}(t). \tag{20}$$

Here, $u_{\mathrm{c}i}(t) \in \mathbb{R}^m$ is the local cooperative controller that receives the event-triggered relative output measurements of the neighboring agents in terms of $y_{\mathrm{fs}i}(t)$ and $y_{\mathrm{Ls}i}(t)$ and $u_{\mathrm{v}i}(t) \in \mathbb{R}^m$ is the agent level controller that receives the internal nonminimal state-space realization based state measurements, i.e., $x_{\mathrm{f}i}(t)$.

4.1. Vehicle-level Control Law. We consider the agent-level control law given by [14]

$$u_{\mathrm{v}i}(t) \triangleq -kx_{\mathrm{f}i}(t), \tag{21}$$

in order to make $A_{\mathrm{fr}} \triangleq A_{\mathrm{f}} - B_{\mathrm{f}}k \in \mathbb{R}^{n_{\mathrm{f}}\times n_{\mathrm{f}}}$ Hurwitz (i.e., internal stability), where $k \in \mathbb{R}^{m_{\mathrm{f}}\times n_{\mathrm{f}}}$ is a feedback matrix designed using pole placement. Then, the follower agent dynamics in (13) become

$$\dot{x}_{\mathrm{f}i}(t) = A_{\mathrm{fr}}x_{\mathrm{f}i}(t) + B_{\mathrm{f}}u_{\mathrm{c}i}(t), \;\; x_{\mathrm{f}i}(0) = x_{\mathrm{f}0i}, \;\; t \geq 0. \tag{22}$$

4.2. Local Cooperative Control Law with Event-triggering. In order to present the cooperative control scheme with event-triggered exchanged information, we first consider the approach in [18, 14, 15] in our theoretical setup. In addition, we assume each ith, $i = 1, \cdots, N_{\mathrm{F}}$, follower agent's controller receives event-trigged relative output measurements form the neighbor agents. For this purpose, let $\tilde{y}(t) \triangleq \left[y_{\mathrm{L}}^{\mathrm{T}}(t), y_{\mathrm{f}}^{\mathrm{T}}(t)\right]^{\mathrm{T}} \in \mathbb{R}^{(N_{\mathrm{L}}\times N_{\mathrm{F}})l}$ be the vector associated with the graph $\mathcal{G}$, where $y_{\mathrm{L}}^{\mathrm{T}}(t) \triangleq [y_{\mathrm{L}1}^{\mathrm{T}}(t), \cdots, y_{\mathrm{L}N_{\mathrm{L}}}^{\mathrm{T}}(t)]^{\mathrm{T}} \in \mathbb{R}^{N_{\mathrm{L}}l}$ denotes the first N_{L} nodes representing the aggregated output vector of the leaders and $y_{\mathrm{f}}^{\mathrm{T}}(t) \triangleq [y_{\mathrm{f}1}^{\mathrm{T}}(t), \cdots, y_{\mathrm{f}N_{\mathrm{F}}}^{\mathrm{T}}(t)]^{\mathrm{T}} \in \mathbb{R}^{N_{\mathrm{F}}l}$ denotes the last N_{F} nodes representing the aggregated filtered output vector of the follower agents. Let in addition, $\tilde{y}_{\mathrm{s}}(t) \triangleq \left[y_{\mathrm{Ls}}^{\mathrm{T}}(t), y_{\mathrm{fs}}^{\mathrm{T}}(t)\right]^{\mathrm{T}} \in \mathbb{R}^{(N_{\mathrm{L}}\times N_{\mathrm{F}})l}$ be the vector associated with the graph $\mathcal{G}$, where $y_{\mathrm{Ls}}(t)$ and $y_{\mathrm{fs}}(t)$ denote the event-triggered version of $y_{\mathrm{L}}(t)$ and $y_{\mathrm{f}}(t)$, respectively. For each agent $i, i = 1, \cdots, N_{\mathrm{F}}$, consider the local cooperative controller receiving the even-triggered relative output measurements of the neighboring agents in terms of $y_{\mathrm{fs}i}(t), i = 1, \cdots, N_{\mathrm{F}}$, and $y_{\mathrm{Ls}i}(t), i = 1, \cdots, N_{\mathrm{L}}$ as [18, 14, 15]

$$u_{\mathrm{c}i}(t) = K_c\Big[-\sum_{i\sim j}\Big(\tilde{y}_i(t) - \tilde{y}_{\mathrm{s}j}(t)\Big) + \theta_i(t)\Big], \tag{23}$$

$$\dot{\theta}_i(t) = \delta\Big[-\sum_{i\sim j} \Big(\tilde{y}_i(t) - \tilde{y}_{\mathrm{s}j}(t)\Big) - \zeta\left(\theta_i(t) - \nu_i(t)\right)\Big], \quad \theta_i(0) = \theta_{i0}, \tag{24}$$

$$\dot{\nu}_i(t) = \eta\left(\theta_i(t) - \nu_i(t)\right), \quad \nu_i(0) = \nu_{i0}, \tag{25}$$

where $K_c \in \mathbb{R}^{m\times l}$ is a gain matrix, $\theta_i(t) \in \mathbb{R}^l$ is the integrator state, $\nu_i(t) \in \mathbb{R}^l$ is the filter state, $\delta \in \mathbb{R}_+$ is the integrator gain, $\zeta \in \mathbb{R}_+$ is the modification gain, and $\eta \in \mathbb{R}_+$ is the filter gain. Next, applying the local cooperative controller (27), (28), and (29) to the follower agent dynamics given by (22) yields

$$\dot{x}_{\mathrm{f}i}(t) = A_{\mathrm{fr}}x_{\mathrm{f}i}(t) - B_{\mathrm{f}}K_c\sum_{i\sim j}\Big(\tilde{y}_i(t) - \tilde{y}_{\mathrm{s}j}(t)\Big) + B_{\mathrm{f}}K_c\theta_i(t). \tag{26}$$

Letting $x_{\mathrm{f}}(t) \triangleq [x_{\mathrm{f}1}^{\mathrm{T}}(t),\cdots,x_{\mathrm{f}N_{\mathrm{F}}}^{\mathrm{T}}(t)]^{\mathrm{T}} \in \mathbb{R}^{N_{\mathrm{F}}n_{\mathrm{f}}}$, $\theta(t) \triangleq [\theta_1^{\mathrm{T}}(t),\cdots,\theta_{N_{\mathrm{F}}}^{\mathrm{T}}(t)]^{\mathrm{T}} \in \mathbb{R}^{N_{\mathrm{F}}l}$, and $\nu(t) \triangleq [\nu_1^{\mathrm{T}}(t),\cdots,\nu_{N_{\mathrm{F}}}^{\mathrm{T}}(t)]^{\mathrm{T}} \in \mathbb{R}^{N_{\mathrm{F}}l}$, and $y_{\mathrm{f}i}(t) = C_o x_{\mathrm{f}i}(t)$ where $C_o \triangleq [I_l,\cdots,0] \in \mathbb{R}^{l\times n_{\mathrm{f}}}$, the follower agent dynamics (22) subject to the local cooperative controller (23), (24), and (25) can be written at the multiagent system level as

$$\begin{aligned}
\dot{x}_{\mathrm{f}}(t) &= (I_{N_{\mathrm{F}}}\otimes A_{\mathrm{fr}})x_{\mathrm{f}}(t) - (F_{\mathrm{p}}(\mathcal{G})\otimes B_{\mathrm{f}}K_c)y_{\mathrm{f}}(t) - (F_{\mathrm{s}}(\mathcal{G})\otimes B_{\mathrm{f}}K_c)y_{\mathrm{fs}}(t)\\
&\quad - (G_{\mathrm{s}}(\mathcal{G})\otimes B_{\mathrm{f}}K_c)y_{\mathrm{Ls}}(t) + (I_{N_{\mathrm{F}}}\otimes B_{\mathrm{f}}K_c)\theta(t)\\
&= [I_{N_{\mathrm{F}}}\otimes A_{\mathrm{fr}} - F(\mathcal{G})\otimes B_{\mathrm{f}}K_cC_o]x_{\mathrm{f}}(t) - (G(\mathcal{G})\otimes B_{\mathrm{f}}K_c)y_{\mathrm{L}}(t) + (I_{N_{\mathrm{F}}}\otimes B_{\mathrm{f}}K_c)\theta(t)\\
&\quad - (G(\mathcal{G})\otimes B_{\mathrm{f}}K_c)y_{\mathrm{Le}}(t) - (F_{\mathrm{s}}(\mathcal{G})\otimes B_{\mathrm{f}}K_c)y_{\mathrm{fe}}(t), \quad x_{\mathrm{f}}(0) = x_{\mathrm{f}0},
\end{aligned} \tag{27}$$

$$\begin{aligned}
\dot{\theta}(t) &= -\delta(F_{\mathrm{p}}(\mathcal{G})\otimes I_l)y_{\mathrm{f}}(t) - \delta(F_{\mathrm{s}}(\mathcal{G})\otimes I_l)y_{\mathrm{fs}}(t) - \delta(G_{\mathrm{s}}(\mathcal{G})\otimes I_l)y_{\mathrm{Ls}}(t)\\
&\quad - \delta\zeta\left(\theta(t) - \nu(t)\right)\\
&= -\delta\left(F(\mathcal{G})\otimes C_o\right)x_{\mathrm{f}}(t) - \delta(G(\mathcal{G})\otimes I_l)y_{\mathrm{L}}(t) - \delta\zeta\left(\theta(t) - \nu(t)\right)\\
&\quad - \delta(F_{\mathrm{s}}(\mathcal{G})\otimes I_l)y_{\mathrm{fe}}(t) - \delta(G(\mathcal{G})\otimes I_l)y_{\mathrm{Le}}(t), \quad \theta(0) = \theta_0,
\end{aligned} \tag{28}$$

$$\dot{\nu}(t) = \eta\left(\theta(t) - \nu(t)\right), \quad \nu(0) = \nu_0. \tag{29}$$

This can further be written compactly as

$$\dot{\xi}(t) = \mathcal{A}(\mathcal{G})\xi(t) + \mathcal{B}(\mathcal{G})y_{\mathrm{L}}(t) + \mathcal{D}_1(\mathcal{G})y_{\mathrm{Le}}(t) + \mathcal{D}_2(\mathcal{G})y_{\mathrm{fe}}(t), \quad \xi(0) = \xi_0. \tag{30}$$

where $\xi \triangleq [x_{\mathrm{f}}^{\mathrm{T}}(t),\ \theta^{\mathrm{T}}(t),\ \nu^{\mathrm{T}}(t)]^{\mathrm{T}} \in \mathbb{R}^{n_\xi}$, $n_\xi \triangleq N_{\mathrm{F}}(n_{\mathrm{f}} + 2l)$, $A_\xi(\mathcal{G}) \triangleq I_{N_{\mathrm{F}}} \otimes A_{\mathrm{fr}} - F(\mathcal{G}) \otimes B_{\mathrm{f}}K_cC_o \in \mathbb{R}^{N_{\mathrm{F}}n_{\mathrm{f}} \times N_{\mathrm{F}}n_{\mathrm{f}}}$, $y_{\mathrm{Le}}(t) \triangleq y_{\mathrm{Ls}}(t) - y_{\mathrm{L}}(t) \in \mathbb{R}^{N_{\mathrm{L}}l}$, $y_{\mathrm{fe}}(t) \triangleq y_{\mathrm{fs}}(t) - y_{\mathrm{f}}(t) \in \mathbb{R}^{N_{\mathrm{F}}l}$ and

$$\mathcal{A}(\mathcal{G}) = \begin{bmatrix} A_\xi(\mathcal{G}) & I_{N_{\mathrm{F}}} \otimes B_{\mathrm{f}}K_c & 0 \\ -\delta\,(F(\mathcal{G}) \otimes C_o) & -\delta\zeta I_{N_{\mathrm{F}}l} & \delta\zeta I_{N_{\mathrm{F}}l} \\ 0 & \eta I_{N_{\mathrm{F}}l} & -\eta I_{N_{\mathrm{F}}l} \end{bmatrix} \in \mathbb{R}^{n_\xi \times n_\xi}, \tag{31}$$

$$\mathcal{B}(\mathcal{G}) = \begin{bmatrix} -G(\mathcal{G}) \otimes B_{\mathrm{f}}K_c \\ -\delta(G(\mathcal{G}) \otimes I_l) \\ 0 \end{bmatrix} \in \mathbb{R}^{n_\xi \times N_{\mathrm{F}}l}, \tag{32}$$

$$\mathcal{D}_1(\mathcal{G}) = \begin{bmatrix} -G(\mathcal{G}) \otimes B_{\mathrm{f}}K_c \\ -\delta(G(\mathcal{G}) \otimes I_l) \\ 0 \end{bmatrix} \in \mathbb{R}^{n_\xi \times N_{\mathrm{F}}l}, \tag{33}$$

$$\mathcal{D}_2(\mathcal{G}) = \begin{bmatrix} -F_{\mathrm{s}}(\mathcal{G}) \otimes B_{\mathrm{f}}K_c \\ -\delta(F_{\mathrm{s}}(\mathcal{G}) \otimes I_l) \\ 0 \end{bmatrix} \in \mathbb{R}^{n_\xi \times N_{\mathrm{F}}l}, \tag{34}$$

where (33) and (34) are additional terms due to event-triggering of the exchanged information resulting from the communication among the agents.

As mentioned before, that the objective of the proposed observer-free agent-level controller given in this section is to stabilize the follower agent dynamics. In addition, the objective of the local cooperative controller given in this subsection based on [18, 14, 15] is to solve the containment problem. For this purpose, we first need to ensure that the solution $\xi(t)$ to (30) is $\mathcal{L}_\infty$ stable [21], that is for every bounded $y_{\mathrm{L}}(t)$, $y_{\mathrm{Le}}(t)$, and $y_{\mathrm{fe}}(t)$, $\xi(t)$ is bounded. So, we know that $y_{\mathrm{L}}(t)$, $y_{\mathrm{Le}}(t)$, and $y_{\mathrm{fe}}(t)$ are bounded, since every $A_{\mathrm{L}i}, i =$

$1, \cdots, N_{\mathrm{L}}$, are Hurwitz. Therefore, in order to conclude that (30) is $\mathcal{L}_\infty$ stable, $\mathcal{A}(\mathcal{G})$ needs to be Hurwitz. A necessary and sufficient condition satisfying this requirement is given in the following remark.

Remark 3 *Similar to the results in [22, 23, 18], let $\mu_i \in spec(F(\mathcal{G})), i = 1, \cdots, N_F$. If*

$$\mathcal{U}_{\mathcal{A}(\mathcal{G})i} = \begin{bmatrix} A_{fr} - \mu_i B_f K_c C_o & B_f K_c & 0 \\ -\mu_i \delta C_o & -\delta\zeta I_l & \delta\zeta I_l \\ 0 & \eta I_l & -\eta I_l \end{bmatrix} \in \mathbb{R}^{(n_f+2l)\times(n_f+2l)}, \tag{35}$$

is Hurwitz for $i = 1, \cdots, N_F$, then $\mathcal{A}(\mathcal{G})$ in (31) is Hurwitz. This shows that (35) can be made Hurwitz for $i = 1, \cdots, N_L$ by arbitrarily choosing the design parameters K_c, δ, ζ, and η. This further implies that the system (30) with the leader dynamical given by (18) and (19) is $\mathcal{L}_\infty$ stable (e.g., see Corollary 6.1 of [18]).

5. USER-DEFINED EVENT-TRIGGERING RULES

Let $\epsilon_{yi} \in \mathbb{R}_+$ be a given, user-defined sensing threshold to allow for output data transmission from the ith follower agent system, $i = 1, \cdots, N_{\mathrm{F}}$, to the neighboring follower agent systems. In addition, let $\epsilon_{y_{\mathrm{L}i}} \in \mathbb{R}_+$ be a given, user-defined sensing threshold to allow for output data transmission from the ith leader system, $i = 1, \cdots, N_{\mathrm{L}}$, to the neighboring follower agent systems. We then define the logic rules for scheduling the data exchange:

$$E_{1i} : \|y_{\mathrm{fs}i}(t) - y_{\mathrm{fi}}(t)\| \leq \epsilon_{yi}, \tag{36}$$

$$E_{2i} : \|y_{\mathrm{Ls}i}(t) - y_{\mathrm{L}i}(t)\| \leq \epsilon_{y_{\mathrm{L}}i}. \tag{37}$$

Specifically, when the inequality in Equation (36) is violated at the $s_{k_i} \in \mathbb{R}_+$ moment of the k_i-th time instant, the follower agent system triggers the filtered measured output signal information, such that $y_{\mathrm{fs}i}(t)$ is sent to the neighboring agent systems along the monotonic sequence $\{s_{k_i}\}_{k_i=1}^{\infty}$. Likewise, when Equation (37) is violated, then the leader system sends

the measured output signal information $y_{\mathrm{L}si}(t)$ to the neighboring agent systems at the $r_{q_i} \in \mathbb{R}_+$ moment of the q_i-th time instant along the monotonic sequence $\left\{r_{q_i}\right\}_{q_i=1}^{\infty}$. Each ith leader agent, $i = 1, \cdots, N_{\mathrm{L}}$ and ith follower agent, $i = 1, \cdots, N_{\mathrm{F}}$ output signal is held by zero-order-hold operator (ZOH) until the next triggering event for the corresponding signal take place. In addition, each ith follower agent ,$i = 1, \cdots, N_{\mathrm{F}}$, receives the event-triggered relative output measurement form its neighboring agent and stores it by a ZOH and update this value whenever it receives a new triggered relative output measurement form that neighboring agent. Furthermore, each agent event-triggers its own output signal asynchronously to the neighbor agents.

Now, consider the agent system given by (22), and compact form of multivechile system subject to the local cooperative control given by (30). Letting the transmission of the follower agent system filtered output to the neighboring agent systems occur when $\bar{E}_{1i}$ is true and letting the transmission of the leader system measured output signal to the neighboring follower agent systems occur when $\bar{E}_{2i}$ is true.

6. SYSTEM-THEORETIC ANALYSIS

In this section, we show the performance of the follower agents' outputs to converge to the leader output. In the analysis, we show that the proposed control architecture solves the containment problem with the presence of event-triggering mechanism. For this purpose, we first let $A_{\mathrm{L}} \triangleq \text{block-diag}(A_{\mathrm{L}1}, \cdots, A_{\mathrm{L}N_{\mathrm{L}}}) \in \mathbb{R}^{n_{\mathrm{L}} \times n_{\mathrm{L}}}$, $B_{\mathrm{L}} \triangleq \text{block-diag}(B_{\mathrm{L}1}, \cdots, B_{\mathrm{L}N_{\mathrm{L}}}) \in \mathbb{R}^{n_{\mathrm{L}} \times m_{\mathrm{L}}}$, $C_{\mathrm{L}} \triangleq \text{block-diag}(C_{\mathrm{L}1}^{\mathrm{T}}, \cdots, C_{\mathrm{L}N_{\mathrm{L}}}^{\mathrm{T}})^{\mathrm{T}} \in \mathbb{R}^{N_{\mathrm{L}}l \times n_{\mathrm{L}}}$, and $c(t) \triangleq [c_1^{\mathrm{T}}(t), \cdots, c_{N_{\mathrm{L}}}^{\mathrm{T}}(t)]^{\mathrm{T}} \in \mathbb{R}^{m_{\mathrm{L}}}$, with $\|c(t)\| \leq c^*$, where $n_{\mathrm{L}} = \sum_{i=1}^{N_{\mathrm{L}}} n_i$, and $m_{\mathrm{L}} = \sum_{i=1}^{N_{\mathrm{L}}} m_i$. In order to analyze the effect of event-triggering of communication among the agents on the closed loop system and controller performance, we consider the dynamical system given by

$$\dot{\bar{\xi}}(t) = \mathcal{A}(\mathcal{G})\bar{\xi}(t) + \mathcal{B}(\mathcal{G})y_{\mathrm{L}}(t), \quad \bar{\xi}(0) = \xi_0, \tag{38}$$

has solution partitioned as $\bar{\xi} \triangleq [\bar{x}_{\mathrm{f}}^{\mathrm{T}}(t),\ \bar{\theta}^{\mathrm{T}}(t),\ \bar{v}^{\mathrm{T}}(t)]^{\mathrm{T}} \in \mathbb{R}^{n_\xi}$, where $\bar{x}_{\mathrm{f}}(t) \in \mathbb{R}^{N_{\mathrm{F}} n_{\mathrm{f}}}$ with $\bar{y}_{\mathrm{f}}(t) = (I_{N_{\mathrm{F}}} \otimes C_o)\bar{x}_{\mathrm{f}}(t)$, $\bar{\theta}(t) \in \mathbb{R}^{N_{\mathrm{F}} l}$, and $\bar{v}(t) \in \mathbb{R}^{N_{\mathrm{F}} l}$.

Note that each ith, $i = 1, \cdots, N_{\mathrm{F}}$, follower agent communicates with its own controller in periodic sampling instances. In addition, the received event-triggered output measurements from the neighboring agents only affect on the cooperative controller scheme performance. Since we utilize ZOH operator to hold the event-triggered outputs form the other neighboring agents that considered as inputs to the cooperative controller, we utilize standard Lyapunov analysis to analyze the performance of overall multiagent systems [11, 24].

Theorem 2 *Consider the follower agent dynamics given compactly by (30) with (31) being Hurwitz and the leader dynamics given by (18) and (19) for $i = 1, \cdots, N_L$, where the reference command is time varying with bounded time rate of change. Furthermore, let the data transmission from the ith follower systems to the neighboring follower agent systems occur when $\bar{E}_{1i}, i = 1, \cdots, N_F$, is true and let the data transmission from the ith leader agent system to the neighboring follower agent systems occur when $\bar{E}_{2i}$, $i = 1, \cdots, N_L$, is true. Then, $y_f(t)$ converge to the neighborhood of the convex hull formed by $(M(\mathcal{G}) \otimes I_l)y_L(t)$ as $t \to \infty$. If, in addition, $N_L = 1$, then $y_f(t)$ converge to the neighborhood of $\mathbf{1}_{N_F} \otimes y_{L1}(t)$ as $t \to \infty$; that is $y_{fi}(t), i = 1, \cdots, N_F$, converge to the neighborhood of the output of the leader.*

Proof. In order to analyses the convergence performance, we consider the augmented state vector given by $\mathcal{Z}(t) \triangleq [x_{\mathrm{L}}^{\mathrm{T}}(t), \xi^{\mathrm{T}}(t)]^{\mathrm{T}} \in \mathbb{R}^{n_{\mathrm{L}}+n_\xi}$, (18) and (30) can be written in a compact form as

$$\dot{\mathcal{Z}}(t) = \mathcal{A}_z(\mathcal{G})\mathcal{Z}(t) + \mathcal{B}_z C(t), \quad \mathcal{Z}(0) = \mathcal{Z}_0, \quad t \geq 0 \tag{39}$$

where

$$\mathcal{A}_z(\mathcal{G}) = \begin{bmatrix} A_{\mathrm{L}} & 0 \\ B(\mathcal{G})C_{\mathrm{L}} & A(\mathcal{G}) \end{bmatrix} \in \mathbb{R}^{(n_{\mathrm{L}}+n_\xi)\times(n_{\mathrm{L}}+n_\xi)}, \tag{40}$$

$$\mathcal{B}_z = \begin{bmatrix} B_{\mathrm{L}} & 0 & 0 \\ 0 & \mathcal{D}_1 & \mathcal{D}_2 \end{bmatrix} \in \mathbb{R}^{(n_{\mathrm{L}}+n_\xi)\times(m_{\mathrm{L}}+2N_{\mathrm{F}}l)}, \tag{41}$$

and $C(t) \triangleq [c^{\mathrm{T}}(t), y_{\mathrm{Le}}^{\mathrm{T}}(t), y_{\mathrm{fe}}^{\mathrm{T}}(t)]^{\mathrm{T}} \in \mathbb{R}^{m_{\mathrm{L}}+2N_{\mathrm{F}}l}$. Since $\mathcal{A}(\mathcal{G})$ is Hurwitz as shown in Remark 4 and A_{L} is Hurwitz, it follows from the upper triangle structure of (40) that $\mathcal{A}_z(\mathcal{G})$ is Hurwitz, and hence, there exists a unique $P_z \in \mathbb{R}_+^{(n_{\mathrm{L}}+n_\xi)\times(n_{\mathrm{L}}+n_\xi)} \cap \mathbb{S}_+^{(n_{\mathrm{L}}+n_\xi)\times(n_{\mathrm{L}}+n_\xi)}$ such that

$$0 = \mathcal{A}(\mathcal{G})_z^{\mathrm{T}}\mathcal{P}_z + \mathcal{P}_z\mathcal{A}_z(\mathcal{G}) + \mathcal{R}_z, \tag{42}$$

holds for $\mathcal{R}_z \in \mathbb{R}_+^{(n_{\mathrm{L}}+n_\xi)\times(n_{\mathrm{L}}+n_\xi)} \cap \mathbb{S}_+^{(n_{\mathrm{L}}+n_\xi)\times(n_{\mathrm{L}}+n_\xi)}$. To show the effect of leader reference command on the convergence performance with isolation of event triggering effect, consider the augmented state vector given by $\bar{\mathcal{Z}}(t) \in \mathbb{R}^{n_{\mathrm{L}}+n_\xi}$, (18) and (38) can be written in a compact form as

$$\dot{\bar{\mathcal{Z}}}(t) = \mathcal{A}_z(\mathcal{G})\bar{\mathcal{Z}}(t) + \mathcal{B}_z\bar{C}(t), \quad \bar{\mathcal{Z}}(0) = \bar{\mathcal{Z}}_0, \quad t \geq 0 \tag{43}$$

where $\bar{C}(t) \triangleq [c^{\mathrm{T}}(t), 0, 0]^{\mathrm{T}} \in \mathbb{R}^{m_{\mathrm{L}}+2N_{\mathrm{F}}l}$. Consider in addition

$$\dot{\tilde{\mathcal{Z}}}(t) = \mathcal{A}_z(\mathcal{G})\tilde{\mathcal{Z}}(t) + \mathcal{B}_z\tilde{C}(t), \quad \tilde{\mathcal{Z}}(0) = \tilde{\mathcal{Z}}_0, \quad t \geq 0 \tag{44}$$

where $\tilde{\mathcal{Z}}(t) = \mathcal{Z}(t) - \bar{\mathcal{Z}}(t)$, and $\tilde{C}(t) \triangleq [0, y_{\mathrm{Le}}^{\mathrm{T}}(t), y_{\mathrm{fe}}^{\mathrm{T}}(t)]^{\mathrm{T}} \in \mathbb{R}^{m_{\mathrm{L}}+2N_{\mathrm{F}}l}$.

Next, similar to the proposed analysis in [25, 14], consider

$$\mathcal{H}(t) \triangleq \bar{\mathcal{Z}}(t) + \mathcal{A}_z(\mathcal{G})^{-1}\mathcal{B}_z\bar{C}(t), \tag{45}$$

where $\mathcal{A}_z(\mathcal{G})$ is invertible since it is Hurwitz. In addition, consider the Lyapunov function candidate given by

$$\mathcal{V}_1(\mathcal{H}(t)) = \mathcal{H}^{\mathrm{T}}(t)\mathcal{P}_z\mathcal{H}(t), \tag{46}$$

where $\mathcal{V}_1(0) = 0$, $\mathcal{V}_1(\mathcal{H}(t)) > 0$ for all $\mathcal{H}(t) \neq 0$, and $\mathcal{V}_1(\mathcal{H}(t))$ is radially unbounded. The time derivative of (46) along the trajectory of (43) and (45) is given by

$$\begin{aligned}\dot{\mathcal{V}}_1(\mathcal{H}(t)) = \;& 2\mathcal{H}^{\mathrm{T}}(t)\mathcal{P}_z\left(\dot{\bar{\mathcal{Z}}}(t) + \mathcal{A}_z(\mathcal{G})^{-1}\mathcal{B}_z\dot{\bar{C}}(t)\right)\\ =\;& -\mathcal{H}^{\mathrm{T}}(t)\mathcal{R}_z\mathcal{H}(t) + 2\mathcal{H}^{\mathrm{T}}(t)\mathcal{P}_z\mathcal{A}_z(\mathcal{G})^{-1}\mathcal{B}_z\dot{\bar{C}}(t).\end{aligned} \tag{47}$$

In the reminder of the proof, we consider two cases.

Case 1: For $\dot{c}(t) = 0$, it follows from (47) that $\lim_{t\to\infty}\mathcal{H}(t) = 0$. Next, similar to [18, 14, 15], since this limit implies $\dot{\bar{\mathcal{Z}}}(t) \to 0$ as $t \to \infty$, (43) can be written as

$$\mathcal{A}_z(\mathcal{G})\bar{\mathcal{Z}}(\infty) + \mathcal{B}_z\bar{C}(\infty) = 0, \tag{48}$$

where $\bar{\mathcal{Z}}(\infty) = \lim_{t\to\infty}\bar{\mathcal{Z}}(t)$ and $\bar{C}(\infty) = \lim_{t\to\infty}\bar{C}(t)$. In addition, letting $x_{\mathrm{L}}(\infty) = \lim_{t\to\infty}x_{\mathrm{L}}(t)$, $\bar{x}_{\mathrm{f}}(\infty) = \lim_{t\to\infty}\bar{x}_{\mathrm{f}}(t)$, $\bar{\theta}(\infty) = \lim_{t\to\infty}\bar{\theta}(t)$, $\bar{\nu}(\infty) = \lim_{t\to\infty}\bar{\nu}(t)$, and using the definition of $\mathcal{A}_z(\mathcal{G})$ and $\mathcal{B}_z$ given by (40) and (41), respectively, in (48) we have

$$0 = A_{\mathrm{L}}x_{\mathrm{L}}(\infty) + B_{\mathrm{L}}c(\infty), \tag{49}$$

$$\begin{aligned}0 =\;& [I_{N_{\mathrm{F}}}\otimes A_{\mathrm{fr}} - F(\mathcal{G})\otimes B_{\mathrm{f}}K_cC_o]\bar{x}_{\mathrm{f}}(\infty) - (G(\mathcal{G})\otimes B_{\mathrm{f}}K_c)y_{\mathrm{L}}(\infty)\\ &+ (I_{N_{\mathrm{F}}}\otimes B_{\mathrm{f}}K_c)\bar{\theta}(\infty),\end{aligned} \tag{50}$$

$$0 = -\delta(F(\mathcal{G})\otimes C_o)\bar{x}_{\mathrm{f}}(\infty) - \delta(G(\mathcal{G})\otimes I_l)y_{\mathrm{L}}(\infty) - \delta\zeta\left(\bar{\theta}(\infty) - \bar{\nu}(\infty)\right), \tag{51}$$

$$0 = \eta\left(\bar{\theta}(\infty) - \bar{\nu}(\infty)\right). \tag{52}$$

Since, $\bar{\theta}(\infty) = \bar{\nu}(\infty)$ in (52), (51) implies

$$\bar{y}_{\mathrm{f}}(\infty) = -(F(\mathcal{G})^{-1}G(\mathcal{G}) \otimes I_l)y_{\mathrm{L}}(\infty), \tag{53}$$

and hence, $\bar{y}_{\mathrm{f}i}(t)$, $i = 1, \cdots, N_{\mathrm{F}}$, asymptotically converge to the convex hull formed by the leaders. In addition, if $N_{\mathrm{L}} = 1$, then $-F(\mathcal{G})^{-1}G(\mathcal{G}) = \mathbf{1}_{N_{\mathrm{F}}}$ and as a direct consequence of (53) we have

$$\begin{aligned}\bar{y}_{\mathrm{f}}(\infty) &= (\mathbf{1}_{N_{\mathrm{F}}} \otimes I_l)y_{\mathrm{L}1}(\infty)\\ &= \mathbf{1}_{N_{\mathrm{F}}} \otimes y_{\mathrm{L}1}(\infty),\end{aligned} \tag{54}$$

and hence, $\bar{y}_{\mathrm{f}i}(t)$, $i = 1, \cdots, N_{\mathrm{F}}$, asymptotically converge to the output of the leader.

Case 2: We now consider $\|\dot{c}(t)\| \leq \dot{c}^*$, where $\dot{c}^* > 0$. For this purpose, (47) can be rewritten as

$$\dot{\mathcal{V}}_1(\mathcal{H}(t)) \leq -\lambda_{\min}(\mathcal{R}_z)\|\mathcal{H}(t)\|\left(\|\mathcal{H}(t)\| - \frac{\Psi_1}{\lambda_{\min}(\mathcal{R}_z)}\right), \tag{55}$$

where $\Psi_1 \triangleq 2\|\mathcal{P}_z\mathcal{A}_z(\mathcal{G})^{-1}\mathcal{B}_z\|_{\mathrm{F}}\dot{c}^*$, with $\|\dot{c}(t)\| \leq \dot{c}^*$. It follows from (55) that $\dot{\mathcal{V}}_1(\mathcal{H}(t)) < 0$ outside the compact set $\Omega_1 \triangleq \left\{\mathcal{H}(t) : \mathcal{H}(t) < \frac{\Psi_1}{\lambda_{\min}(\mathcal{R}_z)}\right\}$, which proves uniform ultimate boundedness of the closed-loop solution $\bar{\mathcal{Z}}(t)+\mathcal{A}_z(\mathcal{G})^{-1}\mathcal{B}_z\bar{\mathcal{C}}(t)$ for all initial conditions[21]. Since $\dot{\mathcal{V}}_1(\mathcal{H}(t)) < 0$ outside the compact set Ω_1, then an ultimate bound for the distance of $\mathcal{H}(t) \triangleq \bar{\mathcal{Z}}(t) + \mathcal{A}_z(\mathcal{G})^{-1}\mathcal{B}_z\bar{\mathcal{C}}(t)$ can be computed as $\|\mathcal{H}(t)\| \leq \sqrt{\frac{\lambda_{\max}(\mathcal{P}_z)}{\lambda_{\min}(\mathcal{P}_z)}}\frac{\Psi_1}{\lambda_{\min}(\mathcal{R}_z)}$, $t \geq T$. Note that if the right side of last inequality is small, then the distance of $\bar{\mathcal{Z}}(t) + \mathcal{A}_z(\mathcal{G})^{-1}\mathcal{B}_z\bar{\mathcal{C}}(t)$ is small for $t \geq 0$, and this can be done by utilizing small bound of time rate of change for the reference command. Therefore, a small $\bar{\mathcal{Z}}(t)+\mathcal{A}_z(\mathcal{G})^{-1}\mathcal{B}_z\bar{\mathcal{C}}(t)$ implies $\bar{y}_{\mathrm{f}i}(t)$, $i = 1, \cdots, N_{\mathrm{F}}$ to stay at the neighborhood of the convex hull formed by those of the leaders.

Then, consider the Lyapunov function candidate given by

$$\mathcal{V}_2(\tilde{\mathcal{Z}}(t)) = \tilde{\mathcal{Z}}(t)^{\mathrm{T}}(t)\mathcal{P}_z\tilde{\mathcal{Z}}(t), \tag{56}$$

where $\mathcal{V}_2(0) = 0$, $\mathcal{V}_2(\tilde{\mathcal{Z}}(t)) > 0$ for all $\tilde{\mathcal{Z}}(t) \neq 0$, and $\mathcal{V}_2(\tilde{\mathcal{Z}}(t))$ is radially unbounded. The time derivative of (56) along the trajectory of (44) is given by

$$\begin{aligned}\dot{\mathcal{V}}_2(\tilde{\mathcal{Z}}(t)) &= 2\tilde{\mathcal{Z}}(t)^{\mathrm{T}}(t)\mathcal{P}_z\left(\mathcal{A}_z(\mathcal{G})\tilde{\mathcal{Z}}(t) + \mathcal{B}_z\tilde{C}(t)\right)\\ &= -\tilde{\mathcal{Z}}(t)^{\mathrm{T}}(t)\mathcal{R}_z\tilde{\mathcal{Z}}(t) + 2\tilde{\mathcal{Z}}(t)^{\mathrm{T}}(t)\mathcal{P}_z\mathcal{B}_z\tilde{C}(t)\\ &\leq -\lambda_{\min}(\mathcal{R}_z)\|\tilde{\mathcal{Z}}(t)\|\left(\|\tilde{\mathcal{Z}}(t)\| - \frac{\Psi_2}{\lambda_{\min}(\mathcal{R}_z)}\right), \end{aligned} \tag{57}$$

where $\Psi_2 \triangleq 2\|\mathcal{P}_z\mathcal{B}_z\|_{\mathrm{F}}\left(\epsilon_{y_{\mathrm{L}}} + \epsilon_y\right)$. It follows from (57) that $\dot{\mathcal{V}}_2(\tilde{\mathcal{Z}}(t)) < 0$ outside the compact set $\Omega_2 \triangleq \left\{\tilde{\mathcal{Z}}(t) : \tilde{\mathcal{Z}}(t) < \frac{\Psi_2}{\lambda_{\min}(\mathcal{R}_z)}\right\}$, which proves uniform ultimate boundedness of the closed-loop solution $\tilde{\mathcal{Z}}(t)$ for all initial conditions[21]. Since $\dot{\mathcal{V}}_2(\tilde{\mathcal{Z}}(t)) < 0$ outside the compact set Ω_2, then an ultimate bound for the distance of $\tilde{\mathcal{Z}}(t)$ can be computed as $\|\tilde{\mathcal{Z}}(t)\| \leq \sqrt{\frac{\lambda_{\max}(\mathcal{P}_z)}{\lambda_{\min}(\mathcal{P}_z)}}\frac{\Psi_2}{\lambda_{\min}(\mathcal{R}_z)}$, $t \geq T$. Note that the distance bound $\|\tilde{\mathcal{Z}}(t)\|$ can be small by reducing the event-triggering thresholds. So, if the triggering threshold values are small enough, then $\mathcal{Z}(t)$ stays close to $\bar{\mathcal{Z}}(t)$, and this implies that $y_{\mathrm{f}}(t)$ stays at the neighborhood of $\bar{y}_{\mathrm{f}}(t)$ with a distance governed by the $\|\tilde{\mathcal{Z}}(t)\|$.

Thereby, first, in case of $\dot{c}(t) = 0$, as a direct consequence of (53) and (57) we have $y_{\mathrm{f}}(t)$ converges to the convex hull formed by $(M(\mathcal{G}) \otimes I_l)y_{\mathrm{L}}(t)$ as $t \to \infty$ with uniformly ultimately bounded deviation governed by $\|\tilde{\mathcal{Z}}(t)\|$. Second, in the case of $\|\dot{c}(t)\| \leq \dot{c}^*$, as a direct consequence of (55) and (57) we have $y_{\mathrm{f}}(t)$ converges to the neighborhood of the convex hull formed by $(M(\mathcal{G}) \otimes I_l)y_{\mathrm{L}}(t)$ as $t \to \infty$ with uniformly ultimately bounded deviation governed by $\|\mathcal{H}(t)\| + \|\tilde{\mathcal{Z}}(t)\|$. Then, in both cases, that is $y_{\mathrm{f}i}(t), i = 1, \cdots, N_{\mathrm{F}}$, converge to the neighborhood of the convex hull formed by the leaders. For a single leader in addition, $y_{\mathrm{f}}(t)$ converge to the neighborhood of $\mathbf{1}_{N_{\mathrm{F}}} \otimes y_{\mathrm{L}1}(t)$ as $t \to \infty$; that is $y_{\mathrm{f}i}(t), i = 1, \cdots, N_{\mathrm{F}}$, converge to the neighborhood of the output of the leader. ■

7. ZENO ANALYSIS

In this section, we show that the proposed event triggered communication between the agents does not yield a Zeno behavior, which implies that it does not require a continuous information exchange and reduce wireless network utilization. We utilize the theoretical Zeno analysis similar in fashion to [26, 27, 28, 29].

Corollary 1 *Consider the follower agent dynamics given compactly by (30) with (31) being Hurwitz and the leader dynamics given by (18) and (19) for $i = 1, \cdots, N_L$, where the reference command is time varying with bounded time rate of change. In addition, let the data transmission from the ith follower systems to the neighboring follower agent systems occur when $\bar{E}_{1i}$, $i = 1, \cdots, N_F$, is true and let the data transmission from the ith leader agent system to the neighboring follower agent systems occur when $\bar{E}_{2i}$, $i = 1, \cdots, N_L$, is true. Then, there is exist positive scalar $\alpha_{1i} \triangleq \frac{\epsilon_{yi}}{\Phi_{1i}}$ and $\alpha_{2i} \triangleq \frac{\epsilon_{yLi}}{\Phi_{2i}}$ such that:*

$$s_{k_i+1} - s_{k_i} \geq \alpha_{1i}, \quad \forall k_i \in \mathbb{N}, \tag{58}$$

$$r_{q_i+1} - r_{q_i} \geq \alpha_{2i}, \quad \forall q_i \in \mathbb{N}, \tag{59}$$

Proof. The time derivative of $\|y_{\mathrm{fs}i}(t) - y_{\mathrm{f}i}(t)\|$ over $t \in (s_{k_i+1}, s_{k_i}), \forall k_i \in \mathbb{N}$ is given by:

$$\begin{aligned}
&\frac{d}{dt}\|y_{\mathrm{s}i}(t) - y_i(t)\| \\
&\quad \leq \|\dot{y}_{\mathrm{s}i}(t) - \dot{y}_i(t)\| = \|\dot{y}_i(t)\| \leq \|C_o\|_{\mathrm{F}}\|\dot{x}_{\mathrm{f}}(t)\| \\
&\quad \leq \|C_o\|_{\mathrm{F}}\|A_{\mathrm{fr}}\|_{\mathrm{F}}\|x_{\mathrm{f}}(t)\| + \|C_o\|_{\mathrm{F}}\|B_{\mathrm{fr}}\|_{\mathrm{F}}K_{\mathrm{c}}\sum_{i\sim j}\mu_{ij} + \|C_o\|_{\mathrm{F}}\|B_{\mathrm{fr}}\|_{\mathrm{F}}K_{\mathrm{c}}\|\theta_i(t)\|,
\end{aligned} \tag{60}$$

where

$$\mu_{ij} \triangleq \begin{cases} \|y_{\mathrm{f}i} - y_{\mathrm{Ls}j}\|, & \text{if } j\text{th neighbore is a leader,} \\ \|y_{\mathrm{f}i} - y_{\mathrm{fs}j}\|, & \text{if } j\text{th neighbore is a follower.} \end{cases} \tag{61}$$

Since the closed-loop dynamical system is uniformly ultimately bounded by Theorem 2, there exists an upper bound to the equation (C.1). Letting Φ_{1i} denote this upper bound and with initial condition satisfying $\lim_{t\to s_{k_i}^+} \|y_{\mathrm{fs}i}(t) - y_{\mathrm{f}i}(t)\| = 0$, it follows from Equation (C.1) that $\|y_{\mathrm{fs}i}(t) - y_{\mathrm{f}i}(t)\| \leq \Phi_{1i}(t - s_{k_i}), \quad \forall t \in (s_{k_i}, s_{k_i+1})$. Therefore, when $\overline{E}_{1i}$ is true, then $\lim_{t\to s_{k_i+1}^-} \|y_{\mathrm{fs}i}(t) - y_{\mathrm{f}i}(t)\| = \epsilon_{yi}$, and it then follows that $s_{k_i+1} - s_{k_i} \geq \alpha_{1i}$.

Proof of (59) follows similarly from the above analysis, and hence, is omitted due to page limit restrictions. ■

8. ILLUSTRATIVE NUMERICAL EXAMPLES

In this section, we present two numerical examples to demonstrate the efficacy of the proposed output feedback control architecture for multiagent systems with event-triggered exchanged information between each connected agents. For this purpose, we consider a graph of leader and follower agents as shown in Figure 1. For the follower agent dynamics we consider system matrices given by

$$A = \begin{bmatrix} 0 & 1 \\ 1 & 1 \end{bmatrix}, \quad B = \begin{bmatrix} 0 \\ 1 \end{bmatrix}, \quad C = \begin{bmatrix} 1 & 0 \end{bmatrix}. \tag{62}$$

In addition, for the leader agent dynamics we consider $A_{\mathrm{L}} = -0.5$, $B_{\mathrm{L}} = 0.5$, $C_{\mathrm{L}} = 1$. We let $\lambda = 0.8$, and desired follower agent system eigenvalues $\lambda(A_{\mathrm{fr}}) = [\, -1.2500 + i2.1651,\ -1.2500 - i2.1651,\ -0.9, -0.7]$ to create the nominal feedback gain $k = [\, 32.68,\ 52.58,\ 25.53,\ 5.47]$ and choose $K_{\mathrm{c}} = 1.5$, $\zeta = 1.5$, $\eta = 2$, $\delta = 5$ for the cooperative control design. In addition, consider event triggering thresholds $\epsilon_{y_L} = 0.1$ and $\epsilon_y = 0.1$.

Throughout the simulation, for each example, we consider two types of reference command for the leader system, constant and time varying reference commands.

Example 1. For the first example, we consider a graph with four follower agents and a single leader as shown in Figure 1a, and our aim is to track a given reference command $c_1(t)$, $t \geq 0$, with the initial conditions $x_{\mathrm{L}01} = 0$, and $y_0 = [0\ ,\ 0.2\ ,\ 0.1\ ,\ -0.2]^{\mathrm{T}}$.

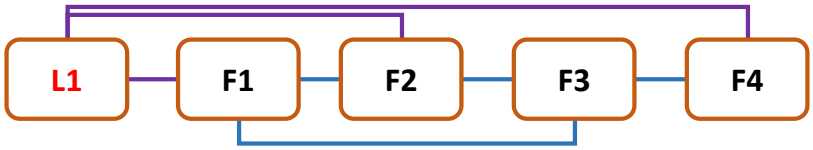

(a) Example 1.

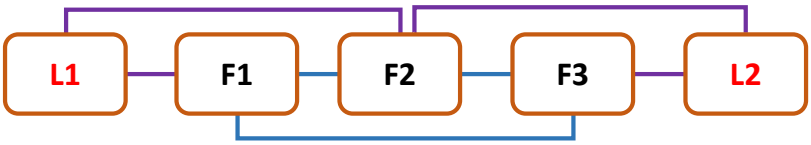

(b) Example 2.

Figure 1. System connection graph.

First we use a unit step reference command as shown in Figure 2, and then we then apply a time varying reference command given by $c_1(t) = 2.5\sin(0.06t)$ as shown in Figure 3. The proposed controller with event-triggering drives the multiagent system output to the desired reference command with bounded deviation. Figure 4 shows a significant reduction in the number of samples throughout the response time due to utilizing the event-triggering mechanism.

Example 2. For the second example, we consider three follower agents and two leaders, as shown in Figure 1b, with different reference commands with the initial conditions $x_{L0} = [0.1\ ,\ -0.1]$, and $y_0 = [0\ ,\ 0.2\ ,\ -0.2]^{\mathrm{T}}$. In this case, the leaders create a convex hull for the followers to (approximately) converge to. First, for a constant reference command, we consider $c(t) = [5\ ,\ 4]^{\mathrm{T}}$ as shown in Figure 5. In Figure 6, we use the time varying commands given by $c_i(t) = 5 * ((-1)^{i+1}0.8 + (-1)^{i+1}0.5\sin((0.06 * i)t))$, $i = 1,2$. In both cases, follower agents converge to the convex hull of leader outputs. Figure 7 shows a significant reduction in the number of samples throughout the response time with each different type reference command due to utilizing the event-triggering mechanism.

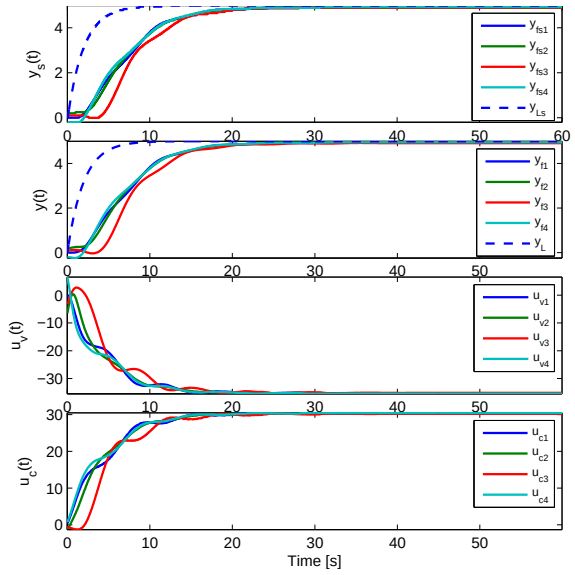

Figure 2. Responses of $y_{\mathrm{f}}(t)$, $y_{\mathrm{L}}(t)$, $y_{\mathrm{fs}}(t)$, $y_{\mathrm{Ls}}(t)$, $u_{\mathrm{v}}(t)$, and $u_{\mathrm{c}}(t)$ for the multiagent system with one leader following a constant command.

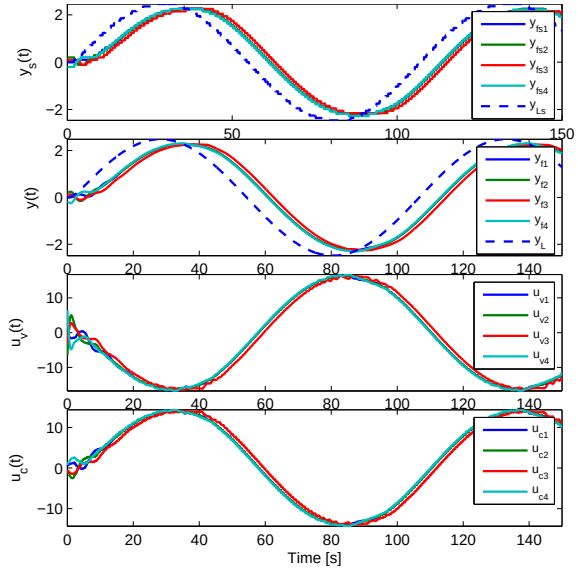

Figure 3. Responses of $y_{\mathrm{f}}(t)$, $y_{\mathrm{L}}(t)$, $y_{\mathrm{fs}}(t)$, $y_{\mathrm{Ls}}(t)$, $u_{\mathrm{v}}(t)$, and $u_{\mathrm{c}}(t)$ for the multiagent system with one leader following a time varying command.

9. CONCLUSIONS

A new event-triggered observer-free output feedback cooperative control architecture was presented for continuous-time, minimum phase, and high-order multiagent systems in the presence of data exchange between the agents. In particular, a nonminimal

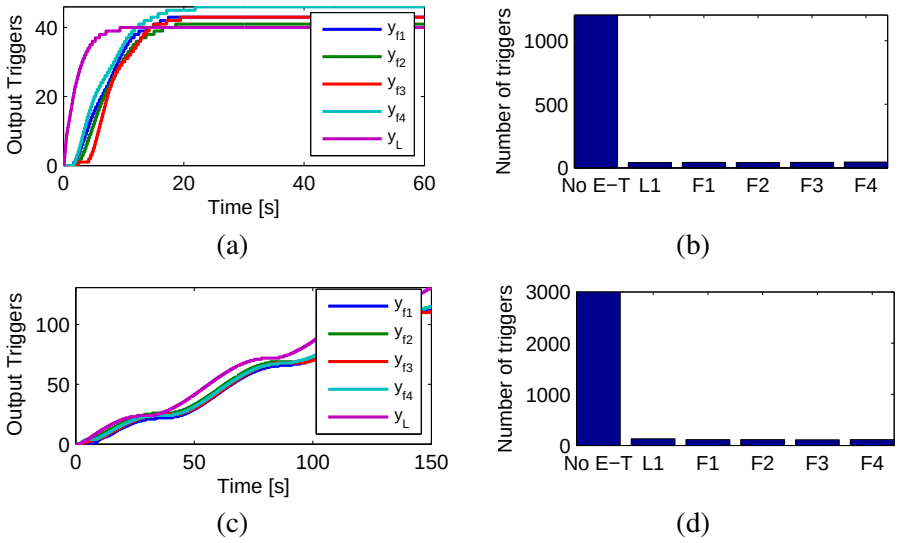

Figure 4. Single leader case; a) Output triggers for constant command; b) Triggers comparison for constant command; c) Output triggers for time varying command; d) Triggers comparison for time varying command.

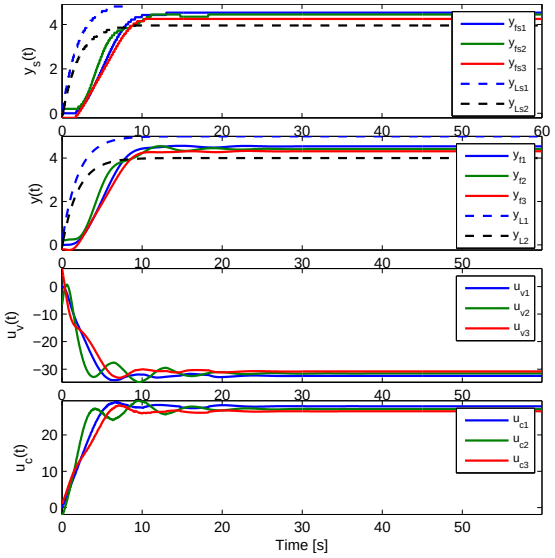

Figure 5. Responses of $y_{\mathrm{f}}(t)$, $y_{\mathrm{L}}(t)$, $y_{\mathrm{fs}}(t)$, $y_{\mathrm{Ls}}(t)$, $u_{\mathrm{v}}(t)$, and $u_{\mathrm{c}}(t)$ for the multiagent system with two leaders creating a constant convex hull.

state-space realization method was utilized to generate an expanded set of states for each agent, where these nonminimal states were then utilized to design a cooperative control architecture to address the containment problem and event-triggering mechanism was utilized

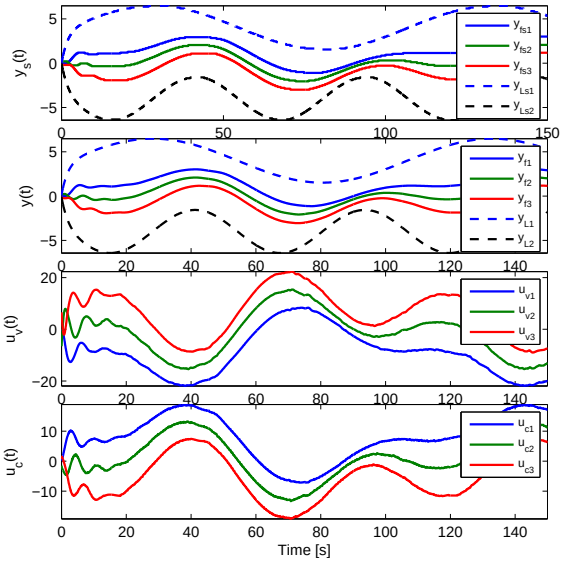

Figure 6. Responses of $y_{\mathrm{f}}(t)$, $y_{\mathrm{L}}(t)$, $y_{\mathrm{fs}}(t)$, $y_{\mathrm{Ls}}(t)$, $u_{\mathrm{v}}(t)$, and $u_{\mathrm{c}}(t)$ for the multiagent system with two leaders creating a time varying convex hull.

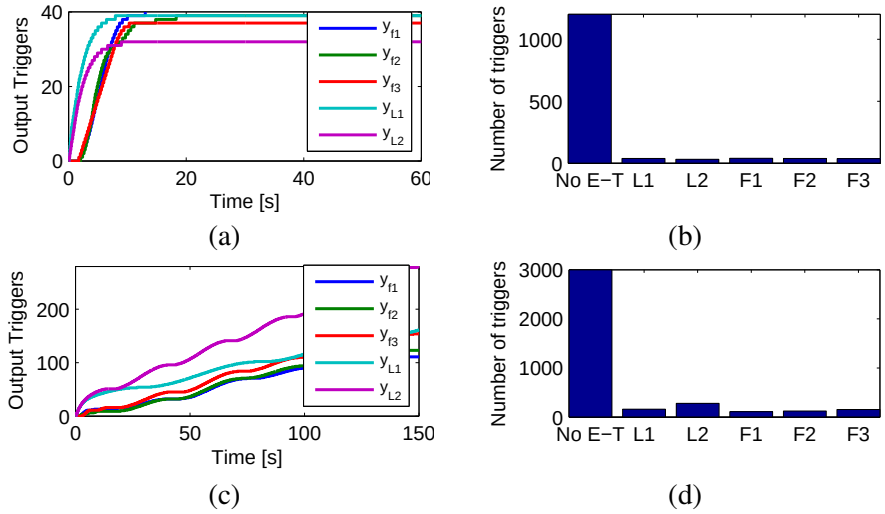

Figure 7. Two leaders case; a) Output triggers for constant commands; b) Triggers comparison for constant commands; c) Output triggers for time varying commands; d) Triggers comparison for time varying commands.

to schedule the exchange information between the agents to reduce the wireless network utilization cost. In addition to rigorous analyses on the performance, two illustrative numerical examples were further included to demonstrate the efficacy of the proposed approach.

ACKNOWLEDGMENT

This research has been supported by the Dynamic Data-Driven Applications Systems Program of the Air Force Office of Scientific Research.

REFERENCES

[1] F. Bullo, J. Cortes, and S. Martinez, *Distributed control of robotic networks: A mathematical approach to motion coordination algorithms*. Princeton University Press, 2009.

[2] M. Mesbahi and M. Egerstedt, *Graph theoretic methods in multiagent networks*. Princeton University Press, 2010.

[3] W. Ren and Y. Cao, *Distributed coordination of multi-agent networks: Emergent problems, models, and issues*. Springer Science & Business Media, 2010.

[4] F. L. Lewis, H. Zhang, K. Hengster-Movric, and A. Das, *Cooperative control of multi-agent systems: optimal and adaptive design approaches*. Springer Science & Business Media, 2013.

[5] P. Tabuada, "Event-triggered real-time scheduling of stabilizing control tasks," *IEEE Transactions on Automatic Control*, vol. 52, no. 9, pp. 1680–1685, 2007.

[6] M. Mazo Jr and P. Tabuada, "On event-triggered and self-triggered control over sensor/actuator networks," in *IEEE Conference on Decision and Control*, pp. 435–440, 2008.

[7] J. Lunze and D. Lehmann, "A state-feedback approach to event-based control," *Automatica*, vol. 46, no. 1, pp. 211–215, 2010.

[8] R. Postoyan, A. Anta, D. Nesic, and P. Tabuada, "A unifying Lyapunov-based framework for the event-triggered control of nonlinear systems," in *IEEE Conference on Decision and Control and European Control Conference*, pp. 2559–2564, 2011.

[9] W. Heemels, K. H. Johansson, and P. Tabuada, "An introduction to event-triggered and self-triggered control," in *IEEE Annual Conference on Decision and Control*, pp. 3270–3285, 2012.

[10] W. Hu, L. Liu, and G. Feng, "Cooperative output regulation of linear multi-agent systems by intermittent communication: A unified framework of time-and event-triggering strategies," *IEEE Transactions on Automatic Control*, 2017.

[11] E. Kharisov, X. Wang, and N. Hovakimyan, "Distributed event-triggered consensus algorithm for uncertain multi-agent systems," *AIAA Guidance, Navigation and Control Conference*, 2010.

[12] P. Zhang and J. Wang, "Event-triggered observer-based tracking control for leader-follower multi-agent systems," *Kybernetika*, vol. 52, no. 4, pp. 589–606, 2016.

[13] C. Yan, M. Yu, and C. Li, "Event-triggered tracking control for couple-group multi-agent systems," *Journal of the Franklin Institute*, 2017.

[14] A. Albattat, T. Yucelen, B. C. Gruenwald, and S. Jagannathan, "An observer-free output feedback cooperative control architecture for multivehicle systems," *ASME Dynamic Systems and Control Conference*, 2017 (Accepted).

[15] A. Albattat, T. Yucelen, B. C. Gruenwald, and J. Sarangapani, "Observer-free output feedback adaptive control for multivehicle systems with exogenous disturbances," *AIAA Guidance, Navigation, and Control Conference*, 2018 (accepted).

[16] T. Yucelen and F. Pourboghrat, "Active noise blocking: Non-minimal modeling, robust control, and implementation," in *American Control Conference, 2009. ACC'09.*, pp. 5492–5497, IEEE, 2009.

[17] T. Yucelen and W. M. Haddad, "Output feedback adaptive stabilization and command following for minimum phase dynamical systems with unmatched uncertainties and disturbances," *International Journal of Control*, vol. 85, no. 6, pp. 706–721, 2012.

[18] T. Yucelen and E. N. Johnson, "Control of multivehicle systems in the presence of uncertain dynamics," *International Journal of Control*, vol. 86, no. 9, pp. 1540–1553, 2013.

[19] C. Godsil and G. Royle, *Algebraic graph theory*. New York, NY: Springer, 2001.

[20] P. J. Antsaklis and A. N. Michel, *Linear systems*. Bosten, MA: Birkhäuser, 2006.

[21] H. K. Khalil, *Nonlinear Systems*. Upper Saddle River, NJ: PrenticeHall, 1996.

[22] J. A. Fax and R. M. Murray, "Information flow and cooperative control of vehicle formations," *IEEE transactions on automatic control*, vol. 49, no. 9, pp. 1465–1476, 2004.

[23] C.-Q. Ma and J.-F. Zhang, "Necessary and sufficient conditions for consensusability of linear multi-agent systems," *IEEE Transactions on Automatic Control*, vol. 55, no. 5, pp. 1263–1268, 2010.

[24] X. Wang and N. Hovakimyan, "Predicting the performance of uncertain multi-agent systems using event-triggering and $\mathcal{L}_1$ adaptation," *AIAA Guidance, Navigation, and Control Conference*, p. 8327, 2010.

[25] D. Tran and T. Yucelen, "On control of multiagent formations through local interactions," in *IEEE Conference on Decision and Control*, 2016.

[26] X. Wang and N. Hovakimyan, "$\mathcal{L}_1$ adaptive control of event-triggered networked systems," *IEEE American Control Conference*, pp. 2458–2463, 2010.

[27] A. Albattat, B. C. Gruenwald, and T. Yucelen, "Design and analysis of adaptive control systems over wireless networks," *Journal of Dynamic Systems, Measurement, and Control*, vol. 139, no. 7, p. 074501, 2017.

[28] A. Albattat, B. C. Gruenwald, and T. Yucelen, *Adaptive Control for Robotic Manipulators*, ch. Output Feedback Adaptive Control of Uncertain Dynamical Systems with Event-Triggering. CRC Press/Taylor & Francis Group: Boca Raton, FL, USA, 2016.

[29] A. Albattat, B. C. Gruenwald, and T. Yucelen, "On event-triggered adaptive architectures for decentralized and distributed control of large-scale modular systems," *Sensors*, vol. 16, no. 8, p. 1297, 2016.

VI. OBSERVER-FREE OUTPUT FEEDBACK ADAPTIVE CONTROL FOR MULTIVEHICLE SYSTEMS WITH EXOGENOUS DISTURBANCES

Ali Albattat[1], Tansel Yucelen[2], Benjamin C. Gruenwald[2], and Sarangapani Jagannathan[1]

[1] Department of Mechanical & Aerospace Engineering

Missouri University of Science and Technology

[2] Department of Mechanical Engineering

University of South Florida

ABSTRACT

A new observer-free output feedback adaptive control, $(OF)^2AC$, method is proposed for continuous-time, minimum phase, and high-order linear multivehicle systems subject to exogenous disturbances (hereinafter referred to as "uncertain multivehicle systems"). In particular, the $(OF)^2AC$ is based on a nonminimal state-space realization for each follower vehicle of the multivehicle system, where this realization generates an expanded set of states using the filtered input, filtered output, and their derivatives of the follower vehicles. The $(OF)^2AC$ consists of *i)* a local cooperative controller and *ii)* a vehicle-level controller for each follower vehicle. Specifically, part *i)* of the proposed control method addresses the leader-follower containment control problem by receiving the relative output measurements of the neighboring vehicles and its part *ii)* consists of an augmenting adaptive controller for stabilization and command following in the presence of exogenous disturbances. Two illustrative numerical examples are provided to demonstrate efficacy of the $(OF)^2AC$.

1. INTRODUCTION

1.1. Literature Review. Multivehicle systems consist of a collection of mobile dynamical systems that sense the surrounding environment and communicate with each other based on a network protocol. In this way, they work cooperatively to achieve shared tasks which may be challenging for an individual vehicle to handle alone. During the past few decades, cooperative control of multivehicle systems has attracted increased attention in the control engineering community owing to its diverse and influential application in areas of science and engineering, such as formation flight of unmanned air, land, and under water vehicles, as well as the control of clusters of satellites and telescopes (see, for example, [1, 2, 3, 4, 5, 6], and references therein).

In general, vehicle system models are represented by the first principles of physics and derived using fundamental physical laws. Due to the system complexity, nonlinearity, and uncertainty, the simplistic approximations create inaccuracies between the model and the the actual system. As a result of this modeling error, it is very important for the cooperative control design to not only achieve system level objectives, but also possess the ability to maintain the stability of each vehicle in the presence of system uncertainties. The most notable results that address cooperative control of uncertain vehicle systems include [7, 8, 9, 10, 11, 12, 13, 14, 15, 16, 17]. Specifically, the authors in [7, 8, 9, 10, 11], consider the uncertain multivehicle systems problem as first and/or second order models which are suitable for a limited number of applications. For more applicable system dynamics, [12, 13, 14, 15, 16, 17] use high-order vehicle models with system uncertainties.

In particular, the authors in [12] consider linear single input and single output vehicle systems with parametric uncertainties that range over an known compact set. The work in [13] uses an internal model based distributed control scheme that makes the vehicle controllers robust to small variation in their models. A finite-time disturbance observer is proposed in [14] to estimate the system uncertainties. A distributed adaptive control for both the uncertain follower and uncertain leaders is considered in [15], where the dis-

tributed adaptive control law is designed based on local consensus error feedback. The authors of [16] design a decentralized adaptive tracking controller under the assumption that the uncertain follower vehicles with Lipschitz-type disturbances are guided by a leader with unknown input. The authors in [17] introduce cooperative control for higher-order multivehicle systems having nonidentical nonlinear uncertain dynamics and large parametric uncertainties with no a prior information on their bound. While the above results are promising, full state feedback is necessary for each proposed controller which requires knowledge of the vehicle system state variables and this is not applicable when the multivehicle system state variables are unknown. Therefore, output feedback is necessary for most applications that involve high-dimensional models with unknown system state variables, such as multiple unmanned aerial vehicles, multiple mobile robots, and multiple manipulators.

To address this problem, [18, 19, 20, 21] propose adaptive output feedback controllers for uncertain dynamical multivehicle systems. In particular, in [18, 19] the adaptive output feedback controller is design for consensus protocols, where the gains rely on the global information of the network which is represented by the Laplacian matrix. The authors of [20] adopt two observer designs, a local observer and an adaptive estimator, for the distributed adaptive output-feedback consensus tracking control for unknown agent dynamics without depending on the Laplacian matrix information. Among the above mentioned works, the common feature is that the adaptive output feedback controller requires an observer for estimating the unknown state variables. In a recent result [22], we employ an output feedback control architecture for dynamical multivehicle systems without observers (outside the context of adaptive control). Specifically, the observer-free nature of our work is an expansion of the original observer-free output feedback adaptive control idea proposed in [23, 24, 25, 26].

1.2. Contribution. In this paper, a new observer-free output feedback adaptive control, $(OF)^2AC$, method is proposed for continuous-time, minimum phase, and high-order linear multivehicle systems subject to exogenous disturbances (hereinafter referred

to as "uncertain multivehicle systems"), where the results reported here can be viewed as an expansion of our recent paper in [22]. In particular, similar to the observer-free methods studied in [23, 24, 25, 26, 22], the $(OF)^2AC$ is based on a nonminimal state-space realization for each follower vehicle of the multivehicle system, where this realization generates an expanded set of states using the filtered input, filtered output, and their derivatives of the follower vehicles. The $(OF)^2AC$ consists of *i)* a local cooperative controller in [17] and *ii)* a vehicle-level controller for each follower vehicle. Specifically, part *i)* of the proposed control method addresses the leader-follower containment control problem by receiving the relative output measurements of the neighboring vehicles and its part *ii)* consists of an augmenting adaptive controller for stabilization and command following in the presence of exogenous disturbances. Two illustrative numerical examples are provided to demonstrate efficacy of the $(OF)^2AC$.

The organization of the paper is as follows. Section 2 present the notation used throughout the paper and recalls some basic results from multivehicle systems. Section 3 presents a nonminimal state space realization [23, 24, 25, 26] technique. The proposed method is given in Section 4. The stability of the overall multivehilce system is analyzed in Section 5 and convergence properties are highlighted in Section 6. Two illustrative numerical examples are provided to show the efficacy of the proposed control architecture in Section 7. Finally, conclusions are drawn in Section 8.

2. NOTATION AND MATHEMATICAL PRELIMINARIES

The notation used in this paper is fairly standard and similar to, for example, our earlier work in [22]. For self-containedness, $\mathbb{R}$ denotes the set of real numbers, $\mathbb{R}^n$ denotes the set of $n \times 1$ real column vectors, $\mathbb{R}^{n\times m}$ denotes the set of $n \times m$ real matrices, $\mathbb{R}_+$ denotes the set of positive real numbers, $\mathbb{R}_+^{n\times n}$ denotes the set of $n \times n$ positive-definite real matrices, $\mathbb{S}^{n\times n}$ denotes the set of $n \times n$ symmetric real matrices, $\mathbb{D}^{n\times n}$ denotes the set of $n \times n$ real matrices with diagonal scalar entries, $(\cdot)^{\mathrm{T}}$ denotes transpose, $(\cdot)^{-1}$ denotes

inverse, $(\cdot)^{\dagger}$ denotes Pseudo inverse, $\mathrm{tr}(\cdot)$ denotes the trace operator, $\mathrm{diag}(a)$ denotes the diagonal matrix with the vector a on its diagonal, and "$\triangleq$" denotes equality by definition. In addition, we write $\lambda_{\min}(A)$ (respectively, $\lambda_{\max}(A)$) for the minimum and respectively maximum eigenvalue of the Hermitian matrix A, $\|\cdot\|$ for the Euclidean norm, and $\|\cdot\|_{\mathrm{F}}$ for the Frobenius matrix norm.

In addition, we adopt graph theoretical notation (e.g., see excellent books on the topic [27, 6]) to encode interactions between vehicles. In particular, an undirected graph $\mathcal{G}$ is defined by $\mathcal{V}_{\mathcal{G}} = \{1, \cdots, N\}$ of nodes and a set $\mathcal{E}_{\mathcal{G}} \in \mathcal{V}_{\mathcal{G}} \times \mathcal{V}_{\mathcal{G}}$ of edges. If $(i, j) \in \mathcal{E}_{\mathcal{G}}$, then the nodes i and j are neighbors, and the neighboring relation is indicated with $i \sim j$. The degree d_i of node i is defined by the number of its neighbors and the degree matrix of graph $\mathcal{G}$ is then given by $\mathcal{D}(\mathcal{G}) \triangleq \mathrm{diag}(d) \in \mathbb{R}^{N\times N}$, $d = [d_1, \cdots, d_N]^{\mathrm{T}}$. A path $i_0 i_1 \cdots i_L$ is a finite sequence of nodes such that $i_{k-1} \sim i_k$, $k = 1, \cdots, L$, and if any pair of district nodes has a path, then a graph $\mathcal{G}$ is connected. Furthermore, we write $\mathcal{A}(\mathcal{G}) \in \mathbb{R}^{N\times N}$ for the adjacency matrix of a graph $\mathcal{G}$ defined by

$$[\mathcal{A}(\mathcal{G})]_{ij} \triangleq \begin{cases} 1, & \text{if } (i,j) \in \mathcal{E}_{\mathcal{G}} \\ 0, & \text{otherwise,} \end{cases} \tag{1}$$

and $\mathcal{B}(\mathcal{G}) \in \mathbb{R}^{N\times M}$ for the (node-edge) incidence matrix of the graph $\mathcal{G}$ defined by

$$[\mathcal{B}(\mathcal{G})]_{ij} \triangleq \begin{cases} 1, & \text{if node} i \text{ is the head of the edge } j, \\ -1, & \text{if node} i \text{ is the tail of the edge } j, \\ 0, & \text{otherwise,} \end{cases} \tag{2}$$

where M is the number of edges, i is an index for the node set, and j is an index for the edge set. Finally, the graph Laplacian matrix, $\mathcal{L}(\mathcal{G}) \in \overline{\mathbb{R}}_{+}^{N\times N} \cap \mathbb{S}^{N\times N}$, is defined by

$$\mathcal{L}(\mathcal{G}) \triangleq \mathcal{D}(\mathcal{G}) - \mathcal{A}(\mathcal{G}), \tag{3}$$

or equivalently,

$$\mathcal{L}(\mathcal{G}) = \mathcal{B}(\mathcal{G})\mathcal{B}(\mathcal{G})^{\mathrm{T}}. \tag{4}$$

Next, we recall some of the basic results for first-order multivehicle systems [6]. Specifically, let nodes and edges represent vehicles and information exchange links between vehicles, respectively. Then, we can model a given multivehicle system by a graph $\mathcal{G}$. For example, let $x_i(t) \in \mathbb{R}$ be the state of node i, $i = 1, ..., N$, satisfying

$$\dot{x}_i(t) = u_i(t), \quad x_i(0) = x_{i0}, \tag{5}$$

where $u_i(t) \in \mathbb{R}$ is the control input. If each vehicle receives the relative state information with respect to its neighbors, then

$$u_i(t) = -\sum_{i\sim j} \left(x_i(t) - x_j(t)\right), \tag{6}$$

solves the rendezvous problem, where (5) subject to (6) can be written at the multivehicle system level as

$$\dot{x}(t) = -\mathcal{L}(\mathcal{G})x(t), \quad x_i(0) = x_{i0}, \tag{7}$$

with $x(t) = \left[x_1^{\mathrm{T}}(t), \cdots, x_N^{\mathrm{T}}(t)\right]$ denoting the aggregated state vector. Note that the spectrum of $\mathcal{L}(\mathcal{G})$ has one zero eigenvalue and $N-1$ positive real eigenvalues if and only if the graph $\mathcal{G}$ is connected and undirected. In this case, the solution of the multivehicle system given by (7) evolves as $x(t) \to (\mathbf{1}_N\mathbf{1}_N^{\mathrm{T}}/N)x_0$ as $t \to \infty$.

Furthermore, we recall some results on leader-follower frameworks. For this purpose, let the incidence matrix (2) be partitioned as

$$\mathcal{B}(\mathcal{G}) = \begin{bmatrix} \mathcal{B}_{\mathrm{L}}(\mathcal{G}) \\ \mathcal{B}_{\mathrm{F}}(\mathcal{G}) \end{bmatrix}, \tag{8}$$

where $\mathcal{B}_{\mathrm{L}}(\mathcal{G}) \in \mathbb{R}^{N_{\mathrm{L}} \times M}$ and $\mathcal{B}_{\mathrm{F}}(\mathcal{G}) \in \mathbb{R}^{N_{\mathrm{F}} \times M}$ with N_{L} and N_{F} denoting cardinalities of the leader and follower groups, respectively, such that $N = N_{\mathrm{L}} + N_{\mathrm{F}}$. Then, using (4) and (8) the partitioned graph Laplacian matrix $\mathcal{L}(\mathcal{G})$ is given by

$$\mathcal{L}(\mathcal{G}) = \begin{bmatrix} L(\mathcal{G}) & G(\mathcal{G})^{\mathrm{T}} \\ G(\mathcal{G}) & F(\mathcal{G}) \end{bmatrix}, \tag{9}$$

where $L(\mathcal{G}) \triangleq \mathcal{B}_{\mathrm{L}}(\mathcal{G})\mathcal{B}_{\mathrm{L}}(\mathcal{G})^{\mathrm{T}}$, $G(\mathcal{G}) = \mathcal{B}_{\mathrm{F}}(\mathcal{G})\mathcal{B}_{\mathrm{L}}(\mathcal{G})^{\mathrm{T}}$ and $F(\mathcal{G}) = \mathcal{B}_{\mathrm{F}}(\mathcal{G})\mathcal{B}_{\mathrm{F}}(\mathcal{G})^{\mathrm{T}}$. Note that $F(\mathcal{G}) \in \mathbb{R}_{+}^{N_{\mathrm{F}} \times N_{\mathrm{F}}} \cap \mathbb{S}^{N_{\mathrm{F}} \times N_{\mathrm{F}}}$, and hence, $F(\mathcal{G})$ is nonsingular since $\det(F(\mathcal{G})) \neq 0$. Furthermore $F(\mathcal{G})\mathbf{1}_{N_{\mathrm{F}}} = -G(\mathcal{G})\mathbf{1}_{N_{\mathrm{L}}}$, or equivalently, each row of $-F(\mathcal{G})^{\mathrm{T}}G(\mathcal{G})$ has a sum equal to 1. Now, we can model a given multivehicle system with a leader-follower framework. In particular, let $x_{\mathrm{L}}(t) \in \mathbb{R}^{N_{\mathrm{L}}}$ and $x_{\mathrm{F}}(t) \in \mathbb{R}^{N_{\mathrm{F}}}$ be the aggregated state vector of the leaders and followers, respectively. Then, the followers evolve through the Laplacian-based dynamics as

$$\dot{x}_{\mathrm{F}}(t) = -F(\mathcal{G})x_{\mathrm{F}}(t) - G(\mathcal{G})x_{\mathrm{L}}(t), \quad x_{\mathrm{F}}(0) = x_{\mathrm{F0}}. \tag{10}$$

Throughout this paper, we consider leaders as command generators for the neighboring followers and that a connected, undirected graph $\mathcal{G}$ represents the interaction topology between the vehicles.

Finally, we provide the following definition necessary for the main results in this paper.

Definition 1. Let $\phi : \mathbb{R}^n \to \mathbb{R}$ be a continuously differentiable convex function given by $\phi(\theta) \triangleq \left((\epsilon_\theta + 1)\,\theta^T \cdot \theta - \theta_{\max}^2\right)/\left(\epsilon_\theta \theta_{\max}^2\right)$, where $\theta_{\max} \in \mathbb{R}$ is a projection norm bound imposed on $\theta \in \mathbb{R}^n$ and $\epsilon > 0$ is a projection tolerance bound. Then, for $y \in \mathbb{R}^n$, the

projection operator Proj : $\mathbb{R}^n \times \mathbb{R}^n \to \mathbb{R}^n$ is defined by

$$\mathrm{Proj}(\theta, y) \triangleq \begin{cases} y, & \text{if } \phi(\theta) < 0, \\ y, & \text{if } \phi(\theta) \geq 0 \text{ and } \phi'(\theta)y \leq 0, \\ y - \dfrac{\phi'^{\mathrm{T}}(\theta)\phi'(\theta)y}{\phi'(\theta)\phi'^{\mathrm{T}}(\theta)}\phi(\theta), & \text{if } \phi(\theta) \geq 0 \text{ and } \phi'(\theta)y > 0. \end{cases} \tag{11}$$

It follows from Definition 1 that $(\theta - \theta^*)^{\mathrm{T}}(\mathrm{Proj}(\theta, y) - y) \geq 0$, $\theta^* \in \mathbb{R}^n$ holds [28]. The definition of the projection operator can be generalized to matrices as $\mathrm{Proj}_{\mathrm{m}}(\Theta, Y) = \big(\mathrm{Proj}(\mathrm{col}_1(\Theta), \mathrm{col}_1(Y)), \ldots, \mathrm{Proj}(\mathrm{col}_m(\Theta), \mathrm{col}_m(Y))\big)$, where $\Theta \in \mathbb{R}^{n\times m}$, $Y \in \mathbb{R}^{n\times m}$, and $\mathrm{col}_i(\cdot)$ denotes the ith column operator. In this case, $\mathrm{tr}\left[(\Theta - \Theta^*)^{\mathrm{T}}(\mathrm{Proj}_{\mathrm{m}}(\Theta, Y) - Y)\right] = \sum_{i=1}^{m}\left[\mathrm{col}_i(\Theta - \Theta^*)^{\mathrm{T}}(\mathrm{Proj}(\mathrm{col}_i(\Theta), \mathrm{col}_i(Y)) - \mathrm{col}_i(Y))\right] \leq 0$ holds, where $\Theta^* \in \mathbb{R}^{n\times m}$.

3. NONMINIMAL STATE SPACE REALIZATION: AN OVERVIEW

In this section, we overview the nonminimal state space representation employed in [29, 25] in the context of the problem considered in this paper, that is, for the follower vehicle dynamics $i, i = 1, \cdots, N_{\mathrm{F}}$, in order to obtain equivalent input-output system dynamics representation for applying the $(\mathrm{OF})^2\mathrm{AC}$ in the next section. For this purpose, consider the controllable and observable minimum phase linear uncertain dynamical follower vehicle system $i, i = 1, \cdots, N_{\mathrm{F}}$, given by

$$\dot{x}_i(t) = Ax_i(t) + Bu_i(t) + Bw_i(t), \quad x_i(0) = x_{0i}, \quad t \geq 0, \tag{12}$$

$$y_i(t) = Cx_i(t), \tag{13}$$

where $x_i(t) \in \mathbb{R}^n$, $t \geq 0$ is the unknown state vector, $u_i(t) \in \mathbb{R}^m$, $t \geq 0$ is the known control input, $y_i(t) \in \mathbb{R}^l$, $t \geq 0$ is the known system output, $w_i(t) \in \mathbb{R}^m$, $t \geq 0$ is the unknown input disturbance with $\|w_i(t)\| \leq w_i^*$ and $\|w_i^{(k)}(t)\| \leq w_i^{(k)*}$, where $Z^{(k)} = \frac{dZ^k}{d^k t}$, $i = 1, \cdots, N_{\mathrm{F}}$, and $k = 1, \cdots, n-1$. In addition, $A \in \mathbb{R}^{n\times n}$, $B \in \mathbb{R}^{n\times m}$, $C \in \mathbb{R}^{l\times n}$, are known follower system matrices and are minimal. An input-output equivalent (from control inputs

$u_i(t),\ t \geq 0$, to system outputs $y_i(t),\ t \geq 0$) nonminimal observer canonical state-space model of (12) and (13) for $l > 1$ is given by [30]

$$\dot{x}_{oi}(t) = A_o x_{oi}(t) + B_o u_i(t) + B_o w_i(t), \quad x_{oi}(0) = x_{o0i},\ t \geq 0, \tag{14}$$

$$y_i(t) = C_o x_{oi}(t), \tag{15}$$

where $x_{oi}(t) \in \mathbb{R}^{ln},\ t \geq 0$ is the state vector,

$$A_o = \begin{bmatrix} 0 & I_l & \cdots & 0 \\ \vdots & \ddots & \ddots & \vdots \\ 0 & \cdots & 0 & I_l \\ -a_0 I_l & -a_1 I_l & \cdots & -a_{n-1} I_l \end{bmatrix} \in \mathbb{R}^{ln \times ln}, \tag{16}$$

$$B_o = \begin{bmatrix} CB \\ CAB \\ \vdots \\ CA^{n-1}B \end{bmatrix} \in \mathbb{R}^{ln \times m}, \tag{17}$$

$$C_o = \begin{bmatrix} 0 I_l \cdots 0 \end{bmatrix} \in \mathbb{R}^{l \times ln}. \tag{18}$$

Note that $a_k,\ k = 0, 1, \cdots, n-1$, in (16) are the coefficients of the characteristic polynomial of the matrix A in (12).

Next, define

$$\bar{B}_0 \triangleq C_o(a_1 I_{ln} + a_2 A_o + \cdots + a_{n-2} A_o^{n-3} + a_{n-1} A_o^{n-2} + A_o^{n-1}) B_o, \tag{19}$$

$$\bar{B}_1 \triangleq C_o(a_2 I_{ln} + a_3 A_o + \cdots + a_{n-1} A_o^{n-3} + A_o^{n-2}) B_o, \tag{20}$$

$$\vdots$$

$$\bar{B}_{n-1} \triangleq C_o B_o. \tag{21}$$

Now, an alternative input-output equivalent nonminimal controllable state-space realization of (12) and (13) is given by

$$\dot{x}_{\mathrm{f}i}(t) = A_{\mathrm{f}}x_{\mathrm{f}i}(t) + B_{\mathrm{f}}u_i(t) + D_{\mathrm{f}}\bar{w}_{\mathrm{f}i}(t), \quad x_{\mathrm{f}i}(0) = x_{\mathrm{f}0i}, \ t \geq 0, \tag{22}$$

$$y_i(t) = C_{\mathrm{f}}x_{\mathrm{f}i}(t), \tag{23}$$

where $x_{\mathrm{f}i}(t) \in \mathbb{R}^{n_{\mathrm{f}}}$, $t \geq 0$, $n_{\mathrm{f}} \triangleq (m + l)n$, is the known filtered expanded state vector given by

$$x_{\mathrm{f}i}(t) = \left[q_{1i}^{\mathrm{T}}(t), \cdots, q_{ni}^{\mathrm{T}}(t), \nu_{1i}^{\mathrm{T}}, \cdots, \nu_{ni}^{\mathrm{T}}\right]^{\mathrm{T}}, \tag{24}$$

where $q_{ki}(t) \triangleq y_{\mathrm{f}i}^{k-1}(t)$, $\nu_{ki} = u_{\mathrm{f}i}^{k-1}(t)$, $k = 1,2,\cdots,n$, $z^{(n)} \triangleq \mathrm{d}^n z(t)/\mathrm{d}t^n$, and where $x_{\mathrm{f}i}(t)$ is obtained by filtering $u_i(t)$ and $y_i(t)$ though the filter $\lambda^n/\Lambda(s)$, where

$$\Lambda(s) = (s + \lambda)^n = \sum_{p=0}^{n} \binom{n}{p} s^{n-p}\lambda^p = s^n + n\lambda s^{n-1} + \cdots + \lambda^n, \tag{25}$$

is a monic Hurwitz polynomial of degree n with $\lambda > 0$. In addition,

$$A_{\mathrm{f}} = \begin{bmatrix} 0 & I_l & 0 & \cdots & & & \cdots & 0 \\ \vdots & & \ddots & & & & & \vdots \\ 0 & \cdots & 0 & I_l & 0 & \cdots\cdots & & 0 \\ -a_0 I_l & \cdots\cdots & & -a_{n-1}I_l & \bar{B}_0 & \cdots\cdots & & \bar{B}_{n-1} \\ 0 & \cdots & & \cdots & 0 & I_m & 0 & 0 \\ \vdots & & & & & & \ddots & \vdots \\ \vdots & & & & & & \cdots\ 0 & I_m \\ 0 & \cdots\cdots & & 0 & -\lambda^n I_m & \cdots\cdots & & -n\lambda I_m \end{bmatrix} \in \mathbb{R}^{n_{\mathrm{f}} \times n_{\mathrm{f}}}, \tag{26}$$

$$B_{\mathrm{f}} = \begin{bmatrix} 0 0 \cdots \lambda^n I_m \end{bmatrix}^{\mathrm{T}} \in \mathbb{R}^{n_{\mathrm{f}} \times m}, \tag{27}$$

$$C_{\rm f} = \left[-\lambda^{-n}(a_0 I_l + \lambda^n I_l) \cdots \cdots -\lambda^{-n}(a_{n-1} I_l + n\lambda^n I_l)\, \lambda^{-n}\bar{B}_0 \cdots \cdots \lambda^{-n}\bar{B}_{n-1} \right] \in \mathbb{R}^{l \times n_{\rm f}}, \tag{28}$$

$$D_{\rm f} = \left[0 \cdots 0 I_l 0 \cdots 00 \right]^{\rm T} \in \mathbb{R}^{n_{\rm f} \times l}, \tag{29}$$

and

$$\begin{aligned} \bar{w}_{{\rm f}i}(t) =& a_1 C_o B_o w_{{\rm f}i}(t) + \cdots + a_{n-1}[C_o A_o^{n-2} B_o w_{{\rm f}i}(t) + \cdots + C_o B_o w_{{\rm f}i}^{(n-2)}(t)] \\ &+ C_o A_o^{n-1} B_o w_{{\rm f}i}(t) + \cdots + C_o B_o w_{{\rm f}i}^{(n-1)}(t),\ t \geq 0, \end{aligned} \tag{30}$$

where $w_{{\rm f}i}(t)$ is obtained by filtering $w_i(t)$ through the filter $\lambda^n/\Lambda(s)$. Now, following the results documented in [29, 25], the ith follower vehicle dynamics (12) and (13) are input-output equivalent to the dynamics given by (22) and (23) (e.g., see Theorem 2.1 of [25]).

4. (OF)^{2}AC CONSTRUCTION FOR THE FOLLOWER VEHICLES

In this section, we introduce the (OF)^{2}AC method for the follower vehicles; but before this, we first provide the leader vehicle dynamics, i, $i = 1, \cdots, N_{\rm L}$, given by

$$\dot{x}_{{\rm L}i}(t) = A_{{\rm L}i} x_{{\rm L}i}(t) + B_{{\rm L}i} c_i(t),\ x_{{\rm L}i}(0) = x_{{\rm L}0i},\ \ t \geq 0, \tag{31}$$

$$y_{{\rm L}i}(t) = C_{{\rm L}i} x_{{\rm L}i}(t), \tag{32}$$

where $x_{{\rm L}i}(t) \in \mathbb{R}^{n_i}$ is the leader vehicle state vector, $c_i(t) \in \mathbb{R}^{m_i}$ is a leader vehicle bounded input command (i.e., $\|c_i(t)\| \leq c_i^*$) with bounded time rate change (i.e., $\|\dot{c}_i(t)\| \leq \dot{c}_i^*$), $y_{{\rm L}i}(t) \in \mathbb{R}^l$ is the leader vehicle output, $A_{{\rm L}i} \in \mathbb{R}^{n_i \times n_i}$ is the leader vehicle system matrix, $B_{{\rm L}i} \in \mathbb{R}^{n_i \times m_i}$ is the leader vehicle command input matrix, $C_{{\rm L}i} \in \mathbb{R}^{l \times n_i}$ is the leader vehicle output matrix, $(A_{{\rm L}i}, B_{{\rm L}i}, C_{{\rm L}i})$ is minimal, and $A_{{\rm L}i}$ is Hurwitz.

Next, for the follower vehicle dynamics, we assume that the system (12) and (13) is minimum phase and let d be the known smallest positive integer i such that the ith Markov parameter of the original system (12) and (13) given by

$$CA^{i-1}B, \tag{33}$$

is nonzero. In this case, it follows from (20)-(21) that

$$\bar{B}_{n-1} = C_o B_o = CB = 0, \tag{34}$$

$$\bar{B}_{n-2} = C_o(a_1 I_{ln} + A_o)B_o = a_1 CB + CAB = 0, \tag{35}$$

$$\vdots$$

$$\bar{B}_{n-d+1} = 0, \tag{36}$$

$$\bar{B}_{n-d} = CA^{d-1}B \neq 0. \tag{37}$$

The first Markov parameter can then be parameterized as

$$CA^{d-1}B = \bar{B}, \tag{38}$$

where $\bar{B} \in \mathbb{R}^{l\times m}$ is a known matrix since A, B, and C are known.

Now, the nonminimal state-space model (22) can be separated into the set of dynamics similar to [25] as

$$\dot{q}_i(t) = A_0 q_i(t) + B_0 v_{0i}(t) + B_1 \phi_i(t) + D_1 \bar{w}_{\mathrm{f}i}(t), \quad q_i(0) = q_{0i}, \quad t \geq 0, \tag{39}$$

$$\dot{v}_i(t) = A_v v_i(t) + B_v u_i(t), \quad v_i(0) = v_{0i}, \quad t \geq 0, \tag{40}$$

where $q_i(t) \triangleq [q_{1i}^{\mathrm{T}}(t), \cdots, q_{ni}^{\mathrm{T}}(t)]^{\mathrm{T}} \in \mathbb{R}^{ln}$, $v_{0i}(t) \triangleq [v_{1i}^{\mathrm{T}}(t), \cdots, v_{(n-d)i}^{\mathrm{T}}(t)]^{\mathrm{T}} \in \mathbb{R}^{m(n-d)}$, $\phi_i(t) \triangleq v_{(n-d+1)i}(t) \in \mathbb{R}^m, v_i(t) \triangleq [v_{1i}^{\mathrm{T}}(t), \cdots, v_{ni}^{\mathrm{T}}(t)]^{\mathrm{T}} \in \mathbb{R}^{mn}$, $i = 1, \cdots, N_{\mathrm{F}}$,

$$A_0 \triangleq \begin{bmatrix} 0 & I_l & \cdots & 0 \\ \vdots & \ddots & \ddots & \vdots \\ 0 & \cdots & 0 & I_l \\ -a_0 I_l & -a_1 I_l & \cdots & -a_{n-1} I_l \end{bmatrix} \in \mathbb{R}^{ln \times ln}, \tag{41}$$

$$B_0 \triangleq \begin{bmatrix} 0 & \cdots & 0 \\ \vdots & \ddots & \vdots \\ 0 & \cdots & 0 \\ \bar{B}_o & \cdots & \bar{B}_{n-d-1} \end{bmatrix} \in \mathbb{R}^{ln \times m(n-d)}, \tag{42}$$

$$B_1 \triangleq \begin{bmatrix} 0 \cdots 0 \bar{B}^{\mathrm{T}} \end{bmatrix}^{\mathrm{T}} \in \mathbb{R}^{ln \times m}, \tag{43}$$

$$D_1 \triangleq \begin{bmatrix} 0 \cdots 0 I_l \end{bmatrix}^{\mathrm{T}} \in \mathbb{R}^{ln \times l}, \tag{44}$$

$$A_v \triangleq \begin{bmatrix} 0 & I_m & \cdots & 0 \\ \vdots & \ddots & \ddots & \vdots \\ 0 & \cdots & 0 & I_m \\ -\zeta_1 I_m & \cdots & \cdots & -\zeta_n I_m \end{bmatrix} \in \mathbb{R}^{mn \times mn}, \tag{45}$$

and

$$B_v \triangleq \begin{bmatrix} 0 \cdots 0 \lambda^n I_m \end{bmatrix}^{\mathrm{T}} \in \mathbb{R}^{mn \times m}, \tag{46}$$

where $\zeta_1 \triangleq \lambda^n, \cdots, \zeta_n \triangleq n\lambda$.

We use a two-stage design [17] for the virtual control signal $\phi_i(t), t \geq 0$, such that the virtual control can suppress the effect of the unmatched disturbances and stabilize the follower vehicles, and drive the uncertain follower vehicles to the convex hull spanned by the leaders. Then, the actual control signal $u_i(t), t \geq 0$, is designed using the follower second dynamical subsystem in (39). This design process is covered in detail in the following subsections.

4.1. Vehicle-level Controller Design. We now design the virtual controller as

$$\phi_i(t) \triangleq \phi_{\mathrm{n}i}(t) + \phi_{\mathrm{a}i}(t) + \phi_{\mathrm{c}i}(t), \tag{47}$$

where $\phi_{\mathrm{n}i}(t)$ is the nominal control, $\phi_{\mathrm{a}i}(t)$ is the adaptive control, and $\phi_{\mathrm{c}i}(t)$ is the cooperative control that is addressed in the next subsection.

The vehicle-level controller consists of the nominal and adaptive control (an augmenting adaptive control viewpoint is adopted here), where the nominal portion is designed as

$$\phi_{\mathrm{n}i}(t) \triangleq K_{\mathrm{q}} q_i(t) - K_v v_{0i}(t), \tag{48}$$

where $K_{\mathrm{q}} \in \mathbb{R}^{m\times ln}$ and $K_v \in \mathbb{R}^{m\times m(n-d)}$, such that $A_{\mathrm{m}} \triangleq A_0 + B_1 K_{\mathrm{q}}$ is Hurwitz and $B_0 \triangleq B_1 K_v$. The existence of a virtual adaptive control $\phi_{\mathrm{a}i}(t), t \geq 0$ is guaranteed under the following assumption.

Assumption 1 *The matrix $\bar{B} \in \mathbb{R}^{l\times m}$ has the dimension satisfying $m \geq l$. In addition, if $m = l$, then $\bar{B}$ is nonsingular (i.e., $\bar{B}\bar{B}^{-1} = \bar{B}^{-1}\bar{B} = I$). Furthermore, if $m > l$, then $\bar{B}$ satisfies $\bar{B}\bar{B}^{\dagger} = I$.*

Using (47), (39) can be written as

$$\begin{aligned}
\dot{q}_i(t) &= A_{\mathrm{m}} q_i(t) + B_1 \phi_{\mathrm{c}i}(t) + B_1 \phi_{\mathrm{a}i}(t) + D_1 \bar{w}_{\mathrm{f}i}(t) \\
&= A_{\mathrm{m}} q_i(t) + B_1 \phi_{\mathrm{c}i}(t) + B_1 \phi_{\mathrm{a}i}(t) + D_1 \bar{B}\bar{B}^{\dagger} \bar{w}_{\mathrm{f}i}(t) \\
&= A_{\mathrm{m}} q_i(t) + B_1 \phi_{\mathrm{c}i}(t) + B_1 \phi_{\mathrm{a}i}(t) + B_1 \bar{B}^{\dagger} \bar{w}_{\mathrm{f}i}(t) \\
&= A_{\mathrm{m}} q_i(t) + B_1 \phi_{\mathrm{c}i}(t) + B_1 \left[\phi_{\mathrm{a}i}(t) + d_{\mathrm{f}i}(t)\right].
\end{aligned} \tag{49}$$

where $d_{\mathrm{f}i}(t) \triangleq \bar{B}^{\dagger} \bar{w}_{\mathrm{f}i}(t)$ is unknown. Now, consider the reference system given by

$$\dot{q}_{\mathrm{m}i}(t) = A_{\mathrm{m}} q_{\mathrm{m}i}(t) + B_1 \phi_{\mathrm{c}i}(t). \tag{50}$$

The error dynamics then follow from the state error vector $e_i(t) \triangleq q_i(t) - q_{\mathrm{m}i}(t)$, (49), and (50) as

$$\dot{e}_i(t) = A_{\mathrm{m}} e_i(t) + B_1 \left[\phi_{\mathrm{a}i}(t) + d_{\mathrm{f}i}(t)\right]. \tag{51}$$

Next, let the virtual adaptive control law of the vehicle $i, i = 1, \cdots, N_{\mathrm{F}}$, be given by

$$\phi_{\mathrm{a}i}(t) \triangleq -\hat{d}_{\mathrm{f}i}(t), \tag{52}$$

where, $\hat{d}_{\mathrm{f}i}(t) \in \mathbb{R}^l$ is the estimate of $d_{\mathrm{f}i}(t)$ satisfying the update law

$$\dot{\hat{d}}_{\mathrm{f}i}(t) = \Gamma \mathrm{Proj}\left[\hat{d}_{\mathrm{f}i}(t), e_i^{\mathrm{T}}(t) P B_1\right], \quad \hat{d}_{\mathrm{f}i}(0) = \hat{d}_{\mathrm{f}0i} \tag{53}$$

where $\Gamma = \gamma I_l \in \mathbb{R}^{l \times l}$ is a positive-definite learning rate matrix and $P \in \mathbb{R}^{ln \times ln}$ is a positive definite solution of the Lyapunov equation

$$0 = A_{\mathrm{m}}^{\mathrm{T}} P + P A_{\mathrm{m}} + R, \tag{54}$$

where $R \in \mathbb{R}^{ln \times ln}$ is a positive definite matrix. It then follows that (51) can be written using (52) as

$$\dot{e}_i(t) = A_{\mathrm{m}} e_i(t) - B_1 \tilde{d}_{\mathrm{f}i}(t), \tag{55}$$

where $\tilde{d}_{\mathrm{f}i}(t) \triangleq \hat{d}_{\mathrm{f}i}(t) - d_{\mathrm{f}i}(t)$ is the weight update error.

4.2. Local Cooperative Control Design. For the virtual control architecture, let $\tilde{y}(t) \triangleq \left[y_{\mathrm{L}}^{\mathrm{T}}(t), y_{\mathrm{f}}^{\mathrm{T}}(t)\right]^{\mathrm{T}} \in \mathbb{R}^{(N_{\mathrm{L}} \times N_{\mathrm{F}})l}$ be the vector associated with the graph $\mathcal{G}$, where $y_{\mathrm{L}}^{\mathrm{T}}(t) \triangleq [y_{\mathrm{L}1}^{\mathrm{T}}(t), \cdots, y_{\mathrm{L}N_{\mathrm{L}}}^{\mathrm{T}}(t)]^{\mathrm{T}} \in \mathbb{R}^{N_{\mathrm{L}}l}$ denotes the first N_{L} nodes representing the aggregated output vector of the leaders and $y_{\mathrm{f}}^{\mathrm{T}}(t) \triangleq [y_{\mathrm{f}1}^{\mathrm{T}}(t), \cdots, y_{\mathrm{f}N_{\mathrm{F}}}^{\mathrm{T}}(t)]^{\mathrm{T}} \in \mathbb{R}^{N_{\mathrm{F}}l}$ denotes the last N_{F} nodes representing the aggregated output vector of the follower vehicles. Then,

for each follower vehicle, consider the local cooperative controller, receiving the relative output measurements of the neighboring vehicles in terms of $y_{\mathrm{f}i}(t), i = 1, \cdots, N_{\mathrm{F}}$, and $y_{\mathrm{L}i}(t), i = 1, \cdots, N_{\mathrm{L}}$, as [17]

$$u_{\mathrm{c}i}(t) = K_c\Big[-\sum_{i\sim j}\Big(\tilde{y}_i(t) - \tilde{y}_j(t)\Big) + \theta_i(t)\Big], \tag{56}$$

$$\dot{\theta}_i(t) = \delta\Big[-\sum_{i\sim j}\Big(\tilde{y}_i(t) - \tilde{y}_j(t)\Big) - \zeta\left(\theta_i(t) - \nu_i(t)\right)\Big], \quad \theta_i(0) = \theta_{i0}, \tag{57}$$

$$\dot{\nu}_i(t) = \eta\left(\theta_i(t) - \nu_i(t)\right), \quad \nu_i(0) = \nu_{i0}, \tag{58}$$

where $K_c \in \mathbb{R}^{m\times l}$ is a gain matrix, $\theta_i(t) \in \mathbb{R}^l$ is the integrator state, $\nu_i(t) \in \mathbb{R}^l$ is the filter state, $\delta \in \mathbb{R}_+$ is the integrator gain, $\zeta \in \mathbb{R}_+$ is a modification gain, and $\eta \in \mathbb{R}_+$ is the filter gain. Next, applying the local cooperative controller (56), (57), and (58) to the reference system given by (50) yields

$$\dot{q}_{\mathrm{m}i}(t) = A_{\mathrm{m}}q_{\mathrm{m}i}(t) - B_1K_c\sum_{i\sim j}\Big(\tilde{y}_i(t) - \tilde{y}_j(t)\Big) + B_1K_c\theta_i(t). \tag{59}$$

Letting $q_{\mathrm{m}}(t) \triangleq [q_{\mathrm{m}1}^{\mathrm{T}}(t), \cdots, q_{\mathrm{m}N_{\mathrm{F}}}^{\mathrm{T}}(t)]^{\mathrm{T}} \in \mathbb{R}^{N_{\mathrm{F}}ln}$, $q(t) \triangleq [q_1^{\mathrm{T}}(t), \cdots, q_{N_{\mathrm{F}}}^{\mathrm{T}}(t)]^{\mathrm{T}} \in \mathbb{R}^{N_{\mathrm{F}}ln}$, $e(t) = q(t) - q_{\mathrm{m}}(t) \in \mathbb{R}^{N_{\mathrm{F}}ln}$, $\theta(t) \triangleq [\theta_1^{\mathrm{T}}(t), \cdots, \theta_{N_{\mathrm{F}}}^{\mathrm{T}}(t)]^{\mathrm{T}} \in \mathbb{R}^{N_{\mathrm{F}}l}$, $\nu(t) \triangleq [\nu_1^{\mathrm{T}}(t), \cdots, \nu_{N_{\mathrm{F}}}^{\mathrm{T}}(t)]^{\mathrm{T}} \in \mathbb{R}^{N_{\mathrm{F}}l}$, and

$$y_{\mathrm{f}i}(t) = C_q q_i(t), \tag{60}$$

where $C_q \triangleq [I_l, \cdots, 0] \in \mathbb{R}^{l\times ln}$, the reference system (50) subject to the local cooperative controller (56), (57), and (58) can be written at the multivehicle system level as

$$\begin{aligned}\dot{q}_{\mathrm{m}}(t) &= (I_{N_{\mathrm{F}}} \otimes A_{\mathrm{m}})q_{\mathrm{m}}(t) - (F(\mathcal{G}) \otimes B_1K_c)y_{\mathrm{f}}(t) - (G(\mathcal{G}) \otimes B_1K_c)y_{\mathrm{L}}(t)\\ &\quad + (I_{N_{\mathrm{F}}} \otimes B1K_c)\theta(t)\\ &= [I_{N_{\mathrm{F}}} \otimes A_{\mathrm{m}} - F(\mathcal{G}) \otimes B_1K_cC_q]q_{\mathrm{m}}(t) - (F(\mathcal{G}) \otimes B_1K_cC_q)e(t)\\ &\quad - (G(\mathcal{G}) \otimes B_1K_c)y_{\mathrm{L}}(t) + (I_{N_{\mathrm{F}}} \otimes B_1K_c)\theta(t), \quad q_{\mathrm{m}}(0) = q_{\mathrm{m}0}, \end{aligned} \tag{61}$$

$$\begin{aligned}\dot{\theta}(t) &= -\delta(F(\mathcal{G}) \otimes I_l)y_{\mathrm{f}}(t) - \delta(G(\mathcal{G}) \otimes I_l)y_{\mathrm{L}}(t) - \delta\zeta\,(\theta(t) - \nu(t))\\ &= -\delta(F(\mathcal{G}) \otimes C_q)q_{\mathrm{m}}(t) - \delta(F(\mathcal{G}) \otimes C_q)e(t) - \delta(G(\mathcal{G}) \otimes I_l)y_{\mathrm{L}}(t)\\ &\quad - \delta\zeta\,(\theta(t) - \nu(t))\,, \quad \theta(0) = \theta_0, \end{aligned} \tag{62}$$

$$\dot{\nu}(t) = \eta\,(\theta(t) - \nu(t))\,, \quad \nu(0) = \nu_0. \tag{63}$$

Now, with $\xi(t) \triangleq [q_{\mathrm{m}}^{\mathrm{T}}(t),\ \theta^{\mathrm{T}}(t),\ \nu^{\mathrm{T}}(t)]^{\mathrm{T}} \in \mathbb{R}^{n_\xi}$, $n_\xi \triangleq N_{\mathrm{F}}(ln + 2l)$, $A_\xi(\mathcal{G}) \triangleq I_{N_{\mathrm{F}}} \otimes A_{\mathrm{m}} - F(\mathcal{G}) \otimes B_1K_cC_q \in \mathbb{R}^{N_{\mathrm{F}}ln \times N_{\mathrm{F}}ln}$, (61), (62), and (63) can be written in compact form as

$$\dot{\xi}(t) = \mathcal{A}(\mathcal{G})\xi(t) + \mathcal{B}(\mathcal{G})y_{\mathrm{L}}(t) + \mathcal{E}(\mathcal{G})e(t), \quad \xi(0) = \xi_0, \tag{64}$$

where

$$\mathcal{A}(\mathcal{G}) = \begin{bmatrix} A_\xi(\mathcal{G}) & I_{N_{\mathrm{F}}} \otimes B_1K_c & 0\\ -\delta(F(\mathcal{G}) \otimes C_q) & -\delta\zeta I_{N_{\mathrm{F}}l} & \delta\zeta I_{N_{\mathrm{F}}l}\\ 0 & \eta I_{N_{\mathrm{F}}l} & -\eta I_{N_{\mathrm{F}}l} \end{bmatrix} \in \mathbb{R}^{n_\xi \times n_\xi}, \tag{65}$$

$$\mathcal{B}(\mathcal{G}) = \begin{bmatrix} -G(\mathcal{G}) \otimes B_1K_c\\ -\delta(G(\mathcal{G}) \otimes I_l)\\ 0 \end{bmatrix} \in \mathbb{R}^{n_\xi \times N_{\mathrm{F}}ln}, \tag{66}$$

$$\mathcal{E}(\mathcal{G}) = \begin{bmatrix} -F(\mathcal{G}) \otimes B_1K_cC_q\\ -\delta(F(\mathcal{G}) \otimes C_q)\\ 0 \end{bmatrix} \in \mathbb{R}^{n_\xi \times N_{\mathrm{F}}ln}. \tag{67}$$

The objective of the proposed observer-free vehicle-level controller given in the previous section is to stabilize the uncertain follower vehicle dynamics. Furthermore, the objective of the local cooperative controller given in this section based on [17] is to solve the containment problem. For this purpose, we first need to ensure that the solution $\xi(t)$ to (64) is $\mathcal{L}_\infty$ stable [31]; that is, for every bounded $y_{\mathrm{L}}(t)$ and $e(t)$, then $\xi(t)$ is either bounded. We know that $y_{\mathrm{L}}(t)$ is bounded, since every $A_{\mathrm{L}i}, i = 1, \cdots, N_{\mathrm{L}}$, are Hurwitz, and it will be shown that $e(t)$ is either $\lim_{t\to\infty} e(t) = 0$ or bounded in the later analysis. Therefore, in order to conclude that (64) is $\mathcal{L}_\infty$ stable, $\mathcal{A}(\mathcal{G})$ needs to be Hurwitz. The desired system $\mathcal{L}_\infty$ stability can be equivalently viewed by

$$\dot{\bar{\xi}}(t) = \mathcal{A}(\mathcal{G})\bar{\xi}(t) + \mathcal{B}(\mathcal{G})y_{\mathrm{L}}(t), \quad \bar{\xi}(0) = \bar{\xi}_0, \tag{68}$$

where $\bar{\xi}(t) \in \mathbb{R}^{n_\xi}$. A necessary and sufficient condition satisfying this requirement is given in the following remark.

Remark 4 *Similar to the results in [32, 33, 17], let $\mu_i \in spec(F(\mathcal{G})), i = 1, \cdots, N_F$. If the matrix storing known parts of the system dynamics as well as the controller parameters*

$$\mathcal{U}_{\mathcal{A}(\mathcal{G})i} = \begin{bmatrix} A_m - \mu_i B_1 K_c C_q & B_1 K_c & 0 \\ -\mu_i \delta C_q & -\delta\zeta I_l & \delta\zeta I_l \\ 0 & \eta I_l & \eta I_l \end{bmatrix} \in \mathbb{R}^{(ln+2l)\times(ln+2l)}, \tag{69}$$

is Hurwitz for $i = 1, \cdots, N_F$, then $\mathcal{A}(\mathcal{G})$ in (53) is Hurwitz.

Note that (69) can be made Hurwitz for $i = 1, \cdots, N_{\mathrm{L}}$ by judiciously choosing the design parameters K_{c}, δ, ζ, and η. This further implies that the system (64) with the leader dynamical given by (31) and (32) is $\mathcal{L}_\infty$ stable (e.g., see Corollary 6.1 of [17]).

4.3. Actual Control Construction. We construct the actual control signal $u_i(t)$, $t > 0$, for the $(\text{OF})^2\text{AC}$ using the system dynamics in (40) as

$$u_i(t) = \dot{v}_i(t) + \zeta_n v_{ni} + \zeta_{n-1} v_{(n-1)i} + \zeta_{n-2} v_{(n-2)i} + \cdots + \zeta_{n-d+2} v_{(n-d+2)i} + \zeta_{n-d+1} v_{(n-d+1)i} + \zeta_{n-d} v_{(n-d)i} + \cdots + \zeta_2 v_{2i} + \zeta_1 v_{1i}, \quad t \geq 0. \tag{70}$$

Using $\phi(t), t \geq 0$ given by (47), it then follows from (70) that [25]

$$\begin{aligned} u_i(t) =& \phi_i^{(d)}(t) + \zeta_n \phi_i^{(d-1)}(t) + \zeta_{n-1} \phi_i^{(d-2)}(t) + \zeta_{n-2} \phi_i^{(d-3)}(t) + \cdots + \zeta_{n-d+2} \dot{\phi}_i(t) + \zeta_{n-d+1} \phi_i(t) \\ &+ \zeta_{n-d} \int_0^t \phi_i(\sigma_1) \mathrm{d}\sigma_1 + \cdots + \zeta_2 \left(\int_0^t \cdots \int_0^t \left(\int_0^t \phi_i(\sigma_1) \mathrm{d}\sigma_1 \right) \mathrm{d}\sigma_2 \cdots \mathrm{d}\sigma_{n-d-1} \right) \\ &+ \zeta_1 \left(\int_0^t \cdots \int_0^t \left(\int_0^t \phi_i(\sigma_1) \mathrm{d}\sigma_1 \right) \mathrm{d}\sigma_2 \cdots \mathrm{d}\sigma_{n-d} \right), \quad t \geq 0. \end{aligned} \tag{71}$$

5. STABILITY ANALYSIS OF THE $(\text{OF})^2\text{AC}$

In order to analyze the stability of the overall multivehicle system, let $\tilde{w}(t) \triangleq [\tilde{d}_{\text{f1}}^{\text{T}}(t), \cdots, \tilde{d}_{\text{f}N_{\text{F}}}^{\text{T}}(t)]^{\text{T}} \in \mathbb{R}^{N_{\text{F}}l}$ and $\dot{w}(t) \triangleq [\dot{d}_{\text{f1}}^{\text{T}}(t), \cdots, \dot{d}_{\text{f}N_{\text{F}}}^{\text{T}}(t)]^{\text{T}} \in \mathbb{R}^{N_{\text{F}}l}$. The rest of this section presents stability analysis, first for the constant disturbance case and then the time-varying disturbance case. Consider in addition

$$\dot{\tilde{\xi}}(t) = \mathcal{A}(\mathcal{G})\tilde{\xi}(t) + \mathcal{E}(\mathcal{G})e(t), \quad \tilde{\xi}(0) = \tilde{\xi}_0, \tag{72}$$

where $\tilde{\xi}(t) \triangleq \xi(t) - \bar{\xi}(t)$, $\tilde{\xi}(t) \in \mathbb{R}^{n_\xi}$.

5.1. Constant Disturbance Case. In the case of ith follower vehicle, $i = 1, \cdots, N_{\text{F}}$, has constant disturbance. For stability analysis of the overall multivehicle system, consider the vehicle error dynamics given by (51) and consider the weight update error dynamics given by

$$\dot{\tilde{d}}_{\text{f}i}(t) = \Gamma \text{Proj}\left[\hat{d}_{\text{f}i}(t), e_i^{\text{T}}(t) P B_1\right], \tag{73}$$

for vehicle $i, i = 1, \cdots, N_{\mathrm{F}}$.

Theorem 3 *Consider a multivehicle system consisting of N_F nonlinear uncertain vehicles with the dynamics given by (39), for $i = 1, \cdots, N_F$, with constant input disturbance, subject to Assumption 1, the reference model given by (50), the virtual vehicle-level controller given by (47), (48), (52), and (53). In addition, let the virtual local cooperative control for vehicle $i = 1, \cdots, N_F$, be given by (56), (57), and (58), such that (65) is Hurwitz. Then, the solution $(e(t), \tilde{\xi}(t), \tilde{w}(t))$ is Lyapunov stable for all $(e(0), \tilde{\xi}(0), \tilde{w}(0))$, and $\lim_{t\to\infty} e(t) = 0$ and $\lim_{t\to\infty} \tilde{\xi}(t) = 0$.*

Proof. To show uniform ultimate boundedness of the solution $(e(t), \xi(t), \tilde{w}(t))$ for all $(e(0), \xi(0), \tilde{w}(0)) \in \mathbb{R}^{N_{\mathrm{F}}ln} \times \mathbb{R}^{n_\xi} \times \mathbb{R}^{N_{\mathrm{F}}l}$ and $t \in \overline{\mathbb{R}}_+$, first consider

$$\mathcal{V}_{1i}(e_i(t), \tilde{d}_{\mathrm{f}i}(t)) = e_i^{\mathrm{T}}(t) P e_i(t) + \tilde{d}_{\mathrm{f}i}^{\mathrm{T}}(t) \Gamma^{-1} \tilde{d}_{\mathrm{f}i}(t), \tag{74}$$

and note that $\mathcal{V}_{1i}(0,0) = 0$, $\mathcal{V}_{1i}(e_i(t), \tilde{d}_{\mathrm{f}i}(t)) > 0$ for all $(e_i(t), \tilde{d}_{\mathrm{f}i}(t)) \neq (0,0)$, and $\mathcal{V}_{1i}(e_i(t), \tilde{d}_{\mathrm{f}i}(t))$ is radially unbounded. The time derivative of (74) is then given by

$$\begin{aligned} \dot{\mathcal{V}}_{1i}(\cdot) &= 2e_i^{\mathrm{T}}(t) P \left(A_{\mathrm{m}} e_i(t) - B_1 \tilde{d}_{\mathrm{f}i}(t) \right) + 2\tilde{d}_{\mathrm{f}}^{\mathrm{T}}(t) \Gamma^{-1} \left(\Gamma \mathrm{Proj} \left[\hat{d}_{\mathrm{f}i}(t), e_i^{\mathrm{T}}(t) P B_1 \right] \right) \\ &\leq -e_i^{\mathrm{T}}(t) R e_i(t). \end{aligned} \tag{75}$$

Now, by introducing

$$\mathcal{V}_1(e(t), \tilde{w}(t)) = \sum_{i=1}^{N_{\mathrm{F}}} \mathcal{V}_{1i}(e_i(t), \tilde{d}_{\mathrm{f}i}(t)), \tag{76}$$

it follows from (75) that

$$\dot{\mathcal{V}}_1(\cdot) \leq -e^{\mathrm{T}}(t) (I_{N_{\mathrm{F}}} \otimes R) e(t). \tag{77}$$

Next, consider

$$\mathcal{V}_2(\tilde{\xi}(t)) = \tilde{\xi}^{\mathrm{T}}(t)\mathcal{P}\tilde{\xi}(t), \tag{78}$$

where since $\mathcal{A}(\mathcal{G})$ is Hurwitz, it follows from converse Lyapunov theory [34] that there is exists a unique $\mathcal{P} \in \mathbb{R}_+^{n_\xi \times n_\xi} \cap \mathbb{S}_+^{n_\xi \times n_\xi}$ satisfying

$$0 = \mathcal{A}(\mathcal{G})^{\mathrm{T}}\mathcal{P} + \mathcal{P}\mathcal{A}(\mathcal{G}) + \mathcal{R}, \tag{79}$$

with given $\mathcal{R} \in \mathbb{R}_+^{n_\xi \times n_\xi} \cap \mathbb{S}_+^{n_\xi \times n_\xi}$. Furthermore, note that $\mathcal{V}_2(0) = 0$, $\mathcal{V}_2(\tilde{\xi}(t)) > 0$ for all $\tilde{\xi}(t) \neq 0$, and $\mathcal{V}_2(\tilde{\xi}(t))$ is radially unbounded. Differentiation of (78) yields

$$\begin{aligned}\dot{\mathcal{V}}_2(\tilde{\xi}(t)) &= 2\tilde{\xi}^{\mathrm{T}}(t)\mathcal{P}\left(\mathcal{A}(\mathcal{G})\tilde{\xi}(t) + \mathcal{E}(\mathcal{G})e(t)\right)\\ &= -\tilde{\xi}^{\mathrm{T}}(t)\mathcal{R}\tilde{\xi}(t) + 2\tilde{\xi}^{\mathrm{T}}(t)\mathcal{P}\mathcal{E}(\mathcal{G})e(t).\end{aligned} \tag{80}$$

Applying Young's inequality [35] to the last term of (80) gives

$$2\tilde{\xi}^{\mathrm{T}}(t)\mathcal{P}\mathcal{E}(\mathcal{G})e(t) \leq \frac{1}{k}e^{\mathrm{T}}(t)\mathcal{E}(\mathcal{G})^{\mathrm{T}}\mathcal{P}^2\mathcal{E}(\mathcal{G})e(t) + k\tilde{\xi}^{\mathrm{T}}(t)\tilde{\xi}(t), \tag{81}$$

where $k \in \mathbb{R}_+$ is an arbitrary constant that satisfies $\mathcal{R} - kI_{n_\xi} > 0$. Now, using (81) in (80) yields

$$\dot{\mathcal{V}}_2(\tilde{\xi}(t)) \leq -\tilde{\xi}^{\mathrm{T}}(t)\left(\mathcal{R} - kI_{n_\xi}\right)\tilde{\xi}(t) + \frac{1}{k}e^{\mathrm{T}}(t)\mathcal{E}(\mathcal{G})^{\mathrm{T}}\mathcal{P}^2\mathcal{E}(\mathcal{G})e(t). \tag{82}$$

Consider now, the Lyapunov function candidate using (76) and (78) as

$$\mathcal{V}_{\mathrm{s}}(e(t), \tilde{\xi}(t), \tilde{w}(t)) = \mathcal{V}_1(e(t), \tilde{w}(t)) + \alpha\mathcal{V}_2(\tilde{\xi}(t)), \tag{83}$$

where $\alpha \triangleq k\tilde{\alpha} \in \mathbb{R}_+$ satisfies $I_{N_\mathrm{F}} \otimes R - \tilde{\alpha}\mathcal{E}(\mathcal{G})^{\mathrm{T}}\mathcal{P}^2\mathcal{E}(\mathcal{G}) > 0$. Differentiating (83) along (55), (86), and (64), and defining $\mathcal{Q}_1 \triangleq I_{N_\mathrm{F}} \otimes R - \tilde{\alpha}\mathcal{E}(\mathcal{G})^{\mathrm{T}}\mathcal{P}^2\mathcal{E}(\mathcal{G}) > 0$ and $\mathcal{Q}_2 \triangleq \alpha(\mathcal{R} - kI_{n_\xi}) > 0$, it follows from (77) and (82) that

$$\dot{\mathcal{V}}_{\mathrm{s}}(\cdot) \leq -e^{\mathrm{T}}(t)\mathcal{Q}_1 e(t) - \tilde{\xi}^{\mathrm{T}}(t)\mathcal{Q}_2\tilde{\xi}(t) \leq 0, \quad t \geq 0. \tag{84}$$

Hence, the solution $(e(t), \tilde{\xi}(t), \tilde{w}(t))$ is Lyapunov stable for all $(e(0), \tilde{\xi}(0), \tilde{w}(0))$ and $t \in \overline{\mathbb{R}}_+$.

Finally, since $e_i(t), i = 1, \cdots, N_\mathrm{F}$, in (55), is bounded for all $t \in \overline{\mathbb{R}}_+$, $e(t)$ is bounded for all $t \in \overline{\mathbb{R}}_+$. Therefore, $\ddot{\mathcal{V}}_{\mathrm{s}}(e(t), \tilde{\xi}(t), \tilde{w}(t))$ is bounded for all $t \in \overline{\mathbb{R}}_+$. Now, it follows from Barbalat's Lemma [31] that

$$\lim_{t\to\infty} \dot{\mathcal{V}}_{\mathrm{s}}(e(t), \tilde{\xi}(t), \tilde{w}(t)) = 0, \tag{85}$$

which consequently shows that $\lim_{t\to\infty} e(t) = 0$ and $\lim_{t\to\infty} \tilde{\xi}(t) = 0$. Then, this completes the proof. ■

Remark 5 *Theorem 3 shows that* $\lim_{t\to\infty} \tilde{\xi}(t) = \lim_{t\to\infty} \xi(t) - \bar{\xi}(t) = 0$*, and hence the solution of (64) converges to the solution of (68) asymptotically. Then the solution of (64) is bounded for vehicle* $i, i = 1, \cdots, N_F$ *since in Remark 4, (64) is* $\mathcal{L}_\infty$ *stable. Theorem 3 in addition implies that the solution of (12) is bounded since the solution of (64) is partitioned as* $\xi \triangleq [q_m^{\mathrm{T}}(t),\ \theta^{\mathrm{T}}(t),\ \nu^{\mathrm{T}}(t)]^{\mathrm{T}}$ *and* $\lim_{t\to\infty} e(t) = 0$*. Therefore, the trajectories of overall mulrivehicle system are bounded. In addition, Theorem 3 implies that the convergence properties of overall multivehicle system in (64) are identical to the convergence properties of (68) since* $q(t) \to q_m(t)$ *and* $\xi(t) \to \bar{\xi}(t)$ *as* $t \to \infty$.

5.2. Time-varying Disturbance Case. In order to analyze the stability of the overall multivehicle system in case of ith follower vehicle, $i = 1, \cdots, N_\mathrm{F}$, has time-varying disturbance, consider the vehicle error dynamics given by (51) and consider the weight update

error dynamics given by

$$\dot{\hat{d}}_{\mathrm{f}i}(t) = \Gamma \mathrm{Proj}\left[\hat{d}_{\mathrm{f}i}(t), e_i^{\mathrm{T}}(t)PB_1\right] - \dot{d}_{\mathrm{f}i}(t), \tag{86}$$

for vehicle $i, i = 1, \cdots, N_{\mathrm{F}}$. In addition, consider the compact form of the vehicle reference model and cooperative control given by (64).

Theorem 4 *Consider a multivehicle system consisting of N_F nonlinear uncertain vehicles with the dynamics given by (39), for $i = 1, \cdots, N_F$, with time-varying input disturbance, subject to Assumption 1, the reference model given by (50), the virtual vehicle-level controller given by (47), (48), (52), and (53). In addition, let the virtual local cooperative control for vehicle $i = 1, \cdots, N_F$, be given by (56), (57), and (58), such that (65) is Hurwitz. Then, the solution $(e(t), \tilde{\xi}(t), \tilde{w}(t))$ is uniformly ultimately bounded for all initial conditions.*

Proof. To show uniform ultimate boundedness of the solution $(e(t), \tilde{\xi}(t), \tilde{w}(t))$ for all $(e(0), \tilde{\xi}(0), \tilde{w}(0)) \in \mathbb{R}^{N_{\mathrm{F}}ln} \times \mathbb{R}^{n_\xi} \times \mathbb{R}^{N_{\mathrm{F}}l}$ and $t \in \overline{\mathbb{R}}_+$, first consider (74) and note that $\mathcal{V}_{1i}(0,0) = 0$, $\mathcal{V}_{1i}(e_i(t), \tilde{d}_{\mathrm{f}i}(t)) > 0$ for all $(e_i(t), \tilde{d}_{\mathrm{f}i}(t)) \neq (0,0)$, and $\mathcal{V}_{1i}(e_i(t), \tilde{d}_{\mathrm{f}i}(t))$ is radially unbounded. The time derivative of (74) is then given by

$$\begin{aligned}\dot{\mathcal{V}}_{1i}(\cdot) &= 2e_i^{\mathrm{T}}(t)P\left(A_{\mathrm{m}}e_i(t) - B_1\tilde{d}_{\mathrm{f}i}(t)\right) + 2\tilde{d}_{\mathrm{f}}^{\mathrm{T}}(t)\Gamma^{-1}\left(\Gamma\mathrm{Proj}\left[\hat{d}_{\mathrm{f}i}(t), e_i^{\mathrm{T}}(t)PB_1\right] - \dot{d}_{\mathrm{f}i}(t)\right) \\ &\leq -e_i^{\mathrm{T}}(t)Re_i(t) - 2\tilde{d}_{\mathrm{f}i}^{\mathrm{T}}(t)\Gamma^{-1}\dot{d}_{\mathrm{f}i}(t).\end{aligned} \tag{87}$$

Now, by introducing (76), it follows from (87) that

$$\dot{\mathcal{V}}_1(\cdot) \leq -e^{\mathrm{T}}(t)(I_{N_{\mathrm{F}}} \otimes R)e(t) - 2\tilde{w}^{\mathrm{T}}(t)(I_{N_{\mathrm{F}}} \otimes \Gamma^{-1})\dot{w}(t). \tag{88}$$

Next, consider (78), where since $\mathcal{A}(\mathcal{G})$ is Hurwitz, it follows from converse Lyapunov theory [34] that there is exists a unique $\mathcal{P} \in \mathbb{R}_+^{n_\xi \times n_\xi} \cap \mathbb{S}_+^{n_\xi \times n_\xi}$ satisfying (79) with given $\mathcal{R} \in \mathbb{R}_+^{n_\xi \times n_\xi} \cap \mathbb{S}_+^{n_\xi \times n_\xi}$. Furthermore, note that $\mathcal{V}_2(0) = 0$, $\mathcal{V}_2(\xi(t)) > 0$ for all $\tilde{\xi}(t) \neq 0$, and $\mathcal{V}_2(\tilde{\xi}(t))$ is radially unbounded. Differentiation of (78) yields (80). Consider

now, the Lyapnunov function candidate using (76) and (78) as (83), where $\alpha \triangleq k\tilde{\alpha} \in \mathbb{R}_+$ satisfies $I_{N_\mathrm{F}} \otimes R - \tilde{\alpha}\mathcal{E}(\mathcal{G})^\mathrm{T}\mathcal{P}^2\mathcal{E}(\mathcal{G}) > 0$. Differentiating (83) along (55), (86), and (64), and defining $\mathcal{Q}_1 \triangleq I_{N_\mathrm{F}} \otimes R - \tilde{\alpha}\mathcal{E}(\mathcal{G})^\mathrm{T}\mathcal{P}^2\mathcal{E}(\mathcal{G}) > 0$ and $\mathcal{Q}_2 \triangleq \alpha(\mathcal{R} - kI_{n_\xi}) > 0$, it follows from (88) and (82) that

$$\begin{aligned}\dot{\mathcal{V}}_\mathrm{s}(\cdot) \leq & - e^\mathrm{T}(t)\mathcal{Q}_1 e(t) - \tilde{\xi}^\mathrm{T}(t)\mathcal{Q}_2\tilde{\xi}(t) - 2\tilde{w}^\mathrm{T}(t)(I_{N_\mathrm{F}} \otimes \Gamma^{-1})\dot{w}(t)\\ \leq & - \lambda_{\min}(\mathcal{Q}_1)\|e(t)\|^2 - \lambda_{\min}(\mathcal{Q}_2)\|\tilde{\xi}(t)\|^2 + d_1, \end{aligned} \tag{89}$$

where $d_1 \triangleq 2\tilde{w}^*\|(I_{N_\mathrm{F}} \otimes \Gamma^{-1})\|_\mathrm{F}\dot{w}^*$ with $\|\tilde{w}(t)\| \leq \tilde{w}^*$ due to utilizing the projection operator in the weight update law given by (86) and $\|\dot{w}(t)\| \leq \dot{w}^*$. Now, it shows that $\dot{\mathcal{V}}(e(t), \tilde{\xi}(t), \tilde{w}(t)) < 0$ when either $\|e_i(t)\| \geq \psi_1$ or $\left\|\tilde{\xi}(t)\right\| \geq \psi_2$, where $\psi_1 \triangleq \sqrt{d_1/\lambda_{\min}(\mathcal{Q}_1)}$ and $\psi_2 \triangleq \sqrt{d_1/\lambda_{\min}(\mathcal{Q}_2)}$. This argument proves uniform ultimate boundedness of the closed-loop solution $(e(t), \tilde{\xi}(t), \tilde{w}(t))$ for all initial conditions [31, 28]. ■

The next corollary presents a computation of the ultimate bound.

Corollary 2 *Consider a multivehicle system consisting of N_F nonlinear uncertain vehicles with the dynamics given by (39), for $i = 1, \cdots, N_F$, with time-varying input disturbance, subject to Assumption 1, the reference model given by (50), the virtual vehicle-level controller given by (47), (48), (52), (52), and (53). In addition, let the virtual local cooperative control for vehicle $i = 1, \cdots, N_F$, be given by (56), (57), and (58), such that (65) is Hurwitz. Then, the ultimate bound of the solution $(e(t), \tilde{\xi}(t), \tilde{w}(t))$ is given by*

$$||e(t)|| \leq \tilde{\Phi}\lambda_{\min}^{-\frac{1}{2}}(P), \quad t \geq T \tag{90}$$

and

$$||\tilde{\xi}(t)|| \leq \tilde{\Phi}\lambda_{\min}^{-\frac{1}{2}}(\mathcal{P}), \quad t \geq T \tag{91}$$

where $\tilde{\Phi} \triangleq \left[\lambda_{\max}(P)\psi_1^2 + \lambda_{\max}(\mathcal{P})\psi_2^2 + \lambda_{max}(\Gamma^{-1})\tilde{w}^{*2}\right]^{\frac{1}{2}}$.

Proof. It follows from the proof of Theorem 4 that $\dot{\mathcal{V}}(e(t),\tilde{\xi}(t),\tilde{w}(t)) < 0$ outside the compact set given by $\mathcal{S} \triangleq \left\{(e(t),\tilde{\xi}(t)) : \|e(t)\| \leq \psi_1\right\} \bigcap \{(e(t),\tilde{\xi}(t)) : \left\|\tilde{\xi}(t)\right\| \leq \psi_2\}$. That is, since $\dot{\mathcal{V}}(e(t),\tilde{\xi}(t),\tilde{w}(t)) < 0$, $\mathcal{V}(e(t),\tilde{\xi}(t),\tilde{w}(t))$ cannot grow outside $\mathcal{S}$, and hence, evolution of $\mathcal{V}(e(t),\tilde{\xi}(t),\tilde{w}(t))$ is upper bounded by $\mathcal{V}(e(t),\tilde{\xi}(t),\tilde{w}(t)) \leq \max_{(e(t),\tilde{\xi}(t))\in\mathcal{S}} \mathcal{V}(e(t),\tilde{\xi}(t),\tilde{w}(t)) = \lambda_{\max}(P)\psi_1^2 + \lambda_{\max}(\mathcal{P})\psi_2^2 + \lambda_{\max}(\Gamma^{-1})\tilde{w}^{*2} = \tilde{\Phi}^2$. Now, it follows from $e^{\mathrm{T}}(t)(I_{N_{\mathrm{F}}}\otimes P)e(t) \leq \mathcal{V}(e(t),\tilde{\xi}(t),\tilde{w}(t))$ and $\tilde{\xi}(t)^{\mathrm{T}}\mathcal{P}\tilde{\xi}(t) \leq \mathcal{V}(e(t),\tilde{\xi}(t),\tilde{w}(t))$ that $\|e(t)\|^2 \leq \frac{\tilde{\Phi}^2}{\lambda_{\min}(P)}$ and $\left\|\tilde{\xi}(t)\right\|^2 \leq \frac{\tilde{\Phi}^2}{\lambda_{\min}(\mathcal{P})}$. ■

Remark 6 *Theorem 4 shows that the solution of (64) differs that the solution of (68) with uniform ultimate bound. Then the solution of (64) is bounded for vehicle $i, i = 1,\cdots,N_F$ since in Remark 4, (64) is $\mathcal{L}_\infty$ stable. Theorem 4 in addition implies that the solution of (12) is bounded since the solution of (64) is partitioned as $\xi \triangleq [q_m^{\mathrm{T}}(t),\ \theta^{\mathrm{T}}(t),\ \nu^{\mathrm{T}}(t)]^{\mathrm{T}}$ and $e(t)$ is uniformly ultimately bounded. Therefore, the trajectories of overall mulrivehicle system are bounded. In addition, Theorem 4 implies that the convergence properties of overall multivehicle system in (64) are different than the convergence properties of (68) with uniform ultimate bound since $\|q(t) - q_m(t)\| \leq \tilde{\Phi}\lambda_{\min}^{-\frac{1}{2}}(P)$ and $\left\|\xi(t) - \bar{\xi}(t)\right\| \leq \tilde{\Phi}\lambda_{\min}^{-\frac{1}{2}}(\mathcal{P})$ at $t \geq T$.*

5.3. Low-frequency Learning in Adaptive Control: A Practical Extension. To address the high-frequency oscillation prevalent in standard adaptive control with high gain feedback [36], let $\hat{w}_{\mathrm{f}i}(t) \in \mathbb{R}^l, t \geq 0$, be a low-pass filter weight estimate of $\hat{d}_{\mathrm{f}i}(t) \in \mathbb{R}^l, t \geq 0$, given by

$$\dot{\hat{w}}_{\mathrm{f}i}(t) = \Gamma_{\mathrm{f}}\left[\hat{d}_{\mathrm{f}i}(t) - \hat{w}_{\mathrm{f}i}(t)\right], \quad \hat{w}_{\mathrm{f}i}(0)\hat{w}_{\mathrm{f}i0}, \quad t \geq 0, \tag{92}$$

where $\Gamma_{\mathrm{f}} \in \mathbb{R}^{l\times l}$ a positive-definite filter gain matrix. Note that since $\hat{w}_{\mathrm{f}i}(t) \in \mathbb{R}^l, t \geq 0$, is low pass-filter estimate of $\hat{d}_{\mathrm{f}i}(t) \in \mathbb{R}^l, t \geq 0$, the filter gain matrix Γ_{f} is chosen such that $\lambda_{\max}(\Gamma_{\mathrm{f}}) \leq \gamma_{\mathrm{f,max}}$, where $\gamma_{\mathrm{f,max}} > 0$ is design parameter. Next, the modified update law can

be formulated by [36]

$$\dot{\hat{d}}_{\mathrm{fi}}(t) = \Gamma\mathrm{Proj}\left[\hat{d}_{\mathrm{fi}}(t), e_i^{\mathrm{T}}(t)PB_1 - \sigma\left(\hat{d}_{\mathrm{fi}}(t) - \hat{w}_{\mathrm{fi}}(t)\right)\right], \quad \hat{d}_{\mathrm{fi}}(0) = \hat{d}_{\mathrm{f0}i}, \quad t \geq 0, \tag{93}$$

where $\sigma > 0$ is a modification gain. Define $\tilde{w}_{\mathrm{fi}}(t) \triangleq \hat{w}_{\mathrm{fi}}(t) - d_{\mathrm{fi}}(t)$. Then, the weight update error and filtered weight update error dynamics are respectively given by

$$\dot{\tilde{d}}_{\mathrm{fi}}(t) = \Gamma\mathrm{Proj}\left[\hat{d}_{\mathrm{fi}}(t), e_i^{\mathrm{T}}(t)PB_1 - \sigma\left(\hat{d}_{\mathrm{fi}}(t) - \hat{w}_{\mathrm{fi}}(t)\right)\right] - \dot{d}_{\mathrm{fi}}(t), \quad \tilde{d}_{\mathrm{fi}}(0) = \tilde{d}_{\mathrm{f0}i}, \quad t \geq 0, \tag{94}$$

$$\dot{\tilde{w}}_{\mathrm{fi}}(t) = \Gamma_{\mathrm{f}}\left[\hat{d}_{\mathrm{fi}}(t) - \hat{w}_{\mathrm{fi}}(t)\right] - \dot{d}_{\mathrm{fi}}(t), \quad \tilde{w}_{\mathrm{fi}}(0) = \tilde{w}_{\mathrm{fi}0}, \quad t \geq 0, \tag{95}$$

for vehicle $i, i = 1, \cdots, N_{\mathrm{F}}$. Furthermore, let $\tilde{w}_{\mathrm{f}}(t) \triangleq [\tilde{w}_{\mathrm{f1}}^{\mathrm{T}}(t), \cdots, \tilde{w}_{\mathrm{f}N_{\mathrm{F}}}^{\mathrm{T}}(t)]^{\mathrm{T}} \in \mathbb{R}^{N_{\mathrm{F}}l}$. The next theorem presents the system stability analysis of the overall multivehicle system in the presennce of the modified update law and is the second main result of this section.

Theorem 5 *Consider a multivehicle system consisting of N_F nonlinear uncertain vehicles with the dynamics given by (39), for $i = 1, \cdots, N_F$, with time-varying input disturbance, subject to Assumption 1, the reference model given by (50), the virtual vehicle-level controller given by (47), (48), (52), with the update laws (92) and (93). In addition, let the virtual local cooperative control for vehicle $i = 1, \cdots, N_F$, be given by (56), (57), and (58), such that (65) is Hurwitz. Then, the solution $(e(t), \tilde{\xi}(t), \tilde{w}(t), \tilde{w}_f(t))$ is uniformly ultimately bounded for all initial conditions.*

Proof. To show uniform ultimate boundedness of the solution $(e(t), \xi(t), \tilde{w}(t), \tilde{w}_{\mathrm{f}}(t))$ for all $(e(0), \xi(0), \tilde{w}(0),$
$\tilde{w}_{\mathrm{f}}(0)) \in \mathbb{R}^{N_{\mathrm{F}}ln} \times \mathbb{R}^{n_\xi} \times \mathbb{R}^{N_{\mathrm{F}}l} \times \mathbb{R}^{N_{\mathrm{F}}l}$ and $t \in \overline{\mathbb{R}}_+$, first consider

$$\mathcal{V}_{1i}(e_i(t), \tilde{d}_{\mathrm{fi}}(t), \tilde{w}_{\mathrm{fi}}(t)) = e_i^{\mathrm{T}}(t)Pe_i(t) + \tilde{d}_{\mathrm{fi}}^{\mathrm{T}}(t)\Gamma^{-1}\tilde{d}_{\mathrm{fi}}(t) + \sigma\tilde{w}_{\mathrm{fi}}^{\mathrm{T}}(t)\Gamma_{\mathrm{f}}^{-1}\tilde{w}_{\mathrm{fi}}(t), \tag{96}$$

and note that $\mathcal{V}_{1i}(0,0,0) = 0$, $\mathcal{V}_{1i}(e_i(t),\tilde{d}_{\mathrm{f}i}(t),\tilde{w}_{\mathrm{f}i}(t)) > 0$ for all $(e_i(t),\tilde{d}_{\mathrm{f}i}(t),\tilde{w}_{\mathrm{f}i}(t)) \neq (0,0,0)$, and $\mathcal{V}_{1i}(e_i(t),$
$\tilde{d}_{\mathrm{f}i}(t),\tilde{w}_{\mathrm{f}i}(t))$ is radially unbounded. The time derivative of (96) is given by

$$\begin{aligned}
\dot{\mathcal{V}}_{1i}(\cdot) = \; & 2e_i^{\mathrm{T}}(t)P\left(A_{\mathrm{m}}e_i(t) - B_1\tilde{d}_{\mathrm{f}i}(t)\right) + 2\tilde{d}_{\mathrm{f}i}^{\mathrm{T}}(t)\Gamma^{-1}\Big(\Gamma\mathrm{Proj}_{\mathrm{m}}\left[\hat{d}_{\mathrm{f}i}(t), e_i^{\mathrm{T}}(t)PB_1\right. \\
& \left.-\sigma\left(\hat{d}_{\mathrm{f}i}(t) - \hat{w}_{\mathrm{f}i}(t)\right)\right] - \dot{d}_{\mathrm{f}i}(t)\Big) + 2\sigma\tilde{w}_{\mathrm{f}i}^{\mathrm{T}}(t)\Gamma_{\mathrm{f}}^{-1}\left(\Gamma_{\mathrm{f}}\left[\tilde{d}_{\mathrm{f}i}(t) - \tilde{w}_{\mathrm{f}i}(t)\right] - \dot{d}_{\mathrm{f}i}(t)\right) \\
\leq \; & 2e_i^{\mathrm{T}}(t)PA_{\mathrm{m}}e_i(t) - 2\sigma\tilde{d}_{\mathrm{f}i}^{\mathrm{T}}(t)\left(\hat{d}_{\mathrm{f}i}(t) - \hat{w}_{\mathrm{f}i}(t)\right) - 2\tilde{d}_{\mathrm{f}i}^{\mathrm{T}}(t)\Gamma^{-1}\dot{d}_{\mathrm{f}i}(t) \\
& + 2\sigma\tilde{w}_{\mathrm{f}i}^{\mathrm{T}}(t)\left(\hat{d}_{\mathrm{f}i}(t) - \hat{w}_{\mathrm{f}i}(t)\right) - 2\sigma\tilde{w}_{\mathrm{f}i}^{\mathrm{T}}(t)\Gamma_{\mathrm{f}}^{-1}\dot{d}_{\mathrm{f}i}(t) \\
\leq \; & -e_i^{\mathrm{T}}(t)Re_i(t) - 2\sigma\left(\tilde{d}_{\mathrm{f}i}(t) - \tilde{w}_{\mathrm{f}i}(t)\right)^{\mathrm{T}}\left(\tilde{d}_{\mathrm{f}i}(t) - \tilde{w}_{\mathrm{f}i}(t)\right) - 2\tilde{d}_{\mathrm{f}i}^{\mathrm{T}}(t)\Gamma^{-1}\dot{d}_{\mathrm{f}i}(t) \\
& - 2\sigma\tilde{w}_{\mathrm{f}i}^{\mathrm{T}}(t)\Gamma_{\mathrm{f}}^{-1}\dot{d}_{\mathrm{f}i}(t). \qquad (97)
\end{aligned}$$

By introducing

$$\mathcal{V}_1(e(t),\tilde{w}(t),\tilde{w}_{\mathrm{f}}(t)) = \sum_{i=1}^{N_{\mathrm{F}}}\mathcal{V}_{1i}(e_i(t),\tilde{d}_{\mathrm{f}i}(t),\tilde{w}_{\mathrm{f}i}(t)), \qquad (98)$$

it follows from (97) that

$$\begin{aligned}
\dot{\mathcal{V}}_1(\cdot) \leq & -e^{\mathrm{T}}(t)(I_{N_{\mathrm{F}}}\otimes R)e(t) - 2\left(\tilde{d}_{\mathrm{f}}(t) - \tilde{w}_{\mathrm{f}}(t)\right)^{\mathrm{T}}(I_{N_{\mathrm{F}}}\otimes\sigma)\left(\tilde{d}_{\mathrm{f}}(t) - \tilde{w}_{\mathrm{f}}(t)\right) \\
& - 2\tilde{d}_{\mathrm{f}}^{\mathrm{T}}(t)(I_{N_{\mathrm{F}}}\otimes\Gamma^{-1})\dot{d}_{\mathrm{f}}(t) - 2\tilde{w}_{\mathrm{f}}^{\mathrm{T}}(t)(I_{N_{\mathrm{F}}}\otimes\sigma\Gamma_{\mathrm{f}}^{-1})\dot{d}_{\mathrm{f}}(t). \qquad (99)
\end{aligned}$$

Next, consider the same $\mathcal{V}_2(\tilde{\xi}(t))$ in (78) and its time derivation given by (82). Using (96) and (78), the Lyapnunov function candidate is given by

$$\mathcal{V}_{\mathrm{s}}(e(t),\tilde{\xi}(t),\tilde{w}(t),\tilde{w}_{\mathrm{f}}(t)) = \mathcal{V}_1(e(t),\tilde{w}(t),\tilde{w}_{\mathrm{f}}(t)) + \alpha\mathcal{V}_2(\tilde{\xi}(t)), \qquad (100)$$

where we let $\alpha \triangleq k\tilde{\alpha} \in \mathbb{R}_+$ to satisfy $I_{N_{\mathrm{F}}}\otimes R - \tilde{\alpha}\mathcal{E}(\mathcal{G})^{\mathrm{T}}\mathcal{P}^2\mathcal{E}(\mathcal{G}) > 0$, since it is an arbitrary constant. Differentiating (100) along (55), (64), (94), and (95), and defining $\mathcal{Q}_1 \triangleq I_{N_{\mathrm{F}}}\otimes R - \tilde{\alpha}\mathcal{E}(\mathcal{G})^{\mathrm{T}}\mathcal{P}^2\mathcal{E}(\mathcal{G}) > 0$ and $\mathcal{Q}_2 \triangleq \alpha(\mathcal{R} - kI_{n_\xi}) > 0$, it follows from (82) and (99)

that

$$\begin{aligned}\dot{\mathcal{V}}_{\rm s}(\cdot) \leq & - e^{\rm T}(t)Q_1e(t) - \tilde{\xi}^{\rm T}(t)Q_2\tilde{\xi}(t) - 2\left(\tilde{d}_{\rm f}(t) - \tilde{w}_{\rm f}(t)\right)^{\rm T}(I_{N_{\rm F}} \otimes \sigma) \\ & \cdot \left(\tilde{d}_{\rm f}(t) - \tilde{w}_{\rm f}(t)\right) - 2\tilde{d}_{\rm f}^{\rm T}(t)(I_{N_{\rm F}} \otimes \Gamma^{-1})\dot{d}_{\rm f}(t) - 2\tilde{w}_{\rm f}^{\rm T}(t)(I_{N_{\rm F}} \otimes \sigma\Gamma_{\rm f}^{-1})\dot{d}_{\rm f}(t) \\ \leq & - \lambda_{\min}(Q_1)\|e(t)\|^2 - \lambda_{\min}(Q_2)\|\tilde{\xi}(t)\|^2 - 2\|I_{N_{\rm F}} \otimes \sigma\|\|\tilde{d}_{\rm f}(t) - \tilde{w}_{\rm f}(t)\|^2 \\ & + 2\|\tilde{w}(t)\|_{\rm F}\|(I_{N_{\rm F}} \otimes \Gamma^{-1})\|_{\rm F}\|\dot{w}(t)\|_{\rm F} + 2\|\tilde{w}_{\rm f}(t)\|_{\rm F}\|(I_{N_{\rm F}} \otimes \sigma\Gamma_{\rm f}^{-1})\|_{\rm F}\|\dot{w}(t)\|_{\rm F} \\ \leq & - \lambda_{\min}(Q_1)\|e(t)\|^2 - \lambda_{\min}(Q_2)\|\tilde{\xi}(t)\|^2 - d_1\|\tilde{d}_{\rm f}(t) - \tilde{w}_{\rm f}(t)\|^2 + d_2, \end{aligned} \tag{101}$$

where $d_1 \triangleq 2\|I_{N_{\rm F}} \otimes \sigma\|$, and $d_2 \triangleq 2\tilde{w}^*\|(I_{N_{\rm F}} \otimes \Gamma^{-1})\|_{\rm F}\dot{w}^* + 2\tilde{w}_{\rm f}^*\|(I_{N_{\rm F}} \otimes \sigma\Gamma_{\rm f}^{-1})\|_{\rm F}\dot{w}^*$ with $\|\tilde{w}_{\rm f}(t)\| \leq \tilde{w}_{\rm f}^*$. Now, it shows that $\dot{\mathcal{V}}(e(t), \tilde{\xi}(t), \tilde{w}(t), \tilde{w}_{\rm f}(t)) < 0$ when $\|e(t)\| \geq \psi_1$, or $\left\|\tilde{\xi}(t)\right\| \geq \psi_2$, where $\psi_1 \triangleq \sqrt{d_2/\lambda_{\min}(Q_1)}$ and $\psi_2 \triangleq \sqrt{d_2/\lambda_{\min}(Q_2)}$. This argument proves uniform ultimate boundedness of the closed-loop solution $(e(t), \tilde{\xi}(t), \tilde{w}(t), \tilde{w}_{\rm f}(t))$ for all initial conditions [31, 28]. ■

Corollary 3 *Consider a multivehicle system consisting of N_F nonlinear uncertain vehicles with the dynamics given by (39), for $i = 1, \cdots, N_F$, with time-varying input disturbance, subject to Assumption 1, the reference model given by (50), the virtual vehicle-level controller given by (47), (48), (52), with the update laws (92) and (93). In addition, let the virtual local cooperative control for vehicle $i = 1, \cdots, N_F$, be given by (56), (57), and (58), such that (65) is Hurwitz. Then, the ultimate bound of the solution $(e(t), \tilde{\xi}(t), \tilde{w}(t), \tilde{w}_f(t))$ is given by*

$$||e(t)|| \leq \tilde{\Phi}\lambda_{\min}^{-\frac{1}{2}}(P), \quad t \geq T \tag{102}$$

and

$$||\tilde{\xi}(t)|| \leq \tilde{\Phi}\lambda_{\min}^{-\frac{1}{2}}(\mathcal{P}), \quad t \geq T \tag{103}$$

where $\tilde{\Phi} \triangleq \left[\lambda_{\max}(P)\psi_1^2 + \lambda_{\max}(\mathcal{P})\psi_2^2 + \lambda_{\max}(\Gamma^{-1})\tilde{w}^{*2} + \sigma\lambda_{\max}(\Gamma_f^{-1})\tilde{w}_f^{*2}\right]^{\frac{1}{2}}$.

Proof. The proof follows using similar steps as the proof of Corollary 2, and hence, is omitted. ■

6. CONVERGENCE ANALYSIS OF THE (OF)^{2}AC

This section shows that the (OF)^{2}AC method solves the containment problem. For overall system analysis purpose, let $A_{\mathrm{L}} \triangleq \text{block-diag}(A_{\mathrm{L}1}, \cdots, A_{\mathrm{L}N_{\mathrm{L}}}) \in \mathbb{R}^{n_{\mathrm{L}} \times n_{\mathrm{L}}}$, $B_{\mathrm{L}} \triangleq \text{block-diag}(B_{\mathrm{L}1}, \cdots, B_{\mathrm{L}N_{\mathrm{L}}}) \in \mathbb{R}^{n_{\mathrm{L}} \times m_{\mathrm{L}}}$, $C_{\mathrm{L}} \triangleq \text{block-diag}(C_{\mathrm{L}1}^{\mathrm{T}}, \cdots, C_{\mathrm{L}N_{\mathrm{L}}}^{\mathrm{T}})^{\mathrm{T}} \in \mathbb{R}^{N_{\mathrm{L}} l \times n_{\mathrm{L}}}$, and $c(t) \triangleq [c_1^{\mathrm{T}}(t), \cdots, c_{N_{\mathrm{L}}}^{\mathrm{T}}(t)]^{\mathrm{T}} \in \mathbb{R}^{m_{\mathrm{L}}}$, with $\|c(t)\| \leq c^*$, where $n_{\mathrm{L}} = \sum_{i=1}^{N_{\mathrm{L}}} n_i$, and $m_{\mathrm{L}} = \sum_{i=1}^{N_{\mathrm{L}}} m_i$. Further more, let the solution of (68) be partitioned as $\bar{\xi} \triangleq [\bar{q}_{\mathrm{m}}^{\mathrm{T}}(t), \bar{\theta}^{\mathrm{T}}(t), \bar{\nu}^{\mathrm{T}}(t)]^{\mathrm{T}} \in \mathbb{R}^{n_\xi}$, with $\bar{q}_{\mathrm{m}}(t) \in \mathbb{R}^{N_{\mathrm{F}} l n}$, $\bar{\theta}(t) \in \mathbb{R}^{N_{\mathrm{F}} l}$, and $\bar{\nu}(t) \in \mathbb{R}^{N_{\mathrm{F}} l}$. Finally, let $\bar{y}_{\mathrm{m}}(t) \triangleq (I_{N_{\mathrm{F}}} \otimes C_q)\bar{q}_{\mathrm{m}}(t) \in \mathbb{R}^{N_{\mathrm{F}} l}$ and $M(\mathcal{G}) \triangleq F(\mathcal{G})^{-1} G(\mathcal{G})$.

Theorem 6 *Consider a multivehicle system consisting of N_F nonlinear uncertain vehicles with the dynamics given by (39), for $i = 1, \cdots, N_F$, subject to Assumption 1, the reference model given by (50), the virtual vehicle-level controller given by (47), (48), (52), and (53). In addition, let the virtual local cooperative control for vehicle $i = 1, \cdots, N_F$, be given by (56), (57), and (58), such that (69) is Hurwitz for $i = 1, \cdots, N_F$. Furthermore, consider the leader dynamics given by (31) and (32) for $i = 1, \cdots, N_L$. First, if the reference command is constant (i.e. $\dot{c}_i^* = 0, i = 1, \cdots, N_L$), then $\bar{y}_m(t) \to (M(\mathcal{G}) \otimes I_l) y_L(t)$ as $t \to \infty$; that is $\bar{y}_{mi}, i = 1, \cdots, N_F$, asymptotically converge to the convex hull formed by the leaders. If, in addition, $N_L = 1$, then $\bar{y}_m(t) \to \mathbf{1}_{N_F} \otimes y_{L1}(t)$ as $t \to \infty$; that is $y_{mi}, i = 1, \cdots, N_F$, asymptotically converge to the output of the leader. Second, if reference command is time varying with bounded time rate of change, then $\bar{y}_m(t)$ converge to the neighborhood of the convex hull formed by $(M(\mathcal{G}) \otimes I_l) y_L(t)$ as $t \to \infty$. If, in addition, $N_L = 1$, then $\bar{y}_m(t)$ converge to the neighborhood of $\mathbf{1}_{N_F} \otimes y_{L1}(t)$ as $t \to \infty$; that is $\bar{y}_{mi}, i = 1, \cdots, N_F$, converge to the neighborhood of the output of the leader.*

Proof. Let $\bar{\mathcal{Z}}(t) \triangleq [x_{\mathrm{L}}^{\mathrm{T}}(t), \bar{\xi}^{\mathrm{T}}(t)]^{\mathrm{T}} \in \mathbb{R}^{n_{\mathrm{L}}+n_{\xi}}$, then, (31) and (68) can be written in the compact form as

$$\dot{\bar{\mathcal{Z}}}(t) = \mathcal{A}_z(\mathcal{G})\bar{\mathcal{Z}}(t) + \mathcal{B}_z c(t), \quad \bar{\mathcal{Z}}(0) = \bar{\mathcal{Z}}_0, \quad t \geq 0, \tag{104}$$

where

$$\mathcal{A}_z(\mathcal{G}) = \begin{bmatrix} A_{\mathrm{L}} & 0 \\ B(\mathcal{G})C_{\mathrm{L}} & A(\mathcal{G}) \end{bmatrix} \in \mathbb{R}^{(n_{\mathrm{L}}+n_{\xi})\times(n_{\mathrm{L}}+n_{\xi})}, \tag{105}$$

$$\mathcal{B}_z = \begin{bmatrix} B_{\mathrm{L}} \\ 0 \end{bmatrix} \in \mathbb{R}^{(n_{\mathrm{L}}+n_{\xi})\times(m_{\mathrm{L}}+N_{\mathrm{F}}ln)}. \tag{106}$$

Since $\mathcal{A}(\mathcal{G})$ is Hurwitz as shown in Remark 4 and A_{L} is Hurwitz, it follows from the lower triangular structure of (105) that $\mathcal{A}_z(\mathcal{G})$ is Hurwitz, and hence, there exists a unique positive definite matrix P_z such that

$$0 = \mathcal{A}_z(\mathcal{G})^{\mathrm{T}}\mathcal{P}_z + \mathcal{P}_z\mathcal{A}_z(\mathcal{G}) + \mathcal{R}_z, \tag{107}$$

holds for a positive-definite matrix $\mathcal{R}_z$. Now, similar to the proposed analysis in [37], consider

$$\bar{\mathcal{H}}(t) \triangleq \bar{\mathcal{Z}}(t) + \mathcal{A}_z(\mathcal{G})^{-1}\mathcal{B}_z c(t), \tag{108}$$

where $\mathcal{A}_z(\mathcal{G})$ is invertible since it has a nonzero determinant. Using (108), consider the Lyapunov function candidate given by

$$\mathcal{V}(\bar{\mathcal{H}}(t)) = \bar{\mathcal{H}}^{\mathrm{T}}(t)\mathcal{P}_z\bar{\mathcal{H}}(t), \tag{109}$$

where $\mathcal{V}(0) = 0$, $\mathcal{V}(\bar{\mathcal{H}}(t)) > 0$ for all $\bar{\mathcal{H}}(t) \neq 0$, and $\mathcal{V}(\bar{\mathcal{H}}(t))$ is radially unbounded.

The time derivative of (109) along the trajectory of (104) and (108) is given by

$$\begin{aligned}\dot{\mathcal{V}}(\bar{\mathcal{H}}(t)) &= 2\bar{\mathcal{H}}^{\mathrm{T}}(t)\mathcal{P}_z\left(\dot{\mathcal{Z}}(t) + \mathcal{A}_z(\mathcal{G})^{-1}\mathcal{B}_z\dot{c}(t)\right)\\ &= 2\bar{\mathcal{H}}^{\mathrm{T}}\mathcal{P}_z\dot{\mathcal{Z}}(t) + 2\bar{\mathcal{H}}^{\mathrm{T}}(t)\mathcal{P}_z\mathcal{A}_z(\mathcal{G})^{-1}\mathcal{B}_z\dot{c}(t)\\ &= 2\bar{\mathcal{H}}^{\mathrm{T}}(t)\mathcal{P}_z\left(\mathcal{A}_z(\mathcal{G})\mathcal{Z}(t) + \mathcal{B}_z(\mathcal{G})\mathcal{E}_z(t)\right) + 2\bar{\mathcal{H}}^{\mathrm{T}}(t)\mathcal{P}_z\mathcal{A}_z(\mathcal{G})^{-1}\mathcal{B}_z\dot{c}(t)\\ &= 2\bar{\mathcal{H}}^{\mathrm{T}}(t)\mathcal{P}_z\mathcal{A}_z(\mathcal{G})\bar{\mathcal{H}}(t) + 2\bar{\mathcal{H}}^{\mathrm{T}}(t)\mathcal{P}_z\mathcal{A}_z(\mathcal{G})^{-1}\mathcal{B}_z\dot{c}(t)\\ &= -\bar{\mathcal{H}}^{\mathrm{T}}(t)\mathcal{R}_z\bar{\mathcal{H}}(t) + 2\bar{\mathcal{H}}^{\mathrm{T}}(t)\mathcal{P}_z\mathcal{A}_z(\mathcal{G})^{-1}\mathcal{B}_z\dot{c}(t). \end{aligned} \tag{110}$$

In the remainder of this proof, we consider two cases.

Case 1: For $\dot{c}(t) = 0$, (110) can be written as

$$\dot{\mathcal{V}}(\bar{\mathcal{H}}(t)) = -\bar{\mathcal{H}}^{\mathrm{T}}(t)\mathcal{R}_z\bar{\mathcal{H}}(t) < 0, \tag{111}$$

and hence,

$$\lim_{t\to\infty}\bar{\mathcal{H}}(t) = 0. \tag{112}$$

Next, since (112) implies $\dot{\bar{\mathcal{Z}}}(t) \to 0$ as $t \to \infty$, (104) can be written as

$$\mathcal{A}_z(\mathcal{G})\bar{\mathcal{Z}}(\infty) + \mathcal{B}_z c(\infty) = 0, \tag{113}$$

where $\bar{\mathcal{Z}}(\infty) = \lim_{t\to\infty}\bar{\mathcal{Z}}(t)$ and $c(\infty) = \lim_{t\to\infty} c(t)$. In addition, letting $x_{\mathrm{L}}(\infty) = \lim_{t\to\infty} x_{\mathrm{L}}(t)$, $\bar{q}_{\mathrm{m}}(\infty) = \lim_{t\to\infty}\bar{q}_{\mathrm{m}}(t)$, $\bar{\theta}(\infty) = \lim_{t\to\infty}\bar{\theta}(t)$, $\bar{v}(\infty) = \lim_{t\to\infty}\bar{v}(t)$, and using the definition of $\mathcal{A}_z(\mathcal{G})$ and $\mathcal{B}_z$ given by (105) and (106), respectively, in (113) we have

$$0 = A_{\mathrm{L}}x_{\mathrm{L}}(\infty) + B_{\mathrm{L}}c(\infty), \tag{114}$$

$$0 = [I_{N_\mathrm{F}} \otimes A_\mathrm{m} - F(\mathcal{G}) \otimes B_1 K_c C_q]\bar{q}_\mathrm{m}(\infty) - (G(\mathcal{G}) \otimes B_1 K_c) y_\mathrm{L}(\infty) + (I_{N_\mathrm{F}} \otimes B_1 K_c)\bar{\theta}(\infty), \tag{115}$$

$$0 = -\delta(F(\mathcal{G}) \otimes C_q)\bar{q}_\mathrm{m}(\infty) - \delta(G(\mathcal{G}) \otimes I_l) y_\mathrm{L}(\infty) - \delta\zeta\left(\bar{\theta}(\infty) - \bar{\nu}(\infty)\right), \tag{116}$$

$$0 = \eta\left(\bar{\theta}(\infty) - \bar{\nu}(\infty)\right). \tag{117}$$

Since, $\bar{\theta}(\infty) = \bar{\nu}(\infty)$ in (117), (116) follows as

$$0 = -\delta(F(\mathcal{G}) \otimes C_q)\bar{q}_\mathrm{m}(\infty) - \delta(G(\mathcal{G}) \otimes I_l) y_\mathrm{L}(\infty), \tag{118}$$

or, equivalently,

$$(F(\mathcal{G}) \otimes I_l)\bar{y}_\mathrm{m}(\infty) = -(G(\mathcal{G}) \otimes I_l) y_\mathrm{L}(\infty), \tag{119}$$

and since $(F(\mathcal{G}) \otimes I_l)$ is invertible, (119) yields

$$\bar{y}_\mathrm{m}(\infty) = -(F(\mathcal{G})^{-1} G(\mathcal{G}) \otimes I_l) y_\mathrm{L}(\infty), \tag{120}$$

and hence, $\bar{y}_{\mathrm{m}i}(t)$, $i = 1, \cdots, N_\mathrm{F}$, asymptotically converge to the convex hull formed by the leaders. In addition, if $N_\mathrm{L} = 1$, then $-F(\mathcal{G})^{-1}G(\mathcal{G}) = \mathbf{1}_{N_\mathrm{F}}$, and as a direct consequence of (120) we have

$$\begin{aligned} \bar{y}_\mathrm{m}(\infty) &= (\mathbf{1}_{N_\mathrm{F}} \otimes I_l) y_{\mathrm{L}1}(\infty) \\ &= \mathbf{1}_{N_\mathrm{F}} \otimes y_{\mathrm{L}1}(\infty), \end{aligned} \tag{121}$$

and hence, $\bar{y}_{\mathrm{m}i}(t)$, $i = 1, \cdots, N_\mathrm{F}$, asymptotically convergence to the output of the leader.

Case 2: We now consider $\|\dot{c}(t)\| \leq \dot{c}^*$, and $\dot{c}^* \in \mathbb{R}^+$. In this case, (110) follows as

$$\dot{\mathcal{V}}(\bar{\mathcal{H}}(t)) \leq -\lambda_{\min}(\mathcal{R}_z)\|\bar{\mathcal{H}}(t)\|^2 + 2\|\mathcal{P}_z \mathcal{A}_z(\mathcal{G})^{-1}\mathcal{B}_z\|_\mathrm{F}\dot{c}^*\|\bar{\mathcal{H}}(t)\|$$

$$= -\lambda_{\min}(\mathcal{R}_z)\|\bar{\mathcal{H}}(t)\|^2 + \Psi\|\bar{\mathcal{H}}(t)\|, \tag{122}$$

where $\Psi \triangleq 2\|\mathcal{P}_z\mathcal{A}_z(\mathcal{G})^{-1}\mathcal{B}_z\|_{\mathrm{F}}\dot{c}^*$. Rearranging (122), we can equivalently write

$$\dot{\mathcal{V}}(\bar{\mathcal{H}}(t)) \leq -\lambda_{\min}(\mathcal{R}_z)\|\bar{\mathcal{H}}(t)\|\left(\|\bar{\mathcal{H}}(t)\| - \frac{\Psi}{\lambda_{\min}(\mathcal{R}_z)}\right). \tag{123}$$

Therefore, $\dot{\mathcal{V}}(\bar{\mathcal{H}}(t)) < 0$ outside the compact set

$$\Omega \triangleq \left\{\bar{\mathcal{H}}(t) : \bar{\mathcal{H}}(t) \leq \frac{\Psi}{\lambda_{\min}(\mathcal{R}_z)}\right\}, \tag{124}$$

which proves uniform ultimate boundedness of the closed-loop solution $\bar{\mathcal{Z}}(t)+\mathcal{A}_z(\mathcal{G})^{-1}\mathcal{B}_z c(t)$ for all initial conditions [31]. Since $\dot{\mathcal{V}}(\bar{\mathcal{H}}(t)) < 0$ outside the compact set (124), then an ultimate bound for the distance of $\bar{\mathcal{H}}(t) \triangleq \bar{\mathcal{Z}}(t) + \mathcal{A}_z(\mathcal{G})^{-1}\mathcal{B}_z c(t)$ can be computed as

$$\|\bar{\mathcal{H}}(t)\| \leq \sqrt{\frac{\lambda_{\max}(\mathcal{P}_z)}{\lambda_{\min}(\mathcal{P}_z)}}\frac{\Psi}{\lambda_{\min}(\mathcal{R}_z)}, \quad t \geq T. \tag{125}$$

Specifically, if the right side of (125) is small, then the distance of $\bar{\mathcal{Z}}(t) + \mathcal{A}_z(\mathcal{G})^{-1}\mathcal{B}_z c(t)$ is small for $t \geq 0$. This implies $\bar{y}_{\mathrm{m}i}(t)$, $i = 1, \cdots, N_{\mathrm{F}}$, stay in the neighborhood of the convex hull formed by the leaders. In addition, if $N_{\mathrm{L}} = 1$, then $-F(\mathcal{G})^{-1}G(\mathcal{G}) = \mathbf{1}_{N_{\mathrm{F}}}$, implies $\bar{y}_{\mathrm{m}i}(t)$, $i = 1, \cdots, N_{\mathrm{F}}$, stay close to the output of the leader. ■

Remark 7 *As a direct consequence from Theorem 3 and Remark 5, $y_f(t) \to y_m(t)$ and $y_m(t) \to \bar{y}_m(t)$ as $t \to \infty$. Then first, recalling the results of constant reference input case of Theorem 6, yields $y_f(t) \to M(\mathcal{G}) \otimes I_l)y_L(t)$ as $t \to \infty$; that is $y_{fi}(t), i = 1, \cdots, N_F$, asymptotically converge to the convex hull formed by the leaders. In addition, for a single leader, $y_f(t) \to \mathbf{1}_{N_F} \otimes y_{L1}(t)$ as $t \to \infty$; that is $y_{fi}(t), i = 1, \cdots, N_F$, asymptotically converge to the output of the leader. Second, recalling the results of time-varying reference command case of Theorem 6, then since the bound of $\|\bar{y}_m(t) - y_L(t)\|$ is governed by the bound of $\|\bar{\mathcal{H}}(t)\|$ in (125), $y_f(t)$ converges with bounded divergence to the convex hull formed by $(M(\mathcal{G}) \otimes I_l)y_L(t)$ as $t \to \infty$; that is $y_{fi}(t), i = 1, \cdots, N_F$, converge to the neighborhood of*

the convex hull formed by the leaders. For a single leader in addition, $y_f(t)$ converge to the neighborhood of $\mathbf{1}_{N_F} \otimes y_{L1}(t)$ as $t \to \infty$; that is $y_{fi}(t), i = 1, \cdots, N_F$, converge to the neighborhood of the output of the leader.

Remark 8 *As a direct consequence from Theorem 4 and Remark 6, there is a uniformly ultimately bounded error in (90), yields to output error bound*

$$\left\|y_f(t) - y_m(t)\right\| + \|y_m(t) - \bar{y}_m(t)\| \leq \left\|(I_{N_F} \otimes C_q)\right\|_F \tilde{\Phi}\left(\lambda_{\min}^{-\frac{1}{2}}(P) + \lambda_{\min}^{-\frac{1}{2}}(\mathcal{P})\right),\ t \geq T, \tag{126}$$

and $y_m(t) \to \bar{y}_m(t)$ as $t \to \infty$. Then first, recalling the results of constant reference input case of Theorem 6, then, $y_f(t)$ converges to the neighborhood of the convex hull formed by $(M(\mathcal{G}) \otimes I_l) y_L(t)$ as $t \to \infty$ with uniformly ultimately bounded deviation equivalent to the right side of (126) ; that is $y_{fi}(t), i = 1, \cdots, N_F$, converge to the neighborhood of the convex hull formed by the leaders with uniformly ultimately bounded deviation. For a single leader in addition, $y_f(t)$ converge to the neighborhood of $\mathbf{1}_{N_F} \otimes y_{L1}(t)$ as $t \to \infty$ with uniformly ultimately bounded deviation; that is $y_{fi}(t), i = 1, \cdots, N_F$, converge to the neighborhood of the output of the leader with uniformly ultimately bounded deviation. Second, recalling the results of time-varying reference command case of Theorem 6, then since the bound of $\|\bar{y}_m(t) - y_L(t)\|$ is governed by the bound of $\|\bar{\mathcal{H}}(t)\|$ in (125), $y_f(t)$ converges to the neighborhood of the convex hull formed by $(M(\mathcal{G}) \otimes I_l) y_L(t)$ as $t \to \infty$ with uniformly ultimately bounded deviation

$$\left\|y_f(t) - y_L(t)\right\| \leq \left\|y_f(t) - y_m(t)\right\| + \|y_m(t) - \bar{y}_m(t)\| + \|\bar{y}_m(t) - y_L(t)\|, \tag{127}$$

that is $y_{fi}(t), i = 1, \cdots, N_F$, converge to the neighborhood of the convex hull formed by the leaders with uniformly ultimately bounded deviation. For a single leader in addition, $y_f(t)$ converge to the neighborhood of $\mathbf{1}_{N_F} \otimes y_{L1}(t)$ as $t \to \infty$ with uniformly ultimately bounded deviation; that is $y_{fi}(t), i = 1, \cdots, N_F$, converge to the neighborhood of the output of the leader with uniformly ultimately bounded deviation.

The next section illustrates the ability of the proposed adaptive output feedback controller to drive follower vehicles to the output of the leader vehicle, as well as a convex hull created by two leaders.

7. ILLUSTRATIVE NUMERICAL EXAMPLES

In this section, we present two numerical examples to demonstrate the efficacy of the $(\mathrm{OF})^2$AC for multivehicle systems. For this purpose, we consider a line graph of leader and follower vehicles. Specifically, for each follower vehicle, we consider the dynamics given by (12) and (13) with

$$A = \begin{bmatrix} 0 & 1 \\ 1 & 1 \end{bmatrix}, \quad B = \begin{bmatrix} 0 \\ 1 \end{bmatrix}, \quad C = \begin{bmatrix} 1 & 0 \end{bmatrix}, \tag{128}$$

with the different vehicle-level uncertainties given by $w_1(t) = 0.4\sin(0.4t)$, $w_2(t) = 0.6\sin(0.2t)$, $w_3(t) = 0.4\sin(0.2t)$, $w_4(t) = -0.6\sin(0.4t)$, and the intial conditions $q_{10}^{\mathrm{T}} = [0.5\ ,\ 0]$, $q_{20}^{\mathrm{T}} = [0.85\ ,\ 0]$, $q_{10}^{\mathrm{T}} = [0.5\ ,\ 0]$, $q_{30}^{\mathrm{T}} = [0.5\ ,\ 0]$, and $q_{40}^{\mathrm{T}} = [0.5\ ,\ 0]$. For the leader vehicle(s), we consider the dynamics given by (31) and (32) with $A_{\mathrm{L}} = -0.5$, $B_{\mathrm{L}} = 0.5$, $C_{\mathrm{L}} = 1$, and $x_{\mathrm{L}1}(0) = 0$. We let $\lambda = 10$ and

$$A_{\mathrm{m}} = \begin{bmatrix} 0 & 1 \\ -1 & -2 \end{bmatrix}, \tag{129}$$

to create the nominal feedback gain $K_{\mathrm{q}} = [-1\ ,\ -1.5]$, $K_{\mathrm{v}} = 0.5$. In addition, for the cooperative control design, we choose $K_{\mathrm{c}} = 1.5$, $\zeta = 1.5$, $\eta = 2$, $\delta = 5$. Furthermore, for the adaptive control design, we use $\Gamma = 80$, $R = I_2$, and

$$P = \begin{bmatrix} 1.5 & 0.5 \\ 0.5 & 0.5 \end{bmatrix}. \tag{130}$$

Finally, for the second-order follower vehicle with $d = 1$, the actual control signal given by (71) becomes

$$u_i(t) = \dot{\phi}_i(t) + 2\lambda\phi_i(t) + \lambda^2 \int_0^t \phi_i(\sigma_1)\mathrm{d}\sigma_1, \quad t \geq 0. \tag{131}$$

Throughout this section, in order to show efficacy of the proposed $(\mathrm{OF})^2$AC method, we consider both step and sine wave reference commands.

Example 1. For the first example, we consider a line graph with four follower vehicles and a single leader and our aim is to track a given reference command $c_1(t)$, $t \geq 0$. The closed-loop response along with the control signal is shown Figure 1. The proposed controller drives the multivehicle system output to the desired reference command since there is no input disturbance. Utilizing the $(\mathrm{OF})^2$AC without the adaptive controller, Figure 2 shows an undesired closed-loop response for the disturbed follower vehicle systems due to the existence of the input disturbance. Next, we employ the $(\mathrm{OF})^2$AC with the adaptive controller, where the closed-loop response along with the control signal can be seen in Figure 3. Note that the proposed controller achieves better performance in terms of command following in the presence of input disturbance, but the response still contains high-frequency oscillations. In order to remove these oscillations, we now employ the modified update law adaptive control with $\Gamma = 200$, $\Gamma_\mathrm{f} = 4$, and $\sigma = 0.1$ for step reference command, and $\Gamma = 100$, $\Gamma_\mathrm{f} = 4$, and $\sigma = 0.1$ for sine-wave reference command. As shown in Figure 4, the resulting closed-loop response is further improved by suppressing the high frequency content.

Example 2. For the second example, we consider four follower vehicles and two leaders with different reference commands. In this way, the leaders create a convex hull for the followers to (approximately) converge to. We employ the modified update law adaptive control with the same parameters as in Example 1. For a constant reference command, we consider $c(t) = [1\ ,\ 0.8]^\mathrm{T}$ as shown in Figure 5a, and in Figure 5b, we apply time varying

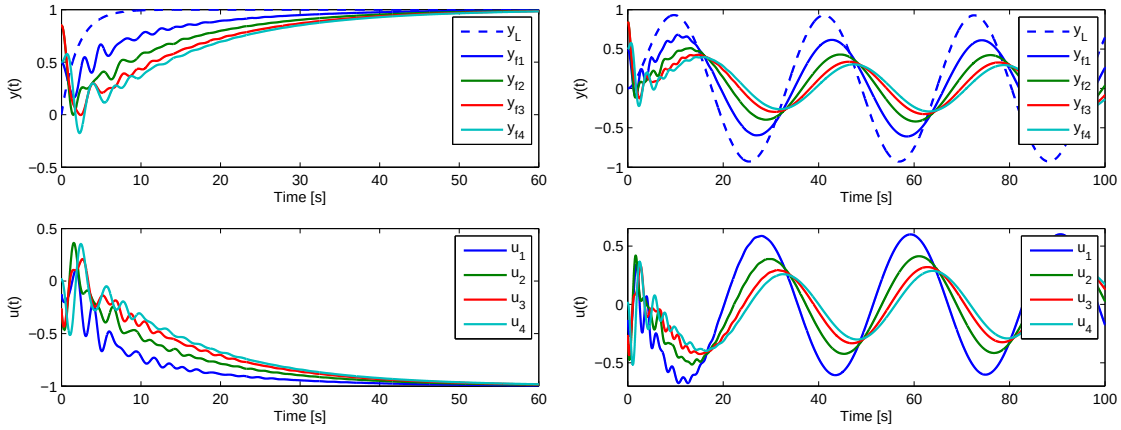

(a) Step reference command. (b) Sine-wave reference command.

Figure 1. Responses of $y(t)$, $y_{\mathrm{L}}(t)$, and $u(t)$ for the multivehicle system for Example 1.

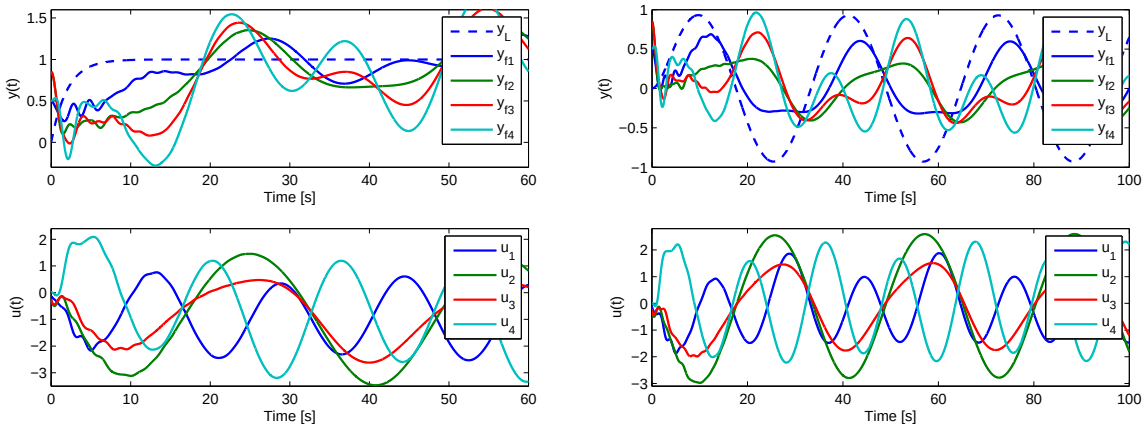

(a) Step reference command. (b) Sine-wave reference command.

Figure 2. Responses of $y(t)$, $y_{\mathrm{L}}(t)$, and $u(t)$ for the multivehicle system with input disturbance for Example 1.

commands given by $c_i(t) = (-1)^{i+1}0.8 + (-1)^{i+1}0.5\sin((0.06*i)t)$, $i = 1,2$. In both cases, it can be seen that the follower vehicles converge to the convex hull created by the leader outputs.

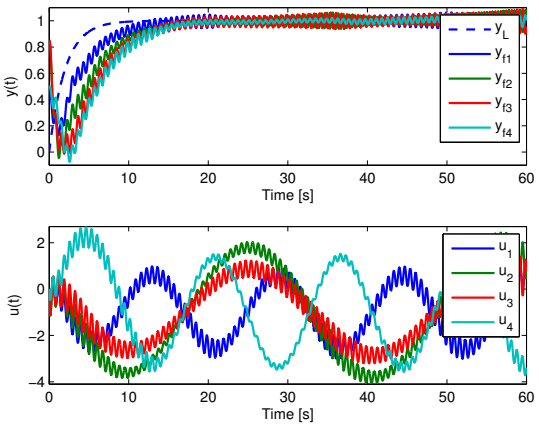

(a) Step reference command.

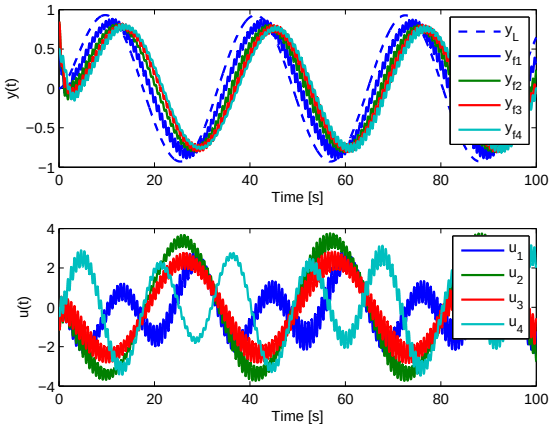

(b) Sine-wave reference command.

Figure 3. Responses of $y(t)$, $y_{\mathrm{L}}(t)$, and $u(t)$ for multivehicle system with proposed adaptive output feedback control architecture in presence of input disturbance for Example 1.

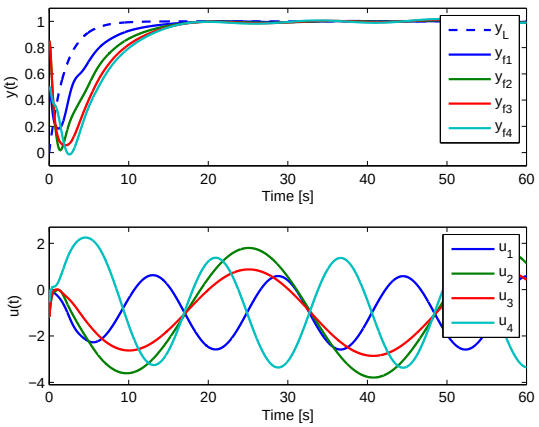

(a) Step reference command.

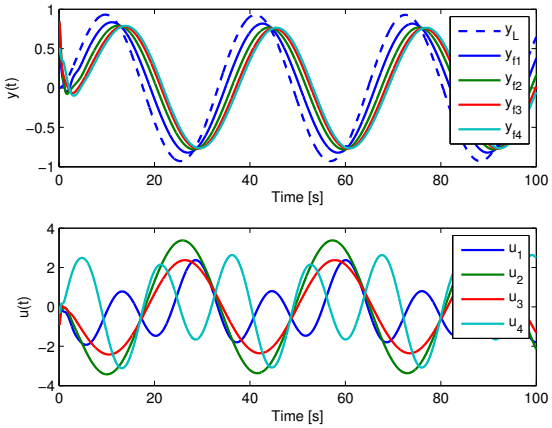

(b) Sine-wave reference command.

Figure 4. Responses of $y(t)$, $y_{\mathrm{L}}(t)$, and $u(t)$ for the multivehicle system with low-frequency version of the proposed adaptive output feedback control architecture in presence of input disturbance for Example 1.

8. CONCLUSION

In this paper, a new observer-free output feedback adaptive control method was presented for continuous-time, minimum phase, and high-order linear multivehicle systems subject to exogenous disturbances. The proposed method was based on a nonminimal state-space realization for each follower vehicle of the multivehicle system. In particular, it

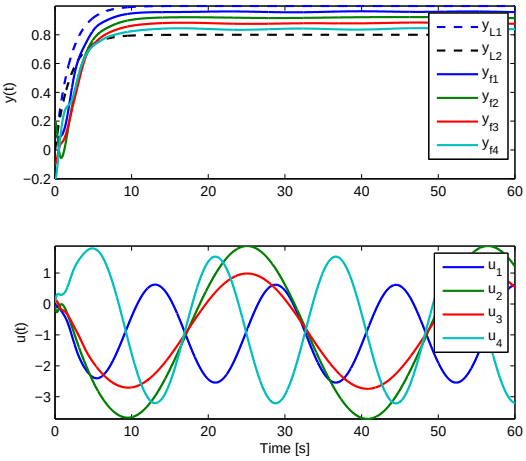

(a) Step reference commands for two leaders creating a constant convex hull.

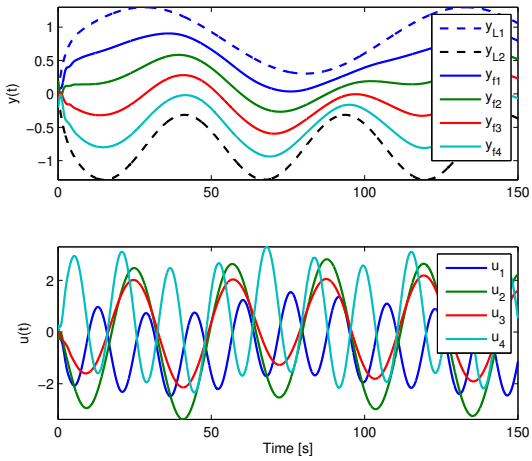

(b) Sine-wave reference commands for two leaders creating a time varying convex hull.

Figure 5. Responses of $y(t)$, $y_{\mathrm{L}}(t)$, and $u(t)$ for the multivehicle system with low-frequency version of the proposed adaptive output feedback control architecture in presence of input disturbance for Example 2.

consisted of a local cooperative controller and a vehicle-level controller for each follower vehicle, where the stability guarantees of the overall scheme were also derived. Finally, two illustrated numerical examples demonstrated the efficacy of the proposed method.

ACKNOWLEDGMENT

This research has been supported by the Dynamic Data-Driven Applications Systems Program of the Air Force Office of Scientific Research.

REFERENCES

[1] Y. Kim, M. Mesbahi, and F. Y. Hadaegh, "Multiple-spacecraft reconfiguration through collision avoidance, bouncing, and stalemate," *Journal of Optimization Theory and Applications*, vol. 122, no. 2, pp. 323–343, 2004.

[2] Q. Jia and G. Li, "Formation control and obstacle avoidance algorithm of multiple autonomous underwater vehicles (auvs) based on potential function and behavior rules," *IEEE International Conference on Automation and Logistics*, pp. 569–573, 2007.

[3] C. W. Reynolds, "Interaction with groups of autonomous characters," *Game Developers Conference*, vol. 2000, pp. 449–460, 2000.

[4] W. Ren, R. W. Beard, and E. M. Atkins, "A survey of consensus problems in multiagent coordination," *Proceedings of the American Control Conference*, pp. 1859–1864, 2005.

[5] R. Olfati-Saber, J. A. Fax, and R. M. Murray, "Consensus and cooperation in networked multi-agent systems," *Proceedings of the IEEE*, vol. 95, no. 1, pp. 215–233, 2007.

[6] M. Mesbahi and M. Egerstedt, *Graph theoretic methods in multiagent networks*. Princeton University Press, 2010.

[7] Z.-G. Hou, L. Cheng, and M. Tan, "Decentralized robust adaptive control for the multiagent system consensus problem using neural networks," *IEEE Transactions on Systems, Man, and Cybernetics - Part B: Cybernetics*, vol. 39, no. 3, pp. 636–647, 2009.

[8] A. Das and F. L. Lewis, "Distributed adaptive control for synchronization of unknown nonlinear networked systems," *Automatica*, vol. 46, no. 12, pp. 2014–2021, 2010.

[9] A. Das and F. L. Lewis, "Cooperative adaptive control for synchronization of second-order systems with unknown nonlinearities," *International Journal of Robust and Nonlinear Control*, vol. 21, no. 13, pp. 1509–1524, 2011.

[10] Y. Miyasato, "Adaptive H_∞ consensus control of multi-agent systems on directed graph by utilizing neural network approximators," *IFAC-PapersOnLine*, vol. 49, no. 13, pp. 36–41, 2016.

[11] Z. Tu, H. Yu, and X. Xia, "Decentralized finite-time adaptive consensus of multiagent systems with fixed and switching network topologies," *Neurocomputing*, vol. 219, pp. 59–67, 2017.

[12] H. Kim, H. Shim, and J. H. Seo, "Output consensus of heterogeneous uncertain linear multi-agent systems," *IEEE Transactions on Automatic Control*, vol. 56, no. 1, pp. 200–206, 2011.

[13] X. Wang, Y. Hong, J. Huang, and Z.-P. Jiang, "A distributed control approach to a robust output regulation problem for multi-agent linear systems," *IEEE Transactions on Automatic control*, vol. 55, no. 12, pp. 2891–2895, 2010.

[14] S. Mondal, R. Su, and L. Xie, "Heterogeneous consensus of higher-order multi-agent systems with mismatched uncertainties using sliding mode control," *International Journal of Robust and Nonlinear Control*, 2016.

[15] J. Wang, K. Chen, and Q. Ma, "Adaptive leader-following consensus of multi-agent systems with unknown nonlinear dynamics," *Entropy*, vol. 16, no. 9, pp. 5020–5031, 2014.

[16] J. Sun and Z. Geng, "Adaptive consensus tracking for linear multi-agent systems with heterogeneous unknown nonlinear dynamics," *International Journal of Robust and Nonlinear Control*, vol. 26, no. 1, pp. 154–173, 2016.

[17] T. Yucelen and E. N. Johnson, "Control of multivehicle systems in the presence of uncertain dynamics," *International Journal of Control*, vol. 86, no. 9, pp. 1540–1553, 2013.

[18] J. Hu and W. X. Zheng, "Adaptive tracking control of leader–follower systems with unknown dynamics and partial measurements," *Automatica*, vol. 50, no. 5, pp. 1416–1423, 2014.

[19] Z. Peng, D. Wang, H. Zhang, and G. Sun, "Distributed neural network control for adaptive synchronization of uncertain dynamical multiagent systems," *IEEE transactions on neural networks and learning systems*, vol. 25, no. 8, pp. 1508–1519, 2014.

[20] J. Sun, Z. Geng, and Y. Lv, "Adaptive output feedback consensus tracking for heterogeneous multi-agent systems with unknown dynamics under directed graphs," *Systems & Control Letters*, vol. 87, pp. 16–22, 2016.

[21] H. Cai, F. L. Lewis, G. Hu, and J. Huang, "The adaptive distributed observer approach to the cooperative output regulation of linear multi-agent systems," *Automatica*, vol. 75, pp. 299–305, 2017.

[22] A. Albattat, T. Yucelen, B. C. Gruenwald, and S. Jagannathan, "An observer-free output feedback cooperative control architecture for multivehicle systems," *ASME Dynamic Systems and Control Conference*, 2017 (Accepted).

[23] T. Yucelen, W. M. Haddad, and A. J. Calise, "Output feedback adaptive command following for nonminimum phase uncertain dynamical systems," *American Control Conference*, pp. 123–128, 2010.

[24] T. Yucelen and W. M. Haddad, "Output feedback adaptive stabilization and command following for minimum phase dynamical systems with unmatched uncertainties," *American Control Conference*, pp. 1163–1168, 2011.

[25] T. Yucelen and W. M. Haddad, "Output feedback adaptive stabilization and command following for minimum phase dynamical systems with unmatched uncertainties and disturbances," *International Journal of Control*, vol. 85, no. 6, pp. 706–721, 2012.

[26] T. Yucelen and A. J. Calise, "Derivative-free model reference adaptive control," *Journal of Guidance, Control, and Dynamics*, vol. 34, no. 4, pp. 933–950, 2011.

[27] C. Godsil and G. Royle, *Algebraic graph theory*. New York, NY: Springer, 2001.

[28] E. Lavretsky and K. A. Wise, "Robust adaptive control," in *Robust and Adaptive Control*, Springer, 2013.

[29] T. Yucelen and F. Pourboghrat, "Active noise blocking: Non-minimal modeling, robust control, and implementation," in *American Control Conference, 2009. ACC'09.*, pp. 5492–5497, IEEE, 2009.

[30] P. J. Antsaklis and A. N. Michel, *Linear systems*. Bosten, MA: Birkhäuser, 2006.

[31] H. K. Khalil, *Nonlinear Systems*. Upper Saddle River, NJ: PrenticeHall, 1996.

[32] J. A. Fax and R. M. Murray, "Information flow and cooperative control of vehicle formations," *IEEE transactions on automatic control*, vol. 49, no. 9, pp. 1465–1476, 2004.

[33] C.-Q. Ma and J.-F. Zhang, "Necessary and sufficient conditions for consensusability of linear multi-agent systems," *IEEE Transactions on Automatic Control*, vol. 55, no. 5, pp. 1263–1268, 2010.

[34] W. M. Haddad and V. Chellaboina, *Nonlinear Dynamical Systems and Control:* A L*yapunov-Based Approach*. Princeton University Press, 2008.

[35] D. S. Bernstein, *Matrix mathematics: Theory, Facts, and Formulas*. Princeton University Press, 2009.

[36] T. Yucelen and W. M. Haddad, "Low-frequency learning and fast adaptation in model reference adaptive control," *IEEE Transactions on Automatic Control*, vol. 58, no. 4, pp. 1080–1085, 2013.

[37] D. Tran and T. Yucelen, "On control of multiagent formations through local interactions," in *IEEE Conference on Decision and Control*, 2016.

SECTION

2. CONCLUDING REMARKS AND FUTURE WORK

2.1. CONCLUDING REMARKS

A critical task in the design and implementation of networked control systems is to guarantee system stability while reducing wireless network utilization and achieving a given system performance in the presence of system uncertainties. Motivating from this standpoint, in the first paper, we presented the design and analysis of an event-triggered adaptive control methodology for a class of uncertain dynamical systems in the presence of two-way data exchange between the physical system and the proposed controller over a wireless network. In particular, using tools and methods from nonlinear systems and Lyapunov stability, we showed that the proposed approach reduces wireless network utilization, guarantees system stability and command following performance in the presence of system uncertainties, and does not yield to a Zeno behavior. In addition, the effect of user-defined thresholds and adaptive controller design parameters to the system performance were characterized and discussed in detail. As a byproduct, we further found that the actuation threshold can be chosen larger than the sensing threshold to reduce wireless network utilization between the physical system and the adaptive controller without necessarily sacrificing closed-loop dynamical system performance.

We then presented, in the second paper, the design and analysis of an event-triggered output feedback adaptive control methodology for a class of uncertain dynamical systems in the presence of two-way data exchange between the physical system and the proposed controller over a wireless network. This approach was a generalization of the results in the first paper where instead of considering state feedback adaptive control architecture, we

consider output feedback adaptive control for such systems where the measuring full states is inapplicable. Specifically, we showed using tools and methods from nonlinear systems theory and Lyapunov stability in particular that the proposed feedback control approach guarantees system stability in the presence of system uncertainties. In addition, we characterized the effect of user-defined thresholds and output feedback adaptive controller design parameters to the system performance and showed that the proposed methodology does not yield to a Zeno behavior.

We next presented, in the third paper, the design and analysis of event-triggered decentralized and distributed adaptive control architectures for uncertain networked large-scale modular systems. For the decentralized case, we showed that the proposed event-triggered adaptive control architecture guarantees system stability and performance with no Zeno behavior under certain structural conditions that depend on the parameters of the large-scale modular systems and the proposed architecture. For the distributed case, we showed that the proposed event-triggered adaptive control architecture guarantees the same system stability and performance with no Zeno behavior without such structural conditions under the assumption that physically-interconnected modules can locally communicate with each other for exchanging their state information. In addition to the presented theoretical findings, the efficacy of the proposed event-triggered decentralized and distributed adaptive control approaches were demonstrated on an illustrative numerical example, where significant reduction on the overall communication cost was obtained for large-scale modular systems in the presence of system uncertainties resulting from modeling and degraded modes of operation of the modules and their interconnections between each other.

In addition, in the fourth paper, we presented a new observer-free output feedback cooperative control architecture. Specifically, the proposed architecture will be predicated on a nonminimal state-space realization that generates an expanded set of states only using the filtered input and filtered output and their derivatives for each vehicles, without the

need for designing an observer for each vehicle. The utilized output feedback cooperative control architecture is in the context of a containment problem (i.e., outputs of the follower agents convergence to the convex hull spanned by those of the leader agents).

Furthermore, based on the above results, we presented in the fifth paper, an event-triggering mechanism on the exchanged output measurements between agents that are controlled by an observer-free output feedback cooperative control architecture for continuous-time, minimum phase, and high-order linear multiagent systems. The proposed event-triggering methodology is applied on the relative output measurements of the agents, where each agent has its own event-triggering threshold to transmit its own output measurements to the neighbor agents asynchronously. Since the information exchanged happening in the event-triggering manner, additional terms in the Laplacian matrices are observed, and these additional terms are utilized in the controller scheme design.

Finally, we presented in sixth paper, new observer-free output feedback adaptive control, $(OF)^2AC$, method for continuous-time, minimum phase, and high-order linear multivehicle systems subject to exogenous disturbances. The $(OF)^2AC$ consists of *i)* a local cooperative controller and *ii)* a vehicle-level controller for each follower vehicle Specifically, the former part of the proposed control method addresses the leader-follower containment control problem by receiving the relative output measurements of the neighboring vehicles, and the later part consists of an augmenting adaptive controller for stabilization and command following in the presence of exogenous disturbances.

2.2. FUTURE RESEARCH SUGGESTIONS

We recommend the following future research topics: i) The results of Papers I, II, and III can be extended by considering sampling, data transmission, and computation delays since they also play an important role in the performance of networked control systems. ii) The results of Papers I can be extended by optimizing the triggering thresholds and controller parameter in order to get minimal closed loop error bound. iii) The results

of Paper III can be extended to the output feedback adaptive control. *iv*) The result of Paper IV can be extended by analyzing the stability during the intersampling time using input-state-stability (ISS) approach in addition to the regular Lyapunov stability analysis. *v*) The result of Paper IV can be extended by applying the event-triggering mechanism on the exchanged information between the vehicles in order to save the communication effort. *vi*) The result of Paper IV can be also extended by considering the time delay in the transmitted information between the vehicles. *vii*) In order to mitigate the high frequency oscillation in the adaptive controller response in Paper VI one can propose output emulator based adaptive controller instead of using low pass filter-modified update law. The resulting adaptive controller can have less parameter to tune in order to obtain an acceptable response. Finally, *vi*) all the results reported in this dissertation can be extended first for discrete time dynamical systems and then for hybrid dynamical systems.

APPENDIX A

SYSTEM CONTROLLABILITY AND THE STRUCTURAL MATCHING CONDITION IN PAPER I

The assumption on controllability of (A, B) implies that it is possible to come up with a control strategy in order to stabilize each individual system. For example, consider the following system matrices as an example:

$$A = \begin{bmatrix} 0 & 1 \\ 0 & 0 \end{bmatrix}, B = \begin{bmatrix} 0 \\ 1 \end{bmatrix}. \tag{A.1}$$

In this case, since the given pair (A, B) is controllable, there always exists a stabilizing gain K_1 to make $A - BK_1$ Hurwitz. On the other hand, standard Assumption 2 puts a structural constraint on the selection of the reference model. Following the above example, consider, for example, the following reference model system matrix:

$$A_{\text{ref}} = \begin{bmatrix} -\alpha & 0 \\ 0 & -\beta \end{bmatrix}, \quad \alpha, \beta \in \mathbb{R}_+. \tag{A.2}$$

Clearly, A_{ref} is Hurwitz, but there does not structurally exist a K_1 satisfying $A_{\text{ref}} = A - BK_1$ in this case with the given A and B above. Instead, for example, consider the following reference model system matrix:

$$A_{\text{ref}} = \begin{bmatrix} 0 & 1 \\ -\alpha & -\beta \end{bmatrix}, \quad \alpha, \beta \in \mathbb{R}_+. \tag{A.3}$$

Once again, A_{ref} is Hurwitz. In this case, there always structurally exist a K_1 satisfying $A_{\text{ref}} = A - BK_1$. A similar comment can be identically made for $B_{\text{ref}} = BK_2$ case.

From this standpoint, the assumption on controllability and Assumption 2 do not contradict each other. The later assumption actually adds a constraint on the former assumption that structurally influences the selection of the reference model dynamics. Note that Assumption 2 is a standard assumption in the literature and often referred as the matching condition, where it holds for many practical systems when the control actions are gen-

erated through moments such as in aircraft, spacecraft, underwater vehicles, and industrial robotic systems just to mention a few. For further explanation, three different physical examples are presented showing the validity of the adopted structural matching condition.

Example 1. Consider aircraft short-period dynamics for longitudinal motion of a conventional aircraft from Section 10.2 of [33]

$$\underbrace{\begin{bmatrix} \dot{\alpha}(t) \\ \dot{q}(t) \end{bmatrix}}_{\dot{x}_{\mathrm{p}}(t)} = \underbrace{\begin{bmatrix} -0.08060 & 1 \\ -9.1484 & -4.59 \end{bmatrix}}_{A_{\mathrm{p}}} \underbrace{\begin{bmatrix} \alpha(t) \\ q(t) \end{bmatrix}}_{x_{\mathrm{p}}(t)} + \underbrace{\begin{bmatrix} -0.04 \\ -4.59 \end{bmatrix}}_{B_{\mathrm{p}}} \Lambda \left(\underbrace{\delta_e(t)}_{u(t)} + \Delta(x_{\mathbf{p}}(t)) \right), \tag{A.4}$$

where $\alpha(t)$ (rad) is the aircraft angle of attack, q (rad/s) is the pitch rate, $\delta_e(t)$ (rad) is the elevator deflection (the control input), $\Lambda = 0.5$ represents a loss-of-control effectiveness, and $\Delta(x_{\mathbf{p}}(t))$ is the matched uncertainty of the system. In addition, let the aircraft angle of attack α be the system regulated output given by

$$y(t) = \begin{bmatrix} 1 & 0 \end{bmatrix} x_{\mathrm{p}}(t). \tag{A.5}$$

Then, the system is augmented with the integrated output tracking error and yields the extended open-loop dynamics

$$\underbrace{\begin{bmatrix} \dot{e}_{yI}(t) \\ \dot{\alpha}(t) \\ \dot{q}(t) \end{bmatrix}}_{\dot{x}(t)} = \underbrace{\begin{bmatrix} 0 & 1 & 0 \\ 0 & -0.08060 & 1 \\ 0 & -9.1484 & -4.59 \end{bmatrix}}_{A} \underbrace{\begin{bmatrix} e_{yI}(t) \\ \alpha(t) \\ q(t) \end{bmatrix}}_{x(t)} + \underbrace{\begin{bmatrix} 0 \\ -0.04 \\ -4.59 \end{bmatrix}}_{B} \Lambda \left(\delta_e(t) + \Delta(x_{\mathbf{p}}(t)) \right) + \begin{bmatrix} -1 \\ 0 \\ 0 \end{bmatrix} y_{\mathbf{cmd}}(t), \tag{A.6}$$

where $e_{yI}(t) = y(t) - y_{\text{cmd}}$ is the system output tracking error, y_{cmd} is bounded time varying command. It can be easily verified that this is a controllable system. A suitable reference model for this system is given in the same section of [33] as:

$$A_{\text{ref}} = \begin{bmatrix} 0 & 1 & 0 \\ -0.1328 & -0.8522 & 0.9910 \\ -14.5149 & -14.2048 & -5.5779 \end{bmatrix}, \tag{A.7}$$

Example 2. Consider lateral-directional motion dynamics of a conventional aircraft from Section 11.5 of [33]

$$\underbrace{\begin{bmatrix} \dot{\varphi}(t) \\ \dot{\beta}(t) \\ \dot{p}(t) \\ \dot{r}(t) \end{bmatrix}}_{\dot{x}_{\text{p}}(t)} = \underbrace{\begin{bmatrix} 0 & 0 & 1 & 0 \\ 0.0487 & -0.0829 & 0 & -1 \\ 0 & -4.56 & -1.699 & 0.1717 \\ 0 & 3.382 & -0.0654 & -0.0893 \end{bmatrix}}_{A_{\text{p}}} \underbrace{\begin{bmatrix} \varphi(t) \\ \beta(t) \\ p(t) \\ r(t) \end{bmatrix}}_{x_{\text{p}}(t)}$$
$$+ \underbrace{\begin{bmatrix} 0 & 0 \\ 0 & 0.0116 \\ 27.276 & 0.5758 \\ 0.3952 & -1.362 \end{bmatrix}}_{B_{\text{p}}} \Lambda \underbrace{\begin{bmatrix} \delta_a(t) \\ \delta_r(t) \end{bmatrix}}_{u(t)}, \tag{A.8}$$

$$y(t) = \underbrace{\begin{bmatrix} 1 & 0 & 0 & 0 \\ 0 & 1 & 0 & 0 \end{bmatrix}}_{C_{\text{p}}} x_{\text{p}}(t), \tag{A.9}$$

$$y_{\text{cmd}}(t) = \begin{bmatrix} \varphi_{\text{cmd}}(t) & \beta_{\text{cmd}}(t) \end{bmatrix}^{\text{T}} \tag{A.10}$$

where $\varphi(t)$ is the bank angle , $\beta(t)$ is the sideslip angle, $p(t)$ is the roll rate, $r(t)$ is the vehicle yaw rate, $\delta_a(t)$ is the aileron trailing angle, and $\delta_r(t)$ is the rudder angle. The control task is to generate control input is to stabilize the open loop system and enable the

independent an simultaneous tracking of the bank angle and sideslip angle that are given in (A.9). Then, the augmented system with two integral tracking errors is given by

$$\underbrace{\begin{bmatrix} \dot{e}_{\varphi I}(t) \\ \dot{e}_{\beta I}(t) \\ \dot{x}_{\mathrm{p}}(t) \end{bmatrix}}_{\dot{x}(t)} = \underbrace{\begin{bmatrix} 0_{2\times 2} & C_{\mathrm{p}} \\ 0_{4\times 2} & A_{\mathrm{p}} \end{bmatrix}}_{A} \underbrace{\begin{bmatrix} e_{\varphi I}(t) \\ e_{\beta I}(t) \\ x_{\mathrm{p}}(t) \end{bmatrix}}_{x(t)} + \underbrace{\begin{bmatrix} 0_{2\times 2} \\ B_{\mathrm{p}} \end{bmatrix}}_{B} \Lambda \underbrace{\begin{bmatrix} \delta_a(t) \\ \delta_r(t) \end{bmatrix}}_{u(t)} + \underbrace{\begin{bmatrix} -I_{2\times 2} \\ 0_{4\times 2} \end{bmatrix}}_{B_{\mathrm{cmd}}} \underbrace{\begin{bmatrix} \varphi_{\mathrm{cmd}}(t) \\ \beta_{\mathrm{cmd}}(t) \end{bmatrix}}_{y_{\mathrm{cmd}}(t)}, \tag{A.11}$$

$$y(t) = \underbrace{\begin{bmatrix} 0_{2\times 2} & C_{\mathrm{p}} \end{bmatrix}}_{C} x(t) = \begin{bmatrix} \varphi(t) & \beta(t) \end{bmatrix}^{\mathrm{T}} \tag{A.12}$$

where $\dot{e}_{\varphi I}(t) = \varphi(t) - \varphi_{\mathrm{cmd}}(t)$, and $\dot{e}_{\beta I}(t) = \beta(t) - \beta_{\mathrm{cmd}}(t)$ are the dynamics of the two integral tracking error signal. Next, a suitable reference model for this system is given in the same section of [33] as

$$A_{\mathrm{ref}} = \begin{bmatrix} 0 & 0 & 1 & 0 & 0 & 0 \\ 0 & 0 & 0 & 1 & 0 & 0 \\ 0 & 0 & 0 & 0 & 1 & 0 \\ 0.0006 & -0.0366 & 0.0478 & -0.1095 & -0.0006 & -0.9677 \\ -27.2103 & -6.2552 & -25.0926 & -8.3100 & -11.3540 & 2.2303 \\ -0.4647 & 4.2370 & -0.2600 & 6.4665 & -0.1385 & -3.8807 \end{bmatrix}, \tag{A.13}$$

Example 3. In this example, consider an nth dimensional system in controllable canonical form given by

$$\begin{bmatrix} \dot{x}_1(t) \\ \dot{x}_2(t) \\ \vdots \\ \dot{x}_{n-1}(t) \\ \dot{x}_n(t) \end{bmatrix} = \begin{bmatrix} 0 & 1 & 0 & \cdots & 0 \\ 0 & 0 & 1 & \cdots & 0 \\ \vdots & \vdots & \vdots & \ddots & \vdots \\ 0 & 0 & 0 & \cdots & 1 \\ -a_n & -a_{n-1} & -a_{n-2} & \cdots & -a_1 \end{bmatrix} \begin{bmatrix} x_1(t) \\ x_2(t) \\ \vdots \\ x_{n-1}(t) \\ x_n(t) \end{bmatrix} + \begin{bmatrix} 0 \\ 0 \\ \vdots \\ 0 \\ 1 \end{bmatrix} u(t), \tag{A.14}$$

Depending on the known system structure,one can choose A_{ref} as

$$A_{\text{ref}} = \begin{bmatrix} 0 & 1 & 0 & \cdots & 0 \\ 0 & 0 & 1 & \cdots & 0 \\ \vdots & \vdots & \vdots & \ddots & \vdots \\ 0 & 0 & 0 & \cdots & 1 \\ -a_n^* & -a_{n-1}^* & -a_{n-2}^* & \cdots & -a_1^* \end{bmatrix}. \tag{A.15}$$

where $a_i^*, i = 1, \cdots, n$ are the desired polynomial parameters leading to an asymptotically stable A_{ref}.

APPENDIX B

NONMINIMAL STATE SPACE REALIZATION FOR THE FOLLOWER VEHICLE SYSTEMS IN PAPER IV

Nonminimal State space representation explanation . we present the explanation of how system (22) and (23) is input-output equivalent to system (32) and (33). For tis purpose, using the input-output equivalence of (24) and (25) with (22) and (23), it follows that

$$a_0 y_i(t) = a_0 C_o x_{oi}(t),\ t \geq 0 \tag{B.1}$$

$$a_1 \dot{y}_i(t) = a_1[C_o A_o x_{oi}(t) + C_o B_o u_i(t)], \tag{B.2}$$

$$\vdots$$

$$a_{n-1} y_i^{(n-1)}(t) = a_{n-1}[C_o A_o^{n-1} x_{oi}(t) + C_o A_o^{n-2} B_o u_i(t) + \cdots + C_o B_o u_i^{(n-2)}(t)], \tag{B.3}$$

$$y_i^{(n)}(t) = C_o A_o^n x_{oi}(t) + C_o A_o^{n-1} B_o u_i(t) + \cdots + C_o B_o u_i^{(n-1)}(t), \tag{B.4}$$

Now, adding the $n+1$ equations in (B.1) and (B.2) we obtain

$$\begin{aligned} y_i^{(n)}(t) = &- [a_0 I_l\ a_1 I_l \cdots a_{n-1} I_l] Y_i(t) + [\bar{B}_0\ \bar{B}_1 \cdots \bar{B}_{n-1}] U_i(t) + C_o[A_o^n + a_{n-1} A_o^{n-1} \\ &+ \cdots + a_1 A_o + a_0 I_{ln}] x_{oi}(t), \end{aligned} \tag{B.5}$$

where $\bar{B}_0, \bar{B}_1, \cdots, \bar{B}_{n-1}$ are given in (29)-(31), and $Y_i(t),\ t \geq 0$, and $U_i(t),\ t \geq 0$ are defined as

$$Y_i(t) \triangleq [y_i(t),\ \dot{y}_i(t),\ \cdots,\ y_i^{(n-1)}(t)]^{\mathrm{T}}, \tag{B.6}$$

$$U_i(t) \triangleq [u_i(t),\ \dot{u}_i(t),\ \cdots,\ u_i^{(n-1)}(t)]^{\mathrm{T}}, \tag{B.7}$$

Next, using the Cayly-Hamilton theorem [107] to consider every square matrix is a root of its characteristic polynomial, and noting that $a_k,\ k = 0, 1, \cdots, n-1$ are the coefficients of the characteristic polynomial of the matrix A_o in (24), it follows that

$$A_o^n + a_{n-1}A_o^{n-1} + \cdots + a_1 A_o + a_0 I_{ln} = 0. \tag{B.8}$$

Hence, (B.5) reduces to

$$y_i^{(n)}(t) = -\,[a_0 I_l\ a_1 I_l \cdots a_{n-1} I_l] Y_i(t) + [\bar{B}_0\ \bar{B}_1 \cdots \bar{B}_{n-1}] U_i(t), \tag{B.9}$$

Now, define the expanded state vector

$$\begin{aligned} x_{\mathrm{nm}i}(t) \triangleq & [Y_i^{\mathrm{T}}(t),\ U_i^{\mathrm{T}}(t)]^{\mathrm{T}} \\ = & [y_i(t),\ \dot{y}_i(t),\ \cdots,\ y_i^{(n-1)}(t),\ u_i(t), \dot{u}_i(t),\ \cdots,\ u_i^{(n-1)}(t)]^{\mathrm{T}}, \end{aligned} \tag{B.10}$$

so that(B.5) can be written as

$$y_i^{(n)}(t) = \Phi x_{\mathrm{nm}i}(t), \tag{B.11}$$

where

$$\Phi = [-a_0 I_l - a_1 I_l \cdots - a_{n-1} I_l\ \bar{B}_0\ \bar{B}_1 \cdots \bar{B}_{n-1}] \in \mathbb{R}^{l \times n_{\mathrm{f}}}. \tag{B.12}$$

Next consider the $\mathrm{n_f}$-th order nonminimal state space model given by

$$\dot{x}_{\mathrm{nm}i}(t) = A_{\mathrm{nm}} x_{\mathrm{nm}i}(t) + B_{\mathrm{nm}} u_i^{(n)}(t), \quad x_{\mathrm{nm}i}(0) = x_{\mathrm{nm}0i}, t \geq 0, \tag{B.13}$$

$$y_i(t) = C_{\mathrm{nm}} x_{\mathrm{nm}i}(t), \tag{B.14}$$

where

$$A_{\mathrm{nm}} = \begin{bmatrix} 0 & I_l & 0 & \cdots & & \cdots & 0 \\ \vdots & & \ddots & & & & \vdots \\ 0 & \cdots & 0 & I_l & 0 \cdots & \cdots & 0 \\ -a_0 I_l & \cdots & \cdots & -a_{n-1} I_l & \bar{B}_0 \cdots & \cdots & \bar{B}_{n-1} \\ 0 & \cdots & & \cdots & 0 \; I_m & 0 & 0 \\ \vdots & & & & & \ddots & \vdots \\ \vdots & & & & \cdots & 0 & I_m \\ 0 & \cdots & & & & \cdots & 0 \end{bmatrix} \in \mathbb{R}^{n_{\mathrm{f}} \times n_{\mathrm{f}}}, \tag{B.15}$$

$$B_{\mathrm{nm}} = \begin{bmatrix} 0 & 0 \cdots & I_m \end{bmatrix}^{\mathrm{T}} \in \mathbb{R}^{n_{\mathrm{f}} \times m}, \tag{B.16}$$

$$C_{\mathrm{nm}} = [I_l \; 0 \cdots \quad \cdots \; 0] \in \mathbb{R}^{l \times n_{\mathrm{f}}}. \tag{B.17}$$

To eliminate differentiating the actual input and output signals in (B.13), we filter the input signals in (B.13)and the output signals in (B.14) through the filter $\lambda^n/\Lambda(s)$, where $\Lambda(s)$ is defined by (35). In this case, the states $x_{\mathrm{nm}i}(t), t \geq 0$ become $x_{\mathrm{f}i}(t), t \geq 0$, given by (34).

Now, let $\bar{\lambda} = [\lambda^n, \cdots, n\lambda]^{\mathrm{T}}$, and note that the Laplace transform of the filtered input signal $u_{\mathrm{f}i}^{(n)}$, $t \geq 0$ can be written as

$$\begin{aligned} \mathcal{L}\{u_{\mathrm{f}i}^{(n)}(t)\} &= \frac{\lambda^n s^n}{(s+\lambda)^n} \mathcal{L}\{u_i(t)\} \\ &= \frac{\lambda^n s^n - (s+\lambda)^n + ((s+\lambda)^n)}{(s+\lambda)^n} \mathcal{L}\{u_i(t)\} \\ &= \left[s^n - \lambda^{-n}(s+\lambda)^n\right] \mathcal{L}\{u_{\mathrm{f}i}(t)\} + \mathcal{L}\{u_i(t)\} \\ &= \left[s^n - (\lambda^{-n} s^n + n\lambda^{-n+1} s^{(n-1)} + \cdots + 1)\right] \mathcal{L}\{u_{\mathrm{f}i}(t)\} + \mathcal{L}\{u_i(t)\}, \end{aligned} \tag{B.18}$$

and after rearranging (B.18), it can be written as

$$\mathcal{L}\{u_{\mathrm{f}i}^{(n)}(t)\} = -\left[n\lambda s^{(n-1)} + \cdots + \lambda^n\right]\mathcal{L}\{u_{\mathrm{f}i}(t)\} + \lambda^n\mathcal{L}\{u_i(t)\}, \tag{B.19}$$

where $\mathcal{L}\{\cdot\}$ denotes the Laplace transform operator. Next, the inverse Laplace transform for (B.19) is given by

$$\begin{aligned} u_{\mathrm{f}i}^{(n)}(t) &= -\bar{\lambda}^{\mathrm{T}}\left[u_{\mathrm{f}i}^{\mathrm{T}}(t),\, \dot{u}_{\mathrm{f}i}^{\mathrm{T}}(t), \cdots, u_{\mathrm{f}i}^{\mathrm{T}(n-1)}(t)\right]^{\mathrm{T}} + \lambda^n u_i(t) \\ &= -\bar{\lambda}^{\mathrm{T}} U_{\mathrm{f}}(t) + \lambda^n u_i(t). \end{aligned} \tag{B.20}$$

Analogously, the filtered output signals can be written as

$$\begin{aligned} y_{\mathrm{f}i}^{(n)}(t) &= -\bar{\lambda}^{\mathrm{T}}\left[y_{\mathrm{f}i}^{\mathrm{T}}(t),\, \dot{y}_{\mathrm{f}i}^{\mathrm{T}}(t), \cdots, y_{\mathrm{f}i}^{\mathrm{T}(n-1)}(t)\right]^{\mathrm{T}} + \lambda^n y_i(t) \\ &= -\bar{\lambda}^{\mathrm{T}} Y_{\mathrm{f}i}(t) + \lambda^n y_i(t). \end{aligned} \tag{B.21}$$

Furthermore, the filtered version of (B.11) id given by

$$y_{\mathrm{f}i}^{(n)}(t) = \Phi x_{\mathrm{f}i}(t). \tag{B.22}$$

Using (B.21) and (B.22), it follows that the actual system output is given by

$$y(t) = \left(\lambda^{-n}\Phi + \left[\lambda^{-n}\bar{\lambda}^{\mathrm{T}},\, 0\right]\right) x_{\mathrm{f}i}(t). \tag{B.23}$$

Now, filtering the signal in (B.13) and (B.14), and using (B.19) and (B.23), a nonminimal state-space realization of (22) and (23) is given by (32) and (33), where $x_{\mathrm{f}i}(t), t \geq 0$, is the known filtered expanded state vector given by (34) and $A_{\mathrm{f}} \in \mathbb{R}^{n_{\mathrm{f}} \times n_{\mathrm{f}}}$, $B_{\mathrm{f}} \in \mathbb{R}^{n_{\mathrm{f}} \times m}$ and

$C_{\mathrm{f}} \in \mathbb{R}^{l \times n_{\mathrm{f}}}$ are given by (36)-(38) respectively with

$$A_{\mathrm{f}} = A_{\mathrm{nm}} - [0 \; B_{\mathrm{nm}} \bar{\lambda}^{\mathrm{T}}], \tag{B.24}$$

$$B_{\mathrm{f}} = \lambda^{n} B_{\mathrm{nm}}, \tag{B.25}$$

$$C_{\mathrm{f}} = \lambda^{-n} \Phi + [\lambda^{-n} \bar{\lambda}^{\mathrm{T}} \; 0]. \tag{B.26}$$

APPENDIX C

INTERSAMPLING TIME ANALYSIS FOR THE EVENT-TRIGGERED OUTPUT OF THE LEADER SYSTEMS IN PAPER V

Proof: [Proof of (59) in Corollary 1 in Paper V] The time derivative of $\|y_{\mathrm{fs}i}(t) - y_{\mathrm{f}i}(t)\|$ over $t \in (s_{k_i+1}, s_{k_i}), \forall k_i \in \mathbb{N}$ is given by:

$$\begin{aligned}
&\frac{d}{dt}\|y_{\mathrm{Ls}i}(t) - y_{\mathrm{L}i}(t)\| \\
&\quad \leq \|\dot{y}_{\mathrm{Ls}i}(t) - \dot{y}_{\mathrm{L}i}(t)\| = \|\dot{y}_{\mathrm{L}i}(t)\| \leq \|C_{\mathrm{L}i}\|_{\mathrm{F}}\|\dot{x}_{\mathrm{L}i}(t)\| \\
&\quad \leq \|C_{\mathrm{L}i}\|_{\mathrm{F}}\|A_{\mathrm{L}i}\|_{\mathrm{F}}\|x_{\mathrm{L}i}(t)\| + \|C_{\mathrm{L}i}\|_{\mathrm{F}}\|B_{\mathrm{L}i}\|_{\mathrm{F}}\|r_i(t)\| \\
&\quad \leq \|C_{\mathrm{L}i}\|_{\mathrm{F}}\|A_{\mathrm{L}i}\|_{\mathrm{F}}x^*_{\mathrm{L}i} + \|C_{\mathrm{L}i}\|_{\mathrm{F}}\|B_{\mathrm{L}i}\|_{\mathrm{F}}r^*_i, \qquad \text{(C.1)}
\end{aligned}$$

where $\|x_{\mathrm{L}i}(t)\| \leq x^*_{\mathrm{L}i}$. Since the closed-loop dynamical system is bounded, there exists an upper bound to the equation (C.1). Letting Φ_{2i} denote this upper bound and with initial condition satisfying $\lim_{t\to r^+_{q_i}} \|y_{\mathrm{Ls}i}(t) - y_{\mathrm{L}i}(t)\| = 0$, it follows from Equation (C.1) that $\|y_{\mathrm{Ls}i}(t) - y_{\mathrm{L}i}(t)\| \leq \Phi_{2i}(t - r_{q_i}), \quad \forall t \in (r_{q_i}, r_{q_i+1})$. Therefore, when $\overline{E}_{2i}$ is true, then $\lim_{t\to r^-_{q_i+1}} \|y_{\mathrm{Ls}i}(t) - y_{\mathrm{L}i}(t)\| = \epsilon_{y_{\mathrm{L}}i}$, and it then follows that $r_{q_i+1} - r_{q_i} \geq \alpha_{2i}$. ■

APPENDIX D

COPYRIGHT PERMISSION FOR PAPER II

Taylor and Francis Group LLC Books LICENSE
TERMS AND CONDITIONS

Nov 07, 2017

This is a License Agreement between Missouri University of science and technology -- Ali Albattat ("You") and Taylor and Francis Group LLC Books ("Taylor and Francis Group LLC Books") provided by Copyright Clearance Center ("CCC"). The license consists of your order details, the terms and conditions provided by Taylor and Francis Group LLC Books, and the payment terms and conditions.

All payments must be made in full to CCC. For payment instructions, please see information listed at the bottom of this form.

License Number	4223790983509
License date	Nov 07, 2017
Licensed content publisher	Taylor and Francis Group LLC Books
Licensed content title	Adaptive Control for Robotic Manipulators
Licensed content date	Nov 10, 2016
Type of Use	Thesis/Dissertation
Requestor type	Author of requested content
Format	Print, Electronic
Portion	chapter/article
Number of pages in chapter/article	26
The requesting person/organization is:	Ali Albattat
Title or numeric reference of the portion(s)	full article
Title of the article or chapter the portion is from	Output Feedback Adaptive Control of Uncertain Dynamical Systems with Event-Triggering
Editor of portion(s)	N/A
Author of portion(s)	Ali Albattat, Benjamin C. Gruenwald, and Tansel Yucelen
Volume of serial or monograph.	N/A
Page range of the portion	98-123
Publication date of portion	2016
Rights for	Main product
Duration of use	Life of current edition
Creation of copies for the disabled	no
With minor editing privileges	no
For distribution to	United States
In the following language(s)	Original language of publication

With incidental promotional use	no
The lifetime unit quantity of new product	Up to 4,999
Title	Event-Triggering Architectures for Adaptive Control of Uncertain Dynamical Systems
Instructor name	Dr. Tansel Yucelen
Institution name	Missouri University of Science and Technology
Expected presentation date	Nov 2017
Total (may include CCC user fee)	0.00 USD
Terms and Conditions	

TERMS AND CONDITIONS

The following terms are individual to this publisher:

Taylor and Francis Group and Informa healthcare are division of Informa plc. Permission will be void if material exceeds 10% of all the total pages in your publication and over 20% of the original publication. This includes permission granted by Informa plc and all of its subsidaries.

Other Terms and Conditions:

STANDARD TERMS AND CONDITIONS

1. Description of Service; Defined Terms. This Republication License enables the User to obtain licenses for republication of one or more copyrighted works as described in detail on the relevant Order Confirmation (the "Work(s)"). Copyright Clearance Center, Inc. ("CCC") grants licenses through the Service on behalf of the rightsholder identified on the Order Confirmation (the "Rightsholder"). "Republication", as used herein, generally means the inclusion of a Work, in whole or in part, in a new work or works, also as described on the Order Confirmation. "User", as used herein, means the person or entity making such republication.

2. The terms set forth in the relevant Order Confirmation, and any terms set by the Rightsholder with respect to a particular Work, govern the terms of use of Works in connection with the Service. By using the Service, the person transacting for a republication license on behalf of the User represents and warrants that he/she/it (a) has been duly authorized by the User to accept, and hereby does accept, all such terms and conditions on behalf of User, and (b) shall inform User of all such terms and conditions. In the event such person is a "freelancer" or other third party independent of User and CCC, such party shall be deemed jointly a "User" for purposes of these terms and conditions. In any event, User shall be deemed to have accepted and agreed to all such terms and conditions if User republishes the Work in any fashion.

3. Scope of License; Limitations and Obligations.

3.1 All Works and all rights therein, including copyright rights, remain the sole and exclusive property of the Rightsholder. The license created by the exchange of an Order Confirmation (and/or any invoice) and payment by User of the full amount set forth on that document includes only those rights expressly set forth in the Order Confirmation and in these terms and conditions, and conveys no other rights in the Work(s) to User. All rights not expressly granted are hereby reserved.

3.2 General Payment Terms: You may pay by credit card or through an account with us

payable at the end of the month. If you and we agree that you may establish a standing account with CCC, then the following terms apply: Remit Payment to: Copyright Clearance Center, 29118 Network Place, Chicago, IL 60673-1291. Payments Due: Invoices are payable upon their delivery to you (or upon our notice to you that they are available to you for downloading). After 30 days, outstanding amounts will be subject to a service charge of 1-1/2% per month or, if less, the maximum rate allowed by applicable law. Unless otherwise specifically set forth in the Order Confirmation or in a separate written agreement signed by CCC, invoices are due and payable on “net 30” terms. While User may exercise the rights licensed immediately upon issuance of the Order Confirmation, the license is automatically revoked and is null and void, as if it had never been issued, if complete payment for the license is not received on a timely basis either from User directly or through a payment agent, such as a credit card company.

3.3 Unless otherwise provided in the Order Confirmation, any grant of rights to User (i) is “one-time” (including the editions and product family specified in the license), (ii) is non-exclusive and non-transferable and (iii) is subject to any and all limitations and restrictions (such as, but not limited to, limitations on duration of use or circulation) included in the Order Confirmation or invoice and/or in these terms and conditions. Upon completion of the licensed use, User shall either secure a new permission for further use of the Work(s) or immediately cease any new use of the Work(s) and shall render inaccessible (such as by deleting or by removing or severing links or other locators) any further copies of the Work (except for copies printed on paper in accordance with this license and still in User's stock at the end of such period).

3.4 In the event that the material for which a republication license is sought includes third party materials (such as photographs, illustrations, graphs, inserts and similar materials) which are identified in such material as having been used by permission, User is responsible for identifying, and seeking separate licenses (under this Service or otherwise) for, any of such third party materials; without a separate license, such third party materials may not be used.

3.5 Use of proper copyright notice for a Work is required as a condition of any license granted under the Service. Unless otherwise provided in the Order Confirmation, a proper copyright notice will read substantially as follows: “Republished with permission of [Rightsholder’s name], from [Work's title, author, volume, edition number and year of copyright]; permission conveyed through Copyright Clearance Center, Inc. ” Such notice must be provided in a reasonably legible font size and must be placed either immediately adjacent to the Work as used (for example, as part of a by-line or footnote but not as a separate electronic link) or in the place where substantially all other credits or notices for the new work containing the republished Work are located. Failure to include the required notice results in loss to the Rightsholder and CCC, and the User shall be liable to pay liquidated damages for each such failure equal to twice the use fee specified in the Order Confirmation, in addition to the use fee itself and any other fees and charges specified.

3.6 User may only make alterations to the Work if and as expressly set forth in the Order Confirmation. No Work may be used in any way that is defamatory, violates the rights of third parties (including such third parties' rights of copyright, privacy, publicity, or other tangible or intangible property), or is otherwise illegal, sexually explicit or obscene. In addition, User may not conjoin a Work with any other material that may result in damage to the reputation of the Rightsholder. User agrees to inform CCC if it becomes aware of any infringement of any rights in a Work and to cooperate with any reasonable request of CCC

or the Rightsholder in connection therewith.
4. Indemnity. User hereby indemnifies and agrees to defend the Rightsholder and CCC, and their respective employees and directors, against all claims, liability, damages, costs and expenses, including legal fees and expenses, arising out of any use of a Work beyond the scope of the rights granted herein, or any use of a Work which has been altered in any unauthorized way by User, including claims of defamation or infringement of rights of copyright, publicity, privacy or other tangible or intangible property.
5. Limitation of Liability. UNDER NO CIRCUMSTANCES WILL CCC OR THE RIGHTSHOLDER BE LIABLE FOR ANY DIRECT, INDIRECT, CONSEQUENTIAL OR INCIDENTAL DAMAGES (INCLUDING WITHOUT LIMITATION DAMAGES FOR LOSS OF BUSINESS PROFITS OR INFORMATION, OR FOR BUSINESS INTERRUPTION) ARISING OUT OF THE USE OR INABILITY TO USE A WORK, EVEN IF ONE OF THEM HAS BEEN ADVISED OF THE POSSIBILITY OF SUCH DAMAGES. In any event, the total liability of the Rightsholder and CCC (including their respective employees and directors) shall not exceed the total amount actually paid by User for this license. User assumes full liability for the actions and omissions of its principals, employees, agents, affiliates, successors and assigns.
6. Limited Warranties. THE WORK(S) AND RIGHT(S) ARE PROVIDED “AS IS”. CCC HAS THE RIGHT TO GRANT TO USER THE RIGHTS GRANTED IN THE ORDER CONFIRMATION DOCUMENT. CCC AND THE RIGHTSHOLDER DISCLAIM ALL OTHER WARRANTIES RELATING TO THE WORK(S) AND RIGHT(S), EITHER EXPRESS OR IMPLIED, INCLUDING WITHOUT LIMITATION IMPLIED WARRANTIES OF MERCHANTABILITY OR FITNESS FOR A PARTICULAR PURPOSE. ADDITIONAL RIGHTS MAY BE REQUIRED TO USE ILLUSTRATIONS, GRAPHS, PHOTOGRAPHS, ABSTRACTS, INSERTS OR OTHER PORTIONS OF THE WORK (AS OPPOSED TO THE ENTIRE WORK) IN A MANNER CONTEMPLATED BY USER; USER UNDERSTANDS AND AGREES THAT NEITHER CCC NOR THE RIGHTSHOLDER MAY HAVE SUCH ADDITIONAL RIGHTS TO GRANT.
7. Effect of Breach. Any failure by User to pay any amount when due, or any use by User of a Work beyond the scope of the license set forth in the Order Confirmation and/or these terms and conditions, shall be a material breach of the license created by the Order Confirmation and these terms and conditions. Any breach not cured within 30 days of written notice thereof shall result in immediate termination of such license without further notice. Any unauthorized (but licensable) use of a Work that is terminated immediately upon notice thereof may be liquidated by payment of the Rightsholder's ordinary license price therefor; any unauthorized (and unlicensable) use that is not terminated immediately for any reason (including, for example, because materials containing the Work cannot reasonably be recalled) will be subject to all remedies available at law or in equity, but in no event to a payment of less than three times the Rightsholder's ordinary license price for the most closely analogous licensable use plus Rightsholder's and/or CCC's costs and expenses incurred in collecting such payment.
8. **Miscellaneous.**
8.1 User acknowledges that CCC may, from time to time, make changes or additions to the Service or to these terms and conditions, and CCC reserves the right to send notice to the User by electronic mail or otherwise for the purposes of notifying User of such changes or additions; provided that any such changes or additions shall not apply to permissions already secured and paid for.

8.2 Use of User-related information collected through the Service is governed by CCC's privacy policy, available online here: http://www.copyright.com/content/cc3/en/tools/footer/privacypolicy.html.
8.3 The licensing transaction described in the Order Confirmation is personal to User. Therefore, User may not assign or transfer to any other person (whether a natural person or an organization of any kind) the license created by the Order Confirmation and these terms and conditions or any rights granted hereunder; provided, however, that User may assign such license in its entirety on written notice to CCC in the event of a transfer of all or substantially all of User's rights in the new material which includes the Work(s) licensed under this Service.
8.4 No amendment or waiver of any terms is binding unless set forth in writing and signed by the parties. The Rightsholder and CCC hereby object to any terms contained in any writing prepared by the User or its principals, employees, agents or affiliates and purporting to govern or otherwise relate to the licensing transaction described in the Order Confirmation, which terms are in any way inconsistent with any terms set forth in the Order Confirmation and/or in these terms and conditions or CCC's standard operating procedures, whether such writing is prepared prior to, simultaneously with or subsequent to the Order Confirmation, and whether such writing appears on a copy of the Order Confirmation or in a separate instrument.
8.5 The licensing transaction described in the Order Confirmation document shall be governed by and construed under the law of the State of New York, USA, without regard to the principles thereof of conflicts of law. Any case, controversy, suit, action, or proceeding arising out of, in connection with, or related to such licensing transaction shall be brought, at CCC's sole discretion, in any federal or state court located in the County of New York, State of New York, USA, or in any federal or state court whose geographical jurisdiction covers the location of the Rightsholder set forth in the Order Confirmation. The parties expressly submit to the personal jurisdiction and venue of each such federal or state court.If you have any comments or questions about the Service or Copyright Clearance Center, please contact us at 978-750-8400 or send an e-mail to info@copyright.com.
v 1.1

Questions? customercare@copyright.com or +1-855-239-3415 (toll free in the US) or +1-978-646-2777.

REFERENCES

[1] W. Zhang, M. S. Branicky, and S. M. Phillips, "Stability of networked control systems," *IEEE Control Systems Magazine*, vol. 21, no. 1, pp. 84–99, 2001.

[2] Y. Tipsuwan and M.-Y. Chow, "Control methodologies in networked control systems," *Control engineering practice*, vol. 11, no. 10, pp. 1099–1111, 2003.

[3] J. P. Hespanha, P. Naghshtabrizi, and Y. Xu, "A survey of recent results in networked control systems," *Proceedings of the IEEE*, vol. 95, no. 1, pp. 138–162, 2007.

[4] F.-Y. Wang and D. Liu, *Networked Control Systems*. Springer, 2008.

[5] A. Bemporad, M. Heemels, and M. Johansson, *Networked Control Systems*. Springer, 2010.

[6] K. Zhou and J. C. Doyle, *Essentials of Robust Control*. Upper Saddle River, NJ: Prentice Hall, 1998.

[7] G. Dullerud and F. Paganini, *Course in Robust Control Theory*. Springer-Verlag New York, 2000.

[8] P. A. Ioannou and J. Sun, *Robust Adaptive Control*. Courier Corporation, 2012.

[9] K. S. Narendra and A. M. Annaswamy, *Stable Adaptive Systems*. Courier Corporation, 2012.

[10] K. J. Åström and B. Wittenmark, *Adaptive Control*. Courier Corporation, 2013.

[11] T. Yucelen and W. M. Haddad, "A robust adaptive control architecture for disturbance rejection and uncertainty suppression with $\mathcal{L}_\infty$ transient and steady-state performance guarantees," *International Journal of Adaptive Control and Signal Processing*, vol. 26, no. 11, pp. 1024–1055, 2012.

[12] T. Yucelen and E. Johnson, "A new command governor architecture for transient response shaping," *International Journal of Adaptive Control and Signal Processing*, vol. 27, no. 12, pp. 1065–1085, 2013.

[13] A. Sahoo, H. Xu, and S. Jagannathan, "Neural network-based adaptive event-triggered control of nonlinear continuous-time systems," *IEEE International Symposium on Intelligent Control*, pp. 35–40, 2013.

[14] A. Sahoo, H. Xu, and S. Jagannathan, "Neural network approximation-based event-triggered control of uncertain mimo nonlinear discrete time systems," *IEEE American Control Conference*, pp. 2017–2022, 2014.

[15] X. Wang and N. Hovakimyan, "$\mathcal{L}_1$ adaptive control of event-triggered networked systems," *IEEE American Control Conference*, pp. 2458–2463, 2010.

[16] X. Wang, E. Kharisov, and N. Hovakimyan, "Real-time adaptive control for uncertain networked control systems," *IEEE Transactions on Automatic Control*, vol. 60, no. 9, pp. 2500–2505, 2015.

[17] T. Yucelen and A. J. Calise, "Derivative-free model reference adaptive control," *Journal of Guidance, Control, and Dynamics*, vol. 34, no. 4, pp. 933–950, 2011.

[18] P. Tabuada, "Event-triggered real-time scheduling of stabilizing control tasks," *IEEE Transactions on Automatic Control*, vol. 52, no. 9, pp. 1680–1685, 2007.

[19] M. Mazo Jr and P. Tabuada, "On event-triggered and self-triggered control over sensor/actuator networks," in *IEEE Conference on Decision and Control*, pp. 435–440, 2008.

[20] M. Mazo Jr, A. Anta, and P. Tabuada, "On self-triggered control for linear systems: Guarantees and complexity," in *IEEE European Control Conference*, pp. 3767–3772, 2009.

[21] J. Lunze and D. Lehmann, "A state-feedback approach to event-based control," *Automatica*, vol. 46, no. 1, pp. 211–215, 2010.

[22] R. Postoyan, A. Anta, D. Nesic, and P. Tabuada, "A unifying Lyapunov-based framework for the event-triggered control of nonlinear systems," in *IEEE Conference on Decision and Control and European Control Conference*, pp. 2559–2564, 2011.

[23] W. Heemels, K. H. Johansson, and P. Tabuada, "An introduction to event-triggered and self-triggered control," in *IEEE Annual Conference on Decision and Control*, pp. 3270–3285, 2012.

[24] H. Li and Y. Shi, "Event-triggered robust model predictive control of continuous-time nonlinear systems," *Automatica*, vol. 50, no. 5, pp. 1507–1513, 2014.

[25] D. Shi, T. Chen, and L. Shi, "An event-triggered approach to state estimation with multiple point-and set-valued measurements," *Automatica*, vol. 50, no. 6, pp. 1641–1648, 2014.

[26] E. Lavretsky, R. Gadient, and I. M. Gregory, "Predictor-based model reference adaptive control," *Journal of Guidance, Control, and Dynamics*, vol. 33, no. 4, pp. 1195–1201, 2010.

[27] J. A. Muse and A. J. Calise, "H_∞ adaptive flight control of the generic transport model," *AIAA Infotech@Aerospace*, 2010.

[28] V. Stepanyan and K. Krishnakumar, "MRAC revisited: guaranteed performance with reference model modification," *IEEE American Control Conference*, pp. 93–98, 2010.

[29] V. Stepanyan and K. Krishnakumar, "M-MRAC for nonlinear systems with bounded disturbances," *IEEE Decision and Control and European Control Conference*, pp. 5419–5424, 2011.

[30] T. E. Gibson, A. M. Annaswamy, and E. Lavretsky, "Improved transient response in adaptive control using projection algorithms and closed loop reference models," *AIAA Guidance Navigation and Control Conference*, 2012.

[31] T. Yucelen, G. De La Torre, and E. N. Johnson, "Improving transient performance of adaptive control architectures using frequency-limited system error dynamics," *International Journal of Control*, vol. 87, no. 11, pp. 2383–2397, 2014.

[32] T. E. Gibson, A. M. Annaswamy, and E. Lavretsky, "Adaptive systems with closed-loop reference models: Stability, robustness and transient performance," *arXiv preprint arXiv:1201.4897*, 2012.

[33] E. Lavretsky and K. Wise, *Robust and Adaptive Control: With Aerospace Applications*. Springer, 2012.

[34] H. K. Khalil, "Adaptive output feedback control of nonlinear systems represented by input-output models," *Automatic Control, IEEE Transactions on*, vol. 41, no. 2, pp. 177–188, 1996.

[35] A. J. Calise, N. Hovakimyan, and M. Idan, "Adaptive output feedback control of nonlinear systems using neural networks," *Automatica*, vol. 37, no. 8, pp. 1201–1211, 2001.

[36] N. Hovakimyan, F. Nardi, A. Calise, and N. Kim, "Adaptive output feedback control of uncertain nonlinear systems using single-hidden-layer neural networks," *Neural Networks, IEEE Transactions on*, vol. 13, no. 6, pp. 1420–1431, 2002.

[37] K. Y. Volyanskyy, W. M. Haddad, and A. J. Calise, "A new neuroadaptive control architecture for nonlinear uncertain dynamical systems: Beyond-and-modifications," *IEEE Transactions on Neural Networks*, vol. 20, no. 11, pp. 1707–1723, 2009.

[38] T. Yucelen and W. M. Haddad, "Output feedback adaptive stabilization and command following for minimum phase dynamical systems with unmatched uncertainties and disturbances," *International Journal of Control*, vol. 85, no. 6, pp. 706–721, 2012.

[39] E. Lavretsky, "Adaptive output feedback design using asymptotic properties of LQG/LTR controllers," *Automatic Control, IEEE Transactions on*, vol. 57, no. 6, pp. 1587–1591, 2012.

[40] T. E. Gibson, Z. Qu, A. M. Annaswamy, and E. Lavretsky, "Adaptive output feedback based on closed-loop reference models," *arXiv preprint arXiv:1410.1944*, 2014.

[41] E. Lavretsky, "Transients in output feedback adaptive systems with observer-like reference models," *International Journal of Adaptive Control and Signal Processing*, vol. 29, no. 12, pp. 1515–1525, 2015.

[42] K. Kaneko and R. Horowitz, "Repetitive and adaptive control of robot manipulators with velocity estimation," *Robotics and Automation, IEEE Transactions on*, vol. 13, no. 2, pp. 204–217, 1997.

[43] T. Burg, D. Dawson, and P. Vedagarbha, "A redesigned dcal controller without velocity measurements: theory and demonstration," *Robotica*, vol. 15, no. 03, pp. 337–346, 1997.

[44] E. Zergeroglu, W. Dixon, D. Haste, and D. Dawson, "A composite adaptive output feedback tracking controller for robotic manipulators," *Robotica*, vol. 17, no. 06, pp. 591–600, 1999.

[45] F. Zhang, D. M. Dawson, M. S. de Queiroz, W. E. Dixon, *et al.*, "Global adaptive output feedback tracking control of robot manipulators," *IEEE Transactions on Automatic Control*, vol. 45, no. 6, pp. 1203–1208, 2000.

[46] F. Bullo, J. Cortes, and S. Martinez, *Distributed control of robotic networks: A mathematical approach to motion coordination algorithms*. Princeton University Press, 2009.

[47] M. Mesbahi and M. Egerstedt, *Graph theoretic methods in multiagent networks*. Princeton University Press, 2010.

[48] D. D. Siljak, *Decentralized control of complex systems*. Courier Corporation, 2011.

[49] T. Yucelen and E. N. Johnson, "Control of multivehicle systems in the presence of uncertain dynamics," *International Journal of Control*, vol. 86, no. 9, pp. 1540–1553, 2013.

[50] E. J. Davison and A. G. Aghdam, *Decentralized control of large-scale systems*. Springer Publishing Company, Incorporated, 2014.

[51] T. Yucelen and J. S. Shamma, "Adaptive architectures for distributed control of modular systems," in *American Control Conference*, pp. 1328–1333, 2014.

[52] E. Lavretsky and K. A. Wise, "Robust adaptive control," in *Robust and Adaptive Control*, Springer, 2013.

[53] T. Yucelen and W. M. Haddad, "Low-frequency learning and fast adaptation in model reference adaptive control," *IEEE Transactions on Automatic Control*, vol. 58, no. 4, pp. 1080–1085, 2013.

[54] K. J. Åström and B. Bernhardsson, "Comparison of riemann and lebesque sampling for first order stochastic systems," in *Proceedings of the 41st IEEE Conference on Decision and Control*, vol. 2, pp. 2011–2016, 2002.

[55] W. Heemels, M. Donkers, and A. R. Teel, "Periodic event-triggered control for linear systems," *IEEE Transactions on Automatic Control*, vol. 58, no. 4, pp. 847–861, 2013.

[56] P. Ioannou, "Decentralized adaptive control of interconnected systems," *IEEE Transactions on Automatic Control*, vol. 31, no. 4, pp. 291–298, 1986.

[57] D. T. Gavel and D. Siljak, "Decentralized adaptive control: structural conditions for stability," *IEEE Transactions on Automatic Control*, vol. 34, no. 4, pp. 413–426, 1989.

[58] L. Shi and S. K. Singh, "Decentralized adaptive controller design for large-scale systems with higher order interconnections," *IEEE Transactions on Automatic Control*, vol. 37, no. 8, pp. 1106–1118, 1992.

[59] J. T. Spooner and K. M. Passino, "Decentralized adaptive control of nonlinear systems using radial basis neural networks," *IEEE transactions on automatic control*, vol. 44, no. 11, pp. 2050–2057, 1999.

[60] B. M. Mirkin, "Decentralized adaptive controller with zero residual tracking errors," in *Proceedings of the 7th Mediterranean Conference on Control and Automation (MED99)*, pp. 28–30, 1999.

[61] K. S. Narendra and N. O. Oleng, "Exact output tracking in decentralized adaptive control systems," *IEEE Transactions on Automatic Control*, vol. 47, no. 2, pp. 390–395, 2002.

[62] M. Mazo and P. Tabuada, "Decentralized event-triggered control over wireless sensor/actuator networks," *IEEE Transactions on Automatic Control*, vol. 56, no. 10, pp. 2456–2461, 2011.

[63] A. Molin and S. Hirche, "Optimal design of decentralized event-triggered controllers for large-scale systems with contention-based communication," in *IEEE Conference on Decision and Control and European Control*, pp. 4710–4716, 2011.

[64] D. V. Dimarogonas, E. Frazzoli, and K. H. Johansson, "Distributed event-triggered control for multi-agent systems," *IEEE Transactions on Automatic Control*, vol. 57, no. 5, pp. 1291–1297, 2012.

[65] M. Donkers and W. Heemels, "Output-based event-triggered control with guaranteed-gain and improved and decentralized event-triggering," *IEEE Transactions on Automatic Control*, vol. 57, no. 6, pp. 1362–1376, 2012.

[66] E. Garcia, Y. Cao, H. Yu, P. Antsaklis, and D. Casbeer, "Decentralised event-triggered cooperative control with limited communication," *International Journal of Control*, vol. 86, no. 9, pp. 1479–1488, 2013.

[67] Y. Fan, G. Feng, Y. Wang, and C. Song, "Distributed event-triggered control of multi-agent systems with combinational measurements," *Automatica*, vol. 49, no. 2, pp. 671–675, 2013.

[68] E. Garcia, Y. Cao, and D. W. Casbeer, "Cooperative control with general linear dynamics and limited communication: centralized and decentralized event-triggered control strategies," in *IEEE American Control Conference*, pp. 159–164, 2014.

[69] X. Wang, E. Kharisov, and N. Hovakimyan, "Real-time $\mathcal{L}_1$ adaptive control for uncertain networked control systems," *IEEE Transactions on Automatic Control*, vol. 60, no. 9, pp. 2500–2505, 2015.

[70] A. Albattat, B. C. Gruenwald, and T. Yucelen, "Event-triggered adaptive control," in *ASME 2015 Dynamic Systems and Control Conference*, American Society of Mechanical Engineers, 2015.

[71] A. Albattat, B. C. Gruenwald, and T. Yucelen, *Adaptive Control for Robotic Manipulators*, ch. Output Feedback Adaptive Control of Uncertain Dynamical Systems with Event-Triggering. CRC Press/Taylor & Francis Group: Boca Raton, FL, USA, 2016.

[72] W. Ren and Y. Cao, *Distributed coordination of multi-agent networks: Emergent problems, models, and issues*. Springer Science & Business Media, 2010.

[73] F. L. Lewis, H. Zhang, K. Hengster-Movric, and A. Das, *Cooperative control of multi-agent systems: optimal and adaptive design approaches*. Springer Science & Business Media, 2013.

[74] J. Xiang, W. Wei, and Y. Li, "Synchronized output regulation of linear networked systems," *IEEE Transactions on Automatic Control*, vol. 54, no. 6, pp. 1336–1341, 2009.

[75] H. Zhang, F. L. Lewis, and A. Das, "Optimal design for synchronization of cooperative systems: state feedback, observer and output feedback," *IEEE Transactions on Automatic Control*, vol. 56, no. 8, pp. 1948–1952, 2011.

[76] Y. Su and J. Huang, "Cooperative output regulation of linear multi-agent systems," *IEEE Transactions on Automatic Control*, vol. 57, no. 4, pp. 1062–1066, 2012.

[77] R. Cui, B. Ren, and S. Ge, "Synchronised tracking control of multi-agent system with high-order dynamics," *IET Control Theory & Applications*, vol. 6, no. 5, pp. 603–614, 2012.

[78] T. Liu and Z.-P. Jiang, "Distributed output-feedback control of nonlinear multi-agent systems," *IEEE Transactions on Automatic Control*, vol. 58, no. 11, pp. 2912–2917, 2013.

[79] H. Zhang, G. Feng, H. Yan, and Q. Chen, "Observer-based output feedback event-triggered control for consensus of multi-agent systems," *IEEE Transactions on Industrial Electronics*, vol. 61, no. 9, pp. 4885–4894, 2014.

[80] B. Zhou, C. Xu, and G. Duan, "Distributed and truncated reduced-order observer based output feedback consensus of multi-agent systems," *IEEE Transactions on Automatic Control*, vol. 59, no. 8, pp. 2264–2270, 2014.

[81] C. P. Chen, G.-X. Wen, Y.-J. Liu, and Z. Liu, "Observer-based adaptive backstepping consensus tracking control for high-order nonlinear semi-strict-feedback multiagent systems," *IEEE transactions on cybernetics*, vol. 46, no. 7, pp. 1591–1601, 2016.

[82] T. Yucelen and F. Pourboghrat, "Active noise blocking: Non-minimal modeling, robust control, and implementation," in *American Control Conference, 2009. ACC'09.*, pp. 5492–5497, IEEE, 2009.

[83] W. Hu, L. Liu, and G. Feng, "Cooperative output regulation of linear multi-agent systems by intermittent communication: A unified framework of time-and event-triggering strategies," *IEEE Transactions on Automatic Control*, 2017.

[84] E. Kharisov, X. Wang, and N. Hovakimyan, "Distributed event-triggered consensus algorithm for uncertain multi-agent systems," *AIAA Guidance, Navigation and Control Conference*, 2010.

[85] P. Zhang and J. Wang, "Event-triggered observer-based tracking control for leader-follower multi-agent systems," *Kybernetika*, vol. 52, no. 4, pp. 589–606, 2016.

[86] C. Yan, M. Yu, and C. Li, "Event-triggered tracking control for couple-group multi-agent systems," *Journal of the Franklin Institute*, 2017.

[87] A. Albattat, T. Yucelen, B. C. Gruenwald, and S. Jagannathan, "An observer-free output feedback cooperative control architecture for multivehicle systems," *ASME Dynamic Systems and Control Conference*, 2017 (Accepted).

[88] A. Albattat, T. Yucelen, B. C. Gruenwald, and J. Sarangapani, "Observer-free output feedback adaptive control for multivehicle systems with exogenous disturbances," *AIAA Guidance, Navigation, and Control Conference*, 2018 (accepted).

[89] Z.-G. Hou, L. Cheng, and M. Tan, "Decentralized robust adaptive control for the multiagent system consensus problem using neural networks," *IEEE Transactions on Systems, Man, and Cybernetics - Part B: Cybernetics*, vol. 39, no. 3, pp. 636–647, 2009.

[90] A. Das and F. L. Lewis, "Distributed adaptive control for synchronization of unknown nonlinear networked systems," *Automatica*, vol. 46, no. 12, pp. 2014–2021, 2010.

[91] A. Das and F. L. Lewis, "Cooperative adaptive control for synchronization of second-order systems with unknown nonlinearities," *International Journal of Robust and Nonlinear Control*, vol. 21, no. 13, pp. 1509–1524, 2011.

[92] Y. Miyasato, "Adaptive H_∞ consensus control of multi-agent systems on directed graph by utilizing neural network approximators," *IFAC-PapersOnLine*, vol. 49, no. 13, pp. 36–41, 2016.

[93] Z. Tu, H. Yu, and X. Xia, "Decentralized finite-time adaptive consensus of multiagent systems with fixed and switching network topologies," *Neurocomputing*, vol. 219, pp. 59–67, 2017.

[94] H. Kim, H. Shim, and J. H. Seo, "Output consensus of heterogeneous uncertain linear multi-agent systems," *IEEE Transactions on Automatic Control*, vol. 56, no. 1, pp. 200–206, 2011.

[95] X. Wang, Y. Hong, J. Huang, and Z.-P. Jiang, "A distributed control approach to a robust output regulation problem for multi-agent linear systems," *IEEE Transactions on Automatic control*, vol. 55, no. 12, pp. 2891–2895, 2010.

[96] S. Mondal, R. Su, and L. Xie, "Heterogeneous consensus of higher-order multi-agent systems with mismatched uncertainties using sliding mode control," *International Journal of Robust and Nonlinear Control*, 2016.

[97] J. Wang, K. Chen, and Q. Ma, "Adaptive leader-following consensus of multi-agent systems with unknown nonlinear dynamics," *Entropy*, vol. 16, no. 9, pp. 5020–5031, 2014.

[98] J. Sun and Z. Geng, "Adaptive consensus tracking for linear multi-agent systems with heterogeneous unknown nonlinear dynamics," *International Journal of Robust and Nonlinear Control*, vol. 26, no. 1, pp. 154–173, 2016.

[99] J. Hu and W. X. Zheng, "Adaptive tracking control of leader–follower systems with unknown dynamics and partial measurements," *Automatica*, vol. 50, no. 5, pp. 1416–1423, 2014.

[100] Z. Peng, D. Wang, H. Zhang, and G. Sun, "Distributed neural network control for adaptive synchronization of uncertain dynamical multiagent systems," *IEEE transactions on neural networks and learning systems*, vol. 25, no. 8, pp. 1508–1519, 2014.

[101] J. Sun, Z. Geng, and Y. Lv, "Adaptive output feedback consensus tracking for heterogeneous multi-agent systems with unknown dynamics under directed graphs," *Systems & Control Letters*, vol. 87, pp. 16–22, 2016.

[102] H. Cai, F. L. Lewis, G. Hu, and J. Huang, "The adaptive distributed observer approach to the cooperative output regulation of linear multi-agent systems," *Automatica*, vol. 75, pp. 299–305, 2017.

[103] T. Yucelen, W. M. Haddad, and A. J. Calise, "Output feedback adaptive command following for nonminimum phase uncertain dynamical systems," *American Control Conference*, pp. 123–128, 2010.

[104] T. Yucelen and W. M. Haddad, "Output feedback adaptive stabilization and command following for minimum phase dynamical systems with unmatched uncertainties," *American Control Conference*, pp. 1163–1168, 2011.

[105] J.-B. Pomet and L. Praly, "Adaptive nonlinear regulation: estimation from the Lyapunov equation," *IEEE Transactions on Automatic Control*, vol. 37, no. 6, pp. 729–740, 1992.

[106] W. M. Haddad and V. Chellaboina, *Nonlinear Dynamical Systems and Control:* A L*yapunov-Based Approach*. Princeton University Press, 2008.

[107] D. S. Bernstein, *Matrix mathematics: Theory, Facts, and Formulas*. Princeton University Press, 2009.

[108] H. K. Khalil, *Nonlinear Systems*. Upper Saddle River, NJ: PrenticeHall, 1996.

[109] G. C. Walsh and H. Ye, "Scheduling of networked control systems," *Control Systems, IEEE*, vol. 21, no. 1, pp. 57–65, 2001.

[110] L. Zhang and D. Hristu-Varsakelis, "Communication and control co-design for networked control systems," *Automatica*, vol. 42, no. 6, pp. 953–958, 2006.

[111] R. Alur, K.-E. Arzen, J. Baillieul, T. Henzinger, D. Hristu-Varsakelis, and W. S. Levine, *Handbook of networked and embedded control systems*. Springer Science & Business Media, 2007.

[112] J.-J. E. Slotine and W. Li, "On the adaptive control of robot manipulators," *The international journal of robotics research*, vol. 6, no. 3, pp. 49–59, 1987.

[113] M. Krstic, P. V. Kokotovic, and I. Kanellakopoulos, *Nonlinear and adaptive control design*. John Wiley & Sons, Inc., 1995.

[114] K. Zhou, J. C. Doyle, and K. Glover, *Robust and optimal control*, vol. 40. Prentice hall New Jersey, 1996.

[115] K. Kim, T. Yucelen, and A. J. Calise, "A parameter dependent riccati equation approach to output feedback adaptive control," in *AIAA Guidance, Navigation, and Control Conference*, 2011.

[116] K. Kim, A. J. Calise, T. Yucelen, and N. Nguyen, "Adaptive output feedback control for an aeroelastic generic transport model: A parameter dependent riccati equation approach," in *AIAA Guidance, Navigation, and Control Conference*, 2011.

[117] A. Yeşildirek and F. L. Lewis, "Feedback linearization using neural networks," *Automatica*, vol. 31, no. 11, pp. 1659–1664, 1995.

[118] Y. H. Kim and F. L. Lewis, "Neural network output feedback control of robot manipulators," *Robotics and Automation, IEEE Transactions on*, vol. 15, no. 2, pp. 301–309, 1999.

[119] T. E. Lavretsky, Eugene and and A. M. Annaswamy, "Projection operator in adaptive systems," 2011.

[120] J. Kevorkian and J. D. Cole, *Multiple Scale and Singular Perturbation Methods*. Springer-Verlag New York, 1996.

[121] J. D. Murray, *Asymptotic Analysis*. Springer-Verlag New York, 1984.

[122] E. Lavretsky, "Adaptive output feedback design using asymptotic properties of lqg/ltr controllers," *AIAA Guidance, Navigation, and Control Conference*, 2010.

[123] C. Godsil and G. Royle, *Algebraic graph theory*. New York, NY: Springer, 2001.

[124] K. Glover, J. Doyle, P. P. Khargonekar, and B. A. Francis, "State space solutions to standard H_2 and H_∞ control problems," *IEEE transactions on automatic control*, vol. 34, no. 8, 1989.

[125] P. J. Antsaklis and A. N. Michel, *Linear systems*. Bosten, MA: Birkhäuser, 2006.

[126] J. A. Fax and R. M. Murray, "Information flow and cooperative control of vehicle formations," *IEEE transactions on automatic control*, vol. 49, no. 9, pp. 1465–1476, 2004.

[127] C.-Q. Ma and J.-F. Zhang, "Necessary and sufficient conditions for consensusability of linear multi-agent systems," *IEEE Transactions on Automatic Control*, vol. 55, no. 5, pp. 1263–1268, 2010.

[128] D. Tran and T. Yucelen, "On control of multiagent formations through local interactions," in *IEEE Conference on Decision and Control*, 2016.

[129] X. Wang and N. Hovakimyan, "Predicting the performance of uncertain multi-agent systems using event-triggering and $\mathcal{L}_1$ adaptation," *AIAA Guidance, Navigation, and Control Conference*, p. 8327, 2010.

[130] A. Albattat, B. C. Gruenwald, and T. Yucelen, "Design and analysis of adaptive control systems over wireless networks," *Journal of Dynamic Systems, Measurement, and Control*, vol. 139, no. 7, p. 074501, 2017.

[131] A. Albattat, B. C. Gruenwald, and T. Yucelen, "On event-triggered adaptive architectures for decentralized and distributed control of large-scale modular systems," *Sensors*, vol. 16, no. 8, p. 1297, 2016.

[132] Y. Kim, M. Mesbahi, and F. Y. Hadaegh, "Multiple-spacecraft reconfiguration through collision avoidance, bouncing, and stalemate," *Journal of Optimization Theory and Applications*, vol. 122, no. 2, pp. 323–343, 2004.

[133] Q. Jia and G. Li, "Formation control and obstacle avoidance algorithm of multiple autonomous underwater vehicles (auvs) based on potential function and behavior rules," *IEEE International Conference on Automation and Logistics*, pp. 569–573, 2007.

[134] C. W. Reynolds, “Interaction with groups of autonomous characters,” *Game Developers Conference*, vol. 2000, pp. 449–460, 2000.

[135] W. Ren, R. W. Beard, and E. M. Atkins, “A survey of consensus problems in multi-agent coordination,” *Proceedings of the American Control Conference*, pp. 1859–1864, 2005.

[136] R. Olfati-Saber, J. A. Fax, and R. M. Murray, “Consensus and cooperation in networked multi-agent systems,” *Proceedings of the IEEE*, vol. 95, no. 1, pp. 215–233, 2007.

VITA

Ali Albattat received the B.S. and M.S. degree in Mechatronics Engineering from the University of Baghdad, Baghdad, Iraq, in 2005 and 2007, respectively. He received a PhD in Mechanical Engineering from Missouri University of Science and Technology, Rolla, Missouri, United States of America in December 2017.

His dynamical systems and controls research specialized in adaptive control, event-triggered control, decentralized control, and distributed control with applications to networked systems, large-scale complex systems , multivehicle uncertain systems, linear systems, control applications, nonlinear systems, uncertain systems, and stability of nonlinear systems. He was a student member of the American Society of Mechanical Engineers (ASME).